

# Investigating the Role of the Mammalian RAS-Association Domain Family Member 7 (RASSF7)

Recino Scerif, Asha

*Award date:*
2011

*Awarding institution:*
University of Bath

# INVESTIGATING THE ROLE OF THE MAMMALIAN RAS-ASSOCIATION DOMAIN FAMILY MEMBER 7 (RASSF7)

Asha Recino

A thesis submitted for the degree of Doctor of Philosophy

University of Bath

Department of Biology and Biochemistry

February 2011

# Table of Contents

# Abstract

RASSF7 is part of a novel group of proteins, the N-terminal RAS-association domain family, which has been recently described as a distinct and evolutionary conserved group of Ras association domain containing members. The biological function of these members is still unclear, but at least some of these proteins may play a role in oncogenesis.

The aim of this project was to understand the role of mammalian RASSF7, which is up-regulated in a variety of cancers but whose direct contribution to tumour progression has still to be proved. RASSF7 was found to be an integral centrosomal component which is broadly expressed during mouse embryogenesis and in adult tissues. It is also expressed in every human cell line tested so far. Knockdown of RASSF7 severely impairs cell growth in H1792 and HeLa cells and causes major mitotic defects in HeLa cells. In fact, RASSF7 depletion compromises spindle formation and choromosomal congression in these cells. Furthermore Aurora B, which plays a fundamental role in the maintenance of genome integrity, is not activated in the knockdowns. Finally microtubule re-growth assays show that RASSF7 is a key regulator of microtubule dynamics.

Overall, the data presented in this thesis provide the first functional analysis of human RASSF7, indicating that this protein has a key role in regulating microtubules during mitosis, and suggest that the misregulation of RASSF7 in cancer cells might promote genomic instability.

# List of Figures

# List of Tables

# Abbreviations

| | |
|---|---|
| **α** | anti |
| **AP** | Alkaline phosphatase |
| **APC/c** | Anaphase promoting complex/cyclosome |
| **APS** | Ammonium persulphate |
| **ASPP** | Ankyrin-repeat, SH3-domain, and Prolin-rich-region containing Protein |
| **ATP** | Adenosine 5'-triphosphate |
| **bp** | Base pairs |
| **BRCA1** | Breast cancer 1 |
| **BSA** | Bovine serum albumin |
| **Bub** | Budding uninhibited by benzimidazole |
| **BubR1** | Bub1 related protein 1 |
| **°C** | Degrees Celsius |
| **Cdc20** | Cell division cycle 20 |
| **CDK** | Cyclin-dependent kinase |
| **cDNA** | Complementary DNA |
| **CENP-A** | Centromere protein A |
| **CPC** | Chromosomal passenger complex |
| **DAPI** | 4',6-diamidino-2-phenylindole |
| **DEPC** | Diethyl pyrocarbonate |
| **$dH_2O$** | Distilled Water |
| **DMEM** | Dulbecco's modified Eagle's medium |
| **DNA** | Deoxyribonucleic acid |
| **DTT** | Dithiothreitol |
| **E** | Embryonic day |
| **ECL** | Enhanced chemiluminescence |
| **EDTA** | Diaminoethanetetra-acetic acid disodium salt |
| **EST** | Expression sequence tags |

| | |
|---|---|
| **FACS** | Fluorescence-activated cell sorting |
| **FBS** | Fetal bovine serum |
| **G418** | Geneticin selective antibiotic |
| **GDP** | Guanosine diphosphate |
| **GFP** | Green fluorescent protein |
| **GTP** | Guanosine triphosphate |
| **HA** | Haemagglutinin |
| **H a E** | Haematoxylin and eosin |
| **IHC** | Immunohistochemistry |
| **INCENP** | Inner centromere protein |
| **ISH** | In *situ* hybridisation |
| **JNK** | c-Jun-NH2-kinase |
| **kb** | Kilo base |
| **KD** | Knockdown |
| **kDa** | Kilo Daltons |
| **LATS** | Large tumour suppressor |
| **LB** | Luria-Bertani |
| **Mad** | Mitotic arrest deficient |
| **MAP-1** | Modulator of apoptosis-1 |
| **MCAK** | Mitotic centromere-associated kinesin |
| **MCC** | Mitotic checkpoint complex |
| **MEFs** | Mouse embryonic fibroblasts |
| **MKK7** | MAP kinase kinase 7 |
| **mA** | MilliAmpere |
| **mg** | Milligram |
| **ml** | Millilitre |
| **mM** | Millimolar |
| **Mps1** | Monopolar spindle 1 |
| **mRNA** | Messenger ribonucleic acid |
| **MST** | Mammalian sterile20-like |

| | |
|---|---|
| **MTOC** | Microtubule organising centre |
| **n** | population size |
| **NCBI** | National centre for Biotechnology information |
| **ng** | Nanogram |
| **NGS** | Normal goat serum |
| **NSCLC** | Non small cell lung cancer |
| **p** | Probability value |
| **PBS** | Phosphate buffered saline |
| **PBST** | PBS with Tween-20 |
| **PCM** | Pericentriolar material |
| **PCR** | Polymerase chain reaction |
| **PFA** | Paraformaldehyde |
| **PI3-K** | Phosphatidylinositol 3-kinase |
| **PLK1** | Polo like Kinase 1 |
| **RA** | Ras association |
| **RASSF** | Ras association domain family |
| **RCC1** | Regulator of chromosome condensation 1 |
| **RNAi** | RNA interference |
| **RT** | Room temperature |
| **RT-PCR** | reverse transcription-PCR |
| **SCLC** | Small cell lung cancer |
| **SD** | Standard Deviation |
| **SDS** | Sodium dodecyl sulphate |
| **shRNA** | Short hairpin RNA |
| **siRNA** | Small interfering RNA |
| **SSC** | Standard Saline Citrate |
| **TBST** | Tris buffered saline with Tween-20 |
| **TCF** | T-cell factor |
| **TEMED** | N,N,N,N'-tetramethylethylenediamine |
| **TNFα** | tumour necrosis factor α |

| | |
|---|---|
| **tRNA** | Transfer ribonucleic acid |
| **U** | Units of enzyme |
| **UTR** | Untranslated region |
| **UV** | Ultraviolet |
| **V** | Volts |
| **VEGA** | Vertebrate gene annotation |
| **μl** | Microlitre |
| **μm** | Micrometre |
| **μg** | Microgram |
| **μM** | Micromolar |

# List of publications

- **Asha Recino**, Victoria Sherwood, Amy Flaxman, Wendy N Cooper, Farida Latif, Andrew Ward, and Andrew D Chalmers. **(**2010). "*Human RASSF7 regulates the microtubule cytoskeleton and is required for spindle formation, Aurora B activation and chromosomal congression during mitosis".* Biochem J. **430**(2): 207-13.

- Lock, F. E., Underhill-Day N., Dunwell T., Matallanas D., Cooper W., Hesson L., **Recino A**., Ward A., Pavlova T., Zabarovsky E., Grant M. M., Maher E. R., Chalmers A. D., Kolch W. and Latif F. (2010). "*The RASSF8 candidate tumor suppressor inhibits cell growth and regulates the Wnt and NF-kappaB signaling pathways*." Oncogene **29**, 4307-4316.

- Sherwood, V., **Recino A**., Jeffries A., Ward A. and Chalmers A. D. (2010). "*The N-terminal RASSF family: a new group of Ras-association-domain-containing proteins, with emerging links to cancer formation*." Biochem J **425**(2): 303-11.

- **Asha Recino**, Amy Flaxman, Victoria Sherwood, Wendy N Cooper, Andrew Ward, Farida Latif, and Andrew D Chalmers. (2010).*"RASSF7: a new possible therapeutic cancer target?*" Abstracts of papers presented at the twentieth Genetics Society's Mammalian Genetics and Development Workshop held at the Institute of Child Health, University College London, on 19 and 20 November 2009. Edited by: Nicholas D. E. Greene, Andrew Ward and Andrew J Copp. Genet. Res., Camb., **92**, pp. 71–79.

# Acknowledgements

I would like to express my big thanks to my first supervisor, Dr Andrew Chalmers, for giving me the opportunity to undertake this research and for his constant support and enthusiasm throughout all its stages. I would also like to thank my second supervisor, Dr Andrew Ward, for his valuable help and advice.

I would like to thank Dr Victoria Sherwood, a brilliant postdoc who started the RASSF7 project and has continually supported me during the initial phase of my PhD.

I would like to thank Dr Adrian Roger and Iryna Withington for their precious technical assistance, without which I could not have resolved an endless number of problems. A special thank you also to my project students, Amy Flaxman and George Bullock, who helped me with the project and made my experience as students supervisor quite enjoyable.

I would like to thank Dr Momna Hejmadi, Dr Stefan Bagby, Prof. Geoff Holman, Prof Farida Latif, Dr Eric O'Neil, Dr Barbara Reaves, Prof. Cheryll Tickle, Dr Nicolas Tapon, Dr David Tosh, Dr Abhishek Upadhyay, Dr Alan Wheals, Dr Rob Williams and Dr Will Wood for either allowing me to use their laboratory equipment/ materials or giving me valuable suggestions about the project.

My thanks go to ALL members of the Chalmers, Ward and Wood labs for many useful discussions and for their continuous help.

I would also like to thank the Marie Curie funding body for the numerous opportunities I have been given for attending conferences and training courses which I have enormously benefited from.

My family and Malcolm have been tremendous and I cannot thank them enough for all their support and encouragement. Special thanks to all my friends and Giusi, David, Massimo, Navin, Pooja and Spartaco for their help.

# 1 Introduction

Aberrant control of cell division is closely related to tumour formation and many cell cycle regulators are tumour suppressors or oncogenes and potential targets of anti-cancer therapies. This thesis will test the hypothesis that RASSF7 is a new mitotic regulator. Therefore, the introduction will focus on two areas, mitosis and the RASSF family.

## 1.1 An overview of mitosis

### 1.1.1 Mitotic stages

The cell cycle is composed of two main phases termed interphase and mitosis. Genome replication (synthesis or S-phase) and the accumulation of cellular material (gap-phases G1 and G2) take place during interphase. Mitosis leads to the segregation of the duplicated genome into daughter cells and comprises the following stages: prophase, prometaphase, metaphase, anaphase and telophase. These mitotic phases are shown in a schematic diagram (Figure 1.1A), and in confocal images (Figure 1.1B).

**A**

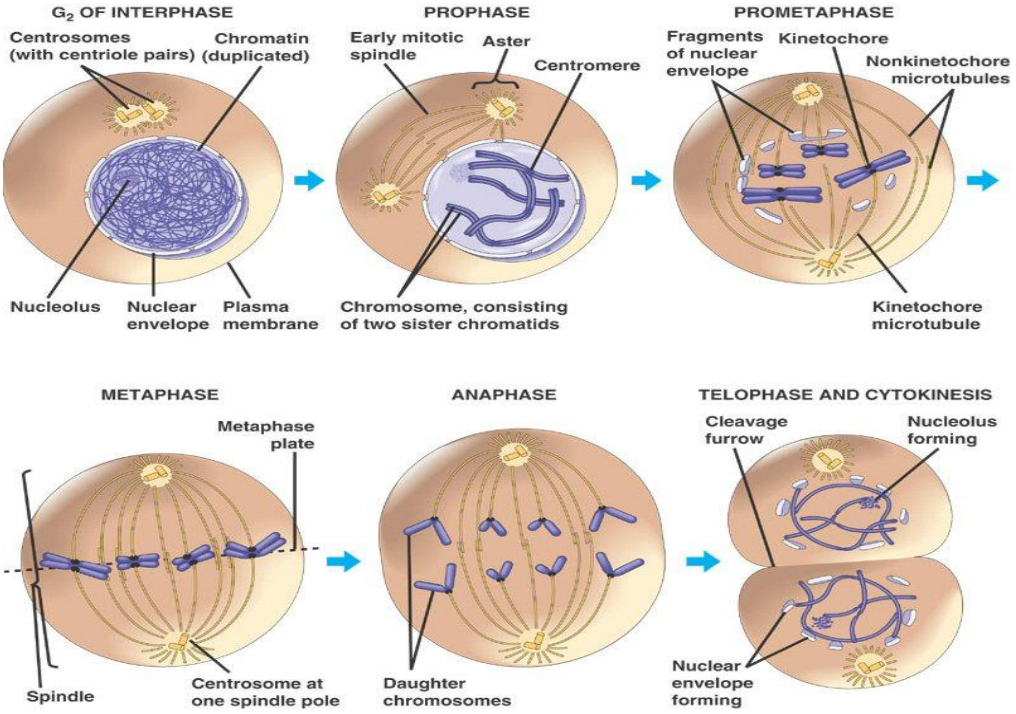


**B**

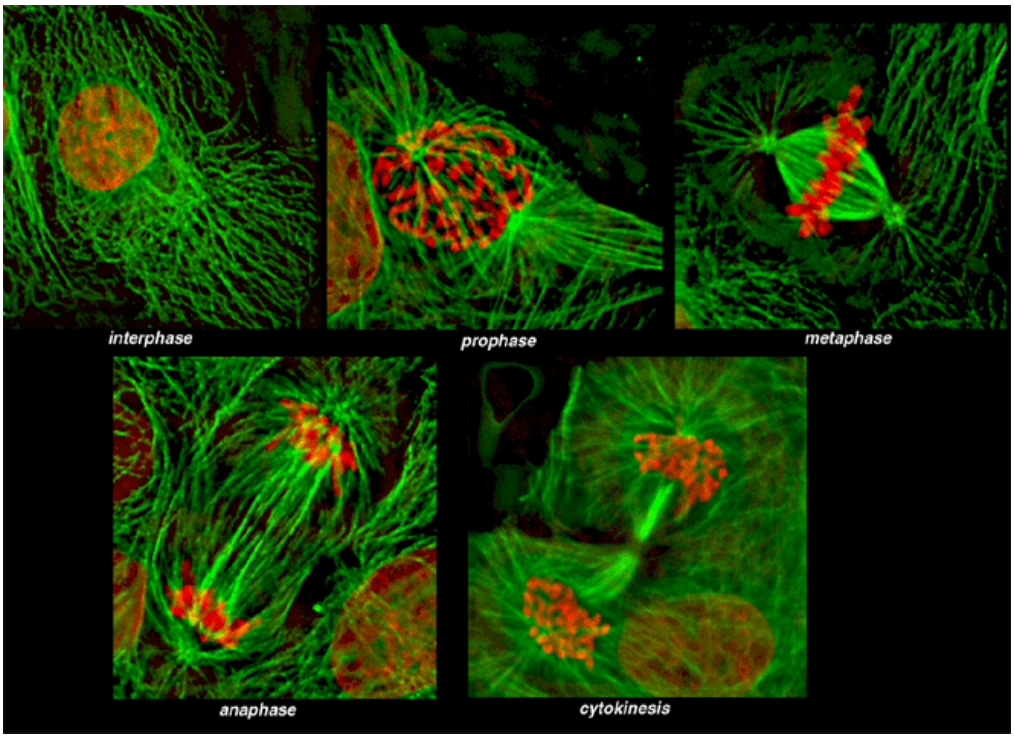


**Figure 1.1: Mitotic phases**. Diagram of the mitotic phases (A). Immunofluorescent images of pig kidney epithelial cells (LLC PK) stained for DNA (red) and tubulin (green) (B). Adapted from http://royaleb.wordpress.com/2009/04/27/mitosis/ and Earnshaw Laboratory's website (http://www.biology.ed.ac.uk/research/groups/earnshaw/Mitosis.htm).

During prophase, condensins are involved in condensing nuclear chromatin into chromosomes (Strunnikov, 2003). Cohesins keep chromosomes (which are namely sister chromatids) connected (Michaelis *et al.*, 1997) from S phase to mitosis the metaphase-to-anaphase transition takes place (Waizenegger *et al.*, 2000). An other important event during phophase is the formation of the mitotic spindle. This event is concomitant to the movement of the centrosomes, also referred to as spindle poles, to the opposite ends of the cell. This occurs in parallel with the nuclear envelope breakdown, which marks the beginning of prometaphase.

In prometaphase, the microtubules originating from the centrosomes reach the chromosomes and start their movement torwards the centre of the cell. The microtubules are extremely active components of the cytoskeleton and capture the chromosomes in the cytoplasm with their plus-ends (Hayden *et al.*, 1990; Holy and Leibler, 1994). Chromosomes initially bind along the microtubules via kinetochores by forming temporary “lateral attachments” (Rieder and Alexander, 1990; Merdes and De Mey, 1990; Hayden *et al.*, 1990). Such transient attachments become subsequently stable when the chromosome-microtubule attachment occurs via the interaction of microtubules with kinetochores.

In the amphitelic attachment, microtubules that originate from opposite centrosomes become attached to sister kinetochores in a bipolar fashion (Figure 1.2). Namely, each sister kinetochore is attached through microtubules to the spindle pole facing that kinetochore. However, since sister kinetochores attachment occurs via microtubules from one pole first and then from the other pole, monotelic, syntelic or merotelic attachments often precede amphitelic attachments (Figure 1.2B). These are improper attachments and need to be made unstable in order to make the cell proceed with the amphitelic attachments (Tanaka, 2008). As illustrated in figure 1.2B, they either lead to only one sister kinetochore bound or both sister kinetochores bound to the same pole or one of the sister kinetochores bound to both poles.

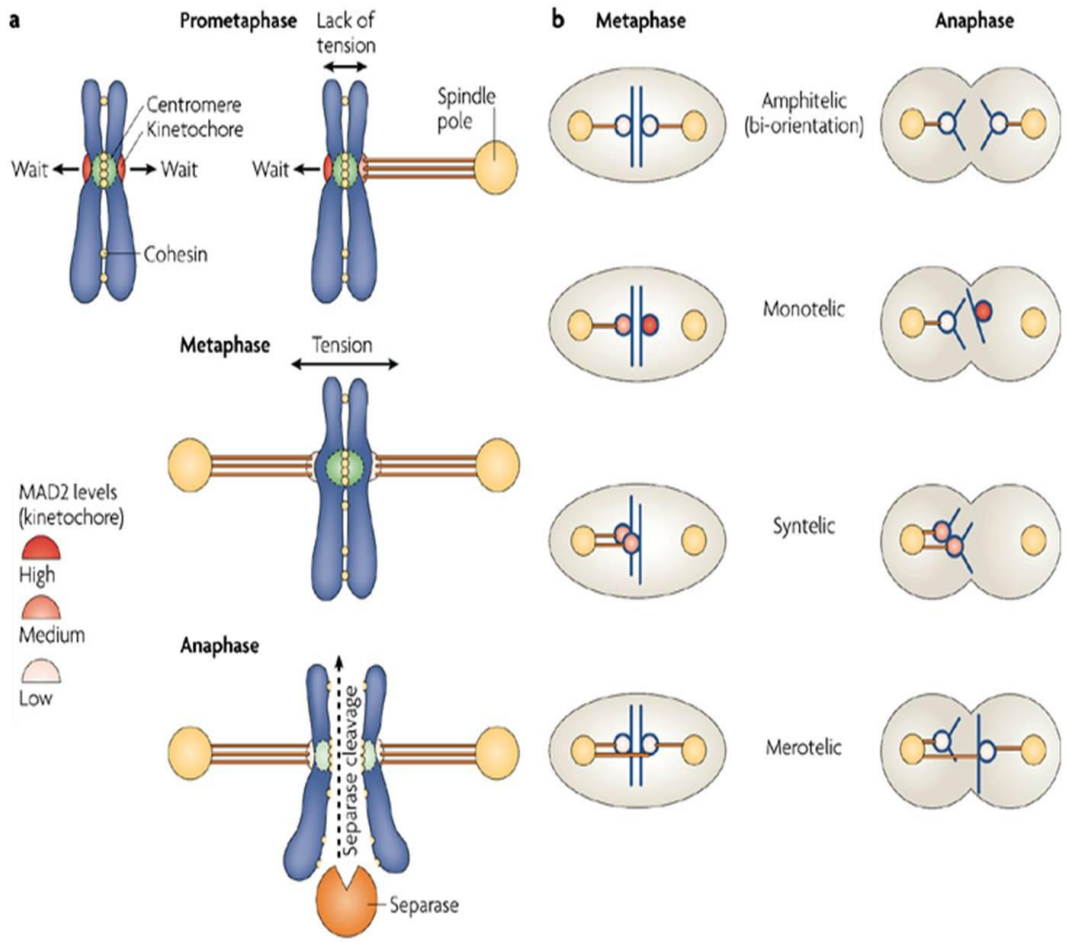


**Figure 1.2:**: **Possible kinetochore attachment errors and subsequent incorrect chromosome inheritance**. A) Unattached kinetochores generate a “wait” signal and recruit the spindle checkpoint proteins. The levels of mitotic-arrest deficient homologue-2 (MAD2) are high at unattached kinetochores (right) and moderately high in case of monotelic attachment (left) (see section 1.1.4.2). B) Correction mechanisms exist to prevent incorrect chromosome division, which would occur if improper attachments (syntelic, merotelic) persisted until anaphase. Monotelic attachment is a normal condition during prometaphase before bi-orientation. Modified from (Musacchio and Salmon, 2007).

During metaphase, chromosomes align at the centre of the cell to form the metaphase plate. Forces that originate from the spindle microtubules and the kinetochores counterbalance each other and make this alignment possible (Inoue and Salmon, 1995). This is a necessary condition for the correct segregation of the duplicated DNA into daughter cells.

Following the removal of cohesin, sister chromatids separate from each other after and anaphase takes place (de Gramont and Cohen-Fix, 2005). Anaphase comprises an initial phase during which sister chromatids are pulled in opposite directions towards their respective mitotic poles (Anaphase A), and a subsequent stage (Anaphase B) when further separation of the sister chromatids occurs. Microtubules with opposite orientation, that form the spindle midzone where the metaphase plate used to lie, and microtubule motor proteins mediate the accomplishment of this process.

In the last mitotic phase, telophase, the cleavage furrow develops where the metaphase plate used to be and segregates the separated chromatids and cytoplasm into new daughter cells in a process called cytokinesis (Barr and Gruneberg, 2007). Numerous regulatory proteins contribute to the correct progression of cytokinesis, which is successfully completed via the abscission of the last element of the cytokinetic furrow, called midbody.

### 1.1.2 Centrosomes and mitotic spindle

In proliferating animal cells, centrosomes organise microtubules to form the mitotic spindle. This requires nucleation of microtubules at their minus end which stabilises and anchors them at the centrosome. Centrosomes consist of two centrioles, barrel shaped structures consisting of microtubule triplets, arranged perpendicularly to one another (Luders and Stearns, 2007). Traditionally, the centrioles were considered to be the structures which organise the microtubules, but studies in which the centrioles have been removed have shown that they have a non-essential role in mitosis (Luders and Stearns, 2007). The other main component of the centrosome is a mass of proteins termed the pericentriolar material (PCM). It is thought that the PCM is responsible for microtubule organisation, and not the centrioles.

γ-tubulin is one of the main components of the PCM and the key protein in microtubule organisation (Stearns *et al.*, 1991; Stearns and Kirschner, 1994; Zheng *et al.*, 1995). γ-tubulin nucleates the α and β-tubulin subunits of microtubules, without being incorporated itself. It does this by forming, with a number of other proteins, a ring complex (γTuRC) which mimics the plus end of the microtubules, causing the latter to bind to them via their minus end. The minus ends are capped which stabilises the microtubules. Other proteins found in the PCM are also involved in the organisation of microtubules, including pericentrin and ninein (Doxsey, 2001; Bornens, 2002; Blagden and Glover, 2003).

Centrosomes undergo a series of events including duplication, separation, and maturation to form the poles of the bipolar spindle [reviewed in (Nigg, 2001)], which are controlled by numerous centrosomal effectors. Polo-like Kinase 1 (PLK1) localises to spindle poles to control these early mitotic events (Lane and Nigg, 1996; McInnes *et al.*, 2006). In fact, It may affect microtubule nucleation at spindle poles through phosphorylation of the Nlp (Ninein –like protein) and recruitment of γ-tubulin, thus contributing to the formation of the mitotic spindle (Lane and Nigg, 1996; McInnes *et al.*, 2006). The activity of another important centrosome controller, Aurora A, is closely correlated with the maturation of mitotic centrosomes (see section

1.1.5.1). Aurora A assists in the centrosome maturation by recruiting proteins such as γ-tubulin (Berdnik and Knoblich, 2002), D-TACC *(Drosophila*-Transforming, Acidic, Coiled Coil containing protein*)* (Giet *et al.*, 2002)*,* SPD-2 (Kemp *et al.*, 2004), centrosomin (Terada *et al.*, 2003) and chTOG (colonic and hepatic tumour overexpressed protein) (Conte *et al.*, 2003), and consequently, participates in spindle assembly and stability. Aurora A localisation and kinase activity is controlled by TPX2 (Kufer *et al.*, 2002; Bayliss *et al.*, 2003), a microtubule binding protein involved in the Ran-GTP mediated pathway, which is not only critical for spindle organisation and function but also for directional microtubule growth (Roscioli *et al.*, 2010).

Many more proteins, which have not yet been identified and/or characterised, may also be involved in co-ordinating the centrosome's role in microtubule organisation. In fact, over 100 regulatory proteins are known to bind to centrosomes (Doxsey *et al.*, 2005). However, the function of many of these proteins is unknown, indicating that cellular processes mediated by centrosomes are complex and must be carefully controlled. More investigation of centrosome proteins is therefore required.

In multicellular eukaryotes, the mitotic spindle is made up of microtubules extending from two opposing spindle poles (Figure 1.3). The less dynamic minus ends of microtubules are located at the spindle poles, while the more dynamic plus ends extend away from the poles (Figure 1.3). A portion of the microtubules' plus ends attaches to sister chromatids at the kinetochore. Kinetochore microtubules form morphologically distinct bundles called K fibers (Figure 1.3), which maintain attachment of chromosomes to the spindle and allow them to align and segregate (Rieder and Salmon, 1998; McIntosh *et al.*, 2002). The remainder of the spindle consists of interpolar microtubules (Figure 1.3). In addition, systems with centrosomes as the primary microtubule organising centre (MTOC) at the spindle poles have astral microtubules extending away from the spindle (Figure 1.3) and play an important role for positioning the mitotic spindle.

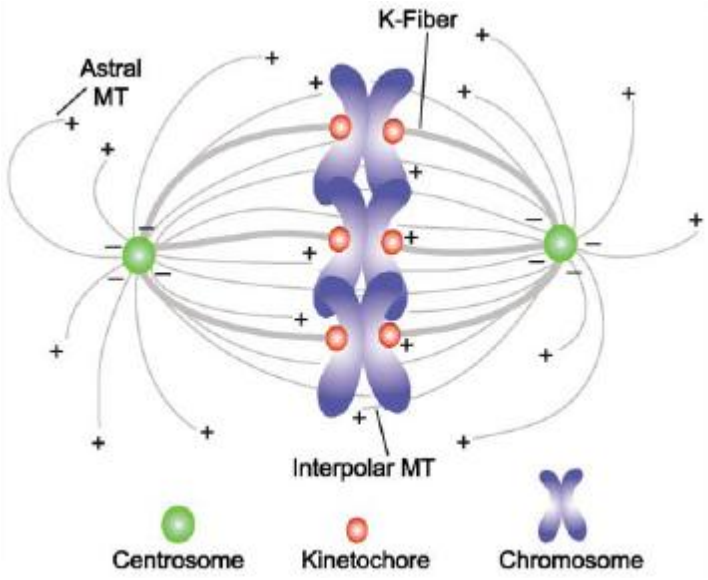


**Figure 1.3**: **Mitotic spindle components.** The schematic diagram shows the basic components of the mitotic spindle in somatic cells. Microtubules (MT) are shown in gray, centrosomes in green, kinetochores in red, and chromosomes in blue. Positions of the microtubule minus (-) ends versus (+) ends are indicated. Adapted from (Kline-Smith and Walczak, 2004).

### 1.1.3 Centromeres and kinetochores

Centromeres are the most condensedand constricted regions of a chromosome, to which the spindle fibers are attached during mitosis (Figure 1.4). Repetitive DNA sequences, called $\alpha$-satellite DNA, form the centromeres. Besides, in the centromeric chromatin a specific histone CenpA, substitutes the normal nucleosomal subunit H3 at certain intervals (Blower *et al.*, 2002). Another peculiar feature of this region is the presence of heterochromatin, which is tightly packed and not transcribed (Pidoux and Allshire, 2005). The structural conformation of the centromere chromatin determines the sites at which the kinetochore proteins and centromere proteins (Cenps) are assembled (Zinkowski *et al.*, 1991; Blower *et al.*, 2002). It is plausible that forms of epigenetic controls determine where the assembly of the proteins mentioned above occurs (Karpen and Allshire, 1997).

The inner, middle and outer layers constitute the vertebrate kinetochore structure (Brinkley and Stubblefield, 1966) (Figure 1.4). It is important to

note the presence of a fourth region called the fibrous corona that originates from the outer kinetochore. The importance of kinetochores is due to the role they have in mediating and monitoring microtubule-chromosome attachments.

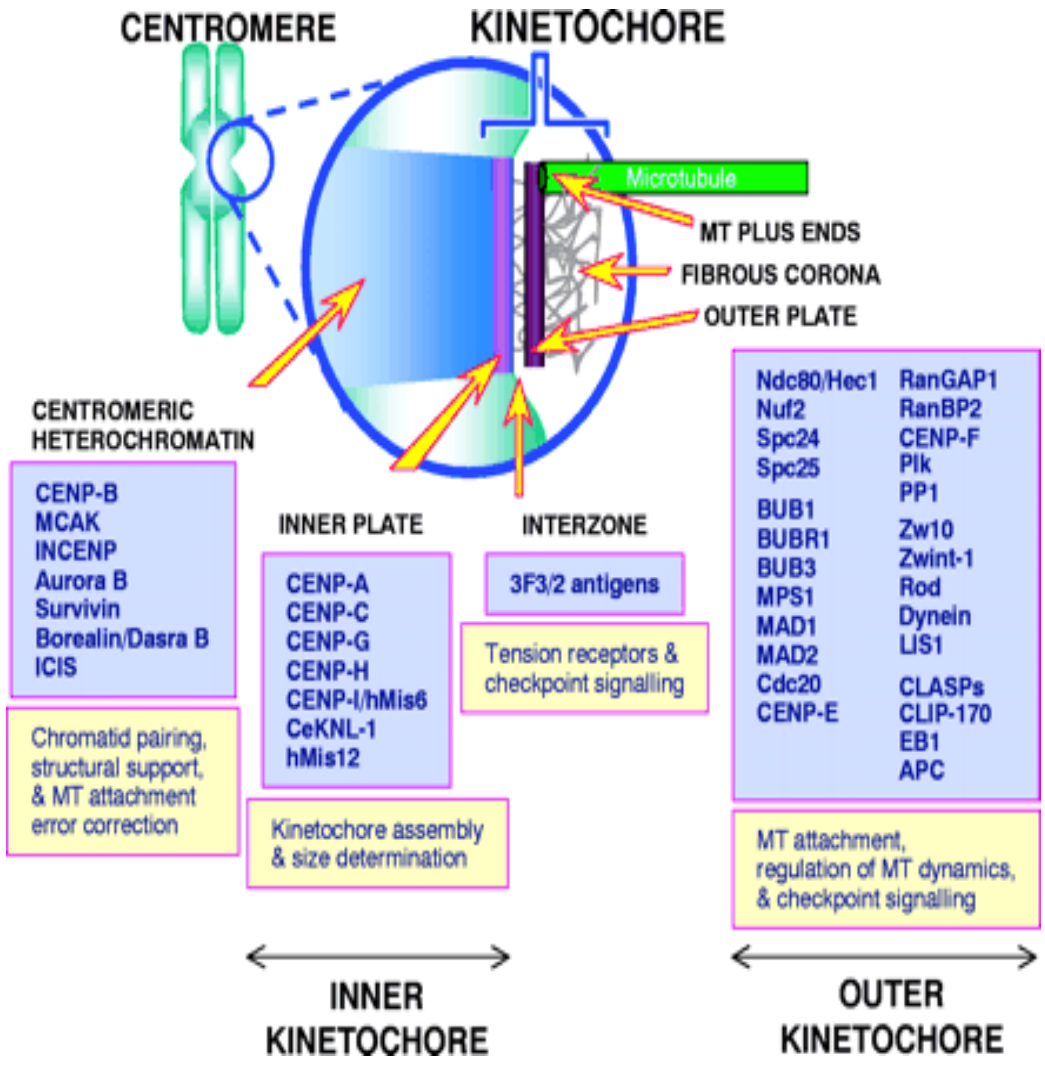


**Figure 1.4: Organisation of the centromere-kinetochore region showing the location of some of its protein constituents**. The kinetochore is composed of several distinct layers. Innermost is an inner plate, a chromatin structure containing nucleosomes with at least one specialised histone, auxiliary proteins and DNA. Outside this is an outer plate composed primarily, if not solely, of proteins (Cooke *et al.*, 1993). Adapted from (Maiato *et al.*, 2004).

The centromere and inner kinetochore regions (Figure 1.4) are made of proteins involved in mediating the binding of the kinetochore to DNA, and in kinetochore assembly (Maiato *et al.*, 2004; Cheeseman and Desai, 2008). Amongst those proteins there the Chromosomal Passenger Complex (CPC) molecules. Molecules that are thought to play a role in sensing tension across the kinetochore as a result of microtubule pulling forces (3F3/2 antigen) reside in the middle kinetochore. The most external layer of the kinetochore and the fibrous corona contain numerous proteins ascribed as part of the spindle checkpoint system (Bub1, Bub3, BubR1, Cdc20 and Mad2), involved in microtubule attachment (CenpE and F, Ndc80/Hec1 and microtubule associated proteins EB1 and CLASPs), or crucial for chromosome movements along microtubules (motor proteins CenpE and dynein).

Kinetochore proteins are differently regulated during mitosis. Some components, such as the microtubule motor proteins CenpE, dyneins and spindle checkpoint proteins (Mad1, Mad2, BubR1 and Cdc20), differ in concentration at the kinetochore depending on the presence of microtubule attachments. In fact during early mitosis, they are higly present at the kinetochores, but their concentrations are reduced by interactions with spindle microtubules in late prometaphase and metaphase (King *et al.*, 2000; Hoffman *et al.*, 2001; Shah *et al.*, 2004; Howell *et al.*, 2004). Kinetochore components' response is further regulated by the turnover of the proteins. In fact, some proteins, such as Cdc20 and Mad2 (Kallio *et al.*, 2002a; Shah *et al.*, 2004; Howell *et al.*, 2004), are frequently synthetised and degraded so that new molecules can bind to the kinetochore.

## 1.1.4 The spindle checkpoint system

### *1.1.4.1 The function of the spindle checkpoint*

The spindle checkpoint monitors the presence of errors in the attachment of the microtubules to chromosomes during mitosis, in order to guarantee that the correct number of chromosomes is inherited by daughter cells (Figure 1.2). It delays cell cycle progression from metaphase to anaphase until all chromosomes have aligned in a bipolar fashion at the metaphase plate [Figure 1.5; reviewed in (Musacchio and Salmon, 2007)].

The activation of the spindle checkpoint occurs in early mitosis when few kinetochores exhibit correct attachment to the microtubules and this activation persists until the establishment of proper bipolar attachments. The presence of one single improperly attached chromosome could inhibit mitotic progression (Rieder *et al.*, 1995). Incorrecly attached kinetochores release inhibitory signals in the cytoplasm therefore preventing all chromosomes from initiating anaphase (Rieder *et al.*, 1994; Rieder *et al.*, 1995).

The spindle checkpoint releases cell cycle inhibitory signals in response to lack of attachment between the kinetochore and the microtubules (Rieder *et al.*, 1994; Rieder *et al.*, 1995). Another aspect of kinetochore microtubule interaction that determines the activation of the spindle checkpoint is the lack of tension (Figure 1.2; synthelic attachment) (Nicklas *et al.*, 1995; Li and Nicklas, 1995). Tension is the result of opposite directional forces generated by kinetochore microtubules attached to chromosomes aligned at the metaphase plate. At this point the spindle checkpoint is switched off. The generation of tension was reported to increase the number of kinetochore microtubule attachments (Nicklas and Ward, 1994; King and Nicklas, 2000). It was suggested that in the absence of tension a small number of unattached kinetochores is generated, so that the spindle checkpoint is maintained active (Pinsky *et al.*, 2006).

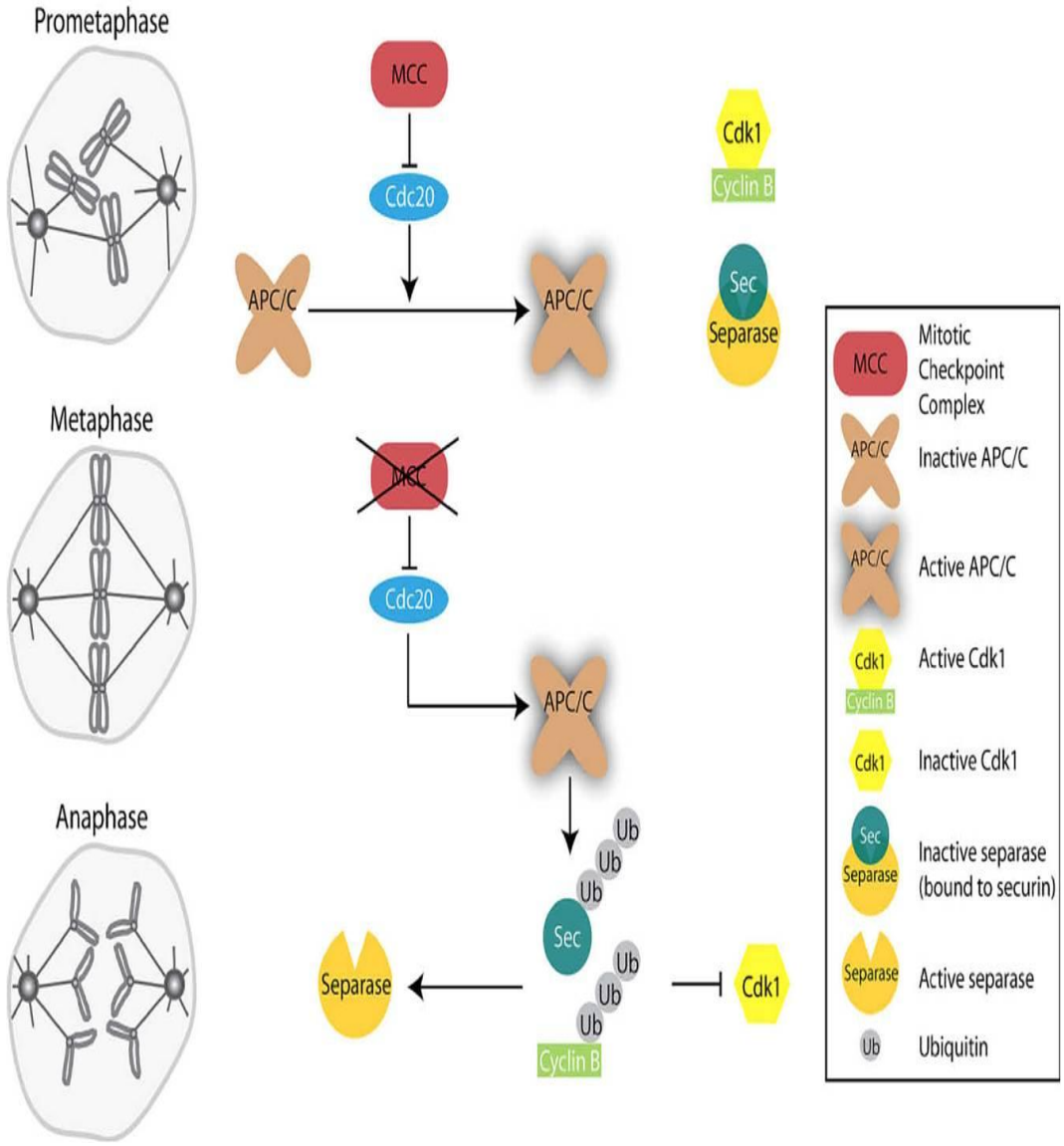


**Figure 1.5: The spindle checkpoint and the cell cycle machinery**. In prometaphase, the lack of microtubule attachment or tension at the level of the kinetochore contributes to the creation of the mitotic checkpoint complex (MCC). The MCC prevents Cdc20 mediated activation of the APC/C. Separase is kept inactive by securin. In metaphase, kinetochores are attached and under tension and no longer originate MCC. Cdc20 can therefore activate the APC/C allowing ubiquitination of securing and cyclin B. Separase is activated and can cleave sister chromatids to promote anaphase onset. Modified from (Musacchio and Salmon, 2007).

#### *1.1.4.2 The inhibitory complexes*

The lack of attachment or tension that activates the spindle checkpoint generates inhibitory signals consisting of various proteins. Bubs and Mads genes (Li and Murray, 1991; Hoyt *et al.*, 1991) were identifired as part of of the inhibitory complexes that prevent Cdc20 (cell division cycle 20) mediated activation of the anaphase promoting complex/cyclosome (APC/c) (Figure 1.5) (Kallio *et al.*, 1998; Sudakin *et al.*, 2001). Free Cdc20 activates APC/c, which subsequently triggers entry into anaphase by polyubiquitination of mitotic substrates, such as cyclin B and securin, which leads to their degradation (Peters *et al.*, 2006).

BubR1 (Bub1 related protein 1), Mad2, Bub3 and Cdc20 proteins form mitotic checkpoint complex, or MCC (Kallio *et al.*, 1998; Sudakin *et al.*, 2001) and diffuse from the incorrectly attached kinetochores throughout the cell to inhibit the APC/c. When kinetochore microtubules are not attached properly, MCC proteins accumulate at kinetochores. Lack of tension triggers BubR1 accumulation to kinetochores, whereas Mad2 levels respond to in the lack of attachment (Skoufias *et al.*, 2001; Logarinho *et al.*, 2004).

Other proteins are thought to contribute to the formation of inhibitory signals at the kinetochores. CenpE, a plus end kinetochore microtubule protein (Abrieu *et al.*, 2000) regulates BubR1 kinase activity and is involved in Mad1 and Mad2 recruitment to the kinetochores (Chan *et al.*, 1998; Mao *et al.*, 2003; Mao *et al.*, 2005). CenpE activity is, in turn, controlled by Bub1 and Mps1 (monopolar spindle 1) kinases, as they are essential for the checkpoint because they are involved in retaining CenpE at kinetochores (Sharp-Baker and Chen, 2001; Abrieu *et al.*, 2001; Mao *et al.*, 2003). Moreover, Bub1 kinase contributes to the MCC-APC/c interaction and Cdc20 phosphorylation (Tang *et al.*, 2004; Morrow *et al.*, 2005). Finally, Aurora B promotes the creation of detached kinetochores that activate the spindle checkpoint (see section 1.1.5.2) (Pinsky *et al.*, 2006) and cooperate with CenpE, BubR1 and Mad2 at the kinetochores (Ditchfield *et al.*, 2003).

#### *1.1.4.3 Inactivation of the spindle checkpoint and entry into anaphase*

When correct attachments and tension are established, Cdc20 is relieved from inhibition and binds to the APC/c (Figure 1.5). The APC/c ubiquitinates securin which becomes degraded, thus eliminating the inhibition of separase, a cysteine protease responsible for the separation of sister chromatids through the hydrolysis of cohesin. Following APC/c activation, also cyclin B becomes degraded, which leads to CDK1 inactivation and exit from mitosis. Consequently, the initiation of anaphase is promoted only by the concomitant cleavage of cohesin and inhibition of CDK1.

However, it is not clear what individual events trigger the inactivation of the spindle checkpoint and the MCC production, as multiple events contribute to switching off the spindle checkpoint signaling pathway. Proper microtubule attachment, modulation of BubR1 kinase activity (Putkey *et al.*, 2002; Mao *et al.*, 2003), Dynein mediated silencing of the spindle checkpoint (Howell *et al.*, 2001), and degradation of Cdc20 (Reddy *et al.*, 2007), are all events required for stopping the inhibitory signal production.

## 1.1.5 Aurora B and the Chromosomal Passenger Complex

### *1.1.5.1 CPC components and localisation*

Aurora B kinase is part of the CPC with Incenp, Survivin and Borealin (Figure 1.6A). The localisation of the complex is subject to cell cycle phases (Figure 1.6B). In early mitosis it localises to the chromosome arms, then it is detected at the inner centromeres until metaphase-to-anaphase transition. CPC proteins then relocate to the spindle midzone and to the cell cortex (Cooke *et al.*, 1987). Aurora B and Incenp were first shown to be part of the CPC complex when co-immunoprecipitated from different model systems and the study of the phenotypes derived from their knockdown showed similar defects, such as failure of chromosome segregation and inhibition of cytokinesis (Kim *et al.*, 1999; Kaitna *et al.*, 2000; Adams *et al.*, 2000). Later on Survivin and Borealin were ascribed as components of the same complex (Bolton *et al.*, 2002; Gassmann *et al.*, 2004).

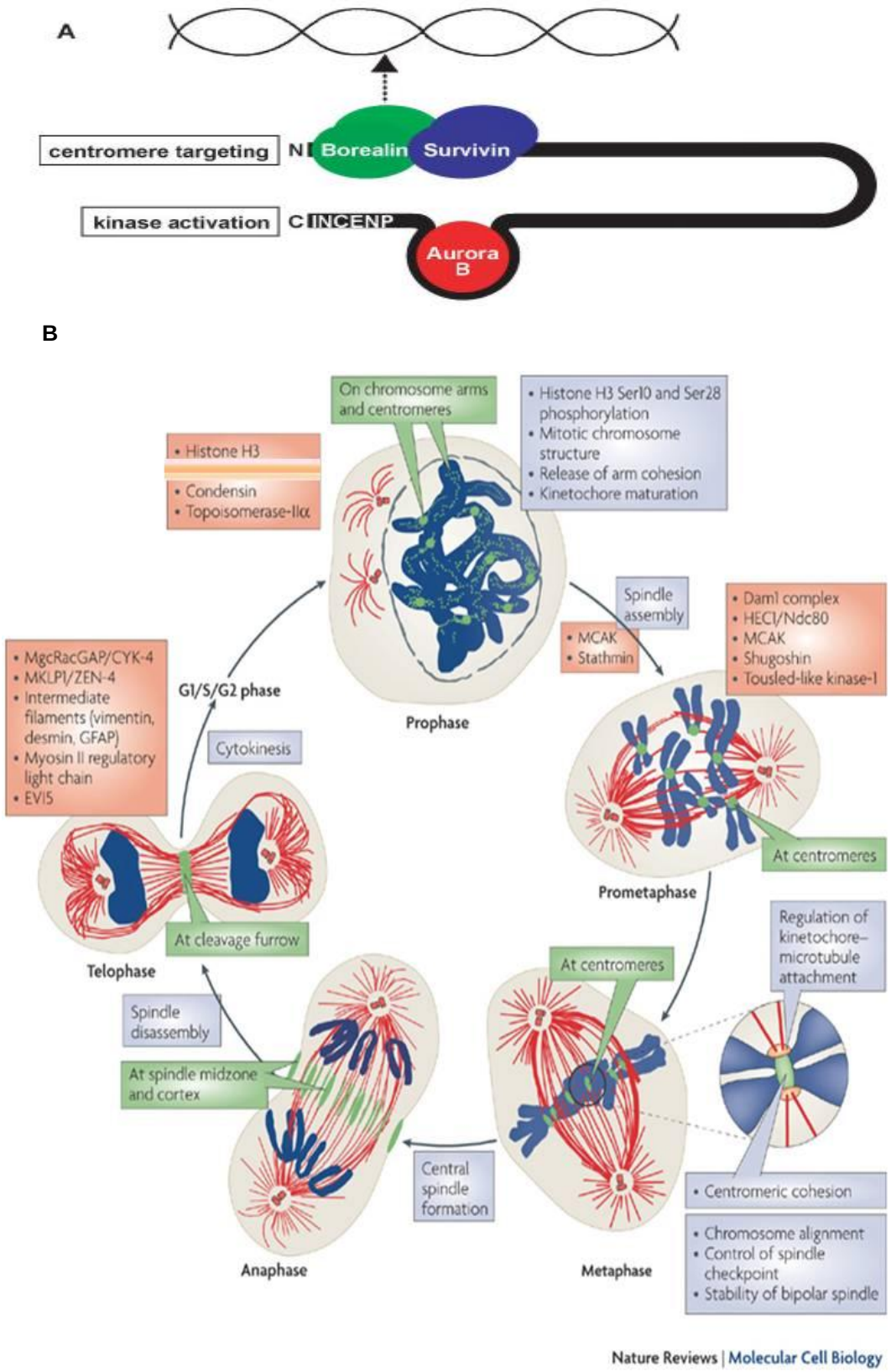


**Figure 1.6: The chromosomal passenger complex (CPC).** Schematic structure of the CPC (A) and mitotic functions (B). In B) the localisation (green boxes) is correlated with the relevant functions (blue boxes) and principal targets (red boxes) during the different phases of mitosis relative to tubulin and chromosome dynamics. Adapted from (Klein *et al.*, 2006) and (Ruchaud *et al.*, 2007).

Three proteins are considered members of the Aurora kinase family: Aurora A, B and C that are Ser/Thr kinases involved in diverse functions during mitosis. Aurora A controls bipolar spindle assembly and the maturation of the centrosomes, where it resides (Glover *et al.*, 1995; Kimura *et al.*, 1997). Moreover, It promotes entry into mitosis by activating PLK1 and CDK1 (Seki *et al.*, 2008; Macurek *et al.*, 2008). Aurora C expression appears to be testis specific and in fact regulates spermatogenesis along with Aurora B (Kimmins *et al.*, 2007). Aurora C could interact with other CPC proteins (Sasai *et al.*, 2004; Li *et al.*, 2004b; Yan *et al.*, 2005), but its role during somatic cell mitosis needs more investigations.

Aurora B kinase is the principal component of the CPC. Incenp is required for Aurora B activation and the recruitment of the other CPC members. The N-terminus of Incenp, which determines the centromere and midzone targeting, interacts with Survivin and Borealin, whereas the region adjacient to the C-terminus of Incenp binds to Aurora B (Figure 1.6A) (Ainsztein *et al.*, 1998; Bolton *et al.*, 2002; Klein *et al.*, 2006). The interaction between Aurora B and Incenp is crucial for the complete activation of the kinase (Bishop and Schumacher, 2002; Sessa *et al.*, 2005).

The site of action and role of the CPC members is determined by their interaction. In fact RNA knockdown experiments or dominant negative mutations showed tha the depletion of one of these proteins compromises the localisation and function of other CPC molecules (Kaitna *et al.*, 2000; Wheatley *et al.*, 2001; Adams *et al.*, 2001; Honda *et al.*, 2003).

### *1.1.5.2 CPC functions*

The localisation of the CPC during the different mitotic phases is in line with the functions of the complex (Figure 1.6B). At the beginning of mitosis, the CPC is involved in chromosome condensation, spindle assembly, correction of improper kinetochore microtubule interactions and control of spindle checkpoint activity. In late mitosis the CPC monitors the completion of cytokinesis.

#### *Chromosome condensation and cohesion*

Following entry into mitosis, chromosomes acquires the necessary rigidity for chromosome segregation in anaphase. Aurora B promotes the recruitment of condensin via its phosphorylation, therefore facilitating chromosome condensation (Giet and Glover, 2001; Lipp *et al.*, 2007). Aurora B provides further contribution to chromosome condensation through the phosphorylation of histone H3 (Wei *et al.*, 1998; Hsu *et al.*, 2000; Giet and Glover, 2001; Adams *et al.*, 2001).

Aurora B plays a crucial role in controlling cohesion between duplicated sister chromatids. As illustrated above, cohesin is lost in two distinct phases during mitosis of vertebrate cells (Waizenegger *et al.*, 2000). Aurora B determines the removal of cohesin from chromosomes arms (Sumara *et al.*, 2002; Losada *et al.*, 2002; Gimenez-Abian *et al.*, 2004) at the onset of mitosis, but it restricts cohesin to centromeres during later phases of mitosis (McGuinness *et al.*, 2005; Resnick *et al.*, 2006).

#### *The error correction system and the regulation of CPC activity*

Aurora B plays a vital role in the re-organisation of incorrect microtubule-kinetochore attachments (Tanaka *et al.*, 2002; Lampson *et al.*, 2004). This is achieved via the destabilisation of improper attachments via inhibitory phosphorylations that regulate the activity of MCAK (Mitotic centromere-associated kinesin) (Sampath *et al.*, 2004; Lan *et al.*, 2004; Andrews *et al.*, 2004).

Aurora B has been also involved in the regulation of Ndc80/Hec1, which contributes to the formation of stable kinetochore microtubule attachments at the outer kinetochore (McCleland *et al.*, 2003; McCleland *et al.*, 2004; DeLuca *et al.*, 2005). In fact, the interaction of Ndc80/Hec1 with microtubules may be affected by the phosphorylation of Ndc80/Hec1 by Aurora B, therefore leading to microtubule release (DeLuca *et al.*, 2006; Cheeseman *et al.*, 2006; Emanuele *et al.*, 2007).

Aurora B plays an important role in correcting merotelic attachments. In these erroneous attachments, one of the two sister kinetochores of a chromosome is attached to both spindle poles (Figure 1.2), causing the kinetochore to be under tension by microtubule pulling forces. If merotelic attachments were not detected by the spindle checkpoint, anaphase could initiate leading to the formation of lagging chromatids. For this reason merotely has been linked to aneuploidy (Cimini *et al.*, 2001). The importance of Aurora B in correcting these erroneous connections was highlighted by the higher rate of merotelic attachments observed in cells where Aurora B activity had been partially inhibited (Cimini *et al.*, 2006). It seems that Aurora B activity is mediated by MCAK, which in turn destabilises inappropriately attached kinetochore microtubules (Knowlton *et al.*, 2006).

The activity of Aurora B is determined by activating and inhibitory proteins (Rosasco-Nitcher *et al.*, 2008). Rosasco-Nitcher and colleagues have proposed that Aurora B is first recruited to centromeres as a result of the phosphorylation mediated by other kinases such as PLK1 (Rosasco-Nitcher *et al.*, 2008). At the centromeres, activating proteins, such as TD-60 (telophase disk 60) and the interaction with the microtubules promote an increase of Aurora activity and autophosphorylation. Aurora B activity is suppressed by interactions with substrates that lack priming phosphorylations. In particular, the model explains why the allosteric changes induced by the physical interaction with the microtubules are necessary for Aurora B activation. The centromeres of unaligned chromosomes frequently make contact with microtubules, and such interaction persists for centromeres of merotelically attached

chromosomes even when they are aligned at the metaphase plate. However, once chromosomes are correctly aligned at the metaphase plate, centromeres detach from the microtubules and Aurora B cannot reach its targets. As a result, the activity of Aurora B would be higher at the centromeres of unaligned and merotelically attached chromosomes, whereas it would be reduced at the centromeres of metaphase chromosomes.

***Spindle checkpoint activity***

Aurora B cooperates with the spindle checkpoint by destabilising incorrect attachments (Pinsky *et al.*, 2006). It has also been suggested a more active role of Aurora B in the spindle checkpoint system. In fact, it is role is crucial for maintaining the mitotic arrest induced by drugs that promote microtubule disassembly (loss of attachment) or hyperstabilisation (loss of tension) and therefore trigger the spindle checkpoint activation (Kallio *et al.*, 2002b; Hauf *et al.*, 2003; Ditchfield *et al.*, 2003). It is likely that Aurora B functions in the tension sensitive branch of the spindle checkpoint given that its chemical inhibition leads to more rapid escape from mitotic arrest induced by taxol (loss of tension) compared to nocodazole block (loss of attachment) (Hauf *et al.*, 2003). Aurora B role has also been linked to the recruitment of checkpoint proteins such as Mad2 and BubR1 to kinetochores (Ditchfield *et al.*, 2003). Besides, Aurora B would modulate BubR1 activity via phosphorylation upon entry into mitosis (Ditchfield *et al.*, 2003) and would therefore regulate the activity of the spindle checkpoint.

***Cytokinesis***

Aurora B and other CPC members have been shown to control chromosome segregation and cytokinesis (Terada *et al.*, 1998; Kaitna *et al.*, 2000; Giet and Glover, 2001; Adams *et al.*, 2001): Aurora B controls contractile ring formation, an element that determines the site of the cytokinetic furrow development, as well as the function of the cytokinetic furrow in numerous ways. It phosphorylates Mklp1 and MgcRacGAP/CYK-4 that are components of the centralspindlin complex, which contributes to the formation of the spindle midzone (Mishima *et al.*, 2002; Minoshima *et al.*, 2003; Guse *et al.*, 2005). Aurora B phosphorylation targets during

cytokinesis comprise components of the cleavage furrow, such as vimentin, myosin II regulatory light chain and desmin (Murata-Hori *et al.*, 2000; Kawajiri *et al.*, 2003; Goto *et al.*, 2003).

## 1.2 Introduction to the RASSF proteins

### 1.2.1 The RAS-Association Domain Family

Ras proteins are small GTPases which alternate between their active, GTP-bound state and their inactive, GDP bound state. Ras proteins mediate their downstream effects through binding to a variety of proteins, termed Ras effectors. Ras effectors bind via their Ras binding domain specifically to GTP-bound Ras proteins (van der Weyden and Adams, 2007). A number of different Ras binding domains exist, including the RalGDS/AF6 Ras association (RA) motif which is supposed to form a three dimensional structure called an ubiquitin fold (Herrmann, 2003) and it is common to over 50 human proteins. One family of proteins which all contain a RA domain are the RAS-association domain family (RASSF).

### 1.2.2 The domain architecture of the Classical and N-terminal RASSF proteins

#### *1.2.2.1 Classical RASSFs*

The RASSF proteins have only been identified in the last 10 years. RASSF1 was first described in 2000 as 3 variants with high homology of their C terminus to the mouse gene, NORE1, which was a known Ras effector (Dammann *et al.*, 2000). A human orthologue of NORE1 was later identified and termed RASSF5 due to its high homology with RASSF1. To date RASSF1 and RASSF5 are the best studied RASSF proteins and so far 10 RASSF members have been found in the human genome.

RASSF1 to 6 are characterised by their RA domain at their carboxy (C)-terminal of the protein, and together these 6 proteins form the Classical RASSF family. A protein-protein interaction domain, the SARAH domain, was identified adjacent to the C terminal RA domain in RASSF1 to 6, as shown in Figure 1.7A . This domain is named after the 3 types of proteins that contain it Salvador (WW45 in vertebrates), RASSF and Hippo (MST1/2 in vertebrates) (Scheel and Hofmann, 2003). SARAH domains

have two α-helices which form a novel antiparallel helix conformation (Hwang *et al.*, 2007). This fold allows dimerisation between SARAH domains so that Salvador, RASSF and Hippo can form homo and heterodimers. RASSF 1 and 5 also contain a diacylglycerol/phorbol ester binding (DAG) domain, known as protein kinase C conserved region (C1).

RASSF proteins have no catalytic domain, but their RA domain allows them to bind to Ras proteins. Therefore they have the potential to function as adaptors which are recruited to activated Ras-GTPases to modulate GTPase activity or to mediate downstream actions of GTPases (Avruch *et al.*, 2009). Several studies have investigated the ability of RASSF proteins to bind to different Ras family proteins. RASSF1 to 5 have been shown to bind Ras or Ras-like GTPases either directly or indirectly. For example, RASSF1A alone binds weakly to Ras, but when it dimerises with RASSF5, it is able to associate with Ras-like GTPases (Ortiz-Vega *et al.*, 2002). Mixed reports exist on the ability of RASSF6 to bind to Ras and so this requires further investigation (Richter *et al.*, 2009).

#### *1.2.2.2 N-terminal RASSFs*

More recently the N-terminal members of the family have been identified. RASSF7 to 10 do not contain the SARAH domain and their RA domain is located at their extreme amino terminus (Figure1.7A) (Sherwood *et al.*, 2008). N-terminal RASSFs contain coiled coil domains, and it is speculated that these are involved in protein-protein interactions to mediate downstream signaling, as SARAH domains may do in classical RASSFs. The presence of an RA domain is the defining feature of classical and N-terminal RASSF proteins. However, the RA domains of the two groups have quite different sequences. In fact, the RA domains of RASSF7-10 form a phylogenetically distinct group from the RA domains of the classical RASSF proteins (Figure 1.7B). The separation between groups is not a recent event, *Drosophila melanogaster* and *Caenorhabditis elegans* have both classical (dmRASSF (Polesello *et al.*, 2006) and *T24F1.3* respectively (Khokhlatchev *et al.*, 2002)) and N-terminal RASSF homologues [Table 1.1 and (Sherwood *et al.*, 2008)].

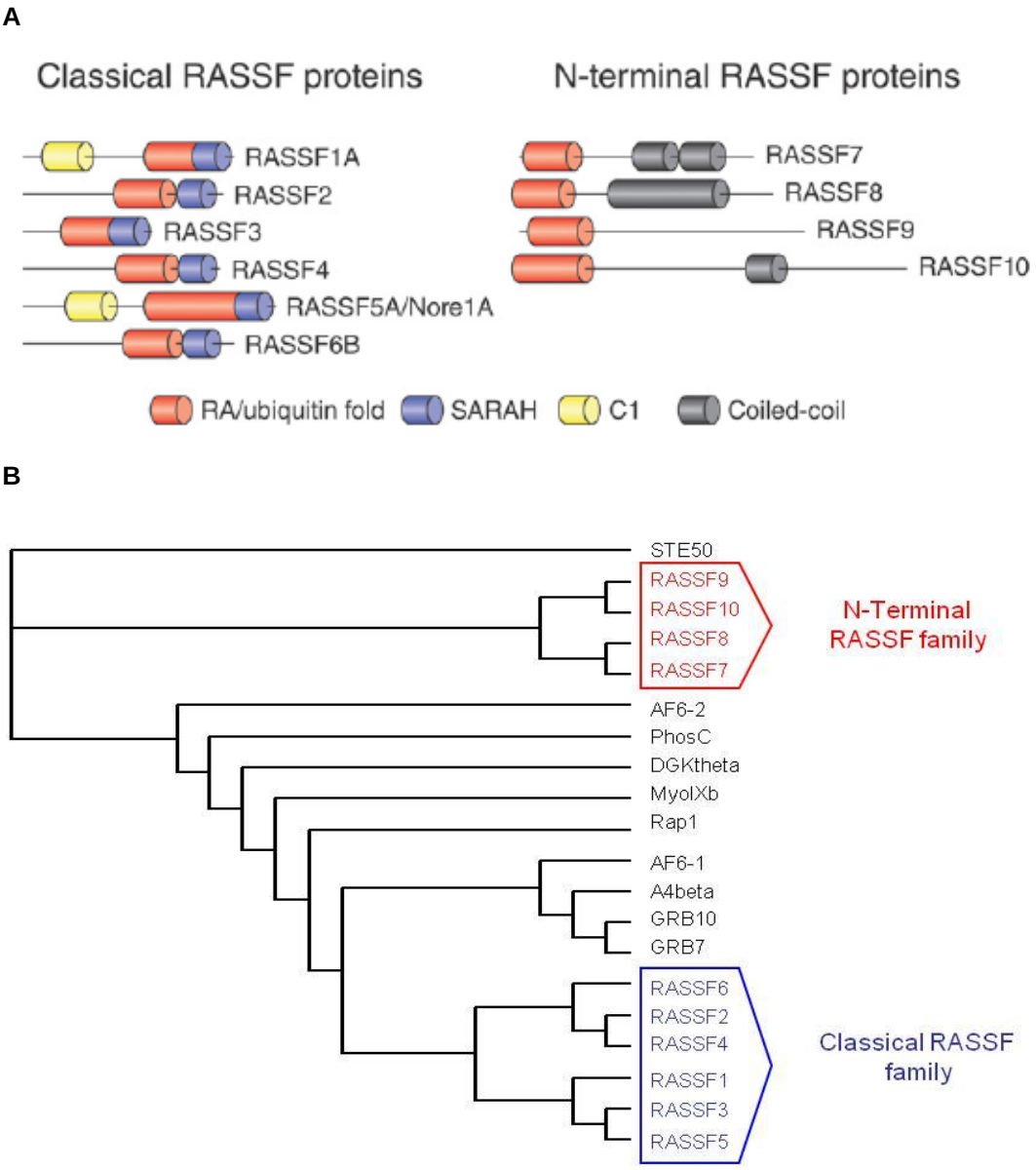


**Figure 1.7: Differences between Classical and N-terminal RASSF proteins**. The 4 members of the newly identified N-terminal RA domain family are both structurally (A) and phylogenetically (B) distinct from the 6 Classical RASSFs. Adapted from (Sherwood *et al.*, 2010).

RASSF7, 8 and 10 are all located close to members of the Ras family in the genome (Weitzel *et al.*, 1992; Falvella *et al.*, 2006; Sherwood *et al.*, 2008). This suggests that the N-terminal RASSF proteins may have co-evolved with members of the Ras family. No similar association has been found between the classical RASSF proteins and members of the Ras family, so this unusual juxtaposition of a Ras gene and a potential Ras

effector represents another distinction between the two groups (Sherwood *et al.*, 2010).

| N-terminal RASSF member | Chromosome | Alternative names | Potential *Drosophila* orthologue | Potential *C. elegans* orthologue |
|---|---|---|---|---|
| RASSF7 | 11p15.5 | HRAS1 cluster1 (HRC1), C11orf13 | CG5053 | K05B2.2 |
| RASSF8 | 12p12.3 | Human carcinoma associated HoJ-1(HoJ-1), C12orf2 | | |
| RASSF9 | 12q21.31 | peptidylglycine alpha-amidating monooxygenase (PAM) C-terminal interactor 1 (P-CIP1), PAMC1 | CG13875 | |
| RASSF10 | 11p15.2 | similar to peptidylglycine alpha-amidating monooxygenase C-terminal interactor 1 | CG32150 | |

**Table 1.1: The N-terminal RASSF family.** The table summarises the nomenclature used for the N-terminal RASSF proteins and their genomic positions. Adapted from (Sherwood *et al.*, 2010).

### *1.2.2.3 RASSF7*

*RASSF7* was first identified by Weitzel and colleagues in a cluster of three genes closely located to *HRas* in the genome and called *HRC-1* (H-Ras1 cluster 1) (Weitzel *et al.*, 1992). *HRC-1* was recently renamed *RASSF7*, presumably because the protein it encodes contains an RA domain/ubiquitin fold and was not part of a recognised family. Through alternative promoter usage and splicing of the exons, three different transcripts have been predicted by Vega- The Vertebrate Gene Annotation database (http://vega.sanger.ac.uk) (Figure 1.8).

Given the close proximity to *HRas* in the genome, Weitzel and colleagues originally suggested that *RASSF7/HRC-1* might be a growth regulator (Weitzel *et al.*, 1992). They also suggested, based on Southern blotting,

that RASSF7/HRC-1 might be part of a large family of related proteins. Only recently the authors predictions about RASSF7 have begun to be confirmed.

Interestingly, *RASSF7* maps also near *HRAS1* minisatellite which is immediately downstream of *HRas*. Rare alleles of this minisatellite were shown to be associated with cancer risk (Krontiris *et al.*, 1985; Krontiris *et al.*, 1993) and it was proposed that altered expression of *RASSF7* might contribute to the increased risk (Weitzel *et al.*, 2000). This generated a great deal of interest in the region, however subsequent studies using improved technology failed to find a link (Firgaira *et al.*, 1999; Tamimi *et al.*, 2003) and the idea that rare alleles of the minisatellite are associated with cancer risk is no longer the consensus.

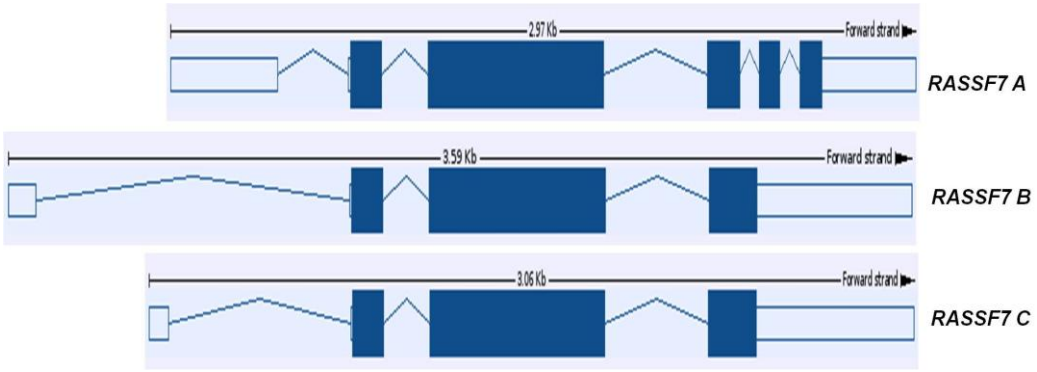


**Figure 1.8: Human RASSF7 transcripts.** Schematic diagram representing the transcripts produced from the *RASSF7* locus due to use of different C-terminal exons. *RASSF7A* (Vega: RASSF7-003, OTTHUMT00000254972) is a 1,928 bp transcript that initiates transcription from the ATG present in exon 2 and utilises different C-terminal exons from the other *RASSF7* transcripts. Its translated product is a 373 amino acid protein. *RASSF7B* (Vega: RASSF7-002, OTTHUMT00000254971) differs from *RASSF7A* for the last exon, and generates a 1,745 bp transcript that translates a 337 amino acid protein. *RASSF7C* (Vega: RASSF7-001, OTTHUMT00000254970) has the same number of exons of *RASSF7B.* Its transcript is 1,731 bp long and translates a 337 amino acid protein. Recently the number of RASSF7 spliced variants predicted by Vega- The Vertebrate Gene Annotation database- has raised to 7. Boxes are exons and lines connecting boxes are introns. Filled boxes are coding sequence, whereas empty, unfilled boxes are UTRs(untranslated regions). Each of these proteins contains an N-terminal RA domain. Modified from (van der Weyden and Adams, 2007).

## 1.2.3 The function of the RASSF proteins

### *1.2.3.1 The tumour suppressor activity of the classical RASSFs*

Several RASSF family proteins are tumour suppressors that are frequently down-regulated during the development of human cancer. However there are differences in the biological activity of the members (Table 1.2).

In mammals, epigenetic inactivation of RASSFF1A is frequently reported in different tumour entities (Dammann *et al.*, 2005; Agathanggelou *et al.*, 2005), suggesting RASSF1A functions as a tumour suppressor. In agreement with this, the constitutive over-expression of *RASSF1A* in different tumour cell lines (non small cell lung cancer (NSCLC), prostate, kidney, nasopharyngeal carcinoma and glioma cell lines) resulted in cells exhibiting less viability, suppressed growth, diminished invasiveness, and reduced anchorage independence (Dammann *et al.*, 2000; Dreijerink *et al.*, 2001; Burbee *et al.*, 2001; Kuzmin *et al.*, 2002; Hesson *et al.*, 2004; Chow *et al.*, 2004). In addition, forced expression of *RASSF1A* in lung, kidney, nasopharyngeal and prostate cancer cell lines caused a substantial attenuation of tumourigenicity both in *vivo* and in *vitro* (Dammann *et al.*, 2000; Dreijerink *et al.*, 2001; Burbee *et al.*, 2001; Kuzmin *et al.*, 2002; Ji *et al.*, 2002; Li *et al.*, 2004a; Chow *et al.*, 2004). The characterisation of *Rassf1a* knockout mice (van der Weyden *et al.*, 2005; Tommasi *et al.*, 2005) corroborated the analysis done in human tumour cell types. Rassf1a null mice exhibited increased tumourigenesis, reduced survival rate and higher physical/ chemical mutagen induced tumour susceptibility compared with controls (van der Weyden *et al.*, 2005; Tommasi *et al.*, 2005). Thus RASSF1A is a tumour suppressor that is frequently impaired in human tumours.

Fragmented and contrasting information is available for another RASSF1 isoform, RASSF1C. *RASSF1C* did not show hypermethylation of its promoter region and was expressed in almost all tumour cell lines tested (Dammann *et al.*, 2000; Burbee *et al.*, 2001). *RASSF1C* ectopic expression did not show any relevant effect on growth, anchorage independent colony forming activity and growth inhibitory activity of

various lung carcinoma cell lines (Burbee *et al.*, 2001; Ji *et al.*, 2002; Li *et al.*, 2004a). However, *RASSF1C* expression was almost undetectable in the KRC/Y renal cell carcinoma cell line (Dreijerink *et al.*, 2001) and *RASSF1C* was reported to exert growth inhibitory effects in the prostate cell line LNCaP, the renal cell carcinoma line KRC/Y (Li *et al.*, 2004a), and embryonic kidney 293T cells upon the presence of activated RasG12V (Vos *et al.*, 2000). In contrast, over-expressed *RASSF1C* was seen to activate osteoblast (Amaar *et al.*, 2005) and MDA-MB231 and T47D breast cancer cell proliferation (Reeves *et al.*, 2010). In accordance with these data, reduced *RASSF1C* expression levels led to decreased lung cancer (Amaar *et al.*, 2006) and breast cancer (Reeves *et al.*, 2010) cell proliferation. Therefore RASSF1C could exert any tumourigenic activity in a tumour type specific fashion, which raises questions over the role of RASSF1C in tumour suppression.

Recently, an explanation for the different mechanism of action of RASSF1A and RASSF1C isoforms has been suggested by Estrabaud and colleagues (Estrabaud *et al.*, 2007). Indeed, the two variants were shown to control the degradation of β-catenin in different ways (Estrabaud *et al.*, 2007). β-catenin links E-cadherin to the actin cytoskeleton through interaction with α-catenin in adherens junctions. Abnormalities of cell adhesion molecules are known to play an important role in invasion and metastasis of cancer cells through loss of cell-to-cell adhesion. β-catenin accumulation was reported to be promoted by over-expression of *RASSF1C* (Estrabaud *et al.*, 2007) or inactivation of *RASSF1A* (Estrabaud *et al.*, 2007; van der Weyden *et al.*, 2008), which suggests that the inhibition of β-catenin accumulation could be one of the mechanisms by which RASSF1A exerts its tumour suppressor function. RASSF1C expression in the absence of RASSF1A could promote tumourigenesis (Estrabaud *et al.*, 2007).

RASSF2 protein was shown to be frequently down-regulated in human lung cancer cell lines (Vos *et al.*, 2003a) and *RASSF2* promoter methylation was observed to occur at a higher incidence rate in primary

colorectal cancer cell lines compared to other *RASSF* genes (Akino *et al.*, 2005). Over-expression of RASSF2 in A549 human lung cancer cells and RKO colorectal cancer cells caused an inhibition of cell growth (Vos *et al.*, 2003a; Akino *et al.*, 2005). In 293-T cells, this RASSF2 mediated growth inhibition was significantly enhanced by the presence of activated K-RAS, which binds directly to RASSF2 (Vos *et al.*, 2003a). RASSF2 down-regulation via siRNA was shown to increase the ability of K-*Ras* to transform rat kidney cells (Akino *et al.*, 2005), suggesting that the inactivation of negative regulators of K-*ras,* such as RASSF2, could result in a growth advantage during tumour cell transformation (Akino *et al.*, 2005; Park *et al.*, 2007; Nosho *et al.*, 2007).

RASSF3 promoter methylation has not been extensively studied and no systematic functional characterisation of RASSF3 has been performed to-date.

*RASSF4* expression is down-regulated in some human tumour cell lines and primary tumours and this correlated well with methylation of the promoter (Eckfeld *et al.*, 2004). RASSF4 was reported to inhibit cell colony formation when over-expressed in MCF-7 cells and A549 lung cancer cells (Eckfeld *et al.*, 2004) and this effect could be enhanced by the presence of activated K-Ras, to which RASSF4 binds directly in a GTP dependent manner via the RA domain (Eckfeld *et al.*, 2004).

*NORE1 (RASSF5)* transcripts were shown to be expressed at very low levels in several cancer cell lines compared to normal tissues (Tommasi *et al.*, 2002; Vos *et al.*, 2003b), although promoter silencing by methylation was reported to be the likely mechanism behind the down-regulation of *NORE1* expression only in some studies (Vos *et al.*, 2003b; Hesson *et al.*, 2003). NORE1 is known to induce growth suppression. The expression of *NORE1A* or *NORE1B* inhibited cell growth in some NORE1 deficient cancer cell lines (namely A549 and G361) (Vos *et al.*, 2003b; Aoyama *et al.*, 2004), but not in others (NCI-H4460 and M14) (Aoyama *et al.*, 2004) despite the RAS signaling being disrupted in all of them primarily due to a RAS activating mutation. Stable expression of NORE1A also impairs the

anchorage independent growth of A549 human lung cells and PC12 pheochromocytoma cells (Aoyama *et al.*, 2004; Li *et al.*, 2005). A possible explanation for the growth suppressive effects of NORE1A could be found in its cytoskeletal localisation and could occur through the ERK signaling pathway (Moshnikova *et al.*, 2006).

Similar to the other classical RASSFs, reduced levels of RASSF6 transcripts were found in numerous primary tumour tissues (Allen *et al.*, 2007), but this phenomenon seemed to be only partially linked to epigenetic mechanisms of silencing (Allen *et al.*, 2007). RASSF6 over-expression caused a decrease in cell survival but this phenomenon was specific for particular tumour cell types. RASSF6 inhibited the growth and cell survival of MCF-7 human breast tumour cells and A549 human lung cancer cells, but not of H1299 human lung tumour cell line (Allen *et al.*, 2007). Conversely, RASSF6 siRNA knockdown (KD) in the H1792 NSCLC cell line enhanced their ability to grow in soft agar, relative to control cells (Allen *et al.*, 2007).

In *Drosophila melanogaster*, a “tumour suppressor” effect of *dRassf* was first observed by Polesello and colleagues in 2006 as *dRASSF* appeared to antagonise Ras1 signaling in growth control and Salvador mediated Hippo activation in *vivo* (Polesello *et al.*, 2006). Recently, the same group has demonstrated the presence of a *dRassf-Hippo* containing complex, which associates with a *Drosophila* PP2A phosphatase complex, *dSTRIPAK* (Drosophila Striatin-interacting phosphatase and kinase), as a negative regulator of Hippo signaling (Ribeiro *et al.*, 2010).

| Classical RASSFs | Effect caused on cell viability/cell growth following protein up-regulation | Effect caused on cell viability/cell growth following protein down-regulation |
|---|---|---|
| RASSF1A | ↓ | ↑ |
| RASSF1C | Contrasting data | ↓ |
| RASSF2 | ↓ | ↑ |
| RASSF3 | Not known | Not known |
| RASSF4 | ↓ | Not known |
| RASSF5 | ↓ | ↑ |
| RASSF6 | ↓ | ↑ |

**Table 1.2**: **The tumour suppressor activity of the classical RASSFs**. Summary of effects caused by up or down- regulation of RASSF proteins on cell viability and cell growth. Arrows pointing upwards indicate enhanced cell ability to grow; arrows pointing downwards indicate reduction or inhibition of cell growth.

### *1.2.3.2 The classical RASSFs and their microtubule activity*

RASSF1A was seen to induce microtubule stabilisation and protect cells from the actions of microtubule depolymerising agents, such as nocodazole, when re-expressed in a RASSF1A negative cell line (Liu *et al.*, 2003; Vos *et al.*, 2004; Rong *et al.*, 2004; Dallol *et al.*, 2004). Such a microtubule stabilising property of RASSF1A was shown to critically depend on RAN-GTP, via the MST2 (mammalian Sterile20-like 2) induced phosphorylation of RCC1 (Regulator of chromosome condensation 1) (Dallol *et al.*, 2009a). The association of RASSF1A with the microtubules could well contribute to the tumour suppressor activity of this protein. In fact the interaction with C19ORF5, a microtubule-associated protein confirmed to interact with RASSF1 (Liu *et al.*, 2002a; Song *et al.*, 2004) was suggested to be required for the proper control of the APC/Cdc20 complex during mitosis (Song *et al.*, 2004), as explained in detail in the following section. Interestingly, RASSF1A was recently proposed by Verma and co-workers as a novel substrate of protein kinase C (PKC), which would play a key role in determining RASSF1A control of microtubule organisation via the RA domain phosphorylation sites (Verma *et al.*, 2008).

RASSF1C, the other RASSF1 isoform, was shown to hyperstabilise microtubules (Liu *et al.*, 2005). However, when its expression was co-

induced with C19ORF5, it did not associate with microtubules and did not hyperstabilise them (Liu *et al.*, 2005). Therefore RASSF1C seems to be less effective at stabilising microtubules compared to RASSF1A.

#### *1.2.3.3 The classical RASSFs and their modulation of the cell cycle*

RASSF1A was demonstrated to play a role at the G1-S checkpoint (Figure 1.9) and showed to modulate the levels of cyclin D1 in numerous human cell lines (Shivakumar *et al.*, 2002; Agathanggelou *et al.*, 2003). Cyclin D production may be induced by growth factors which stimulate the Ras-Raf-Erk signaling cascade. RASSF1 was found to cause inhibition of the epidermal growth factor (EGF) dependent activation of the Erk pathway. When co-expressed with plasma membrane calmodulin dependent calcium ATPase 4b (PMCA4b) in mammalian cells, RASSF1 was indeed able to impair proliferation (Armesilla *et al.*, 2004).

Other studies demonstrated that the RASSF1A induced G1 cell cycle arrest may occur via inhibition of the c-Jun-NH2-kinase (JNK) pathway (Whang *et al.*, 2005) (Figure 1.9). RASSF1A directly interacts with the kinase MST1 (Khokhlatchev *et al.*, 2002) which can modulate JNK activity (Ura *et al.*, 2007). RASSF1A could also affect the G1 transition via its direct interaction with the transcription factor $p120^{E4F}$ (Fenton *et al.*, 2004). RASSF1A enhances the ability of $p120^{E4F}$ to suppress cyclin A2 which in turn regulates CDK2 and thereby controls progression through S phase. In this way RASSF1A synergises with $p120^{E4F}$ to induce cell cycle arrest (Fenton *et al.*, 2004; Ahmed-Choudhury *et al.*, 2005).

In addition to a G1 arrest, RASSF1A can block the cell cycle at G2/M. Over-expression of *RASSF1A* caused G2/M arrest in MCF-7 breast cancer cell line (Rong *et al.*, 2004), in HeLa cells and 293T human embryonic kidney cells (Song *et al.*, 2004; Rong *et al.*, 2004). The RASSF1A mediated M phase arrest observed in 293T and HeLa cells was explained by Song and colleagues through the direct binding of RASSF1A with Cdc20 (Song *et al.*, 2004; Song *et al.*, 2005) (Figure 1.9), although it should be noted that this interaction is controversial (Liu *et al.*, 2007). This blocks the ability of Cdc20 to activate the ubiquitin ligase activity of the

APC, and consequently the degradation of the mitotic cyclins A and B, which is essential for the progression of mitosis (Song *et al.*, 2004). The negative effect exerted by RASSF1A on APC-Cdc20 activity during mitosis appeared to be independent of Mad2 and Emi1 (negative regulators of Cdc20 during mitotic progression) (Song and Lim, 2004; Song *et al.*, 2004) and to be regulated by C19ORF5. The depletion of this RASSF1A-binding protein prevented both the localisation of RASSF1A to the spindle poles and its binding to Cdc20, which resulted in premature destruction of mitotic cyclins and acceleration of mitotic progression (Song *et al.*, 2005). In addition C19ORF5 KD caused mitotic abnormalities and disrupted the MTOC (Dallol *et al.*, 2007). However, in contrast with these data, *Rassf1a* null mouse embryonic fibroblasts (*Rassf1a* $^{-/-}$ MEFs) showed delayed mitosis (Guo *et al.*, 2007). The protracted period of time observed for completing mitosis was also shown to be reverted to a normal period of time by the expression of either RASSF1A or components of the mammalian Hippo pathway (MST2, WW45 and LATS1) (Guo *et al.*, 2007).

The involvement of RASSF1A in mitosis is further underlined by the interaction with Aurora A, an established regulator of cell division. Aurora A phosphorylates RASSF1A on residues located in the microtubule-binding domain, and mutations of these residues which mimic constitutive phosphorylation of RASSF1A disrupt its interaction with the microtubules, and suppress its ability to induce M phase cell cycle arrest (Rong *et al.*, 2007). Interestingly, RASSF1A was also reported to regulate Aurora A activation, as RASSF1A down-regulation, or conversely over-expression, resulted in a marked decrease or increase of Aurora A phosphorylation on Thr288, respectively (Liu *et al.*, 2008).

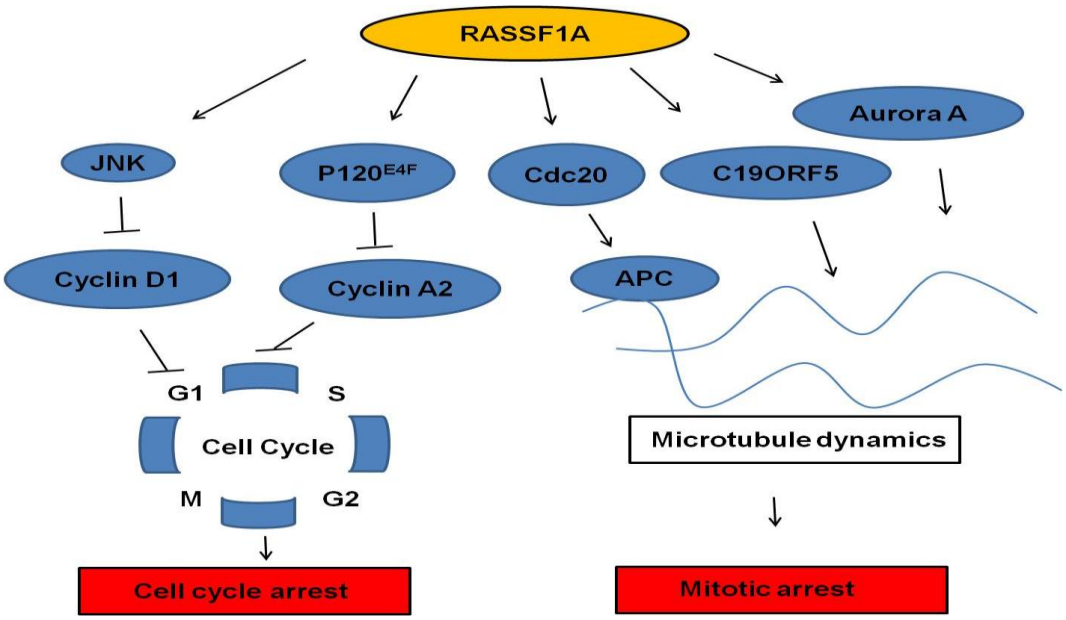


**Figure 1.9: RASSF1A and cell cycle control.** Summary of some of the known partners and pathways of RASSF1A. Direct interaction between RASSF1A and microtubule-associated proteins results in RASSF1A localising the microtubules, stabilising them and regulating mitosis. Repression of cyclins A and D1 by RASSF1A results in cell cycle arrest. Modified from (Donninger *et al.*, 2007).

RASSF1C contribution to cell cycle regulation has been less well studied compared to RASSF1A. RASSF1C over-expression induced cell cycle arrest in the renal cell carcinoma cell line KRC/Y (Li *et al.*, 2004a), but not in HeLa cells (Song *et al.*, 2004).

Cell cycle arrest was suggested as a mechanism of growth inhibition also for RASSF2. RASSF2 expressing 293-T cells showed a 20% decrease in the G2/M phase of the cell cycle, suggesting the cells tended to arrest in the G0/G1 phase (Vos *et al.*, 2003a).

NORE1A was found to induce growth suppression through a mechanism independent of Ras or the MST1/2 kinases. As observed for RASSF1A, expression of NORE1A caused a significant decrease in the number of cells in S phase and a reciprocal increase of the fraction in G1 phase (Aoyama *et al.*, 2004).

#### *1.2.3.4 Classical RASSFs mediated control of genomic stability*

Over-expression of *RASSF1A* or *RASSF1C* in the human embryonic kidney cell line 293T or human lung tumour cell line NCI-H1299 impaired

the ability of activated RAS to induce genomic instability (Vos *et al.*, 2004), such as polyploidy, aneuploidy, and improper organisation of the nuclear structure (Denko *et al.*, 1994; Saavedra *et al.*, 2000; Vos *et al.*, 2004). Human foreskin fibroblasts depleted of *RASSF1A* were reported to be bicentrosomal and showed various mitotic spindle abnormalities including the formation of multi-polar spindles, misalignment of chromosomes, and lagging chromosomes, indicative of chromosome instability (Song *et al.*, 2004). However, cultured fibroblasts from *Rassf1a* null mouse embryos (*Rassf1a*$^{-/-}$ MEFs) did not show a significant increase of polycentrosomal cells or any obvious chromosomal rearrangements by spectral karyotyping analysis (van der Weyden *et al.*, 2005). It has to be noted though, that these cells exhibited delayed mitosis and subsequent cytokinesis failure albeit apparently genomically stable (Guo *et al.*, 2007). Thus, RASSF1A could be potentially involved in the maintenance of genomic stability, but further detailed analysis will be required to determine the specific role of this gene in this context.

#### *1.2.3.5 The classical RASSFs and apoptosis*

Numerous lines of research report the RASSF family proteins to be pro-apoptotic (Vos *et al.*, 2000; Vos *et al.*, 2003a; Vos *et al.*, 2003b; Vos *et al.*, 2004; Eckfeld *et al.*, 2004).

Over-expression of RASSF1A in MCF-7 breast cancer cells caused morphological and biochemical changes indicative of apoptosis (cell rounding, increased annexin V staining and appearance of a sub-G1 population) (Baksh *et al.*, 2005). Apoptosis was also triggered by temporary expression of RASSF1C in 293-T cells and enhanced by co-expression with mutant active Ras (Vos *et al.*, 2000), but others failed to observe this phenomenon in the same cell line over-expressing only wild type RASSF1A or RASSF1C (Rabizadeh *et al.*, 2004).

If the initiation of apoptosis by any over-expressed RASSF1 isoforms can be debated, there is strong evidence that RASSF1A can participate in pro-apoptotic pathways (Figure 1.10). In a yeast two-hybrid assay RASSF1, as NORE1, was shown to specifically bind the pro-apoptotic MST1

(Khokhlatchev *et al.*, 2002). MST1/2 over-expression promotes apoptosis and normally becomes activated by auto-phosphorylation, which can be inhibited by co-transfection with RASSF1A, RASSF1C, or NORE1 (Praskova *et al.*, 2004). NORE1A and RASSF1A are constitutively complexed with MST1 and when endogenous MST1/2 is prevented from associating with these proteins, Ras induced apoptosis is inhibited (Praskova *et al.*, 2004; Avruch *et al.*, 2006).

Hippo, the *Drosophila* homologue of MST1, forms part of an important tumour suppressor network which is crucial for growth control (Saucedo and Edgar, 2007; Harvey and Tapon, 2007). Hippo functions by regulating the kinase Warts which in turn regulates the transcriptional activator Yorkie, which controls apoptosis-associated genes. Recent work shows that RASSF1A induced apoptosis acts via a similar pathway, which involves MST2 activating LATS (large tumour suppressor), causing the release of YAP (yes-associated protein 1) which promotes transcription of p73 (Matallanas *et al.*, 2007). NDR (Nuclear Dbf2-related) kinases, which are related to LATS kinases, can also function downstream of MST1 to promote apoptosis (Vichalkovski *et al.*, 2008).

RASSF1A may also function as a scaffold for the assembly of an apoptotic complex containing CNK1, a pro-apoptotic adapter protein that can bind to RASSF1A or RASSF1C (Rabizadeh *et al.*, 2004) and requires interaction with RASSF1A-MST1 in order to induce apoptosis (Rabizadeh *et al.*, 2004). Furthermore, RASSF1A could control apoptosis by regulating the activity of Bax, a Bcl2 family component involved in the apoptotic machinery (Tan *et al.*, 2001; Sharpe *et al.*, 2004). Stimulation of death receptors with TNF$\alpha$ (tumour necrosis factor $\alpha$) or TNF$\alpha$-related apoptosis-inducing ligand (TRAIL) was shown to cause the recruitment and subsequent interaction of RASSF1A and modulator of apoptosis-1 (MAP-1), a Bax-binding protein (Tan *et al.*, 2001), at the site of the receptor complexes (Baksh *et al.*, 2005). Bax activation was further enhanced by the concomitant presence of K-Ras, RASSF1A, and MAP-1, and knocking down RASSF1A impaired the ability of oncogenic K-Ras to activate Bax (Vos *et al.*, 2006).

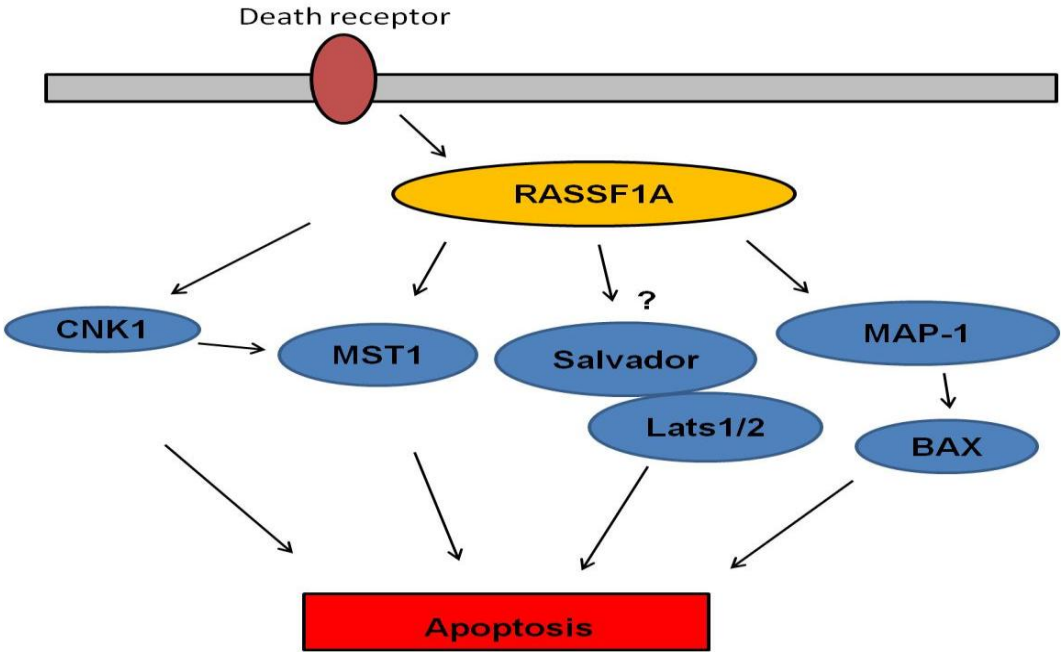


**Figure 1.10: RASSF1A and apoptosis**. Schematic diagram of RASSF1A interactions with CNK1, MST1, Salvador and MAP-1, which may allow RASSF1A to modulate apoptosis. Modified from (Donninger *et al.*, 2007).

It was reported that RASSF1C binds to Daxx (involved in apoptosis and transcriptional repression) in nuclear protein complexes called promyelocytic leukaemia-nuclear bodies (Kitagawa *et al.*, 2006). Following DNA damage, Daxx is degraded and RASSF1C translocates to the microtubules and participates in the activation of stress-activated protein kinase/c-Jun N-terminal kinase (SAPK/JNK) pathway, which plays a crucial role in the regulation of gene expression leading to apoptosis (Kitagawa *et al.*, 2006). In contrast with these data however, Reeves and colleagues have recently published that RASSF1C down-regulates several pro-apoptotic genes, including *Bax* and *Caspase 3,* in breast cancer cells (Reeves *et al.*, 2010). Caspase 3 down-regulation due to *RASSF1C* over-expression was further shown to reduce the sensitivity of breast cancer cells to the apoptosis inducing agent etoposide (Reeves *et al.*, 2010). Therefore it is debatable that RASSF1C has a pro-apoptotic role.

When exogenously expressed, RASSF2 was found to induce actin polymerisation changes and suppression of the Ras-RhoA pathway in colorectal cancer cells. The subsequent loss of adhesion was seen to

cause a suspension dependent apoptosis, called anoikis (Akino *et al.*, 2005).

Over-expressed RASSF4 induced caspase mediated cell death in 293-T cells, which was enhanced by the presence of activated K-Ras, and was shown to interact with exogenously expressed MST1 (Eckfeld *et al.*, 2004).

There are conflicting reports about the ability of NORE1 on its own to induce apoptosis (Khokhlatchev *et al.*, 2002; Vos *et al.*, 2003b; Aoyama *et al.*, 2004; Li *et al.*, 2005). On the other hand, co-expression of NORE1 and MST1, to which NORE1 was shown to bind (Khokhlatchev *et al.*, 2002; Hwang *et al.*, 2007), has a greater pro-apoptotic effect than either protein alone (Khokhlatchev *et al.*, 2002). Apoptosis caused by the over-expression of constitutively active Ki-RasG12V in a variety of cell lines is counteracted by over-expression of either the NORE1-binding domains of MST1 or by the portion of NORE1 that binds MST1 (Khokhlatchev *et al.*, 2002). NORE1/RASSF1 proteins not only would mediate the Ras apoptotic effect, they would also direct MST1 to sites of activation and perhaps co-localisation with endogenous substrates (Praskova *et al.*, 2004).

Similar to what has been found for RASSF1A, forced expression of RASSF6 caused apoptosis in both the MCF-7 cell line (Allen *et al.*, 2007) and the HeLa cervical cancer cell line (Ikeda *et al.*, 2007). On the other hand, *RASSF6* KD was seen to partially block TNF$\alpha$ induced cell death in HeLa cells (Ikeda *et al.*, 2007). Furthermore RASSF6 was shown to activate Bax, induce cytochrome *c* release and initiate caspase dependent and caspase independent pathways of apoptosis (Ikeda *et al.*, 2007). RASSF6 was found to interact with MAP-1 and this binding was made more stable by the presence of activated K-Ras (Allen *et al.*, 2007).

#### *1.2.3.6 The classical RASSFs and cell migration/adhesion*

Agathanggelou and colleagues showed that genes for cell adhesion and motility, such as *tropomyosin I* and *CDH2* were up-regulated in A549 NSCLC cells stably expressing RASSF1A (Agathanggelou *et al.*, 2003).

RASSF1A could well control cell migration given that *RASSF1A* methylation was more frequently observed in tumours showing metastasis (Byun *et al.*, 2001; Calvisi *et al.*, 2006). Over-expressed RASSF1A affects the ability of A549 NSCLC cells to migrate either through a transwell filter or to close a wound (Dallol *et al.*, 2005). If stably transfected with *RASSF1A*, the same cells exhibited increased cell-cell adhesion (Dallol *et al.*, 2005). *Rassf1a* deficient MEFs and RASSF1A KD HeLa cells showed loss of cell-cell adhesion and increased cell migration. This last effect could be Phosphatidylinositol 3-kinase (PI3-K) mediated, given the ability of LY294002, a PI3K inhibitor, to abrogate that effect (Dallol *et al.*, 2005). In addition, activation of the PI3K pathway was also suggested by the detection of increased phosphorylation of the PI3-K downstream effector AKT in the *RASSF1A* depleted cells (Dallol *et al.*, 2005). Interestingly, Rassf1a$^{-/-}$ cells showed also increased levels of the small GTPase Rac1, but the mechanisms behind this phenomenon are still unknown (Dallol *et al.*, 2005).

Over-expressed RASSF1C was recently found to enhance T47D cell invasion/migration in *vitro*, which suggests a role for RASSF1C in stimulating metastasis in breast cancer cells (Reeves *et al.*, 2010).

#### *1.2.3.7 The classical RASSFs in the immune system*

NORE1B has been found to regulate lymphocyte adhesion (under the name of RAPL- regulator of adhesion and polarisation enriched in lymphocytes) (Katagiri *et al.*, 2003). In fact, NORE1B was found to associate with the Ras family member Rap1, which modulates integrin activity (Kinashi and Katagiri, 2005). *Nore1B* knockout mice exhibited defective adhesion and migration of lymphocytes and dendritic cells, which led to an impaired immune response (Katagiri *et al.*, 2004). NORE1B was further linked to lymphocyte polarity and adhesion (via the interaction with the proapoptotic kinase MST1) (Katagiri *et al.*, 2006), T cell migration (Miertzschke *et al.*, 2007), and directional migration of vascular endothelial cells (Fujita *et al.*, 2005). Endogenous NORE1B was also suggested to respond to T-cell receptor (TCR) stimulation by recruiting active Ras, which co-precipitates with NORE1B, to the plasma membrane and by

contributing to the localisation of Carma1, a regulator of TCR induced NF-κB activator (Ishiguro *et al.*, 2006).

RASSF6 was shown to suppress NF-κB pathway in a lung epithelial cell line and suggested to play a role in dictating the degree of inflammatory response to the respiratory syncytial virus (Allen *et al.*, 2007).

In summary, as shown in Table 1.3, the biological function of the classical RASSF proteins is much too complicated to be ascribed to one process only. The members of this family have been linked to microtubule stability, cell cycle control and apoptosis, all of which may contribute to the tumour suppressor activity of these proteins.

| Function | Classical RASSF proteins involved |
|---|---|
| MICROTUBULE ACTIVITY | 1A, 1C |
| MODULATION OF CELL CYCLE | 1A, 1C, 2, 5A |
| APOPTOSIS | 1A, 1C,2, 4, 5, 6 |
| CELL MIGRATION/ ADHESION | 1A, 1C |
| REGULATION OF IMMUNE SYSTEM | 5B, 6 |

**Table 1.3: Functions of the classical RASSFs.** A summary of what is currently known about the function of individual classical RASSFs in different cellular processes.

#### *1.2.3.8 The function of the N-terminal RASSF proteins*

The differences between RASSF7-10 and RASSF1-6 make it important that RASSF7-10 proteins are not assumed to be an extension of the classical RASSF proteins and may therefore have a different role. The N-terminal RASSFs, whose name was given to refer to a distinctive group of proteins, represent a new family of potential Ras effectors which suggests they may have important and specific biological functions. In comparison with the classical RASSFs little is known about the function of the N-terminal RASSF7-10.

RASSF8 may be a tumour suppressor. The first studies that aimed to characterise the function of this protein found that the over-expression of RASSF8 protein in A549 lung cancer cell lines significantly reduced anchorage independent growth, which has been correlated with tumour progression and metastasis (Falvella *et al.*, 2006). More recently, Langton

and colleagues started to shed light on the mechanism of action of the *Drosophila* RASSF8 orthologue, Boa (Langton *et al.*, 2009). Boa acts in concert with dASPP (Ankyrin-repeat, SH3-domain, and Prolin-rich-region containing Protein) at the adherens junctions to promote dCsk (*Drosophila* C-terminal Src kinase) activity (Langton *et al.*, 2009). Boa-dASPP mediated modulation of cell-cell adhesion was shown to be crucial for the normal cellular rearrangements and for normal localisation of the cell adhesion molecule E-cadherin in the *Drosophila* eye (Langton *et al.*, 2009). Boa-dASPP complex at the adherens juctions may be required to locally prevent inappropriate Src activation and in fact Boa mutants exhibited an overgrowth phenotype, reduced apoptosis and cell-cell adhesion defects (Langton *et al.*, 2009). It is known that inappropriate disruption of cell-cell contacts can lead to excess proliferation and is a hallmark of the metastatic process in mammals (Vasioukhin *et al.*, 2001; Yang and Weinberg, 2008).

The regulation of cell-cell adhesion could also be key for understanding a possible tumour suppressor function of human RASSF8. Lock *et al.* found that endogenous RASSF8 interacted with endogenous E-cadherin in lung cancer cells, where E-cadherin, β-catenin and NF-κB p65 localisation at the adherens junctions was abolished following RASSF8 depletion (Lock *et al.*, 2010). In RASSF8 KD lung cells, β-catenin was seen to re-locate back to the nucleus, where the authors observed increased β-catenin/ T-cell factor (TCF) promoter activity, which suggested that RASSF8 depletion may result in increased β-catenin/TCF signaling as part of the canonical Wnt signaling pathway (Lock *et al.*, 2010). A549 RASSF8 depleted cells showed an increase in anchorage independent growth in soft agar when compared to controls and were able to form solid tumours when inoculated into severe combined immunodeficiency (SCID) mice (Lock *et al.*, 2010). The authors of the study also observed that RASSF8 KD led to enhanced cell proliferation in *Xenopus* embryos and A549 confluent cells, indicating loss of contact dependent growth inhibition. Thus RASSF8 suppressed growth in a manner dependent on contact inhibition and was also suggested to control proliferation of NSCLC cells

by modulating Wnt and NF-κB signaling pathway (Lock *et al.*, 2010). Furthermore, there is evidence suggesting a role for RASSF8 in the organisation of the cytoskeleton. A549- RASSF8 RNAi cells exhibited a disorganised actin cytoskeleton and increased in *vitro* motility and migration abilities, which makes it plausible to speculate that a role of RASSF8 in regulating cell-cell adhesion may contribute to the maintenance of normal tissue architecture (Lock *et al.*, 2010).

RASSF9 has been linked to vesicle trafficking (Chen *et al.*, 1998). Rat Rassf9 (also called P-CIP1) interacted with immunoprecipitated PAM-1 (peptidylglycine α-amidating monooxygenase), a transmembrane protein found in secretory vesicles of neurons and endocrine cells (Chen *et al.*, 1998). This result confirmed a previous yeast two-hybrid screen (Alam *et al.*, 1996) and was further substantiated by the association of exogenously expressed Rassf9 with recycling endosomes (Chen *et al.*, 1998). Interestingly, RASSF9 is the only member of the N-terminal RASSF proteins which has currently been shown to bind Ras proteins. Pull-down experiments with RASSF9 and Ras family GTPases showed that RASSF9 binds N-Ras, K-Ras and R-Ras (Rodriguez-Viciana *et al.*, 2004).

RASSF10 was recently proposed as a candidate tumour suppressor gene in gliomagenesis. Hill *et al.* showed that forced expression of *RASSF10* in glioma cell lines not expressing endogenous RASSF10 suppressed the ability to form colonies. Conversely, transient depletion of endogenous RASSF10 in U87 glioma cells exhibited an increased ability in their anchorage independent growth potential compared to control cells (Hill *et al.*, 2010). The growth inhibitory effects of RASSF10 on cell proliferation were further confirmed by cell viability assay and 5-ethynyl-2′-deoxyuridine (EdU) incorporation (Hill *et al.*, 2010).

RASSF7 function has been linked to some key biological processes including the regulation of cell death and proliferation. A large scale RNAi screen suggested that RASSF7 is required for necroptosis (Hitomi *et al.*, 2008), a regulated form of necrosis which is distinct from apoptosis. To date the most informative work on the role of RASSF7 has been carried

out by my colleagues (Sherwood *et al.*, 2008). *Xenopus* rassf7 was demonstrated to be essential for cell cycle progression and cell survival (Sherwood *et al.*, 2008). In embryonic cells where *rassf7* was not expressed, mitotic spindle defects and mitotic arrest occurred with subsequent nuclear fragmentation and apoptosis (Sherwood *et al.*, 2008). However, the signaling pathways in which RASSF7 participates remain a mystery. The physiological functions of RASSF7 in mammals are also unknown, so further work is required.

## 1.3 Aims of the thesis

The primary aim of this project was to understand the role of RASSF7 in mammalian, and in particular in human, cells. In order to address this fundamental question multiple approaches were used:

1) **Analysis of the expression pattern.** This approach was intended for evaluating whether the expression of mammalian RASSF7 is restricted to developmental stages, specific to particular tissues and cell lines or, conversely, broadly expressed.

2) **Study of the subcellular localisation**. This aimed to provide understanding of where RASSF7 functions within the human cells. This is key to understanding the function of the protein.

3) **Characterisation of the function**. To test if human RASSF7 plays a role in mitosis, as its *Xenopus* counterpart (Sherwood *et al.*, 2008), and, more in general, to understand what the consequences of RASSF7 depletion are for the human cells.

# 2 Materials and Methods

## 2.1 Materials

Unless otherwise specified, all chemicals and general laboratory reagents were of molecular biology grade and were purchased from either Sigma-Aldrich Chemical Company or Fisher Scientific UK Ltd.

### 2.1.1 Reagents

*Phosphate Buffered Saline (PBS):*

Purchased from OXID.

*Phosphate Buffered Saline - Tween 20 (PBST):*

PBS 0.1% (v/v) Tween-20.

*Tris Buffered Saline - Tween 20 (TBST):*

10 mM Tris, (pH 7.4), 154 mM NaCl, 0.1% (v/v) Tween-20.

*Luria Broth (LB):*

1% (w/v) Bacto™ Tryptone (BD Biosciences), 0.5% (w/v) Bacto™ Yeast Extract (BD Biosciences), 0.5% (w/v) NaCl. Autoclaved.

*Agar Plates:*

1% (w/v) Bacto™ Tryptone (BD Biosciences), 0.5% (w/v) Bacto™ Yeast Extract (BD Biosciences), 0.5% (w/v) NaCl, 1.5% (w/v) Agar. Autoclaved and once cooled down, the appropriate antibiotic was added (100 μg/ml ampicillin or 30 μg/ml kanamycin) and poured into plastic plates. Kept at 4°C.

#### *2.1.1.1 Buffers for in situ hybridisation*

*Diethyl pyrocarbonate (DEPC)-treated water :*

0.1% (v/v) DEPC in distilled $H_20$ ($dH_2O$) was incubated overnight and autoclaved.

*4% Paraformaldehyde (PFA)*:

The PFA 4% (w/v) was dissolved in PBS, made with DEPC treated water (autoclaved) by heating at 65°C with stirring. When dissolved and cooled, it was adjusted to pH 7.4.

*20X Standard Saline Citrate (SSC) buffer:*

3M NaCl, 0.3 M sodium citrate in dH2O (pH 7, autoclaved).

*Tris-Glycine buffer:*

0.5 M Tris-Cl (pH 8, autoclaved), 0.5 M glycine in DEPC treated $dH_2O$.

*100X Denharts:*

2% (w/v) ficoll, 2% (w/v) polyvinylpyrrolidone, 2% (w/v) Bovine Serum Albumin (BSA) (Fraction V, Sigma 85040C) in $dH_2O$. When dissolved, it was sterilised.

*In situ hybridisation solution:*

40% (v/v) Formamide (Sigma 47671), 1X Denharts, 5X SSC, 100 μg/ml tRNA (Sigma R8508), 100 mg/ml herring sperm (Sigma D7290) in DEPC treated $dH_2O$.

*Post-hybridisation solution:*

20% (v/v) Formamide, 0.5X SSC in $dH_2O$.

RNase A solution:

12.5 μg RNase A (Sigma R5500) in 1 ml 2X SSC.

*10% Blocking solution:*

5% (v/v) sheep serum (Roche 11 096 176 001), 10 mg/ml BSA in PBST.

*NTMT:*

100 mM NaCl, 50 mM $MgCl_2$, 100 mM Tris-HCl pH 9.5, 0.1% (v/v) TritonX-100 in $dH_2O$.

### *2.1.1.2 Buffers for immunohistochemistry*

*Sodium Citrate Buffer:*

10 mM tri-sodium citrate (dehydrate) in $dH_20$ with 0.05% (v/v) Tween-20. pH 6.

*Blocking solution:*

1% (w/v) BSA (Vector Laboratories SP-5050), 1.5% (v/v) goat serum (Vectastain *Elite* ® ABC Kit, Vector Laboratories PK-6101) in PBS.

### *2.1.1.3 Solutions for cell culture*

*RIPA buffer for protein extraction:*

50 mM Tris-HCl, pH 7.5, 150 mM NaCl, 0.5% Na-deoxycholate, 0.1% sodium dodecyl sulphate (SDS), 0.1% NP40 and 10μM protease inhibitor cocktail for mammalian cell extracts (Sigma P8340).

*2X DMEM solution for soft agar assay:*

20% (v/v) 10X DMEM (Sigma), 0.75% (v/v) sodium bicarbonate, 20% fetal calf serum, 1% penicillin/streptomycin/glutamine (Sigma), 0.1 mg/ml Gentamicin (Sigma) in sterile water.

*4% PFA*:

As described above but dissolved in PBS made with $dH_2O$.

*10% Blocking solution for immunocytochemistry:*

Blocking reagent (Roche) was dissolved in maleic acid buffer (100 mM maleic acid, 150 Mm NaCl, pH 7.5) to a final concentration of 10% (w/v) with shaking and heating on a heating block. Autoclaved.

*Propidium iodide buffer for flow citometry:*

20 μg/ml propidium iodide (Sigma, kindly provided by Dr Asma Aroun, University of Bath), 200 mg/ml RNase A, 0.1% (vol/vol) Triton X-100 in PBS.

### *2.1.1.4 Buffers for Western blotting*

*Sample Buffer:*

Protein samples were solubilised in 2% (w/v) SDS, 62.5 mM Tris HCl (pH 6.8), 0.01% (w/v) bromophenol blue, 10% (v/v) glycerol with 100 mM Dithiothreitol (DTT) as reducing agent.

*Resolving Gel Buffer:*

1.5 M Tris HCl, 0.4% (w/v) SDS, (pH 8.8).

*Stacking Gel Buffer:*

0.5 M Tris HCl, 0.4% (w/v) SDS, (pH 6.8).

*Electrophoresis Running Buffer:*

25 mM Tris HCl, (pH 6.3), 0.1% (w/v) SDS, 0.2 M glycine.

*Transfer Buffer:*

39 mM glycine, 48 mM Tris, 0.0375% SDS (w/v), 20% methanol (v/v), (pH 8.8).

*Ponceau S Stain:*

0.1% (w/v) Ponceau S (Sigma), 3% (w/v) trichloroacetic acid.

*Blocking buffer :*

5% (w/v) skimmed milk (Marvel®) in TBST.

*ECL Reagent (home made):*

Solution A – 100 mM glycine (pH 10), 0.4 mM luminol (Sigma 09253), 8 mM 4-iodophenol (Aldrich I10201).

Solution B – 0.12% (w/w) hydrogen peroxide in water.

## 2.1.2 Antibodies

Table 2.1 shows a list of antibodies along with their suppliers and dilutions used for different applications.

| | Antibody | Species | Source | Application-Dilution |
|---|---|---|---|---|
| PRIMARIES | α-active caspase 3 | rabbit | Abcam Ab13847 | IF-1:100 |
| | α–Aurora A (clone 4/IAK1) | mouse, monoclonal | BD biosciences 610938 | IF-1:500 |
| | α–Aurora B (clone 6/AIM-1) | mouse, monoclonal | BD biosciences 611082 | IF-1:200 |
| | α–INCENP (clone 58-217) | mouse, monoclonal | Upstate/Millipore 05-940 | IF-1:250 |
| | α–pericentrin | rabbit | Covance PRB-432C | IF-1:500 |
| | α–phospho Aurora A (Thr288), B (Thr232), C (Thr198) (clone D13A11) | rabbit | Cell Signaling 2914 | IF-1:50 |
| | α–phospho CENP-A (Ser7) (clone NL41) | rabbit | Millipore 04-792 | IF-1:300 |
| | α–phospho histone H3 (Ser10) | mouse, monoclonal | Abcam Ab14955 | IF-1:500 WB-1:1000 |
| | α–phospho PLK1 (Thr210) (clone Poly6186) | rabbit | Biolegend 618601 | IF-1:100 |
| | α–RASSF1A (clone eB114-10H1) | mouse, monoclonal | eBioscience 14-6888 | IF-1:100 |
| | α–RASSF7 | rabbit | Aviva System Biology ARP34390_T100 | IF-1:100 IHC-1:50 WB-1:1000 |

| | Antibody | Species | Source | Application-Dilution |
|---|---|---|---|---|
| PRIMARIES | α–RASSF8 (clone 2G1) | mouse, monoclonal | Abnova H00011228-M01 | IF-1:200 |
| | α-α tubulin (clone DM1A) | mouse, monoclonal | Sigma T9026 | IF-1:250 |
| | α–β tubulin (clone TUB 2.1) | mouse, monoclonal | Sigma T4026 | WB-1:2500 |
| | α–γ tubulin (clone GTU-88) | mouse, monoclonal | Sigma T6557 | IF-1:100 |
| | α-V5 | mouse, monoclonal | Invitrogen R960-25 | IF-1:200 |
| | **Antibody** | **Species** | **Source** | **Application-Diluition** |
| SECONDARIES | α-mouse Alexa® Fluor 488 | goat | Molecular Probes A11001 | IF-1:500 |
| | α-mouse Alexa® Fluor 568 | goat | Molecular Probes A11004 | IF-1:300 |
| | α-rabbit Alexa® Fluor 488 | goat | Molecular Probes A11008 | IF-1:500 |
| | α-rabbit Alexa® Fluor 568 | goat | Molecular Probes A11011 | IF-1:300 |
| | α-rabbit-HRP | goat | Pierce | WB-1:5000 |
| | α-mouse-HRP | goat | Sigma A2554 | WB-1:5000 |

**Table 2.1: List of antibodies used**. Where known, clone and catalogue numbers of primary antibodies are given. Dilutions are of original supplied stocks. For the conditions of antibody utilisation, refer to main text. Abbreviatios: IHC: immunohistochemistry, IF = immunofluorescence, WB = Western Blotting.

## 2.1.3 Plasmids

Table 2.2 shows a list of antibodies used during the current project.

| Plasmid names | Details | Internal database number |
|---|---|---|
| Mouse RASSF7 | Used for In *situ* hybridisation | 305 |
| Mouse RASSF8 | Used for In *situ* hybridisation | 304 |
| Mouse RASSF9 | Used for In *situ* hybridisation | 361 |
| Human RASSF7 clone | Used for subcloning *RASSF7* cDNA into the Gateway entry vectors | 414 |
| pENTR/human RASSF7 with stop codon | Gateway entry vector which contains RASSF7 for cloning into N-terminally tagged destination vectors | Not available |
| pcDNA/DEST53 (Invitrogen) | Gateway destination vector with N-terminal GFP tag (kindly donated by Dr Angelina Felici, IFOM, Milan) | 345 |
| GFP-human RASSF7 | Used for analysing the localisation of ectopic GFP-RASSF7 | 343 |
| pcDNA6.2/V5-DEST (Invitrogen) | Gateway destination vector with C-terminal V5 tag | 318 |
| pENTR/human RASSF7 without stop codon | Gateway entry vector which contains RASSF7 for cloning into C-terminally tagged destination vectors | 382 |
| Human RASSF7-V5 | Used for analysing the localisation of ectopic RASSF7-V5 | 344 |
| Human RASSF8-GFP | Used for analysing the localisation of ectopic RASSF8 (kindly donated by Prof. Farida Latif, University of Birmingham) | 346 |
| Cytoplasmic GFP | Used as control for localisation analysis of ectopically expressed proteins | 39 |
| Human RASSF7 short hairpin RNAi (SuperArray Bioscience) | Used for RASSF7 knockdown | 314 |
| Negative control short hairpin RNAi (SuperArray Bioscience) | Used for RASSF7 knockdown | 315 |

**Table 2.2: List of plasmids used**. Names, details and, where available, internal database numbers of plasmids are given.

## 2.1.4 RNA interference

Tables 2.3 and 2.4 show the siRNA (small interfering RNA) oligonucleotides and shRNA (short hairpin RNA) used for silencing *RASSF7* gene expression.

**A**

| Symbol | Catalogue # | Oligo sequence (5'-> 3') |
|---|---|---|
| RASSF7 KD 1 | 13242 | GGAAGUGGUCAUCGCACUAtt |
| RASSF7 KD 2 | 13338 | GGAGAUGCAUGGACAGUGUtt |

**B**

| Symbol | Catalogue # | Oligo sequence (5'-> 3') |
|---|---|---|
| Luciferase KD | 21204193 | CGUACGCGGAAUACUUCGA |

**Table 2.3: siRNA oligonucleotides used for transient RASSF7 KD in H1792 cells.** RASSF7 KD1 and RASSF7 KD2 were purchased from Ambion (A). A control oligonucleotide targeting luciferase was purchased from MWG (B).

| Symbol | Catalogue # | Oligo sequence (5'-> 3') |
|---|---|---|
| RASSF7 | KH09867N | TCTCGATCGCACTAGCCCAAGCAATACTTCCTGTCATA TTGCTTGGGCTAGTGCGATCT |
| | Control | TCTCGGAATCTCATTCGATGCATACCTTCCTGTCAGTAT GCATCGAATGAGATTCCCT |

**Table 2.4: shRNA used for RASSF7 KD in HeLa cells.** RASSF7 shRNA and scrambled control shRNA were cloned into pGeneClip/Neo vectors and purchased from SuperArray Bioscience.

## 2.2 Methods

### 2.2.1 Molecular biology techniques

#### *2.2.1.1 Restriction digests*

Digestion of DNA was carried out with restriction enzymes (Promega or NEB) according to the manufacturer's instructions. The reactions contained DNA, $^{1}/_{10}$ volume of restriction enzyme buffer, 100 μg/ml BSA, 5U of enzyme per μg of DNA and water to the required volume. Most enzymes were incubated at 37°C for 1-2 hours. When required, restriction enzymes were heat inactivated at 65°C for 15 minutes.

#### *2.2.1.2 Agarose gel electrophoresis*

Digested DNA , synthesised RNA and polymerase chain reaction (PCR) products were loaded into a 0.9% (w/v) agarose Tris-acetate EDTA (TAE) gel and run in the presence of 500 ng of ethidium bromide (10 mg/ml) per ml of agarose to aid visualisation of nucleic acids. Loading dye (6x, Promega) was added to each DNA/RNA sample before loading into the wells of the gel. Samples were elecrophoresed at 100-135V for 20-30 minutes depending on size of DNA/RNA. The DNA/RNA samples were analysed under ultra-violet light with a Spectroline® transilluminator.

#### *2.2.1.3 Bacterial transformations and plasmid DNA separation*

Plasmids which contained specific DNA constructs were transformed into competent *E.Coli* cells. A small amount (2 μl) of the cloned DNA construct was added to 100 μl of competent TOP10 cells (Invitrogen) on ice and incubated for 10 minutes. Cells were subsequently heat shocked by incubating at 42°C for 30 seconds, and then placed back on ice for 2 minutes. LB media (900 μl) was added to the heat shocked DNA-cell mixture and this was incubated at 37°C for 1 hour. Different volumes of this mixture (20-100 μl) were then plated on LB plates that contained the appropriate antibiotic selection that the recipient plasmid had resistance to. This made it possible to select only the colonies which had integrated the plasmids. Plates were grown overnight at 37°C.

Single colonies were selected and grown in 5 or 100 ml cultures (according to the extraction protocol followed) with the relevant antibiotics, in order to highly concentrate the volume of desired DNA. Incubation at 37°C shaking overnight followed. Cultures were pelletted by spinning at 4000 x g for 15 minutes, and DNA was extracted using mini-prep kits (Quiagen) or Maxi-prep kits (Sigma) according to the manufacturer's instructions. The kits are designed to separate plasmid DNA from chromosomal DNA and any other cellular debris such as lipids and proteins. This was achieved by binding the plasmid DNA to the column, removing all other cellular component via washing and then eluting the clean plasmid DNA.

#### *2.2.1.4 Subcloning of DNA constructs*

The human *RASSF7* gene coding region (approximately 1.2 Kb) was amplified from the cDNA clone (IMAGE: 40032773) isolated from a full length human plasmid cDNA library (Geneservice). The clone was identified by BLAST searches after having interrogated the protein database and its translated product corresponds to the RASSF7 protein isoform NP_003466 (RASSF7 A).

In order to subclone *RASSF7* construct, the PCR was used along with specifically designed primers for the template DNA (Table 2.5).

| No. | Primer name | Sequence | Notes |
|---|---|---|---|
| 1 | F7 fwd. | 5'-**cacc**atgttgttgggactggcggcc-3' | Forward primer |
| 2 | F7 rev. | 5'-tcacagagcctggggctgg-3' | Reverse primer with stop codon for cloning into N-terminal GFP containing vector |
| 3 | F7 rev. | 5'-cagagcctggggctgggctg-3' | Reverse primer without stop codon for cloning into C-terminal V5 containing vector |

**Table 2.5: Primers used for cloning human RASSF7 construct**. The description and the sequence of the primers utilised is given. Bold and underlined text indicates the sequence being introduced into the forward primer at the 5' end to enable directional cloning. F7 fwd is RASSF7 forward; F7 rev. is RASSF7 reverse.

PCR reaction was carried out with 400 ng of DNA template, 1X thermal polymerase buffer (Stratagene), 200 μM dNTPs, 1 μM of each oligonucleotide primer, 2.5 U Pfu Turbo polymerase (Stratagene). This mixture was usually made up to a total volume of 50 μl by using $dH_2O$. Table 2.6 shows the cycle for PCR that was used when cloning the construct.

| PCR stage | Temperature | Time | Repeat |
|---|---|---|---|
| 1- Denaturation | 95°C | 2 minutes | |
| 2- Denaturation | 95°C | 30 seconds | |
| 3- Annealing | X°C * | 30 seconds | |
| 4- Elongation | 72°C | 1.5 minutes | Go to step 2 (x29) |
| Hold | 4°C | | |

**Table 2.6 : PCR cycle used**. *Annealing temperatures were 58.4°C for primers 1+2 and 61°C for primers 1+3 (refer to Table 2.5 for primers used).

The PCR products were subsequently gel extracted according to the kit manufacturer's specifications (Quiagen) and were cloned into the pENTR/D-TOPO gateway entry clone using the pENTR Directional TOPO Cloning Kit (Invitrogen). TOP10 supercompetent cells (Invitrogen) were transformed with 2ul of TOPO Cloning reaction using standard transformation techniques. *RASSF7* containing entry clones were sequenced and transferred to the destination vector backbones by mixing the DNAs with the Gateway® LR Clonase™ II enzyme mix (Invitrogen). The destination vectors were green fluorescent protein (GFP) containing pcDNA-DEST53 (Invitrogen) for N-terminal fusion to *RASSF7* and V5 epitope containing pcDNA/V5-DEST (Invitrogen) for C-terminal fusion to *RASSF7*. The resulting recombination reactions were then transformed into *E.Coli* bacteria and GFP-RASSF7 or RASSF7-V5 expressing clones selected. To check for successful clones with integrated PCR products, digestions of the cloned DNA were used, employing BGRI restriction enzyme (NEB), for band size estimations. This method was useful in identifying positive clones prior to sequencing. DNA sequencing was performed via MWG Biotech using vector-specific primers, in order to confirm correct DNA sequences of all constructs cloned.

### *2.2.1.5 In Situ Hybridisation (ISH)*

#### *ISH RNA probe synthesis*

Mouse RASSF7 (Genebank accession number**:** BC011131), mouse RASSF8 (Genebank accession number: BC115779) and mouse RASSF9 (Genebank accession number**:** BG175058) DNA containing plasmids (10 μg ) were linearised approximately 500 bp downstream of the appropriate promoter using the correct enzyme in the right buffer according to the guidelines set out by the suppliers (Table 2.7). Gene-specific antisense or sense digoxigenin (DIG)-labelled cRNA probes were made using 1μg of linearised plasmid DNA and the DIG RNA Labelling Kit (Roche 11 175 025 910) (Table 2.7).

| Probe | Restriction enzyme | RNA polymerase |
|---|---|---|
| RASSF7 sense | STU I (Promega) | SP6 (Promega) |
| RASSF7 αsense | AHD I (NEB) | T7 (Promega) |
| RASSF8 sense | ECONI (NEB) | T7 (Promega) |
| RASSF8 αsense | PSTI (Promega) | SP6 (Promega) |
| RASSF9 sense | ALU I (NEB) | SP6 (Promega) |
| RASSF9 αsense | BGL II (NEB) | T7 (Promega) |

**Table 2.7: List of restriction enzymes and RNA polymerases utilised for producing the *in situ* riboprobes**.

The RNA probes were ethanol precipitated in the presence of LiCl and resuspended in 20 μl of DEPC treated water. RNase Inhibitor (Roche) was added to a concentration of 0.1 unit/μl. The probes were subsequently vortexed and heated to 80°C for a couple of times to fully resuspend the RNA. Agarose gel electrophoresis was performed in order to evaluate and compare the presence and the amount of RNA probe obtained. The probes were stored at -80°C until used.

#### *Specimen preparation for ISH and sectioning*

In order to carry out ISH, mouse embryos (E15.5 or E10.5) or adult tissues were fixed in 4% PFA at 4°C for approximately 16 hours, dehydrated and infiltrated with paraffin wax heated to 60°C through a tissue processor (Leica). The samples were then embedded in excess wax in square blocks which acted as a support during sectioning, with the help provided by Iryna

Withington. Sequential series of sagittal sections (7μm thick) were cut manually with a conventional microtome (Leica), floated onto a water bath and then recovered onto uncoated slides (Fisher Scientific), dried overnight and finally stored at 4°C till used. Prior to initiating the ISH, some of the embryonic sections were haematoxylin and eosin (H a E) stained to verify the integrity of the internal organs (see section 2.2.2.1)

***ISH on mouse slices***

After rehydration, the sections were fixed in freshly prepared 4% PFA for 30 minutes, washed in PBS and permeabilised for 15 minutes at room temperature (RT) with 25 μg/ml proteinase K (Roche 03 115 836 001) in PBS. After additional washes in PBS, the sections were post-fixed for 15 minutes with freshly prepared 4% PFA, washed with 2X SSC and Tris-glycine buffer for 5 and 30 minutes respectively, and finally serially dehydrated in ethanol and air dried for 30 minutes. The sections were subsequently incubated in hybridising solution containing the appropriate digoxigenin- labelled riboprobe diluted 1:50 in a total volume of 500 μl per section. Each section was covered by parafilm and hybridised overnight at 60°C. To remove the excess probe, the sections were washed in 5X SSC at RT 3 times for 15 minutes each, in post-hybridisation buffer at 55°C for 40 minutes, in 2X SSC at RT for 15 minutes, and treated with RNAse A solution at 37°C for 15 minutes to digest away any excess unbound riboprobe. Sections were rinsed in 2X SSC at RT for 15 minutes, washed at a higher stringency in post-hybridisation buffer at 55°C for 20 minutes and then washed twice in 2X SSC with rocking at RT for 15 minutes each time. The sections were incubated at 4°C overnight with alkaline phosphatase (AP) labelled anti-digoxigenin Fab fragments (Roche 11 093 274 910) diluted 1:500 in 1% blocking medium. After 4 hours washes in PBS and 3 washes of 10 minutes in NTMT, the staining reaction for alkaline phosphatase was performed with the AP chromogenic substrate BM purple (Roche 11 442 074 001) at RT in the darkness. Progress of the staining was followed using a dissection microscope. The positive signal was visible as a dark purple staining and once developed, the reaction was stopped for the in *situs* and the corresponding negative controls, by

washing in PBS with 0.5 M EDTA for 5 minutes. The slides were subsequently dehydrated and stored in DPX mounting medium at RT for following analyses. Pictures were taken using a Nikon digital camera on a Leica microscope (David Tosh's laboratory, University of Bath).

## 2.2.2 Histological methods

### *2.2.2.1 H & E staining*

Slides of 7 mm wax embedded organ sections were washed in histoclear clearing solution (National Diagnostics) 2 x2 minutes to remove wax. The slides were then hydrated in 100% (v/v) ethanol (2 x 1 minute), in 95% (v/v) ethanol (1 minute), 90% (v/v) ethanol (1 minute), 70% (v/v) ethanol (1 minute), 50% (v/v) ethanol (1minute). Washes in MilliQ water for 1 minute followed before staining in haematoxylin (provided by Iryna Withington, University of Bath) for 15 minutes. Slides were then washed in running tap water for 3 minutes to avoid non-specific binding of haematoxylin. Washes in 1% (v/v) concentrated hydrochloric acid (HCl) in 70% (v/v) ethanol for 30 seconds, in 1% (v/v) ammonia ($NH_3$) in 70% ethanol for 1 minute and in 70% (v/v) ethanol for 30 seconds followed. Filtered eoosin (provided by Iryna Withington, University of Bath) was then used for 5 minutes to counterstain the slides. Prior to mounting, slides were dehydrated in 70 % (v/v) ethanol (3 seconds), in 95% (v/v) ethanol (5 seconds), in 100% (v/v) ethanol (2 x 1 minute) and in histoclear (2 x 2 minutes). Sections were mounted using DPX mount overlaid with a plastic coverslip (Millipore). Pictures were taken using a Nikon digital camera on a Leica microscope (David Tosh's laboratory, University of Bath).

### *2.2.2.2 Immunohistochemistry (IHC)*

Paraffin-embedded sections of mouse tissues and human xenograft tumours were kindly donated by Dr Jason Gill (University of Bradford). The samples were deparaffinised and rehydrated in histoclear (2 x 5 minutes) and decreasing concentrations of ethanol (100%, 95%, 90%, 70%, 50%) (v/v) for 1 minute each and PBS (1 x 5 minutes). Antigen retrieval of the sections followed by submerging them into boiling sodium citrate buffer in

the microwave for 20 minutes. The samples were then allowed to cool for 45 minutes. A wash in PBS for 5 minutes followed. Tissue sections were then circumscribed with a hydrophobic barrier pen (Vector Laboratories), in order to keep reagents localised on tissue sections. The samples were washed in TBS plus 0.025% (v/v) Triton X-100 with gentle agitation. The slides were subsequently blocked for 2 hours at RT. Primary antibody rabbit $\alpha$-RASSF7 or rabbit serum (kindly given by David Tosh's laboratory, University of Bath) were then diluted 1:50 in TBS with 1% (w/v) BSA (Vector laboratories) and incubated with the sections overnight at 4°C. Washes in PBS (1 x 2 minutes) and TBST (2 x 5 minutes) preceded the quenching in peroxidase solution (0.3% (v/v) $H_2O_2$ in TBS) for 15 minutes at RT. After washing in PBS, sections were incubated for 1 hour at RT with biotinylated secondary antibody (anti rabbit IgG) (Vector Laboratories) diluted in goat serum (Vector Laboratories) and PBS, prepared according to the instructions contained in Vectastain *Elite*®ABC kit (Vector Laboratories PK-6101). After removing the excess of secondary antibody, the antigen-antibody complexes were detected using immunoperoxidase system (Vectastain *Elite* ® ABC Kit, Vector Laboratories) and Diaminobenzidine (DAB) staining according to manufacturer's instructions.

## 2.2.3 Cell culture techniques

All cell culture media and media supplements were purchased from Sigma, unless otherwise specified.

### *2.2.3.1 Cell line maintenance*

All cell lines were grown at 37°C under 5% $CO_2$. A549 (human lung adenocarcinoma, already present in the lab), Caco2 (human colorectal adenocarcinoma, already present in the lab), COS-7 (monkey kidney fibroblast, already present in the lab), H1792 (human lung adenocarinoma, kindly provided by Prof. Farida Latif, University of Birmingham), HeLa (human cervix carcinoma, kindly provided by Prof. Farida Latif, University of Birmingham), HepG2 (human liver carcinoma, kindly provided by Dr David Tosh, University of Bath), PANC-1 (human pancreatic cancer, kindly

provided by Dr David Tosh, University of Bath), OVCAR (ovarian carcinoma, purchased from Cancer Research UK), T293 (human embryonic kidney, already present in the lab) cells were maintained in DMEM (Dulbecco's modified Eagle's medium, Lonza BE12-614F), with 10% fetal bovine serum (FBS, Sigma F9665), 1% penicillin/ streptomycin and 1% glutamine. PC12 rat pheochromocytoma cells (kindly provided by Prof. Sue Wonnacott) were cultured in DMEM medium supplemented with 10% heat-deactivated donor horse serum (Sigma), 5% FBS, 50 U/ml penicillin and 50 μg/ml streptomycin, 2 mM glutamine. Human THP-1 monocytic leukaemia and Jurkat leukemic T cells (kindly provided by Prof. Stephen Ward, University of Bath) were maintained in DMEM-F12 medium containing 10% fetal calf serum, 1% penicillin/ streptomycin and 1% glutamine. SH-SY5Y human neuroblastoma cells (kindly provided by Dr Momna Hejmadi, University of Bath) were cultured in DMEM-F12 medium with 15% FBS, 1% non essential amino acids, 1% penicillin/ streptomycin, 2 mM glutamine.

If required for subsequent immunoblotting analysis, cells were washed with ice-cold PBS then 1 ml ice-cold RIPA buffer was added and incubated with the cells for at least three minutes. The lysates were then scraped off, collected and sonicated on ice for 20/30 seconds, in 3 separate intervals. The lysates were subsequently centrifuged for 10 minutes at 12,000 x g at 4°C. The supernatants were then removed and utilised for Western blotting.

#### *2.2.3.2 Cell cycle synchronisation*

To increase the number of cells in M phase, HeLa cells were grown in T75 (Fisher Scientific 3123-075) tissue culture flasks and treated with 75 ng/ml nocodazole (Sigma) containing growth medium for 18 hours at 37°C. Mitotic cells were then dislodged from the tissue culture flasks by agitation ("Mitotic shake-off ") as recommended in (Soares *et al.*, 2007). Detached mitotic cells (70-90%) were then collected, spun down (1000 x g, 3 minutes) and resuspended in 1 ml cold RIPA buffer. Cells were then sheared by sonication on ice for 20/30 seconds, in 3 separate intervals. The lysates were centrifuged for 10 minutes at 12,000 x g at 4°C. The

supernatants were removed and utilised for subsequent Western blotting analysis.

#### *2.2.3.3 Exposure to hypoxic conditions*

To expose cells to hypoxic conditions, cultures in T25 tissue culture flasks (Fisher Scientific 3103-025) were placed in a humidified 37°C multigas incubator with 5% $CO_2$/ 95% nitrogen (kindly provided by Dr Momna Hejmadi, University of Bath) for 3 hours and 18 hours. Residual $0_2$ levels were monitored regularly and were found to be consistently less than 0.1%. Some samples were subject to hypoxia stress for 18 hours followed by 24 hours recovery in normoxic conditions (21% $0_2$). Control cultures, maintained under normoxic conditions, were processed in parallel. Protein extraction followed as described at the end of section 2.2.3.1, but with 300 μl ice-cold RIPA buffer.

#### *2.2.3.4 Transfection and gene silencing*

***Plasmid transfection***

Hela cells were seeded at 2 x $10^5$ cells per 6 well plate well (Fisher Scientific 3810-006) containing antibiotic free medium one day prior to transfection. On the day of transfection, 3.8 μg of plasmid DNA were incubated with 240 μl of Opti-MEM® Reduced Serum Medium (Invitrogen 31985-062) for 5 minutes at RT. Concomitantly, 9.6 μl of Lipofectamine™ 2000 (Invitrogen 11668-019) were incubated with 240 μl of Opti-MEM® for 5 minutes at RT. The two solutions were then mixed and incubated for 20 minutes at RT. The transfection mixture was added to cells in fresh antibiotic free medium for 6 hours at 37°C and then replaced with fresh growth medium. When over-expressing a *RASSF7* construct, transfected cells were fixed 24 hours after transfection and treated as for immunofluorescence studies (see section 2.2.3.6)

When silencing *RASSF7* gene expression via pGeneClip/Neo plasmid containing either *RASSF7* specific or scrambled shRNA sequence, transfected cells were put in selection with 1.2 mg/ml G418 (Sigma G8168) 24 hours after transfection for 14 days. Cells were then counted

and analysed. The experiment, which was repeated 5 times, was also reproduced as described above, except that the seeding of 2 x $10^5$ HeLa cells was carried out after selection. The analysis was performed via either immunofluorescence studies (see section 2.2.3.6) or Western blotting. In the latter case were treated as described at the end of section 2.2.3.1, but with 100 μl ice-cold RIPA buffer.

***Transfection of siRNA oligonucleotides***

H1792 cells were plated at 5 x $10^4$ cells per well of a 6 well plate in 2 ml of antibiotic free medium one day prior to transfection. On the day of transfection 10 μl of 20 μM siRNA oligonucleotide were diluted in 175 μl Opti-MEM® Reduced Serum Medium (Invitrogen) for 5 minutes at RT. Concomitantly, 4 μl of Oligofectamine™ (Invitrogen 12252-011) were incubated with 15 μl of Opti-MEM® for 5 minutes at RT. The two solutions were combined and incubated for 20 minutes at RT. The transfection mixture was added to cells in fresh antibiotic free medium at 37°C. The results were assayed 3 days later, when cell lysates were collected from some samples as described at the end of section 2.2.3.1, but with 100 μl ice-cold RIPA buffer.

### *2.2.3.5 Soft agar growth assay*

The experiment was set up 24 hours after transfecting H1792 cells with siRNA oligonucleotides. All solutions were kept in a 42°C waterbath. Equal amounts of 2X DMEM and 1.4% (w/v) agar (Sigma) were mixed, 2 ml of the solution were put into each well of a 6 well plate and allowed to set at RT. Transfected H1792 cells were then trypsinised and 5 x $10^4$ cells per well were diluted with 1 ml of 0.35% (w/v) agar (½ 1X DMEM, ¼ 2X DMEM and ¼ 1.4% agar). The cells were then plated on top of the previously formed agar layer. This second layer was allowed to set. Finally, equal amounts of 2X DMEM and 1.4% (w/v) agar were mixed once again, 2 ml of the solution were put on top of the first two solidified agar layers into each well and allowed to set at RT. Cells were cultured at 37°C for two weeks and 200 μl 1X DMEM were added once or twice a week to avoid drying out. Colonies were photographed with a Zeiss microscope digital

camera and the average number of colonies greater than 50 μm was calculated.

#### *2.2.3.6 Immunofluorescence studies*

Cells were grown on glass coverslips (Fisher Scientific MNJ-500-0104) in 6 well plate wells. Cell medium was then removed from cells and cells were rinsed once with PBS. Cells were then differently processed according to the protocol followed:

1) Cells were fixed with 4% PFA at RT for 30 minutes. Washes in PBS followed and the permeabilisation was carried out with 0.1% Triton X-100 at RT for 20 minutes. Non specific binding sites were then blocked by 2% blocking solution at RT for 2 hours prior to adding the primary antibody diluted in 2% blocking solution, and incubating at 4°C overnight. Primary antibodies were: anti-active caspase 3, anti-Aurora A, anti-Aurora B, anti-INCENP, anti-phospho CENP-A, anti-phospho Aurora, anti-phospho histone H3, anti-phospho PLK1, anti-RASSF8 and anti-α-tubulin (for diluitions refer to Table 2.1). After 3 x 15 minutes washes, cells were incubated with the secondary antibody, diluted in 2% blocking buffer, at RT in the dark for 1 hour. Washes in PBS followed again to remove any unbound antibody. Nuclear staining was performed with 1 μg/ml DAPI (4',6-diamidino-2-phenylindole) (Sigma) at RT for 20 minutes in the dark, followed by a quick wash in PBS.

2) Cells were fixed and permeabilised with cold methanol at RT for 5 minutes and subsequently blocked with 1% BSA/ 3% normal goat serum (NGS) in PBS at RT for 2 hours. The incubation with the primary antibody diluted into the blocking solution followed at RT for at least 1 hour. Primary antibodies were: anti-pericentrin, anti-γ-tubulin, anti-RASSF1A and anti-RASSF7 (for diluitions refer to Table 2.1). Appropriate species-specific fluorophore conjugated secondary antibodies and DAPI were also diluted in blocking solution. Incubation with secondary antibodies and 1μg/ml DAPI were for 20 minutes at RT in the dark. Two washes of 5 minutes each in 0.2% BSA/ O.6% NGS/ PBS followed all antibody incubations with further 2 washes in PBS alone. Anti-RASSF7 antibody required antigen

retrieval to unmask the epitope, which involved EDTA treatment (1mM, pH 8) for 1.5 hours at 37°C before blocking.

In both cases, negative controls were conducted in parallel, either by omitting the primary antibodies or by replacing the primary antibody with the pre-immune serum used at the least diluted concentration of the corresponding antibody.

Cells were finally mounted in Mowiol (Merck 475904), visualised using a Zeiss LSM 510 confocal microscope (Bioimaging Suite, University of Bath), and images were captured and processed using LSM image browser software.

#### *2.2.3.7 Fluorescence-Activated Cell Sorting (FACS)*

RASSF7 KD and control HeLa cells were grown onto 10 cm tissue culture dishes (SLS T155318) in the presence of G418. Adherent cells were removed from plates by trypsinisation. Cells were washed once in PBS, fixed in cold 70% (v/v) ethanol/ PBS and stored at -20°C until analysed. On the day of analysis, ethanol-fixed cell samples were washed with PBS, centrifuged for 3 minutes (1000 x g) and resuspended in 500 μl of freshly prepared propidium iodide buffer for 30 minutes at RT. DNA content frequency was acquired using a FACS Canto benchtop cytometer (Becton Dickinson) (Bioimaging Suite, University of Bath), counting 1 x $10^6$ cells per sample. Cell doublets were excluded from the FACS data using doublet discrimination gating: FSC-H/FSC-W gate followed by an SSC-H/SSC-W gate and then a PE-H/PE-A gate. Cell cycle stages were automatically gated by the software, according to the DNA content of the cell population.

#### *2.2.3.8 Microtubule re-growth assay*

RASSF7 KD and control HeLa cells were grown on coverslips in the presence of G418. Cells were washed with PBS and incubated with 300 ng/ml of the depolymerising drug nocodazole dissolved in growth medium at 37°C for 1 hour (Ma *et al.*, 2008). Cells were then shifted on ice for 30 minutes and two quick washes in cold PBS followed. The treated cells were fixed with 4% PFA 0, 5, 15, 30, 60 minutes after adding pre-warmed

nocodazole free medium at 37°C. The subsequent immunofluorescence staining with the microtubule marker α-tubulin made it possible visualise the microtubule growth at different time points. The experiment was repeated twice.

## 2.2.4 Protein biochemistry techniques

### *2.2.4.1 Protein quantification*

Protein concentrations of cultured cells were estimated with Comassie (Bradford) protein assay (Pierce) using a BSA standard curve. Comassie Reagent (250 μl) was added to each of the wells of a 96-well plate containing standard or appropriate samples (5 μl). The solutions within the wells were mixed with a plate shaker for 30 seconds and the plate was subsequently incubated at RT for 10 minutes. The measurement of the absorbance at 595 nm was performed with a Spectra Rainbow Thermo microplate spectrophotometer (Tecan). Results were analysed using Microsoft Excel to determine unknown protein concentration estimations.

### *2.2.4.2 SDS – Poly-Acrylamide Gel Electrophoresis (SDS-PAGE)*

Proteins were separated on the basis of mass by electrophoresis in a polyacrylamide gel under denaturing conditions. SDS containing sample buffers were used to denaturate 25 μg of protein in precleared lysates, and then heated at 95°C for 5 minutes. SDS is an anionic detergent that disrupts nearly all non covalent interactions in native proteins. DTT was also included in the sample buffer to reduce disulfide bonds. The SDS complexes with the denatured proteins were then electrophoresed on a polyacrylamide gel in the form of a thin vertical slab. Vertical gels were of 1.5 mm thickness and were prepared using acrylamide/bis-acrylamide (30% (w/v) acrylamide) (ProtoGel- National Diagnostics ECR 210 010P) and gel buffers previously described. Polymerisation of the gels was induced by the addition of 10% (w/v) ammonium persulphate (APS, Sigma) and N,N,N,N'-tetramethylethylenediamine (TEMED). The gels were composed of two layers: a 12% resolving gel (pH 8.8) that separated

the proteins according to size; and a lower percentage stacking gel (pH 6.8) that insured the proteins simultaneous entry into the separating gel at the same height. The composition of the resolving and stacking gels is given in Table 2.8. Samples were loaded onto the gels with Spectra$^{TM}$ Multicolor Broad Range Protein Ladder (Fermentas). The gels were run at 100 V for about 1.5 hours.

| Solution | Resolving Gel | Stacking Gel |
|---|---|---|
| 30% acrylamide | 3 ml | 850 μl |
| Resolving gel buffer | 2.5 ml | - |
| Stacking gel buffer | - | 1.25 ml |
| $dH_20$ | 2 ml | 1.875 ml |
| 10% APS | 50 μl | 20 μl |
| TEMED | 4 μl | 5 μl |

**Table 2.8: Volumes of solutions used for making SDS-PAGE gels.** Volumes given are for one mini gel.

### *2.2.4.3 Transfer of proteins to nitrocellulose membrane*

Electrophoretically size separated proteins were subsequently transferred from SDS-polyacrilamide gels to membranes. Gels were immersed along with eighteen pieces of filter paper and one nitrocellulose membrane (Whatman), in transfer buffer. The transfer process was performed by placing nine pieces of filter paper, the nitrocellulose membrane, the gel, and finally the last nine pieces of filter paper on the electrophoretic apparatus. Air bubbles were carefully removed. Transfer of proteins was completed by running the electrophoretic apparatus at 54 mA per gel for 110 minutes. Following the transfer, nitrocellulose membranes were briefly incubated with Ponceau S stain for confirming the presence of transferred proteins.

### *2.2.4.4 Western blotting*

Immunodetection of specific proteins transferred onto nitrocellulose membranes was performed via Western blotting. Membranes were washed in TBST to remove all Ponceau S stain and then incubated in blocking buffer for 1 hour at RT. Membranes were then incubated with the primary antibody diluted in the blocking solution for 2 hours at RT or at 4°C

overnight. Membranes were then washed 6 times in TBST, each wash lasting a minimum of 5 minutes. The appropriate peroxidise- conjugated secondary antibody was then diluted in blocking solution and incubated with the membrane for 1 hour at room temperature. Washes followed as described after primary antibody incubations. Membranes were then incubated for 2 minutes with equal volumes of Solution A and B of the ECL Reagent or 5 minutes when using ECL Advanced Reagent (GE-Healthcare). Lastly, membranes were developed and quantification of bands performed using an Optichem detector with associated software (Ultra Violet Products) (Geoff Holman's laboratory, University of Bath).

### 2.2.5 Statistical analysis

Means and Standard Deviations (SDs) were calculated and plotted using Microsoft Excel. Each experiment was repeated in triplicate unless otherwise stated. $P < 0.05$ was considered significant. Statistical analysis was carried out using unpaired Student's *t* tests.

# 3 RASSF7 expression in mammalian tissues

## 3.1 Introduction

***Expression of classical RASSFs***

Alterations in gene expression is a mechanism for loss of tumour suppressor gene function in cancer and the most studied aspect of the expression of the classical RASSF proteins has been associated with hypermethylation of gene promoters and reduced expression during tumourigenesis.

The best characterised *RASSF1* isoforms, *RASSF1A* and *RASSF1C* are ubiquitously expressed in normal tissues (Ponting and Benjamin, 1996; Yamamoto *et al.*, 1999) as confirmed by Northern blot analysis. The expression of the remaining *RASSF1* splice variants (*RASSF1B, D-G*) has been either associated to specific cell types (*RASSF1B*: hematopoietic cells, *RASSF1D*: cardiac cells, *RASSF1E*: pancreatic cells) or not extensively studied (*RASSF1F, RASSF1G*) (Dammann *et al.*, 2000; Burbee *et al.*, 2001).

Loss of *RASSF1A* expression is frequently observed in various human cancers, in association with promoter hypermethylation (Sekido *et al.*, 1998; Pfeifer and Dammann, 2005; Agathanggelou *et al.*, 2005). Epigenetic inactivation of *Rassf1A* was found via bisulphite sequencing in 40% of NSCLC (Agathanggelou *et al.*, 2003), in 72% small cell lung cancers (SCLC) (Dammann *et al.*, 2001a; Burbee *et al.*, 2001), in 62% of breast cancers (Dammann *et al.*, 2001b), in 60% gastric tumours, in 40% ovarian tumours, in 50% prostate tumours (Liu *et al.*, 2002b), in 60% bladder tumours and in 52% neuroblastoma (Yan *et al.*, 2003; Tommasi *et al.*, 2005) and not surprisingly RASSF1A is reported to be one of the most methylated tumour suppressors (Astuti *et al.*, 2001; Harada *et al.*, 2002; Yan *et al.*, 2003; Wong *et al.*, 2004; Banelli *et al.*, 2005; Lazcoz *et al.*, 2006). The association between loss of *RASSF1C* expression and carcinogenesis is more controversial as it was reported only in some transformed ovarian and renal cell carcinoma cell lines (Vos *et al.*, 2000;

Dreijerink *et al.*, 2001). Thus *RASSF1C* may have a tissue specific effect. Loss of expression of other *RASSF1* variants was shown (*RASSF1B*) or predicted (*RASSF1D, RASSF1E, RASSF1F, RASSF1G*) to be concomitant with loss of *RASSF1A* expression mainly because they share the same promoter region (Lee *et al.*, 2001; Burbee *et al.*, 2001; Harada *et al.*, 2002; Endoh *et al.*, 2003).

Northern blot and reverse transcription-PCR (RT-PCR) analyses revealed the presence of *RASSF2, RASSF3* and *RASSF4* transcripts in most normal tissues (Tommasi *et al.*, 2002; Vos *et al.*, 2003a; Eckfeld *et al.*, 2004). *RASSF2A*, the only RASSF2 isoform with a 5' CpG island and predicted promoter region (Hesson *et al.*, 2005), is reported to be methylated in 70% of primary colorectal cancer cell lines (Hesson *et al.*, 2005; Akino *et al.*, 2005), in primary NSCLC, lung tumour cell lines (Vos *et al.*, 2003a; Kaira *et al.*, 2007), gastric cancer and nasopharyngeal carcinoma, in which it positively correlates with lymph node metastasis (Zhang *et al.*, 2007). Similarly to *RASSF2A*, CpG island methylation was also correlated with abnormally low levels of *RASSF4* in breast, lung, colorectal and kidney tumour cell lines and in primary lung and breast tumours (Eckfeld *et al.*, 2004). On the other hand, *RASSF3* was found to be transcribed in all human cancer cell lines (including haematological, colorectal, lung, melanoma and cervical cell lines) examined (Tommasi *et al.*, 2002), which correlates with the absence of methylation in either gliomas (Hesson *et al.*, 2004) or colorectal tumour cell lines (Hesson *et al.*, 2005).

NORE1A is ubiquitously expressed, whereas NORE1B is predominantly expressed in lymphoid tissues, as shown by Northern blotting (Tommasi *et al.*, 2002; Vos *et al.*, 2003b). Several cancer cell lines express very low levels of *NORE1A* transcript (promyelocytic leukaemia HL-60, lymphoblastic leukaemia MOLT-4, Burkitt's lymphoma Raji, lung carcinoma A549 and melanoma G361 cells) and have absent or down-regulated expression of *NORE 1B* (Hela, A549 and G361) (Tommasi *et al.*, 2002; Vos *et al.*, 2003b). *NORE1A* mRNA levels were found to be significantly suppressed in pheochromocytoma primary tumours compared

with normal adrenal medulla (Li *et al.*, 2005). At a protein level, NORE 1A/B expression was reported to be severely reduced or absent in epithelial-derived adenocarcinomas and SCLCs (Vos *et al.*, 2003b). The inactivation of NORE1A commonly results from promoter hypermethylation. The aberrant *NORE1A* promoter methylation is frequently found in lung tumour cell lines, primary lung tumours and breast tumours (Vos *et al.*, 2003b; Hesson *et al.*, 2003). In contrast, *NORE1B* promoter was found to be unmethylated in all lung and breast cell lines and primary tumours examined (Hesson *et al.*, 2003) and gliomas (Hesson *et al.*, 2004). However, more recently *NORE1B* was reported to be epigenetically silenced in human hepatocellular carcinoma (Macheiner *et al.*, 2006).

*RASSF6* transcript was shown to be present in normal blood and numerous tissues analysed including bone marrow where no promoter methylation occurred (Hesson *et al.*, 2009). However, reduced transcript levels were found in 30-60% of primary tumour tissues in the breast, colon, kidney, liver, pancreas, stomach and thyroid gland (Allen *et al.*, 2007). Given that only a minority of tumour cell lines examined showed promoter methylation, Allen and co-workers proposed that loss of *RASSF6* expression in primary tumours may be caused by gene deletions as well as epigenetic mechanisms of silencing (Allen *et al.*, 2007). Exceptions to this theory are the T and B childhood acute lymphoblastic leukaemias, in which *RASSF6* was the only highly methylated classical *RASSF* member (Hesson *et al.*, 2009).

***Expression of N-terminal RASSFs***

There is currently limited data in the literature regarding the expression of the novel members of the RASSF family.

Data published during this project showed that *RASSF8* has a ubiquitous expression pattern in normal human adult tissues, as confirmed by RT- PCR (Lock *et al.*, 2010), and is shown to have reduced transcript levels in lung adenocarcinoma compared to normal tissue via Real-Time PCR (Falvella

*et al.*, 2006) and in male-germ cell tumours via microarray analysis (Korkola *et al.*, 2006).

The expression of *Rassf9* has been examined by Northern blot hybridisation analysis and RT-PCR in the rat. *Rassf9* mRNA transcripts were detected in testis, kidney, skeletal muscle, liver, lung, brain heart, pituitary gland, adrenal gland and ovary (Chen *et al.*, 1998). So far no studies have been undertaken in human samples.

The major findings on human *RASSF10* refer to the methylation status of its promoter. The *RASSF10* CpG island is highly methylated in thyroid cancer (Schagdarsurengin *et al.*, 2009), T-cell acute lymphocytic leukaemia (ALL) and leukaemia cell lines (where *RASSF10* promoter hypermethylation correlated well with low levels of *RASSF10* expression) (Hesson *et al.*, 2009). However, *RASSF10* is unmethylated in normal bone marrow where RT-PCR analysis showed *RASSF10* to be normally present (Hesson *et al.*, 2009). *rassf10* showed a particular strong expression in the *Xenopus* tadpole brain (Hill *et al.*, 2010) and also the potential *Drosophila* orthologue CG32150 is expressed in the nervous system (Reeves and Posakony, 2005). Following on from this study, Hill *et al.* reported the strong association of *RASSF10* promoter methylation with the most malignant astrocytomas and with the worst progression free survival and overall survival in patients with glioblastoma at the early stage of their development (Hill *et al.*, 2010).

The N-terminal RASSF member this thesis focuses on, RASSF7, was previously studied in developing *Xenopus* embryos. *rassf7* expression was detected via ISH in the outer epithelial cells of the *Xenopus* embryo and also at a later stage in the tadpole, with a broad expression including the brain, eye, ear, branchial arches, and embryonic kidney (Sherwood *et al.*, 2008).

The only data referring to RASSF7 expression in organisms other than *Xenopus* derive from microarray studies in which human *RASSF7* is shown to be up-regulated in cancer. *RASSF7* expression is reported to be increased in pancreatic ductal adenocarcinoma (Logsdon *et al.*, 2003;

Friess *et al.*, 2003; Brandt *et al.*, 2004), pancreatic islet cell tumours (Lowe *et al.*, 2007), endometrial cancer (Mutter *et al.*, 2001; Colas *et al.*, 2011), where its under-expression correlated with good prognosis (Mhawech-Fauceglia *et al.*, 2010), and ovarian clear cell carcinoma (Tan *et al.*, 2009) relative to normal tissue. Furthermore, *RASSF7* is down-regulated by the tumour suppressor BRCA 1 (breast cancer 1), suggesting its expression would be increased in cancer cells which have lost BRCA 1 function (Welcsh *et al.*, 2002). Gene-expression studies have also linked RASSF7 to hypoxia, a peculiar feature of many solid tumours (Kenneth and Rocha, 2008). In fact, *RASSF7 mRNA* levels were found to be up-regulated by hypoxia in the MCF7 breast cancer line and in human umbilical vein endothelial cells (Camps *et al.*, 2008; Liang *et al.*, 2009). However, prior to the present study nothing was known about its expression under normal conditions and the consequent functional role of the protein. Therefore the primary aim of the work described in this chapter is to investigate the expression of mammalian RASSF7 expression at either a RNA transcript or protein level by using different approaches such as ISH and western blotting.

## 3.2 Results

### 3.2.1 In *silico* analysis

Initial studies were carried out by interrogating the NCBI database for preliminary predictions about the temporal and spatial expression of the *N-terminal RASSF* family members in the mouse and human. The expression profiles of the selected genes was determined by considering those tissues in which the overall number of ESTs (expression sequence tags) was equal or higher than 50000 (http://www.ncbi.nlm.nih.gov/UniGene/ESTProfile). The frequencies of ESTs were expected to give a rough indication of transcript expression levels.

*RASSF7*, *RASSF8*, *RASSF9* and *RASSF10* appeared to be differently expressed during development (Figure 3.1). Human and mouse *RASSF7* and *RASSF8* transcripts are present from the early stages of embryogenesis to adulthood in mouse (Figure 3.1A) and human (Figure 3.1B). On the contrary, no *RASSF9* and *RASSF10* ESTs were found for the initial developmental stages in mouse (Figure 3.1A) and their presence was either negligible or null in human (Figure 3.1B).

In addition to embryonic stage specific differences, differences were observed among the four genes in adult tissues. Different patterns and levels of expression in both species were seen (Figure 3.2). Overall, *RASSF7* and *RASSF8* seemed to be widely expressed in mouse (Figure 3.2A) and human (Figure 3.2B) samples whereas *RASSF9* and *RASSF10* were generally less expressed in mouse (Figure 3.2A) and with very few transcripts predicted in human tissues (Figure 3.2B).

Overall, the *in silico* analysis used as initial guidance for the subsequent experiments suggested that RASSF7 and RASSF8 were generally found to be broadly transcribed in a wide range of tissues and stages. Human *RASSF9* and *RASSF10* appeared to be less highly expressed.

Figure 3.1

Figure 3.2

## 3.2.2 RASSF7 expression during developmental stages

### *3.2.2.1 ISH on embryonic mouse sections*

To verify if the predictions derived from the *in silico* analysis about the expression pattern of *Rassf7* during murine development were correct, ISH was carried out on sectioned embryos and adult tissues using a *Rassf7 in situ* probe. The riboprobe should recognise the only mouse *Rassf7* transcript variant consistently annotated and reported to translate into a protein in the VEGA database (*Rassf7-001*, OTTMUST00000056147).

E10.5

At this developmental stage relatively high levels of *Rassf7* expression were seen throughout the embryo including the wall of the brain, neural tube and elements of hepatic primordium (Figure 3.3A). Expression was also high in regions of the developing heart (Figure 3.3A). Staining was seen with the antisense probe but not with the sense control.

E 15.5

During late embryogenesis, when most of the organs are distinct and easily distinguishable, *Rassf7* appeared to be expressed in all tissues but at varying levels. Particularly high levels of *Rassf7* RNA expression, detected by the antisense probe, could be seen in the brain, the gut, the heart (Figure 3.3B and 3.4), the lung, and the kidney (Figure 3.3B and 3.5). A slightly lower expression of *Rassf7* was observed in the liver and the pancreas (Figure 3.3B and 3.6).

### *3.2.2.2 ISH and IHC on adult mouse organ sections*

*Rassf7* was expressed in all adult tissues examined. Particularly strong *Rassf7* expression was seen in the respiratory mucosa delimitating the bronchial cavities, the endocrine and exocrine pancreas, and the brain. (Figure 3.7). In the brain there were regions of intense staining coinciding with the high presence of neuron cell bodies, as demonstrated by the H a E staining (Figure 3.8).

Figure 3.3

Figure 3.4

Figure 3.5

Figure 3.6

Figure 3.7

Figure 3.8

As shown in figure 3.8, in both the hippocampus and the cerebellum the grey matter strongly stained, apparently without labelling specific neuron types.

Unlike in the embryo though, the level of *Rassf7* expression was less uniform across the different organs. In the heart, the kidney and the liver the RASSF7 RNA staining was weak even if stronger than the corresponding sense control (Figure 3.9).

***Expression of RASSF7 protein***

The expression of Rassf7 in the mouse was also tested at a protein level by IHC conducted on an adult mouse tissue array kindly donated by Dr Jason Gill, University of Bradford. The high and broad expression of *Rassf7* was confirmed by utilising AVIVA rabbit anti human RASSF7 antibody, which is able to cross-react with mouse Rassf7. The antibody detected the Rassf7 protein in all the analysed samples previously tested for *Rassf7* transcripts (Figure 3.10).

Thus Rassf7 is ubiquitously expressed in embryonic and adult mouse tissues.

#### *3.2.2.3 Murine ISH pattern of other N-terminal RASSFs*

To elucidate whether *Rassf7* expression pattern during mouse development was a distinctive feature of this protein or reflected the expression of the other *N-terminal Rassf* members, hybridisation experiments were performed for *Rassf8* and *Rassf9*. *Rassf10* was investigated as a pseudogene at the time this project was initiated and therefore it was not considered.

In agreement with *Rassf7* results, *Rassf8* hybridisation signals were found to be broadly distributed early in development. At E10.5 the cephalic region, the heart and the primitive gut were evenly labelled (Figure 3.11A). *Rassf8* was ubiquitously expressed also during mid embryogenesis. At E15.5, the level of the *Rassf8* RNA signal was maintained high, if not enhanced, in the major organs, including brain, heart, kidney, liver, lung and spinal cord (Figure 3.11B). For this stage no significant differences

Figure 3.9

Figure 3.10

Figure 3.11

were observed between the level of expression of *Rassf7* and *Rassf8* (Figure 3.3B and 3.11B).

Expression analysis was also performed on adult mouse sections as done for *Rassf7*. In these tissues, a faint label with the *Rassf8* specific probe appeared in the liver, lung and kidney (Figure 3.12, left) but in the case of the brain, the heart and the pancreas no *Rassf8* hybridisation signals above the background were observed (Figure 3.12, right).

The other *N-terminal Rassf* gene, *Rassf9*, exhibited broad distribution in late embryogenesis but the intensity of the signal was less than *Rassf7* and *Rassf8* (Figure 3.13). ISH analysis on adult mouse tissue was not performed for *Rassf9* due to time constraints.

Overall, *Rassf7*, *Rassf8* and *Rassf9* are broadly expressed in the mouse embryo. In adult mouse tissues, such broad expression is maintained at high levels for *Rassf7*, whereas it seems weaker for *Rassf8*.

### 3.2.3 RASSF7 expression in human cell lines

Since cell lines could represent a useful system to study RASSF7 function, an investigation was performed to determine the lines in which RASSF7 was expressed.

The RASSF7 antibody used for the mouse IHC was predicted to react with human samples and recognise all human protein variants (Figure 4.1) and was therefore tested and utilised for probing different mammalian and human cell lines. Details of the cell lines used are shown in Table 3.1. All immunoblotted lysates showed a major band migrating at the predicted molecular weight of RASSF7, 34 kDa, indicating that RASSF7 is expressed in all cell lines tested (Figure 3.14).

Figure 3.12

Figure 3.13

Figure 3.14

| Cell line | Species | Description |
|---|---|---|
| PC12 | Rat | Derived from pheochromocytoma of a adrenal medulla |
| COS-7 | Monkey | Immortalised cell line derived from kidney cells |
| T293 | Human | Derived from embryonic kidney |
| Jurkat | Human | Immortalised cell line of T lymphocytes |
| OVCAR | Human | Ovarian carcinoma cell line |
| HeLa | Human | Immortal cervical cancer cells |
| Caco2 | Human | Epithelial colorectal adenocarcinoma |
| A549 | Human | Adenocarcinomic alveolar basal epithelial cells |
| SHSY5Y | Human | Neuroblastoma |
| HepG2 | Human | Liver carcinoma cell line |
| PANC-1 | Human | Non endocrine pancreatic cancer |
| THP-1 | Human | Acute monocytic leukaemia cell line |

**Table 3.1: List and description of the cell lysates immunoblotted for RASSF7.** Details of the cell lines were obtained from the American Type Culture Collection (ATCC) website: http://www.lgcstandards-atcc.org/ATCCCulturesandProducts/CellBiology/CellLinesandHybridomas/tabid/981/Default.aspx

Noticeably, most of the human cell lines examined were cancerous and still expressed RASSF7. Consistent with this result, IHC studies performed on cancer cell lines, grown as human xenografts in mice, showed intense staining pattern, often throughout the entire tumour cell (Figure 3.15 and 3.16). The level of expression could correlate with specific tumour types as they appeared to show differential expression patterns (Figure 3.15 and 3.16).

Thus RASSF7, unlike RASSF1A, expression, does not appear to be down-regulated in cancer cell lines.

## 3.2.4 Regulation of RASSF7 expression

Given the findings about *Xenopus* rassf7 mitotic function (Sherwood *et al.*, 2008), it is reasonable to wonder if the level of expression of human RASSF7 could be determined by the cell cycle stage. However, it should be noted that many mitotic proteins can be found also in non-dividing cells.

Figure 3.15

Figure 3.16

Disruption of normal cell cycle controls may lead to abnormal levels of proteins, a phenomenon observed in the tumours of various cancers. To address if the human RASSF7 protein was itself regulated in a cell cycle dependent manner, a human cell line expressing RASSF7 at high levels, HeLa (Figure 3.14), was used. HeLa cell lysates were enriched with M phase cells through nocodazole treatment (75 ng/ml) for 18 hours followed by mitotic shake off. Lysates were then probed for either RASSF7 or phospho histone H3 (Ser10) considered as marker for mitotic cells (Figure 3.17). There was no significant change in RASSF7 protein expression levels (Figure 3.17A and 3.17C), whereas the expression of the positive control increased as expected (Figure 3.17A and 3.17B), showing that RASSF7 expression does not increase during mitosis.

#### *3.2.4.1 RASSF7 response under hypoxic insult*

Hypoxia, the condition of insufficient oxygen supply to tissues, is associated with the metastatic potential of tumour cells and increases the expression of genes that also aerobically regulate invasion and metastasis. As a result, many solid tumours contain hypoxic regions. Hypoxia-inducible genes, such as vascular endothelial growth factor (Shweiki *et al.*, 1992), erythropoietin (Huang *et al.*, 1997), and CD105 (Li *et al.*, 2003), promote cell survival mainly by facilitating angiogenesis to sustain tumour growth.

Given the high expression of RASSF7 in numerous cancer cells (Figure 3.14, 3.15 and 3.16) and the results of previous microarray studies on hypoxia induced gene up-regulation (Camps *et al.*, 2008; Liang *et al.*, 2009), another factor to investigate in relation to RASSF7 protein levels could be the effect hypoxia has on RASSF7 expression.

To determine if RASSF7 protein levels were affected by hypoxia, HeLa cells were subjected to hypoxic insult (0.1% Oxygen) for 3 hours, 18 hours and 18 hours + 24 hour recovery in normoxic conditions. Then cell lysates from normoxic and hypoxic samples were probed for RASSF7. Both acute and prolonged hypoxic stress followed by recovery led to a significant RASSF7 over-expression compared to respective controls. A small but not

statistically significant increase in protein levels was found after 18 hours of hypoxic stress without recovery (Figure 3.18).

Figure 3.17

Figure 3.18

## 3.3 Discussion

This study sought to fully characterise the expression of RASSF7 in mammalian tissues. RASSF7 expression was shown to be ubiquitous in the developing and adult mouse and detectable in numerous human cancer cell lines. Hypoxia was demonstrated to induce RASSF7 over-expression at a protein level.

***Rassf7 expression in mouse and Xenopus embryo***

To date RASSF7 expression pattern has been examined exclusively in developing *Xenopus* embryo, where rassf7 has a maternal component and whose transcripts were found in neural tissue, epidermis, eye, ear, branchial arches and pronepheros. The neural and epidermal expression was reported to be maintained also during tadpole stages (Sherwood *et al.*, 2008). However, the lack of a suitable antibody did not allow the authors to ascertain if that pattern coincided with the protein distribution. It was also not known if such expression pattern was evolutionary conserved.

ISH experiments were therefore carried out on embryonic and adult mouse sections by using a mouse *Rassf7* in *situ* probe. *Rassf7* was seen ubiquitously and highly expressed during early embryogenesis, at E10.5, where not all organs are properly differentiated. At E15.5, *Rassf7* expression was still broadly ubiquitous and immuno-reactivity was maintained at high levels.

An interesting question, raised by comparing the RASSF7 expression pattern in *Xenopus* and mouse, is why there is a discrepancy between the tissue distribution. It is possible that the protein plays different roles in the two species. However, given that *Xenopus rassf7* exhibits both maternal and zygotic expression (Sherwood *et al.*, 2008), it cannot be excluded that *rassf7* expression is turned on only in those tissues where the maternal protein is exhausted. Another possible explanation is that in the early *Xenopus* embryo some N-terminal rassfs may have a partial redundant function and could play the same role of rassf7 in tissues in which this protein is not expressed. However, it has to be noted that the

stages considered for analysing the expression pattern in the two systems may not be comparable, and a more ubiquitous staining may be found in tadpoles at later stages. Furthermore ISH was performed on *Xenopus* wholemounts rather than on sections, which may be not sufficiently sensitive for detecting low levels of expression in some tissues.

***Rassf7/Rassf8 expression in the adult mouse***

The ubiquitous expression of *Rassf7* was found during adult stages, even if the level of expression varied, with particularly high levels seen in the lung, the pancreas and the brain. In the brain, the intensity of the immunoreactivity correlated with the cell density rather than with the cell type. An example of this was offered by the dentate gyrus, part of the hippocampus formation. No cell type specific staining was detected across the three layers of neurons forming this region, therefore the signal was determined by the number of cell bodies rather than a subset of cells expressing high levels of *Rassf7*.

Consistent with the above results, the IHC performed on an adult mouse tissue array showed broad expression of Rassf7 protein, thereby confirming the ubiquitous presence of Rassf7, as predicted by preliminary in *silico* analyses. Interestingly, the intensity of the staining appeared more uniform across the different tissues when compared to the one exhibited by the ISH counterparts. This may be due to incomplete fixation of the samples used for ISH. In future, quantitative RT-PCR could be used to confirm differences in mRNA expression between tissues.

A comparative study with the other N-terminal RASSFs showed that *Rassf8* and *Rassf9* were broadly expressed in the mouse embryo. *Rassf8* in particular, whose translated product exhibits 37% identity to Rassf7, was ubiquitously expressed throughout murine embryos, which raised questions over the possible physiological relevance of this expression pattern identical to *Rassf7*. In fact, the two human proteins could have redundant functions but preliminary findings published on *rassf7* and RASSF8 functions (Falvella *et al.*, 2006; Sherwood *et al.*, 2008; Langton *et al.*, 2009; Lock *et al.*, 2010) make this hypothesis unlikely. It is possible

instead that the members of the N-terminal RASSF group have specific distinct functions. A tissue specific role could be indeed suggested for *Xenopus rassf10*, whose striking pattern of expression in the brain was observed by Hill *et al.* (2010).

***RASSF7 expression in human cell lines***

Numerous microarray screenings have shown that *RASSF7* is up-regulated in cancer (Sherwood *et al.*, 2010) but only RNA levels have been investigated. The expression of RASSF7 protein in cancer has not been studied.

To develop a better understanding of RASSF7 expression, various mammalian cell lysates were probed for RASSF7 via a commercially available antibody proved to be suitable for detecting the protein. The immunoblotting showed that RASSF7 was expressed in all cell lines tested, most of which were derived from human cancers. This result was confirmed by immunolabelling different human xenograft tumours grown in mice with the same antibody. Several cancer cell types appeared to show differential expression and the strong staining did not seem to label specific structures within the cells. These data could be even more informative if the experiment was done with primary tumour samples and normal tissue controls to evaluate possible changes in RASSF7 distribution and expression.

***Regulation of RASSF7 expression levels***

Another aspect relating to RASSF7 expression is its regulation. RASSF7 did not exhibit cell cycle dependent changes in the constitutive levels of expression, as RASSF7 protein was not increased in mitotic cells. RASSF7 protein levels are subject to change though, as they were shown to increase in response to hypoxic stress, thus confirming previous microarray studies (Camps *et al.*, 2008; Liang *et al.*, 2009). Both acute and chronic hypoxic insult followed by recovery in normoxic conditions led to a significant over-expression of RASSF7 in HeLa cells. These data suggest a role played by this protein to prepare cells to adapt and survive under a hypoxic environment. This could be achieved, for example, with an

increase of the cell metabolism, namely by increasing glucose transport or by raising the levels of glycolytic enzymes.

Huang and collaborators suggested that the chromatin structure of *RASSF7* chromosomal region could play a role in the hypoxic regulation of gene expression as the genomic positions of *RASSF7* and *AK123483*, whose expression is similarly increased by hypoxia, are close (Huang *et al.*, 2010). In order to explore the RASSF7 regulation further using hypoxia, it would be important to study if RASSF7 is implicated in regulating either the upstream or the downstream signaling of the Hypoxia Inducible Factor (HIF) pathways, not only in malignant but also in physiological conditions.

It has been proved that the down-regulation of many classical RASSF tumour suppressors occurs via promoter methylation (van der Weyden and Adams, 2007; Richter *et al.*, 2009; Avruch *et al.*, 2009) and this seems to be the case also for *RASSF10* (Hesson *et al.*, 2009; Hill *et al.*, 2010). However, our collaborators did not observe any methylation for RASSF7 in any of the carcer (including leukaemia) cell lines analysed (Hesson *et al.*, 2009; Recino *et al.*, 2010). Consistent with these data, RASSF7 is expressed in various cancer cell lines (shown in this study) so it is reasonable to infer that RASSF7 cannot be a tumour suppressor as other RASSF proteins.

## 3.4 Conclusion

The current study has investigated for the first time the expression of mammalian RASSF7. *RASSF7* was found to be ubiquitously and highly expressed in the mouse in a stage and tissue independent manner. Human RASSF7 was also seen expressed in every cell lines analysed, most of which were cancerous. RASSF7 protein levels were not cell cycle dependent but could be up-regulated by hypoxia, a distinctive feature of many tumours which is known to cause a large number of gene-expression changes. The physiological relevance of RASSF7 expression pattern has still to be determined, but the broad expression across tumour cell lines and the lack of promoter methylation demonstrated in previous studies suggest that, unlike other RASSF proteins, RASSF7 cannot act as tumour suppressor.

# 4 Cellular distribution of human RASSF7

## 4.1 Introduction

***Cellular localisation of the classical RASSFs***

RASSF1A represents the best documented RASSF protein in relation to its subcellular distribution (Richter *et al.*, 2009). During interphase, it was shown that epitope tagged and endogenously expressed RASSF1A proteins co-localise with the microtubule network in different mammalian cell lines, including A549, LNCaP, HeLa and NIH-3T3 (Liu *et al.*, 2003; Song *et al.*, 2004). During mitosis RASSF1A, either tagged or endogenous, localises to the centrosomes (prophase) and to the spindle fibres and poles (metaphase and anaphase), whereas during cytokinesis it relocates to the midbody (Liu *et al.*, 2003; Song *et al.*, 2004). However, more recently *Guo et al*. proved that in HeLa cells endogenous RASS1A showed centrosomal localisation throughout the cell cycle (Guo *et al.*, 2007). Ectopic or endogenous RASSF1A was also demonstrated to be recruited to the internalised death receptor TNF-R1 in response to TNF$\alpha$ stimulation in human osteosarcoma U2OS, lung cancer H1299, and monkey kidney COS-1 cell lines (Baksh *et al.*, 2005; Foley *et al.*, 2008). The only other RASSF1 isoform whose localisation has been studied is RASSF1C. Endogenous RASSF1C localises primarily to the nucleus (Song *et al.*, 2004; Kitagawa *et al.*, 2006), where it is anchored in promyelocytic leukaemia-nuclear bodies via the binding with the apoptotic protein Daxx (Kitagawa *et al.*, 2006). However, RASSF1C was also found to localise in the cytoplasm of HeLa cells subjected to ultraviolet (UV) irradiation (Kitagawa *et al.*, 2006). Liu and co-workers reported that an antibody that reacted equally with RASSF1A, RASSF1B and RASSF1C revealed RASSF1 association with mitochondria in interphase cells (Liu *et al.*, 2005). The over-expression of RASSF1A causes the rearrangement of the microtubules into either circular or bundled perinuclear rings (Dallol *et al.*, 2004) and stabilises microtubules from depolymerisation (Liu *et al.*,

2003; Vos *et al.*, 2004; Rong *et al.*, 2004; Dallol *et al.*, 2004), similar to what was reported for RASSF1C (Rong *et al.*, 2004; Liu *et al.*, 2005).

Little is known about the other RASSF proteins. Endogenously expressed RASSF2 was shown to be nuclear via Western blotting analysis performed on nuclear and cytoplasmic fractions of H417 and H720 lung cancer cell lines (Cooper *et al.*, 2008). However, epitope tagged RASSF2 was shown to be both nuclear and cytoplasmic in gastric cancer JRST cells (Maruyama *et al.*, 2008). Ectopic RASSF2 was found to be predominantly nuclear also in COS-7, HeLa, 293 and breast tumour cell lines MCF7 and HTB19, but only when the putative nuclear localisation signal in its N-terminal region was not mutated (Cooper *et al.*, 2008).

The subcellular localisation of RASSF3 and RASSF4 proteins has not been determined.

Endogenous and GFP-NORE1A were seen to localise at the centrosomes of human lung epithelial cells (Moshnikova *et al.*, 2006) and, when over-expressed in cancer A549 and normal cells, NORE1A labelled also the microtubules (Moshnikova *et al.*, 2006). In other reports, GFP-NORE1A was observed in both nucleus and cytoplasm of transfected monkey COS-7 cells (Park *et al.*, 2008; Kumari *et al.*, 2010), where it associated to a variety of subcellular structures or organelles, including microtubules, mitochondria and perinucleus (Park *et al.*, 2008).

RASSF6 localisation has not been extensively investigated. So far it has only been shown that FLAG-RASSF6 localises in both the cytosol and the nucleus of HeLa cells (Ikeda *et al.*, 2007).

Further investigations need to be carried out in order to improve our understanding of the localisation of the classical RASSF proteins, but at the moment centrosomes and microtubules seem to be their best characterised sites of activity.

***Cellular localisation of the N-terminal RASSFs***

Boa, the RASSF8 *Drosophila* orthologue, was found to co-localise with the adherens junction molecule E-cadherin in wing epithelial cells (Langton *et*

*al.*, 2009). In agreement with these data, endogenous human RASSF8 was observed within the nucleus and at the cell membrane at sites of cell-cell contact of A549 and H1792 lung cancer cells, where RASSF8 interacts with E-cadherin (Lock *et al.*, 2010). In both A549 and H1792 cell lines human RASSF8 co-immunocolocalised with β-catenin, which is a subunit of the cadherin protein complex, further confirming the subcellular distribution of the protein (Lock *et al.*, 2010).

Exogenous RASSF9 was found to associate with recycling endosomes in EGFP-RASSF9 transfected CHO cells (Chen *et al.*, 1998), but its endogenous localisation is not known.

Recently RASSF10 was shown to be associated with the spindle poles during metaphase/anaphase in A549 cells. During late cytokinesis RASSF10 was reported to relocate back to the cytoplasm, where it was seen to have a diffuse or perinuclear distribution (Hill *et al.*, 2010).

***RASSF7 localisation in Xenopus***

The first attempt to establish RASSF7 localisation was made by Sherwood and colleagues in 2008 when a *Xenopus* N-terminal GFP-, and a C-terminal HA-fusion constructs were used by injecting *Xenopus* embryos. The authors found that both constructs localised to discrete dots adjacent to the nuclei of expressing cells. This staining localised to the centrosomes, as indicated by the co-immunolabelling with γ-tubulin (Sherwood *et al.*, 2008).

The localisation of the human RASSF7 protein has not been studied so it has been investigated in the present study by analysing the endogenous and ectopic distribution of the protein in human cells via confocal immunofluorescence.

## 4.2 Results

### 4.2.1 Localisation of endogenous human RASSF7

The availability of a reliable anti-RASSF7 antibody on the market made it possible to investigate the subcellular distribution of endogenous human RASSF7. The polyclonal antibody used was produced in rabbits immunised with a synthetic peptide corresponding to a region of human RASSF7 partly overlapping with the first predicted coiled coil domain of the protein (Figure 4.1A and 4.1B). Based on protein sequence analysis, the antibody should recognise all predicted RASSF7 splice variants (Figure 4.1B).

**A**

MLLGLAAMELKVWVDGIQRVVCGVSEQTTCQEVVIALAQAIGQTGRFVLVQRLREKERQLLPQECP
VGAQATCGQFASDVQFVLRRTGPSLAGRPSSDSCPPPERCLIRASLPVKPRAALGCEPRKTLTPEP
APSLSRPGPAAPVTPTPGCCTDLRGLEL**RVQRNAEELGHEAFWEQELRREQARERE**GQARLQ
**ALSAA**TAEHAARLQALDAQARALEAELQLAAEAPGPPSPMASATERLHQDLAVQERQSAEVQGS
LALVSRALEAAERALQAQAQELEELNRELRQCNLQQFIQQTGAALPPPPRPDRGPPGTQGPLPPAR
EESLLGAPSESHAGAQPRPRGGPHDAELLEVAAAPAPEWCPLAAQPQAL

**B**

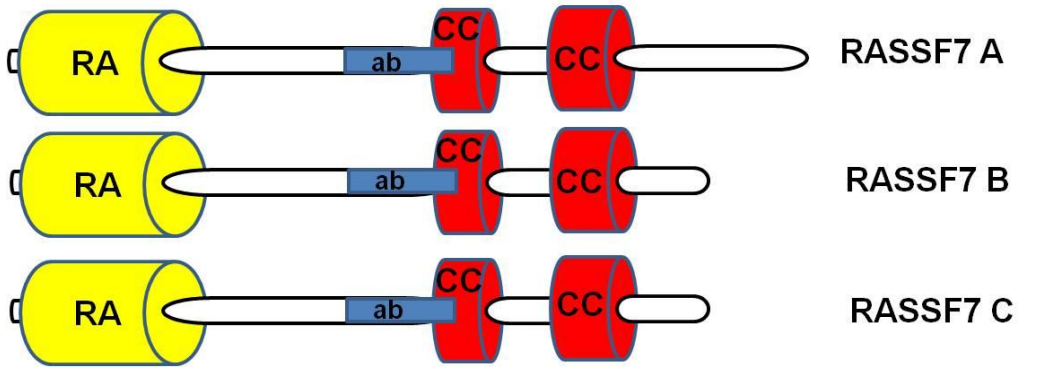


**Figure 4.1: Human RASSF7 protein variants**. RASSF7 A protein sequence (A) and schematic diagram of the domain structure of the three RASSF7 splice variants (B). The RA domain has been highlighted in yellow and the two coiled coil (CC) regions in red. In bold and blue the peptide sequence used for producing the antibody (ab).

Given the high RASSF7 expression levels shown by HeLa cells via immunoblotting (Chapter 3, Figure 3.14), this human cervical cancer cell line was used for localisation analysis. Initial studies failed to detect the

endogenous protein and it was discovered later that the antibody required antigen retrieval to be functional. The specificity of the antibody was confirmed by the lack of staining in RASSF7 KD cells (see chapter 5). RASSF7 was found to localise to specific structures adjacent to the nucleus throughout the cell cycle (Figure 4.2). Double immunolabelling with γ-tubulin showed perfect overlap with the RASSF7, indicating that the endogenous protein localises to the centrosomes in both dividing and non dividing HeLa cells (Figure 4.3). Thus RASSF7 is a centrosomal protein in human cells.

#### *4.2.1.1 Nocodazole treatment for investigating if RASSF7 centrosomal localisation is microtubule dependent*

RASSF7 could be an intrinsic component of the centrosome or alternatively it could be trafficked to these organelles via the microtubules. To see if RASSF7 localisation was maintained when the microtubule network was disrupted, HeLa cells were treated with the microtubule depolymerising drug nocodazole, which was able to depolymerise most of the microtubules within the cells (Figure 4.4A). Following on from the treatment, HeLa cells still exhibited RASSF7 immunoreactivity at the centrosomes (Figure 4.4B). RASSF7 is therefore a centrosomal protein whose localisation is microtubule independent.

### 4.2.2 Localisation of over-expressed human RASSF7

The ectopic expression of a gene often provides insight into its role. As seen in chapter 3, *RASSF7* expression is up-regulated in numerous cancer types (Sherwood *et al.*, 2010) and this could potentially lead to the mislocalisation of the protein from its original site with direct consequences to the protein function.

To understand if RASSF7 over-expression affected its localisation, two differently tagged human *RASSF7A* splice variant containing constructs were engineered with the Gateway cloning system and sequence confirmed. Both N-terminal GFP-, and C-terminal V5 fusion constructs

were transiently transfected into HeLa cells and immunodetection of the tagged proteins followed.

Figure 4.2

Figure 4.3

Figure 4.4

#### *4.2.2.1 Localisation of N-terminal GFP and C-terminal V5 tagged RASSF7 in HeLa cells*

Transfected cells were found to form one cytoplasmic inclusion at moderate levels of N-terminal GFP- and C-terminal V5- tagged RASSF7 over-expression (Figure 4.5A and 4.5B, arrowheads). However, when the level of expression of the ectopic protein was very high, multiple cytoplasmic punctuate structures were seen in the cell (Figure 4.5A and 4.5B, arrows). This phenomenon was not observed when expressing GFP alone (Figure 4.5C).

GFP-RASSF7 and RASSF7-V5 proteins were shown to localise to the same structures when co-transfected into the cell (Figure 4.6). In cells over-expressing RASSF7 at moderate levels, such structures were demonstrated to be centrosomes by the dual labelling experiment with either pericentrin or $\gamma$-tubulin, components of the pericentriolar material (Figure 4.7 and 4.8).

No association with the microtubules was observed when RASSF7 was exogenously expressed and centrosome spots were still visible in cells transfected with fluorescently tagged RASSF7 and immunostained with $\alpha$-tubulin (Figure 4.9). This does not support a possible microtubule stabilising role for RASSF7, as observed for RASSF1A (Liu *et al.*, 2003; Vos *et al.*, 2004; Rong *et al.*, 2004; Dallol *et al.*, 2004). From the data presented, it is clear that RASSF7 maintains its centrosomal localisation pattern when it is moderately over-expressed.

### 4.2.3 Cellular localisation of human RASSF8

RASSF8 is the RASSF protein with the most sequence similarity to RASSF7. Given the identical expression pattern shown in the mouse embryo (Chapter 3), it is plausible that the two proteins localise to the same structures in the human cells.

Figure 4.5

Figure 4.6

Figure 4.7

Figure 4.8 and 4.9

During the performance of this investigation, Lock and colleagues characterised RASSF8 localisation (2010). HeLa cells were stained for endogenous RASSF8 with a commercial antibody and examined by confocal microscopy. RASSF8 was detected within the nucleus (Figure 4.10A, arrowheads) and at the cell membrane (Figure 4.10A, arrows) of non-dividing cells (in agreement with the work of Lock and colleagues), whereas it localised predominantly to the cytoplasm of the cells in M phase (Figure 4.10B). Therefore RASSF8 was proved to be neither centrosomal nor associated to the microtubules. No specific staining above the background was observed for the negative control (data not shown), suggesting that the antibody recognised RASSF8 protein.

When over-expressed, RASSF8 tended to form aggregates which varied in size and number in HeLa cells. Even when expressed at lower levels, RASSF8 forming inclusions were not immunolabelled by pericentrin, indicating that those structures were not centrosomes (Figure 4.11A). In agreement with this result, cells co-transfected with RASSF8-GFP and RASSF7-V5 did not show co-localisation (Figure 4.11B).

Thus, RASSF7 and RASSF8 show a different localisation pattern within human cells.

Figure 4.10

Figure 4.11

## 4.3 Discussion

In the present chapter human RASSF7 localisation has been analysed. Human RASSF7 has been shown to localise to the centrosomes in a microtubule independent manner and to maintain its centrosomal localisation when over-expressed at moderate levels. It has also been demonstrated that human RASSF7 and human RASSF8 do not exhibit the same intracellular localisation within the human cells.

RASSF7 localisation pattern is maintained across species as this protein has been found to localise to the centrosomes in *Xenopus* (Sherwood *et al.*, 2008), mouse embryonic fibroblasts (personal communication from Nicole Antonio, University of Bath), as well as in the dividing and non-dividing human cells examined in the present study. In future, electron microscopy could determine where RASSF7 localises within the centrosome, and whether it is a component of the pericentriolar material or part of the centrioles.

The centrosomes, as main MTOCs, orchestrate microtubule nucleation and spindle assembly during cell division, which involve a complex array of centrosome-associated proteins. *Xenopus* rassf7 has been shown to be essential for progression through mitosis and mitotic spindle formation (Sherwood *et al.*, 2008). Likewise, many centrosomal proteins contribute to the fine control of the cell cycle, and whose deregulation occurs during tumourigenesis. In fact, knocking out *Rassf1A* in mice causes an increased frequency of tumour formation (Tommasi *et al.*, 2005). Therefore it is plausible that human RASSF7 plays an equally important role in regulating mitosis and cancerogenesis.

Human RASSF7 is an integral centrosomal component. In fact human RASSF7 localisation was maintained when microtubules were lost, in contrast to *Xenopus* rassf7 which localised to the centrosomes in a microtubule dependent manner (Sherwood *et al.*, 2008). The discrepancy could be well due to the use of a fusion protein in the *Xenopus* experiments. It would be interesting to test this hypothesis by inducing the expression of fluorescently labelled human RASSF7 prior to treating the

cells with a microtubule depolymerising drug and establishing if the localisation of tagged human RASSF7 is lost.

Assuming that the subcellular distribution of RASSF7 is related to the role it plays in the cell, its mislocalisation could affect its activity. A protein could differently localise within the cell according to its levels of expression. Such a phenomenon was observed in the RASSF family, where the centrosomal NORE1A labelled the microtubules when over-expressed (Moshnikova *et al.*, 2006). This could be the case also for RASSF7, whose levels of expression are up-regulated in numerous tumours (Sherwood *et al.*, 2010). However, the over-expression of RASSF7, obtained via the transfection of fusion constructs in HeLa cells, confirmed the endogenous localisation results, suggesting that RASSF7 localises to the centrosomes when its expression levels are moderately altered. High levels of RASSF7 over-expression could well induce ectopic RASSF7 to form aggregates in the cell, which could explain the formation of numerous inclusions.

To mimic the in *vivo* situation more closely, RASSF7 could be over-expressed without any tag and preferably in normal cells. Nevertheless, the fact that the ectopic RASSF7 behaved in the same way whether it was tagged at its N (GFP) or C (V5) terminus and whether it was exogenously expressed in HeLa or A549 (data not shown) cells made the result more robust. In this respect, a further confirmation could be obtained by analysing RASSF7 localisation in HeLa cells subjected to hypoxia treatment, that, as shown in chapter 3, induces the over-expression of the protein.

The availability of tagged RASSF7 proteins could be useful in future for investigating what RASSF7 protein domains are necessary for its localisation and protein interactions. The use of labelled truncated versions of RASSF7 could verify if RASSF7 protein interactions are mediated by its coiled coil domain, which is a common feature of centrosomal proteins (Andersen *et al.*, 2003).

Despite the structural and phylogenetic differences between RASSF7 and the classical RASSF proteins; RASSF1A, NORE1A and RASSF7 all show a similar localisation at the centrosome. However, ectopic RASSF7 does not seem to be a microtubule-binding protein as previously seen for RASSF1A (Liu *et al.*, 2003) and NORE1A (Moshnikova *et al.*, 2006). Microtubule localisation of RASSF1A was proved to occur when the expression levels of RASSF1A were not physiological (Liu *et al.*, 2003). This result suggests that unlike RASSF1A, RASSF7 does not have a microtubule stabilising role. To ascertain if this was the case, it would be important to determine if forced expression of GFP-RASSF7 preserves microtubule integrity in cells subjected to nocodazole or ice treatment.

The lack of a stabilising effect in RASSF7 over-expressing cells makes it possible to speculate that RASSF7 could promote microtubule polymerisation rather than reducing microtubule dynamics as documented for RASSF1A (Liu *et al.*, 2003). If that was the case, RASSF7 over-expression could lead to cytoskeletal problems different to those reported for RASSF1A, which led to aberrant centrosome separation and bipolar spindle formation (Liu *et al.*, 2003).

The last section of this chapter aimed to analyse the degree of similarity of human RASSF7 and human RASSF8 localisation, given the protein sequence homology. Endogenous RASSF8 was found in the nucleus and at the cell membrane of interphase HeLa cells, and, at low levels, in the cytoplasm of mitotic HeLa cells. When over-expressed RASSF8 forming structures did not co-localise with GFP-RASSF7. Recently, Lock and colleagues shed light on human RASSF8 cellular distribution, by demonstrating that, in both A549 and H1792 cells, RASSF8 immunostaining co-localised with β-catenin at the adherens junction, whose formation and function required RASSF8 expression (Lock *et al.*, 2010). These data confirmed the work published by Langton and colleagues, who characterised Boa, the *Drosophila* RASSF7/8 orthologue, showed that it regulates cell-cell adhesion via dASPP interaction and is required for normal E-cadherin localisation (Langton *et al.*, 2009).

The data discussed here indicate that human RASSF7 is a centrosomal protein whereas human RASSF8 is differently located within the cell. This suggests that there may be substantial differences between the functions of the two proteins. It is possible that RASSF7 function has diverged from RASSF8 during evolution and has developed an independent role. In fact, It is already known that while *Xenopus* RASSF7 is required for completing mitosis (Sherwood *et al.*, 2008), *Drosophila* RASSF7/8 is not required for cell cycle progression (Langton *et al.*, 2009) and knocking down human RASSF8 produces an increase in proliferation (Lock *et al.*, 2010). RASSF8 has been proposed as a tumour suppressor gene in lung cancer (Falvella *et al.*, 2006), and could well exert this function by controlling the actin cytoskeleton organisation and consequently the integrity of the adherens junctions (Langton *et al.*, 2009; Lock *et al.*, 2010). Given the up-regulation in different cancers and the *Xenopus* data, it is tempting to speculate that human RASSF7 could be instead a centrosomally localised proto-oncoprotein involved in microtubule dynamics. The function of human RASSF7 needed to be studied to test this hypothesis. This will be carried out in the next chapter.

## 4.4 Conclusion

Human RASSF7 was shown to be a resident centrosomal component, whose localisation is not microtubule dependent as found in *Xenopus.* Despite localising to the centrosomes as RASSF1A and NORE1A, ectopic RASSF7 did not show any association to the microtubules as previously reported for RASSF1A and NORE1A. Moreover, human RASSF7 and human RASSF8 did not exhibit a similar localisation pattern within the human cells. In view of all these differences and despite the homology with other members of the family, it is therefore plausible that RASSF7 has a distinctive role amongst the RASSF proteins.

# 5 RASSF7 functional analysis

## 5.1 Introduction

The classical RASSF proteins have been implicated in a vast range of biological processes and are generally regarded as tumour suppressors (reviewed in chapter 1). RASSF1A, the best characterised member of the family, is involved in regulating microtubule stability, cell cycle progression, regulation of apoptosis, cell migration and is part of Hippo tumour suppressor network (Hesson *et al.*, 2007; Donninger *et al.*, 2007; Dallol *et al.*, 2009a). Some of the classical RASSF members, such as RASSF1A and NORE1A, have been shown to bind to RAS proteins (Vavvas *et al.*, 1998; Vos and Clark, 2006) and therefore may act as RAS effectors.

Little information is available on the biological properties of the N-terminal RASSF proteins [reviewed in (Sherwood *et al.*, 2010)]. RASSF8 was identified as a candidate gene involved in leukaemia and lymphoma formation in mice (Weiser *et al.*, 2007), may act as a tumour suppressor in lung cancer (Falvella *et al.*, 2006), and controls cell-cell adhesion (Langton *et al.*, 2009; Lock *et al.*, 2010). RASSF9 has been shown to bind to RAS proteins (Rodriguez-Viciana *et al.*, 2004) and could be involved in vesicle trafficking (Chen *et al.*, 1998). RASSF10 has been proposed to be a tumour suppressor in lymphoblastic leukaemias and glioblastomas (Hesson *et al.*, 2009; Hill *et al.*, 2010).

RASSF7 has been demonstrated to play an important role for cell cycle progression and survival in *Xenopus* (Sherwood *et al.*, 2008), but there are no reports on the role of this proteins in other organisms. If such an important role was conserved throughout evolution, RASSF7 could be an interesting therapeutic target in the case of human pathologies.

This chapter will try to broaden the current knowledge on the function of RASSF7 within human cells by analysing the consequences of RASSF7 KD via immunocytochemistry and FACS analyses.

## 5.2 Results

### 5.2.1 RASSF7 depletion prevents anchorage independent growth in H1792 cells

Numerous members of the RASSF family have been shown to be tumour suppressors and to inhibit cell growth (van der Weyden and Adams, 2007; Richter *et al.*, 2009). In particular, it has been shown that *RASSF6* and *RASSF8* depletion results in an increase of anchorage independent growth of the human lung adenocarcinoma cell line H1792 (Allen *et al.*, 2007; Lock *et al.*, 2010). To understand if RASSF7 functions in a similar way, the effect of RASSF7 KD on anchorage independent growth was analysed in H1792 cells. The cells were transfected with two different sets of double-stranded 21-nt short siRNA constructs, RASSF7 KD1 and RASSF7 KD2, which targeted respectively an RA domain coding region in exon 2 and a non coding RNA region in the last exon of all *RASSF7* transcripts (Figure 5.1). The results were assayed 72 hours later via Western blotting. RASSF7 expression was inhibited by RASSF7 KD2 RNA duplexes (Figure 5.2A). In contrast, RASSF7 KD1 did not efficiently knock down RASSF7 and this siRNA was used as an additional negative control along with the standard siRNA control (Figure 5.2A). H1792 cells showed significantly lower colony-forming activity in soft agar ($p<0.01$) after RASSF7 KD2 siRNA treatment as both the size and the numbers of colonies resulted drastically reduced (Figure 5.2B and 5.2C). These findings suggest that RASSF7 is essential for anchorage independent colony formation.

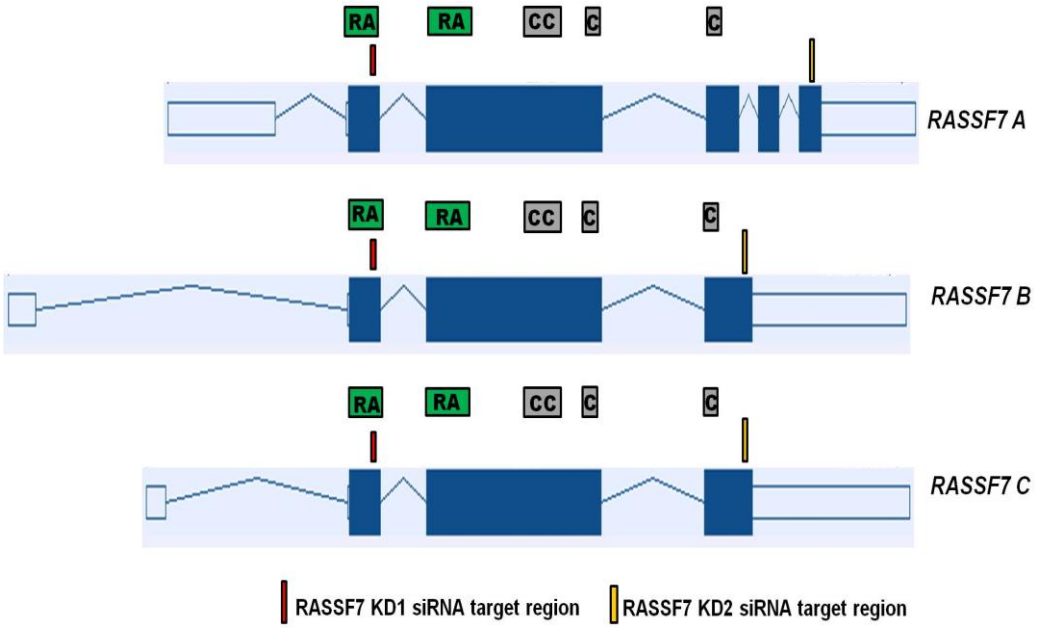


**Figure 5.1: *RASSF7* small interfering (si)RNA target regions.** Schematic representation of *RASSF7* transcript regions targeted by RASSF7 KD1 and RASSF7 KD2 siRNA constructs. The specific protein domains encoded by exon regions have been indicated above each *RASSF7* transcript. Blue and empty boxes are exons and lines connecting boxes are introns. Blue boxes are coding sequence, whereas empty boxes are UTRs. Green boxes: RA protein domains, grey boxes: coiled coil (CC) protein domains.

## 5.2.2 RASSF7 shRNA KD reduces HeLa cell number

RASSF7 function was also investigated via an alternative KD method. This time HeLa cells were used, as they also express RASSF7 (Chapter 3) and are easier to analyse than H1792 cells. Plasmids containing either RASSF7 specific, which targeted an RA domain coding region in exon 2 (Figure 5.3), or scrambled shRNA were transfected into HeLa cells and 24 hours later G418 was added to select for the positive cells.

Figure 5.2

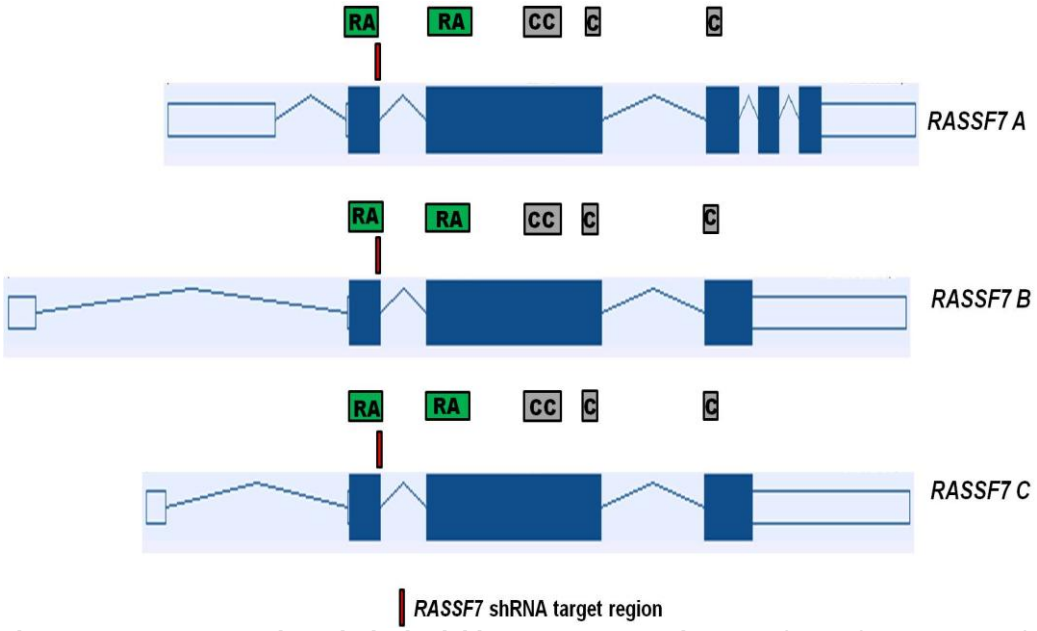


**Figure 5.3: *RASSF7* short hairpin (sh)RNA target regions.** Schematic representation of *RASSF7* transcript regions targeted by *RASSF7* shRNA. The specific protein domains encoded by exon regions have been indicated above each *RASSF7* transcript. Blue and empty boxes are exons and lines connecting boxes are introns. Blue boxes are coding sequence, whereas empty boxes are UTRs. Green boxes: RA protein domains, grey boxes: coiled coil (CC) protein domain.

HeLa cells were efficiently RASSF7 depleted, with more than 70% of the protein removed (Figure 5.4A). Consistent with this result, RASSF7 centrosomal localisation was lost in RASSF7 KD cells (Figure 5.5), which confirmed the specificity of the RASSF7 centrosomal staining. After culturing the cells with G418 for 14 days, the difference in cell number between control and RASSF7 shRNA tested cells was 2.6 $\pm$ 0.6 fold ($p<0.001$) (Figure 5.4B and 5.4C). This reduction in cell number cannot be explained by the G418 selection process as a significant difference in numbers (1.9 $\pm$ 0.4 fold) was observed also after re-plating selected RASSF7 and control KD HeLa cells at the same density. Thus, RASSF7 KD impairs normal cell growth.

Figure 5.4

Figure 5.5

## 5.2.3 Phenotypic characterisation of RASSF7 KD cells

To address why RASSF7 is required for growth, the subsequent characterisation following shRNA treatment was conducted in HeLa cells, as used previously.

### *5.2.3.1 Defects presented by RASSF7 KD cells*

The reduction in cell number observed in RASSF7 KD HeLa cells could be caused by increased apoptosis; however, the percentage of active caspase 3 positive RASSF7 KD cells was not significantly different from controls (Figure 5.6).

***Defects in mitotic cells***

To establish whether the reduction in cell number was caused by defective proliferation the effect of RASSF7 depletion was analysed in dividing cells. After the completion of selection, shRNAi transfected cells were fixed and stained with anti $\alpha$-tubulin antibody (microtubules) and DAPI (DNA) and analysed during different mitotic stages. No prominent differences between RASSF7 KD and control KD cells were observed at the onset of mitosis (Figure 5.7). However, later on in mitosis, once cells have reached metaphase, mitotic aberrations in RASSF7 KD cells became clearly evident (Figure 5.8). Loss of RASSF7 resulted in a failure in chromosomal congression (Figure 5.8B, left panel), demonstrated by an increase in the number of mitotic cells in a prometaphase-like state with no discernible metaphase plate (63% compared with 18% in controls, n=300, $p<0.01$) (Figure 5.8B, white arrows), an increase in metaphase cells with lagging chromosomes (21.5% compared with 6% in controls, n=300, $p<0.01$) (Figure 5.8B, red arrowhead) and a decrease in metaphase cells with correctly aligned DNA (15.7% compared with 75.7% in controls, n=300, $p<0.001$). RASSF7 deficient cells exhibited also spindle defects, with spindles showing less pronounced polarisation towards the DNA and a more radial organisation of microtubules (Figure 5.8B, red arrows). Finally, there was a small increase in the rate of multi-polar spindles (32,6% compared with 23.7% in controls, n=300, $p<0.05$) (Figure 5.8B, white arrowheads).

Figure 5.6

Figure 5.7

Figure 5.8

All these aberrations may have well contributed to the decrease in the number of anaphase cells, which was 5.7% compared with 16.9% in controls (n=180, $p<0.01$). However, despite being reduced in number, anaphase cells looked normal (Figure 5.9).

***Defects in interphase cells***

Given that RASSF7 normally localises to the centrosomes (Chapter 4), interphase centrosomes were analysed in RASSF7 KD cells by immunocytochemistry using an antibody against pericentrin, a component of the pericentriolar material. The rate of polycentrosomal cells was significantly enhanced when RASSF7 was knocked down (6.5 $\pm$ 1.5%) compared to controls (3.5 $\pm$ 0.5%) (n=1500, $p<0.05$) (Figure 5.10). Moreover, a conspicuous population (5.3 $\pm$ 0.7%) of multinucleated cells was generated when RASSF7 was knocked down, whereas control shRNAi cells had only 2.8 $\pm$ 0.5% of polyploid cells (n=1500, $p<0.01$) (Figure 5.11).

These data suggest that RASSF7 KD causes defects in mitosis; this could lead to polyploidy and the increase in the number of centrosomes in HeLa cells.

### *5.2.3.2 Analysis of DNA content of RASSF7 KD cells*

In order to see if the defects caused by RASSF7 KD were able to perturb the cell cycle progression, RASSF7 KD and control cells were fixed and stained with propidium iodide and their cell cycle stage determined by FACS analysis. The lack of RASSF7 did not significantly affect the percentage of diploid (2N DNA), dead and dying cells (<2N DNA) (Figure 5.12). However, RASSF7 depleted cells showed a small but significant increase in the number of cells with 4N DNA (24.55 % $\pm$ 1.35 compared with 21.25% $\pm$ 0.05 in controls, n=3 x $10^6$, $p<0.05$) (Figure 5.12). The number of aneuploid cells (>4N DNA) was not statistically different from control cells (Figure 5.12).

When RASSF7 KD and control HeLa were stained for phospo histone H3 (Ser10), the number of positive cells in the two samples was statistically equivalent (Figure 5.13) indicating that there was no significant difference

Figure 5.9

Figure 5.10

Figure 5.11

Figure 5.12

Figure 5.13

in the number of cells undergoing mitosis between RASSF7 KDs and controls. Thus, RASSF7 KD does not appear to cause a delay in mitosis. However, the increase in RASSF7 KD polyploidy cells suggests that RASSF7 may be required for cells to undergo cytokinesis.

#### *5.2.3.3 Localisation and activation of mitotic signaling proteins in RASSF7 depleted cells*

In order to understand the molecular basis for the mitotic defects described in the previous sections, the effect of RASSF7 KD on established regulators of mitosis was analysed. Analysis of the activation of PLK1 (Barr *et al.*, 2004), using an antibody which recognises its active form ($\alpha$-phospho PLK1, Thr210), showed similar staining in RASSF7 KD and control cells (Figure 5.14).

The localisation of RASSF1A, which is also involved in mitosis, to the centrosome appeared to be the same in control and KD cells (Figure 5.15).

The localisation and activation of Aurora A and Aurora B (Carmena *et al.*, 2009) was also examined (Figures 5.16 and 5.17). An antibody against Aurora A and B and a phospho-specific antibody which recognises the active form of Aurora A and B enzymes [$\alpha$-phospho Aurora A (Thr288), B (Thr232), C (Thr198)] were used. Aurora A was present at the centrosome (Figure 5.16) and Aurora B was present at the kinetochore during metaphase (Figure 5.17A) and at the mid-body during cytokinesis (Figure 5.17B) in both RASSF7 KD and control cells. In the RASSF7 KDs the active Aurora staining was present at the centrosomes (Figure 5.18B, arrows) where it overlapped with Aurora A staining (Figure 5.19B, white arrows), but it was strongly reduced at the kinetochore (Figure 5.18B, white arrowhead) where the co-localisation with Aurora B was almost undetectable (Figure 5.20A, arrowhead). In fact, only 9.3% of RASSF7 depleted cells showed strong active Aurora B staining compared with 83.8% in the controls ($n=240$, $p<0.001$). This loss appeared to be restricted to metaphase as the activation of Aurora B during cytokinesis appeared normal (Figure 5.20B).

Figure 5.14

Figure 5.15

Figure 5.16

Figure 5.17

Figure 5.18

Figure 5.19

Figure 5.20

Loss of Aurora B activity was confirmed by the lack of phosphorylation of CENP-A (Ser7) (Figure 5.21), a centromere specific histone H3 variant phosphorylated by Aurora B during mitosis (Zeitlin *et al.*, 2001). Only 22% of RASSF7 KD cells showed strong phospho CENP-A staining compared with 93,4% of control cells (n=210, $p<0.001$), providing further evidence that Aurora B is not activated normally in the absence of RASSF7.

Aurora B activation requires the recruitment of INCENP, inner centromere protein (Vader *et al.*, 2006b), but RASSF7 KD did not compromise the correct localisation of this protein at the kinetochore (Figure 5.22).

Overall these data suggest that the expression of centrosomal RASSF7 is critical for the correct activation of the mitotic signaling protein Aurora B at the kinetochore, whereas it does not seem to affect the localisation/ activation of PLK1, RASSF1A and Aurora A.

#### *5.2.3.4 Microtubule abnormalities* in RASSF7 *KD cells*

The localisation of RASSF7 at the centrosome and the spindle defects seen in the KDs suggest that RASSF7 might have a role in regulating microtubules. To test whether RASSF7 is required for microtubule polymerisation, microtubule re-growth was studied in RASSF7 depleted HeLa cells. Cells were treated with nocodazole to completely depolymerise the microtubules and then the cells were released into medium at 37°C to allow the microtubules to re-nucleate (Figure 5.23). In RASSF7 KD cells initial microtubule nucleation was not affected (5 minutes) but after 15 minutes microtubule polymerisation was perturbed in terms of timing and organisation, with 53% of RASSF7 KD cells showing a delay in microtubule re-growth compared with 14% of controls (n=100, $p<0.001$) (Figure 5.23). The microtubules in RASSF7 KD cells appeared more bent and looped than controls (Figure 5.23, white arrows). A similar delay in microtubule re-growth was seen also at 30 minutes. After 60 minutes, the number of microtubules in the RASSF7 KD cells resembled the controls (Figure 5.23), showing that RASSF7 KD cells eventually produce similar numbers of microtubules to control cells. However, the microtubule network still appeared quite disorganised, with individual

microtubule fibers less straight than the control microtubules (Figure 5.23, white arrows). RASSF7 is therefore a key regulator of microtubule growth.

Figure 5.21

Figure 5.22

Figure 5.23

## 5.3 Discussion

In the current chapter, RASSF7 function was analysed via a dual *RASSF7* RNAi approach. siRNA and shRNA mediated RASSF7 KD were shown to impair cell growth in H1792 and HeLa cells respectively. In HeLa cells, shRNA induced RASSF7 depletion affected numerous mitotic events and led to a little increase in the tetraploid cell population. RASSF7 depletion did not affect the localisation of PLK1, RASSF1A and Aurora A, but the activity of the mitotic signaling protein Aurora B was found compromised and the microtubule growth was defective.

***RASSF7 KD is required for cell growth***

The first approach used for unraveling RASSF7 function involved the use of two different sets of small interfering RNA oligonucleotides, only one of which specifically inhibited RASSF7 translation. It was found that the siRNA duplex capable of knocking down RASSF7 protein affected H1792 cell growth in soft agar. This result clearly suggests that, unlike RASSF6 and RASSF8 (Allen *et al.*, 2007; Lock *et al.*, 2010), RASSF7 does not seem to restrain cell growth. The fact the RASSF7 is required for growth may explain why its expression is not silenced in the cancer cell lines analysed in chapter 3. It is plausible that RASSF7 could promote cell growth instead. This hypothesis could be tested by over-expressing the protein in this cell line in order to see if the colonies formed would become bigger and more numerous compared to controls.

To address why RASSF7 is required for growth, shRNA KDs were carried out in HeLa cells. The alternative KD strategy ensured the specificity of the phenotype, and HeLa cells were used as they are easier to analyse than H1792 cells. Consistent with the data in H1792 cells, shRNA KD of *RASSF7* caused a reduction in cell number. It is tempting to speculate that if RASSF7 controls cell growth, increased levels of RASSF7 could also increase the tumourigenicity of cancer cells. If that was the case the injection of RASSF7 over-expressing cancer cells into immunocompromised organisms, should result in increased tumour formation. Such a result would confirm that the misregulation of RASSF7

and RASSF8 differently promote cancer progression, as RASSF8 was found to suppress tumour growth in *vivo* (Lock *et al.*, 2010).

***RASSF7 KD causes defects in mitosis***

The cell number reduction in HeLa cells could be caused by increased apoptosis, a phenomenon promoted by *rassf7* KD in the *Xenopus* embryo (Sherwood *et al.*, 2008). However, the percentage of active caspase3 positive human RASSF7 KD cells was not significantly different from controls. This result was further confirmed by flow cytometry as similar sub-G1 populations (which have less than 2N DNA content) were present in RASSF7 KD and control cells. It is possible that if the cells had been left to grow for longer, a higher cell death rate would have been seen in RASSF7 KDs. Another explanation for the reduced HeLa cell number could be a defective cell division. While mitotic spindles fail to form in *Xenopus rassf7* KD cells (Sherwood *et al.*, 2008), their formation in human RASSF7 KD cells is not blocked, although they did form abnormally. However, loss of RASSF7 was found to produce misoriented and lagging chromosomes, a higher rate of multi-polar spindles and a more radial organisation of the microtubules.

RASSF7 KD phenotype partly overlaps with the ones caused by the depletion of other centrosomal proteins involved in mitotic progression. Misaligned metaphase chromosomes were previously observed in HeLa cells following Aurora A siRNA (Marumoto *et al.*, 2003) and PLK1 depleted cells had been found to exhibit chromosomes in a rosette-like arrangement (Hanisch *et al.*, 2006). PLK1 KD cells exhibited spindles with monopolar or abnormally small bipolar microtubule arrays (Hanisch *et al.*, 2006), and also RASSF1A depletion was seen to cause spindle abnormalities (Dallol *et al.*, 2009a). In the examples reported however, the chromosomal congression defects detected seem to be less severe than the ones observed for RASSF7, and seem to be due to a defective centrosome maturation/ separation (Marumoto *et al.*, 2003; Hanisch *et al.*, 2006). On the other hand, RASSF7 KD mitotic cells exhibited apparently normal centrosomes at the opposite poles (data not shown), were able to originate microtubule spindles, but were less good at microtubule

polymerisation. Nevertheless, more work needs to be done: it would be important to test whether in RASSF7 KD cells other centrosomal functions are compromised and the centrioles and the pericentriolar material they consist of are equally partitioned for each spindle pole. The correct distribution of centrioles could be investigated by staining the cells with an antibody raised against centrin 3, a component of centriole (Paoletti *et al.*, 1996).

***RASSF7 KD causes abnormalities in interphase cells***

Both Aurora A and RASSF1A depletions were reported to augment the proportion of cells in the earlier stages of mitosis compared to later stages (Marumoto *et al.*, 2003; Dallol *et al.*, 2009a), with the majority of RASSF1A KD cells failing to proceed into anaphase (Dallol *et al.*, 2009b). Time lapse video microscopy could determine the duration of a cell cycle for RASSF7 KD cells and provide an explanation for the reduced number of anaphase RASSF7 depleted HeLa cells, which was a third of the control counterparts, in agreement with the *Xenopus* data (Sherwood *et al.*, 2008). It would also be interesting to study whether the levels of mitotic cyclin B, whose destruction determines the initiation of anaphase and final events of mitosis, are maintained high after metaphase and its degradation is delayed. RASSF7 KD cells exhibited a two fold increase in polyploid and polycentrosomal interphase cells. This could be due to two consecutive rounds of genome replication during the same cell cycle or a premature exit from mitosis, with subsequent failure to complete cytokinesis. The latter was shown to be the case for Aurora A and RASSF1A KDs, both resulting in an increase of multinucleated cells (Marumoto *et al.*, 2003; Dallol *et al.*, 2009a).

RASSF7 is over-expressed in numerous cancers (Chapter 3), therefore it would be interesting to verify whether the alteration of RASSF7 levels results in genomic instability. The karyotyping of the chromosomes could help to identify genetic problems leading to disorders and diseases. Despite the defects in mitosis, no enhanced phosphorylation of histone H3, a marker of mitotic cells, was detected in RASSF7 KD cells compared to controls, similarly to what was previously shown for *Xenopus rassf7* KD

(Sherwood *et al.*, 2008). Given the fact that mitotic defects did not cause an increase in mitotic cells, it is possible that the chromosome congression defects observed failed to elicit spindle assembly checkpoint activation. Several commercial Mad2 (Li and Murray, 1991) antibodies have been tested to try and investigate this hypothesis, but none of them were suitable for this study (data not shown). If the spindle checkpoint was compromised, cells could experience what is known as “mitotic slippage”, an aberrant exit from mitosis without sister chromatid segregation and cytokinesis. In that case cells could divide also without properly aligned chromosomes. This would cause an increase in tetraploid cells in G1, and could explain the slight but significant increase in the number of RASSF7 KD cells with 4N DNA reported with FACS analysis. These cells could subsequently arrest in G1, but only if the p53 dependent postmitotic G1 checkpoint was active (Vogel *et al.*, 2004). Thus it would be important to test if RASSF7 KD affects also p53 activation.

***RASSF7 KD effects on mitotic signaling proteins***

The consequences of RASSF7 knockdown on signaling proteins involved in mitotic progression were examined. RASSF7 KD did not compromise the correct centrosomal localisation of RASSF1A and phospho PLK1. The analysis was subsequently moved to the Aurora kinases, which are crucially recruited in the control of numerous mitotic events (Nigg, 2001; Carmena and Earnshaw, 2003; Andrews *et al.*, 2003). Aurora A was found to correctly localise and be phosphorylated at the centrosomes. The CPC protein Aurora B (Murata-Hori *et al.*, 2002; Carmena and Earnshaw, 2003; Andrews *et al.*, 2003), localised to the inner centromere adjacent to the kinetochore and at the midbody as expected. The kinetochore is the site where Aurora B exerts is control on DNA condensation, chromosome bi-orientation and kinetochore-microtubule attachment (Carmena and Earnshaw, 2003; Andrews *et al.*, 2003). However, the phospho Aurora staining at the centromere of metaphase RASSF7 depleted cells was barely detectable, which indicates a lack of activity of the protein. Aurora B loss of activity was confirmed by the lack of phosphorylation of CENP-A, a centromere specific histone H3 variant phosphorylated by Aurora B at

mitosis (Zeitlin *et al.*, 2001) and whose deficiency leads to severe chromosome segregation defects (Regnier *et al.*, 2005). Interestingly, however, RASSF7 KD did not compromise the correct centromere recruitment of INCENP, which is required for Aurora B activation (Vader *et al.*, 2006b). The loss of Aurora B activity is likely to contribute to the mitotic defects seen in RASSF7 KDs and, consistent with this hypothesis, inhibiting Aurora B causes chromosomal congression defects similar to those in RASSF7 KD cells (Kallio *et al.*, 2002b; Lampson *et al.*, 2004). Notably, cells in which Aurora B function is impaired often proceed through anaphase despite the presence of misaligned chromosomes. The loss of the spindle checkpoint under these conditions may be due to a lower concentration of Mad2 and BubR1, proteins involved in sensing correct chromosome attachment, at the kinetochores of Aurora B deficient cells (Lens *et al.*, 2003; Hauf *et al.*, 2003). This could explain why the increase in the number of tetraploid RASSF7 KD cells is only small.

Quite intriguingly, Aurora B inactivation was found to be a temporary phenomenon restricted to metaphase as the phospho Aurora signal was detectable again at the midbody of RASSF7 KD cells undergoing cytokinesis. Moreover, given the different activation times for the phosphorylation of histone H3 (late G2), a target of Aurora B which was found to be active in our experiments, and CENP-A (prometaphase) (Zeitlin *et al.*, 2001), it is reasonable to speculate that Aurora B becomes inactive during prophase/prometaphase, after which it cannot phosphorylate its targets anymore. The activity of other CPC members, which have not been checked in the present work, could be compromised in RASSF7 KD cells, and could subsequently reduce Aurora B activity on its endogenous substrates. This was shown to be the case in Mps1 deficient human cells, where the CPC protein Borealin was not phosphorylated and Aurora B was not active, albeit present at normal levels on inner centromeres of chromosomes (Jelluma *et al.*, 2008).

The localisation of RASSF7 at the centrosome (Chapter 4) and the spindle defects seen in the KDs suggest that RASSF7 might have a role in regulating microtubules. In accordance with this hypothesis, microtubule

growth was found to be affected by the loss of RASSF7 in HeLa cells. Microtubule re-growth assay showed that RASSF7 KD microtubules took longer to form and were more looped than the control counterparts. This demonstrates that RASSF7 is a key regulator of microtubule growth and suggests that it could have a role in microtubule polymerisation. This function provides also an explanation for the spindle defects seen in mitosis. It would be interesting to investigate whether the polarised organisation of the microtubules is correctly maintained in RASSF7 depleted cells and if not, how this could affect mitosis. A possible way for looking into this aspect would be to do live imaging of microtubule movements and to specifically analyse the kinetochore bound microtubules by immunostaining, after cold treating the cells to destabilise non kinetochore microtubules.

Changes induced in the microtubule cytoskeleton of RASSF7 mitotic cells were reminiscent of those observed in Aurora B inhibited cells (Kallio *et al.*, 2002b), where astral microtubules were remarkably enhanced. Interestingly, Aurora B activation requires contact with microtubules (Rosasco-Nitcher *et al.*, 2008; Fuller *et al.*, 2008). The spindle formation defects derived from RASSF7 KD could therefore stop the microtubules from correctly interacting with Aurora B, and cause the failure in Aurora B activation, and subsequently in chromosomal congression.

## 5.4 Conclusion

RASSF7 KD impairs colony forming activity and cell growth in H1792 and HeLa cells respectively. Further analysis is needed to understand if RASSF7 actively promotes cell proliferation, and whether it has the complete opposite role compared to the other RASSF members. The characterisation of RASSF7 KD phenotype showed defective mitosis in HeLa cells, leading to malorientated and lagging chromosomes, and a higher rate of multi-polar spindles with more radial microtubules. Eventually such aberrations are the likely cause of the increased numbers of polycentrosomal and polynucleated cells. Despite the major defects observed, RASSF7 depleted cells do not seem to incur in cell death more frequently than controls. RASSF7 depletion also prevents Aurora B activation. Aurora B inhibition is known to cause chromosomal congression defects similar to those in RASSF7 KD cells and it may explain the lack of a pronounced mitotic arrest in RASSF KD dividing cells. It is possible that RASSF7 exerts its control on Aurora B activity by regulating the microtubules and microtubule re-growth assays showed that RASSF7 is an important regulator of microtubule dynamics.

# 6 Final discussion

***Proposed working model***

RASSF7 is a member of the N-terminal RASSF family, an evolutionary conserved group of RA domain proteins that comprise four vertebrate members (Sherwood *et al.*, 2010). So far these proteins have been poorly characterised and their biological function is still unclear, but there is an increasing amount of evidence that, if misregulated, they may promote cancer (Sherwood *et al.*, 2010).

The current project aimed at investigating the role of the mammalian RASSF7, testing the intriguing hypothesis that this protein, as suggested by the *Xenopus* orthologue (Sherwood *et al.*, 2008), could play a role in human cell division.

It has been demonstrated that human RASSF7 is a centrosomal component (Chapter 4) and could promote crosstalk between the centrosome and microtubules, which in turn is required for Aurora B function (Rosasco-Nitcher *et al.*, 2008; Fuller *et al.*, 2008) (Figure 6.1). RASSF7 appears to control microtubule stability and dynamics during formation of a functional mitotic spindle. The down-regulation of RASSF7 would therefore impair the correct assembly of the mitotic microtubules, resulting in Aurora B inactivation and eventually in misalignment of chromosomes on the metaphase plate (Chapter 5). Such an important role in the cell could justify the broad tissue expression observed in mouse and human (Chapter 3) and would be in line with the function of other fundamental centrosomal proteins, such as Aurora A (Giet *et al.*, 1999; Katayama *et al.*, 2001; Kufer *et al.*, 2002; Tsai *et al.*, 2003).

***RASSF7 interactors are crucial to understand RASSF7 function***

The study of RASSF7 binding partners is required to explain the mechanism of action of this protein. RASSF7 could interact with microtubules by direct or indirect binding. A fascinating possibility is that RASSF7 may interact with microtubules via other microtubule dependent

components of the centrosomes. These components comprise elements of the cytoplasmic dynein motor, where the dynactin element is required for anchoring of microtubules at the centrosomes (Quintyne *et al.*, 1999), and are probably involved in mitotic spindle formation and chromosomes motility (Vaisberg *et al.*, 1993).

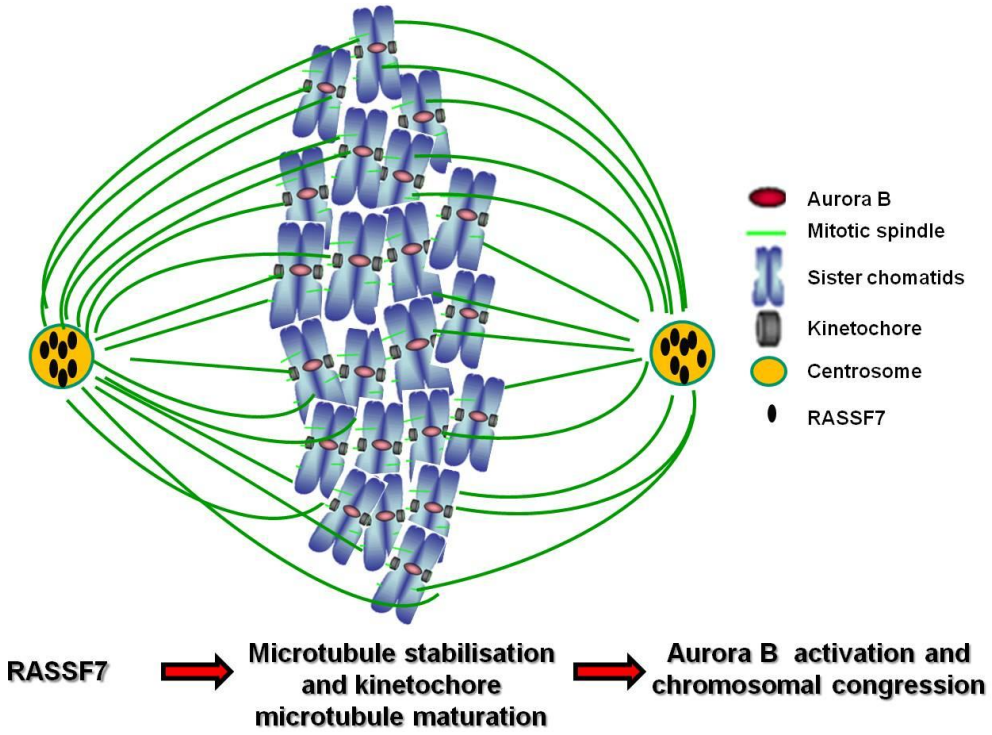


**Figure 6.1: Proposed model for RASSF7- Aurora B interaction.** RASSF7 would allow Aurora B activation and correct completion of mitosis via the stabilisation of the mitotic spindle microtubules.

Potential binding partners for human RASSF7 have been identified via large scale yeast two-hybrid studies. These possible interactors include CHMP1B (chromatin modifying protein 1B), which is associated with endosomal membrane trafficking, and DISC1 (disrupted in schizophrenia 1), which interestingly interacts with microtubules (Morris *et al.*, 2003; Tsang *et al.*, 2006). However, it is crucial to verify these potential protein-protein interactions by immunoprecipitation and Western blotting techniques. Once this is done, it will be interesting to test if the constitutively active/inactive forms of the binding partners are capable of attenuating or reversing the mitotic aberrations observed in RASSF7-deficient cells.

### *RASSF7 and apoptosis*

During the preparation of this thesis, Takashi and colleagues published results demonstrating that RASSF7 physically interacts with phosphorylated MKK7 (MAP kinase kinase 7) to negatively regulate pro-apoptotic JNK signaling in human cells (Takahashi *et al.*, 2011) (Figure 6.2). The authors showed that RASSF7 normally inhibits apoptosis induced by cell stresses, such as UV irradiation, and that its RA domain is required for its inhibitory actions. Immuonoprecipitation assays using recombinant proteins showed that the same RA domain was also capable of binding tightly to active N-Ras, and this interaction was not only enhanced following UV irradiation but also necessary to deliver anti-apoptotic signal in response to short term stresses (Takahashi *et al.*, 2011).

Interestingly, prolonged exposure to UV irradiation induced RASSF7 degradation via the ubiquitin-proteasome pathway in HeLa cells (Figure 6.2). Other cell stress stimuli, such as glucose depletion or treatment with DNA alkylating agents, were shown to induce a temporary up-regulation of RASSF7 and if prolonged to determine the ubiquitination of the protein (Takahashi *et al.*, 2011). It is tempting to speculate that this observation could explain the different levels of RASSF7 expression in HeLa cells after the exposure to acute and chronic hypoxic insults (Chapter 3), as RASSF7 mediated response to stress would not apply to sustained stresses. If this was verified, it would be possible to speculate that the high levels of RASSF7 proteins shown by HeLa cells chronically exposed to hypoxia and then left to recover in normoxic conditions are induced to restore normal cellular metabolism after persistent stress conditions.

Future work is required to establish if there is a link between RASSF7 induced stress response and RASSF7 role in mitosis.

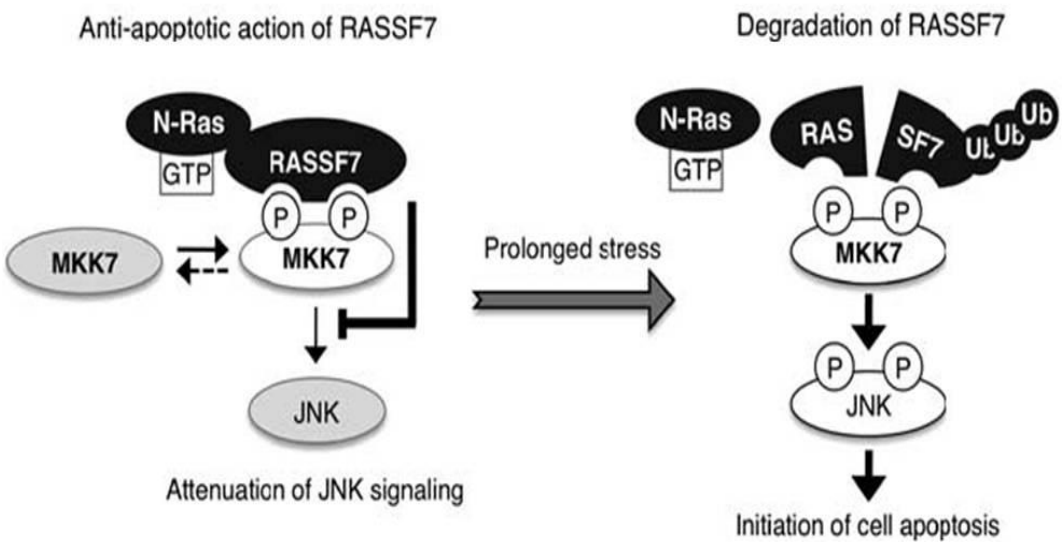


**Figure 6.2: RASSF7 inhibits pro-apoptotic JNK signaling.** Schematic diagram of the relationships among the RASSF7, N-Ras, MKK7 (MAP kinase kinase 7) and Jun (c-Jun N-terminal kinase) proteins as proposed by Takahashi and colleagues (2011). Under resting or low stress conditions (left), the majority of MKK7 protein exists in its dephosphorylated form. RASSF7, in concert with N-Ras, prevents the phosphorylated form of MKK7 from accessing and/or activating its downstream substrate JNK. However, when stress is prolonged (right), the inhibitory action of RASSF7 on MKK7 is eliminated because of degradation of the RASSF7 protein via the Ubiquitin (Ub)–proteasome pathway. In the absence of RASSF7, phosphorylated MKK7 activates JNK, triggering apoptosis. Adapted from (Takahashi *et al.*, 2011).

### *RASSF7 and cancer*

Although gene and protein profiling studies have identified a correlation between abundant expression of RASSF7 and cancer development (Mutter *et al.*, 2001; Logsdon *et al.*, 2003; Friess *et al.*, 2003; Lowe *et al.*, 2007; Tan *et al.*, 2009), the lack of mechanistic or functional data has led to an incomplete understanding of what role, if any, RASSF7 could have in cancer progression. The production of RASSF7 transgenic mouse models will probably elucidate if RASSF7 mutants acquire new oncogenic activities to promote cancer.

For now, the results reported in this thesis and the work of Takashi and colleagues (2011) may account for the association of elevated RASSF7 with tumourigenesis. Unlike other RASSF proteins, RASSF7 would exert an anti-apoptotic function and would also be responsible for correct

completion of mitosis. The two roles could be linked as the MKK7-JNK signaling pathway has been associated to cell cycle progression. In fact *mkk7*$^{-/-}$ MEFs display reduced proliferation caused by cell cycle arrest (Wada *et al.*, 2004).

Targeting mitotic regulators allows the interference with specific molecular targets that have critical roles in tumour growth or progression. However, there is some concern regarding the long term implications of inhibiting molecules such as Aurora B in normal cells, although this could limit the replication of tumour cells. In view of these considerations, RASSF7 could be considered as a possible anti-cancer drug target. In fact, the molecule could potentially integrate cellular networks that are essential for tumour cell proliferation and viability. If further studies were able to confirm its versatile roles in mitosis and apoptosis, inhibiting RASSF7 might provide an opportunity to target a larger subset of cancers compared to single molecule inhibitors.

# 7 References


Abrieu, A., Kahana J. A., Wood K. W. and Cleveland D. W. (2000). "CENP-E as an essential component of the mitotic checkpoint in vitro." *Cell* **102**(6): 817-26.

Abrieu, A., Magnaghi-Jaulin L., Kahana J. A., Peter M., Castro A., Vigneron S., Lorca T., Cleveland D. W. and Labbe J. C. (2001). "Mps1 is a kinetochore-associated kinase essential for the vertebrate mitotic checkpoint." *Cell* **106**(1): 83-93.

Adams, R. R., Maiato H., Earnshaw W. C. and Carmena M. (2001). "Essential roles of Drosophila inner centromere protein (INCENP) and aurora B in histone H3 phosphorylation, metaphase chromosome alignment, kinetochore disjunction, and chromosome segregation." *J Cell Biol* **153**(4): 865-80.

Adams, R. R., Wheatley S. P., Gouldsworthy A. M., Kandels-Lewis S. E., Carmena M., Smythe C., Gerloff D. L. and Earnshaw W. C. (2000). "INCENP binds the Aurora-related kinase AIRK2 and is required to target it to chromosomes, the central spindle and cleavage furrow." *Curr Biol* **10**(17): 1075-8.

Agathanggelou, A., Bieche I., Ahmed-Choudhury J., Nicke B., Dammann R., Baksh S., Gao B., Minna J. D., Downward J., Maher E. R. and Latif F. (2003). "Identification of novel gene expression targets for the Ras association domain family 1 (RASSF1A) tumor suppressor gene in non-small cell lung cancer and neuroblastoma." *Cancer Res* **63**(17): 5344-51.

Agathanggelou, A., Cooper W. N. and Latif F. (2005). "Role of the Ras-association domain family 1 tumor suppressor gene in human cancers." *Cancer Res* **65**(9): 3497-508.

Ahmed-Choudhury, J., Agathanggelou A., Fenton S. L., Ricketts C., Clark G. J., Maher E. R. and Latif F. (2005). "Transcriptional regulation of cyclin A2 by RASSF1A through the enhanced binding of p120E4F to the cyclin A2 promoter." *Cancer Res* **65**(7): 2690-7.

Ainsztein, A. M., Kandels-Lewis S. E., Mackay A. M. and Earnshaw W. C. (1998). "INCENP centromere and spindle targeting: identification of

essential conserved motifs and involvement of heterochromatin protein HP1." *J Cell Biol* **143**(7): 1763-74.

Akino, K., Toyota M., Suzuki H., Mita H., Sasaki Y., Ohe-Toyota M., Issa J. P., Hinoda Y., Imai K. and Tokino T. (2005). "The Ras effector RASSF2 is a novel tumor-suppressor gene in human colorectal cancer." *Gastroenterology* **129**(1): 156-69.

Alam, M. R., Caldwell B. D., Johnson R. C., Darlington D. N., Mains R. E. and Eipper B. A. (1996). "Novel proteins that interact with the COOH-terminal cytosolic routing determinants of an integral membrane peptide-processing enzyme." *J Biol Chem* **271**(45): 28636-40.

Allen, N. P., Donninger H., Vos M. D., Eckfeld K., Hesson L., Gordon L., Birrer M. J., Latif F. and Clark G. J. (2007). "RASSF6 is a novel member of the RASSF family of tumor suppressors." *Oncogene* **26**(42): 6203-11.

Amaar, Y. G., Baylink D. J. and Mohan S. (2005). "Ras-association domain family 1 protein, RASSF1C, is an IGFBP-5 binding partner and a potential regulator of osteoblast cell proliferation." *J Bone Miner Res* **20**(8): 1430-9.

Amaar, Y. G., Minera M. G., Hatran L. K., Strong D. D., Mohan S. and Reeves M. E. (2006). "Ras association domain family 1C protein stimulates human lung cancer cell proliferation." *Am J Physiol Lung Cell Mol Physiol* **291**(6): L1185-90.

Andersen, J. S., Wilkinson C. J., Mayor T., Mortensen P., Nigg E. A. and Mann M. (2003). "Proteomic characterization of the human centrosome by protein correlation profiling." *Nature* **426**(6966): 570-4.

Andrews, P. D., Knatko E., Moore W. J. and Swedlow J. R. (2003). "Mitotic mechanics: the auroras come into view." *Curr Opin Cell Biol* **15**(6): 672-83.

Andrews, P. D., Ovechkina Y., Morrice N., Wagenbach M., Duncan K., Wordeman L. and Swedlow J. R. (2004). "Aurora B regulates MCAK at the mitotic centromere." *Dev Cell* **6**(2): 253-68.

Aoyama, Y., Avruch J. and Zhang X. F. (2004). "Nore1 inhibits tumor cell growth independent of Ras or the MST1/2 kinases." *Oncogene* **23**(19): 3426-33.

Armesilla, A. L., Williams J. C., Buch M. H., Pickard A., Emerson M., Cartwright E. J., Oceandy D., Vos M. D., Gillies S., Clark G. J. and Neyses L. (2004). "Novel functional interaction between the plasma membrane Ca2+ pump 4b and the proapoptotic tumor suppressor Ras-associated factor 1 (RASSF1)." *J Biol Chem* **279**(30): 31318-28.

Astuti, D., Agathanggelou A., Honorio S., Dallol A., Martinsson T., Kogner P., Cummins C., Neumann H. P., Voutilainen R., Dahia P., Eng C., Maher E. R. and Latif F. (2001). "RASSF1A promoter region CpG island hypermethylation in phaeochromocytomas and neuroblastoma tumours." *Oncogene* **20**(51): 7573-7.

Avruch, J., Praskova M., Ortiz-Vega S., Liu M. and Zhang X. F. (2006). "Nore1 and RASSF1 regulation of cell proliferation and of the MST1/2 kinases." *Methods Enzymol* **407**: 290-310.

Avruch, J., Xavier R., Bardeesy N., Zhang X. F., Praskova M., Zhou D. and Xia F. (2009). "Rassf family of tumor suppressor polypeptides." *J Biol Chem* **284**(17): 11001-5.

Baksh, S., Tommasi S., Fenton S., Yu V. C., Martins L. M., Pfeifer G. P., Latif F., Downward J. and Neel B. G. (2005). "The tumor suppressor RASSF1A and MAP-1 link death receptor signaling to Bax conformational change and cell death." *Mol Cell* **18**(6): 637-50.

Banelli, B., Gelvi I., Di Vinci A., Scaruffi P., Casciano I., Allemanni G., Bonassi S., Tonini G. P. and Romani M. (2005). "Distinct CpG methylation profiles characterize different clinical groups of neuroblastic tumors." *Oncogene* **24**(36): 5619-28.

Barr, F. A. and Gruneberg U. (2007). "Cytokinesis: placing and making the final cut." *Cell* **131**(5): 847-60.

Barr, F. A., Sillje H. H. and Nigg E. A. (2004). "Polo-like kinases and the orchestration of cell division." *Nat Rev Mol Cell Biol* **5**(6): 429-40.

Bayliss, R., Sardon T., Vernos I. and Conti E. (2003). "Structural basis of Aurora-A activation by TPX2 at the mitotic spindle." *Mol Cell* **12**(4): 851-62.

Berdnik, D. and Knoblich J. A. (2002). "Drosophila Aurora-A is required for centrosome maturation and actin-dependent asymmetric protein localization during mitosis." *Curr Biol* **12**(8): 640-7.

Bishop, J. D. and Schumacher J. M. (2002). "Phosphorylation of the carboxyl terminus of inner centromere protein (INCENP) by the Aurora B Kinase stimulates Aurora B kinase activity." *J Biol Chem* **277**(31): 27577-80.

Blagden, S. P. and Glover D. M. (2003). "Polar expeditions--provisioning the centrosome for mitosis." *Nat Cell Biol* **5**(6): 505-11.

Blower, M. D., Sullivan B. A. and Karpen G. H. (2002). "Conserved organization of centromeric chromatin in flies and humans." *Dev Cell* **2**(3): 319-30.

Bolton, M. A., Lan W., Powers S. E., McCleland M. L., Kuang J. and Stukenberg P. T. (2002). "Aurora B kinase exists in a complex with survivin and INCENP and its kinase activity is stimulated by survivin binding and phosphorylation." *Mol Biol Cell* **13**(9): 3064-77.

Bornens, M. (2002). "Centrosome composition and microtubule anchoring mechanisms." *Curr Opin Cell Biol* **14**(1): 25-34.

Brandt, R., Grutzmann R., Bauer A., Jesnowski R., Ringel J., Lohr M., Pilarsky C. and Hoheisel J. D. (2004). "DNA microarray analysis of pancreatic malignancies." *Pancreatology* **4**(6): 587-97.

Brinkley, B. R. and Stubblefield E. (1966). "The fine structure of the kinetochore of a mammalian cell in vitro." *Chromosoma* **19**(1): 28-43.

Burbee, D. G., Forgacs E., Zochbauer-Muller S., Shivakumar L., Fong K., Gao B., Randle D., Kondo M., Virmani A., Bader S., Sekido Y., Latif F., Milchgrub S., Toyooka S., Gazdar A. F., Lerman M. I., Zabarovsky E., White M. and Minna J. D. (2001). "Epigenetic inactivation of RASSF1A in lung and breast cancers and malignant phenotype suppression." *J Natl Cancer Inst* **93**(9): 691-9.

Byun, D. S., Lee M. G., Chae K. S., Ryu B. G. and Chi S. G. (2001). "Frequent epigenetic inactivation of RASSF1A by aberrant promoter hypermethylation in human gastric adenocarcinoma." *Cancer Res* **61**(19): 7034-8.

Calvisi, D. F., Ladu S., Gorden A., Farina M., Conner E. A., Lee J. S., Factor V. M. and Thorgeirsson S. S. (2006). "Ubiquitous activation of Ras and Jak/Stat pathways in human HCC." *Gastroenterology* **130**(4): 1117-28.

Camps, C., Buffa F. M., Colella S., Moore J., Sotiriou C., Sheldon H., Harris A. L., Gleadle J. M. and Ragoussis J. (2008). "hsa-miR-210 Is induced by hypoxia and is an independent prognostic factor in breast cancer." *Clin Cancer Res* **14**(5): 1340-8.

Carmena, M. and Earnshaw W. C. (2003). "The cellular geography of aurora kinases." *Nat Rev Mol Cell Biol* **4**(11): 842-54.

Carmena, M., Ruchaud S. and Earnshaw W. C. (2009). "Making the Auroras glow: regulation of Aurora A and B kinase function by interacting proteins." *Curr Opin Cell Biol* **21**(6): 796-805.

Chan, G. K., Schaar B. T. and Yen T. J. (1998). "Characterization of the kinetochore binding domain of CENP-E reveals interactions with the kinetochore proteins CENP-F and hBUBR1." *J Cell Biol* **143**(1): 49-63.

Cheeseman, I. M., Chappie J. S., Wilson-Kubalek E. M. and Desai A. (2006). "The conserved KMN network constitutes the core microtubule-binding site of the kinetochore." *Cell* **127**(5): 983-97.

Cheeseman, I. M. and Desai A. (2008). "Molecular architecture of the kinetochore-microtubule interface." *Nat Rev Mol Cell Biol* **9**(1): 33-46.

Chen, L., Johnson R. C. and Milgram S. L. (1998). "P-CIP1, a novel protein that interacts with the cytosolic domain of peptidylglycine alpha-amidating monooxygenase, is associated with endosomes." *J Biol Chem* **273**(50): 33524-32.

Chow, L. S., Lo K. W., Kwong J., To K. F., Tsang K. S., Lam C. W., Dammann R. and Huang D. P. (2004). "RASSF1A is a target tumor

suppressor from 3p21.3 in nasopharyngeal carcinoma." *Int J Cancer* **109**(6): 839-47.

Cimini, D., Howell B., Maddox P., Khodjakov A., Degrassi F. and Salmon E. D. (2001). "Merotelic kinetochore orientation is a major mechanism of aneuploidy in mitotic mammalian tissue cells." *J Cell Biol* **153**(3): 517-27.

Cimini, D., Wan X., Hirel C. B. and Salmon E. D. (2006). "Aurora kinase promotes turnover of kinetochore microtubules to reduce chromosome segregation errors." *Curr Biol* **16**(17): 1711-8.

Colas, E., Perez C., Cabrera S., Pedrola N., Monge M., Castellvi J., Eyzaguirre F., Gregorio J., Ruiz A., Llaurado M., Rigau M., Garcia M., Ertekin T., Montes M., Lopez-Lopez R., Carreras R., Xercavins J., Ortega A., Maes T., Rosell E., Doll A., Abal M., Reventos J. and Gil-Moreno A. (2011). "Molecular markers of endometrial carcinoma detected in uterine aspirates." *Int J Cancer*.

Conte, N., Delaval B., Ginestier C., Ferrand A., Isnardon D., Larroque C., Prigent C., Seraphin B., Jacquemier J. and Birnbaum D. (2003). "TACC1-chTOG-Aurora A protein complex in breast cancer." *Oncogene* **22**(50): 8102-16.

Cooke, C. A., Bazett-Jones D. P., Earnshaw W. C. and Rattner J. B. (1993). "Mapping DNA within the mammalian kinetochore." *J Cell Biol* **120**(5): 1083-91.

Cooke, C. A., Heck M. M. and Earnshaw W. C. (1987). "The inner centromere protein (INCENP) antigens: movement from inner centromere to midbody during mitosis." *J Cell Biol* **105**(5): 2053-67.

Cooper, W. N., Dickinson R. E., Dallol A., Grigorieva E. V., Pavlova T. V., Hesson L. B., Bieche I., Broggini M., Maher E. R., Zabarovsky E. R., Clark G. J. and Latif F. (2008). "Epigenetic regulation of the ras effector/tumour suppressor RASSF2 in breast and lung cancer." *Oncogene* **27**(12): 1805-11.

Dallol, A., Agathanggelou A., Fenton S. L., Ahmed-Choudhury J., Hesson L., Vos M. D., Clark G. J., Downward J., Maher E. R. and Latif F. (2004). "RASSF1A interacts with microtubule-associated proteins and modulates microtubule dynamics." *Cancer Res* **64**(12): 4112-6.

Dallol, A., Agathanggelou A., Tommasi S., Pfeifer G. P., Maher E. R. and Latif F. (2005). "Involvement of the RASSF1A tumor suppressor gene in controlling cell migration." *Cancer Res* **65**(17): 7653-9.

Dallol, A., Cooper W. N., Al-Mulla F., Agathanggelou A., Maher E. R. and Latif F. (2007). "Depletion of the Ras association domain family 1, isoform A-associated novel microtubule-associated protein, C19ORF5/MAP1S, causes mitotic abnormalities." *Cancer Res* **67**(2): 492-500.

Dallol, A., Hesson L. B., Matallanas D., Cooper W. N., O'Neill E., Maher E. R., Kolch W. and Latif F. (2009a). "RAN GTPase is a RASSF1A effector involved in controlling microtubule organization." *Curr Biol* **19**(14): 1227-32.

Dallol, A., Kolch W. and Latif F. (2009b). "When RASSF1A RAN into tumor suppression: Ran GTPase is a RASSF1A effector involved in controlling microtubule organization." *Cell Cycle* **8**(23): 3796-7.

Dammann, R., Li C., Yoon J. H., Chin P. L., Bates S. and Pfeifer G. P. (2000). "Epigenetic inactivation of a RAS association domain family protein from the lung tumour suppressor locus 3p21.3." *Nat Genet* **25**(3): 315-9.

Dammann, R., Schagdarsurengin U., Seidel C., Strunnikova M., Rastetter M., Baier K. and Pfeifer G. P. (2005). "The tumor suppressor RASSF1A in human carcinogenesis: an update." *Histol Histopathol* **20**(2): 645-63.

Dammann, R., Takahashi T. and Pfeifer G. P. (2001a). "The CpG island of the novel tumor suppressor gene RASSF1A is intensely methylated in primary small cell lung carcinomas." *Oncogene* **20**(27): 3563-7.

Dammann, R., Yang G. and Pfeifer G. P. (2001b). "Hypermethylation of the cpG island of Ras association domain family 1A (RASSF1A), a putative tumor suppressor gene from the 3p21.3 locus, occurs in a large percentage of human breast cancers." *Cancer Res* **61**(7): 3105-9.

de Gramont, A. and Cohen-Fix O. (2005). "The many phases of anaphase." *Trends Biochem Sci* **30**(10): 559-68.

DeLuca, J. G., Dong Y., Hergert P., Strauss J., Hickey J. M., Salmon E. D. and McEwen B. F. (2005). "Hec1 and nuf2 are core components of the kinetochore outer plate essential for organizing microtubule attachment sites." *Mol Biol Cell* **16**(2): 519-31.

DeLuca, J. G., Gall W. E., Ciferri C., Cimini D., Musacchio A. and Salmon E. D. (2006). "Kinetochore microtubule dynamics and attachment stability are regulated by Hec1." *Cell* **127**(5): 969-82.

Denko, N. C., Giaccia A. J., Stringer J. R. and Stambrook P. J. (1994). "The human Ha-ras oncogene induces genomic instability in murine fibroblasts within one cell cycle." *Proc Natl Acad Sci U S A* **91**(11): 5124-8.

Ditchfield, C., Johnson V. L., Tighe A., Ellston R., Haworth C., Johnson T., Mortlock A., Keen N. and Taylor S. S. (2003). "Aurora B couples chromosome alignment with anaphase by targeting BubR1, Mad2, and Cenp-E to kinetochores." *J Cell Biol* **161**(2): 267-80.

Donninger, H., Vos M. D. and Clark G. J. (2007). "The RASSF1A tumor suppressor." *J Cell Sci* **120**(Pt 18): 3163-72.

Doxsey, S. (2001). "Re-evaluating centrosome function." *Nat Rev Mol Cell Biol* **2**(9): 688-98.

Doxsey, S., McCollum D. and Theurkauf W. (2005). "Centrosomes in cellular regulation." *Annu Rev Cell Dev Biol* **21**: 411-34.

Dreijerink, K., Braga E., Kuzmin I., Geil L., Duh F. M., Angeloni D., Zbar B., Lerman M. I., Stanbridge E. J., Minna J. D., Protopopov A., Li J., Kashuba V., Klein G. and Zabarovsky E. R. (2001). "The candidate tumor suppressor gene, RASSF1A, from human chromosome 3p21.3 is involved in kidney tumorigenesis." *Proc Natl Acad Sci U S A* **98**(13): 7504-9.

Eckfeld, K., Hesson L., Vos M. D., Bieche I., Latif F. and Clark G. J. (2004). "RASSF4/AD037 is a potential ras effector/tumor suppressor of the RASSF family." *Cancer Res* **64**(23): 8688-93.

Emanuele, M., Burke D. J. and Stukenberg P. T. (2007). "A Hec of a microtubule attachment." *Nat Struct Mol Biol* **14**(1): 11-3.

Endoh, H., Yatabe Y., Shimizu S., Tajima K., Kuwano H., Takahashi T. and Mitsudomi T. (2003). "RASSF1A gene inactivation in non-small

cell lung cancer and its clinical implication." *Int J Cancer* **106**(1): 45-51.

Estrabaud, E., Lassot I., Blot G., Le Rouzic E., Tanchou V., Quemeneur E., Daviet L., Margottin-Goguet F. and Benarous R. (2007). "RASSF1C, an isoform of the tumor suppressor RASSF1A, promotes the accumulation of beta-catenin by interacting with betaTrCP." *Cancer Res* **67**(3): 1054-61.

Falvella, F. S., Manenti G., Spinola M., Pignatiello C., Conti B., Pastorino U. and Dragani T. A. (2006). "Identification of RASSF8 as a candidate lung tumor suppressor gene." *Oncogene* **25**(28): 3934-8.

Fenton, S. L., Dallol A., Agathanggelou A., Hesson L., Ahmed-Choudhury J., Baksh S., Sardet C., Dammann R., Minna J. D., Downward J., Maher E. R. and Latif F. (2004). "Identification of the E1A-regulated transcription factor p120 E4F as an interacting partner of the RASSF1A candidate tumor suppressor gene." *Cancer Res* **64**(1): 102-7.

Firgaira, F. A., Seshadri R., McEvoy C. R., Dite G. S., Giles G. G., McCredie M. R., Southey M. C., Venter D. J. and Hopper J. L. (1999). "HRAS1 rare minisatellite alleles and breast cancer in Australian women under age forty years." *J Natl Cancer Inst* **91**(24): 2107-11.

Foley, C. J., Freedman H., Choo S. L., Onyskiw C., Fu N. Y., Yu V. C., Tuszynski J., Pratt J. C. and Baksh S. (2008). "Dynamics of RASSF1A/MOAP-1 association with death receptors." *Mol Cell Biol* **28**(14): 4520-35.

Friess, H., Ding J., Kleeff J., Fenkell L., Rosinski J. A., Guweidhi A., Reidhaar-Olson J. F., Korc M., Hammer J. and Buchler M. W. (2003). "Microarray-based identification of differentially expressed growth- and metastasis-associated genes in pancreatic cancer." *Cell Mol Life Sci* **60**(6): 1180-99.

Fujita, H., Fukuhara S., Sakurai A., Yamagishi A., Kamioka Y., Nakaoka Y., Masuda M. and Mochizuki N. (2005). "Local activation of Rap1 contributes to directional vascular endothelial cell migration accompanied by extension of microtubules on which RAPL, a

Rap1-associating molecule, localizes." *J Biol Chem* **280**(6): 5022-31.

Fuller, B. G., Lampson M. A., Foley E. A., Rosasco-Nitcher S., Le K. V., Tobelmann P., Brautigan D. L., Stukenberg P. T. and Kapoor T. M. (2008). "Midzone activation of aurora B in anaphase produces an intracellular phosphorylation gradient." *Nature* **453**(7198): 1132-6.

Gadea, B. B. and Ruderman J. V. (2006). "Aurora B is required for mitotic chromatin-induced phosphorylation of Op18/Stathmin." *Proc Natl Acad Sci U S A* **103**(12): 4493-8.

Gassmann, R., Carvalho A., Henzing A. J., Ruchaud S., Hudson D. F., Honda R., Nigg E. A., Gerloff D. L. and Earnshaw W. C. (2004). "Borealin: a novel chromosomal passenger required for stability of the bipolar mitotic spindle." *J Cell Biol* **166**(2): 179-91.

Giet, R. and Glover D. M. (2001). "Drosophila aurora B kinase is required for histone H3 phosphorylation and condensin recruitment during chromosome condensation and to organize the central spindle during cytokinesis." *J Cell Biol* **152**(4): 669-82.

Giet, R., McLean D., Descamps S., Lee M. J., Raff J. W., Prigent C. and Glover D. M. (2002). "Drosophila Aurora A kinase is required to localize D-TACC to centrosomes and to regulate astral microtubules." *J Cell Biol* **156**(3): 437-51.

Giet, R., Uzbekov R., Cubizolles F., Le Guellec K. and Prigent C. (1999). "The Xenopus laevis aurora-related protein kinase pEg2 associates with and phosphorylates the kinesin-related protein XlEg5." *J Biol Chem* **274**(21): 15005-13.

Gimenez-Abian, J. F., Sumara I., Hirota T., Hauf S., Gerlich D., de la Torre C., Ellenberg J. and Peters J. M. (2004). "Regulation of sister chromatid cohesion between chromosome arms." *Curr Biol* **14**(13): 1187-93.

Glover, D. M., Leibowitz M. H., McLean D. A. and Parry H. (1995). "Mutations in aurora prevent centrosome separation leading to the formation of monopolar spindles." *Cell* **81**(1): 95-105.

Golan, A., Yudkovsky Y. and Hershko A. (2002). "The cyclin-ubiquitin ligase activity of cyclosome/APC is jointly activated by protein kinases Cdk1-cyclin B and Plk." *J Biol Chem* **277**(18): 15552-7.

Goto, H., Yasui Y., Kawajiri A., Nigg E. A., Terada Y., Tatsuka M., Nagata K. and Inagaki M. (2003). "Aurora-B regulates the cleavage furrow-specific vimentin phosphorylation in the cytokinetic process." *J Biol Chem* **278**(10): 8526-30.

Guo, C., Tommasi S., Liu L., Yee J. K., Dammann R. and Pfeifer G. P. (2007). "RASSF1A is part of a complex similar to the Drosophila Hippo/Salvador/Lats tumor-suppressor network." *Curr Biol* **17**(8): 700-5.

Guse, A., Mishima M. and Glotzer M. (2005). "Phosphorylation of ZEN-4/MKLP1 by aurora B regulates completion of cytokinesis." *Curr Biol* **15**(8): 778-86.

Hanisch, A., Wehner A., Nigg E. A. and Sillje H. H. (2006). "Different Plk1 functions show distinct dependencies on Polo-Box domain-mediated targeting." *Mol Biol Cell* **17**(1): 448-59.

Harada, K., Toyooka S., Maitra A., Maruyama R., Toyooka K. O., Timmons C. F., Tomlinson G. E., Mastrangelo D., Hay R. J., Minna J. D. and Gazdar A. F. (2002). "Aberrant promoter methylation and silencing of the RASSF1A gene in pediatric tumors and cell lines." *Oncogene* **21**(27): 4345-9.

Harvey, K. and Tapon N. (2007). "The Salvador-Warts-Hippo pathway - an emerging tumour-suppressor network." *Nat Rev Cancer* **7**(3): 182-91.

Hauf, S., Cole R. W., LaTerra S., Zimmer C., Schnapp G., Walter R., Heckel A., van Meel J., Rieder C. L. and Peters J. M. (2003). "The small molecule Hesperadin reveals a role for Aurora B in correcting kinetochore-microtubule attachment and in maintaining the spindle assembly checkpoint." *J Cell Biol* **161**(2): 281-94.

Hayden, J. H., Bowser S. S. and Rieder C. L. (1990). "Kinetochores capture astral microtubules during chromosome attachment to the mitotic spindle: direct visualization in live newt lung cells." *J Cell Biol* **111**(3): 1039-45.

Herrmann, C. (2003). "Ras-effector interactions: after one decade." *Curr Opin Struct Biol* **13**(1): 122-9.

Hesson, L., Bieche I., Krex D., Criniere E., Hoang-Xuan K., Maher E. R. and Latif F. (2004). "Frequent epigenetic inactivation of RASSF1A and BLU genes located within the critical 3p21.3 region in gliomas." *Oncogene* **23**(13): 2408-19.

Hesson, L., Dallol A., Minna J. D., Maher E. R. and Latif F. (2003). "NORE1A, a homologue of RASSF1A tumour suppressor gene is inactivated in human cancers." *Oncogene* **22**(6): 947-54.

Hesson, L. B., Cooper W. N. and Latif F. (2007). "Evaluation of the 3p21.3 tumour-suppressor gene cluster." *Oncogene* **26**(52): 7283-301.

Hesson, L. B., Dunwell T. L., Cooper W. N., Catchpoole D., Brini A. T., Chiaramonte R., Griffiths M., Chalmers A. D., Maher E. R. and Latif F. (2009). "The novel RASSF6 and RASSF10 candidate tumour suppressor genes are frequently epigenetically inactivated in childhood leukaemias." *Mol Cancer* **8**: 42.

Hesson, L. B., Wilson R., Morton D., Adams C., Walker M., Maher E. R. and Latif F. (2005). "CpG island promoter hypermethylation of a novel Ras-effector gene RASSF2A is an early event in colon carcinogenesis and correlates inversely with K-ras mutations." *Oncogene* **24**(24): 3987-94.

Hill, V. K., Underhill-Day N., Krex D., Robel K., Sangan C. B., Summersgill H. R., Morris M., Gentle D., Chalmers A. D., Maher E. R. and Latif F. (2010). "Epigenetic inactivation of the RASSF10 candidate tumor suppressor gene is a frequent and an early event in gliomagenesis." *Oncogene* **30**(8): 978-89.

Hitomi, J., Christofferson D. E., Ng A., Yao J., Degterev A., Xavier R. J. and Yuan J. (2008). "Identification of a molecular signaling network that regulates a cellular necrotic cell death pathway." *Cell* **135**(7): 1311-23.

Hoffman, D. B., Pearson C. G., Yen T. J., Howell B. J. and Salmon E. D. (2001). "Microtubule-dependent changes in assembly of microtubule motor proteins and mitotic spindle checkpoint proteins at PtK1 kinetochores." *Mol Biol Cell* **12**(7): 1995-2009.

Holy, T. E. and Leibler S. (1994). "Dynamic instability of microtubules as an efficient way to search in space." *Proc Natl Acad Sci U S A* **91**(12): 5682-5.

Honda, R., Korner R. and Nigg E. A. (2003). "Exploring the functional interactions between Aurora B, INCENP, and survivin in mitosis." *Mol Biol Cell* **14**(8): 3325-41.

Hori, T., Haraguchi T., Hiraoka Y., Kimura H. and Fukagawa T. (2003). "Dynamic behavior of Nuf2-Hec1 complex that localizes to the centrosome and centromere and is essential for mitotic progression in vertebrate cells." *J Cell Sci* **116**(Pt 16): 3347-62.

Howell, B. J., McEwen B. F., Canman J. C., Hoffman D. B., Farrar E. M., Rieder C. L. and Salmon E. D. (2001). "Cytoplasmic dynein/dynactin drives kinetochore protein transport to the spindle poles and has a role in mitotic spindle checkpoint inactivation." *J Cell Biol* **155**(7): 1159-72.

Howell, B. J., Moree B., Farrar E. M., Stewart S., Fang G. and Salmon E. D. (2004). "Spindle checkpoint protein dynamics at kinetochores in living cells." *Curr Biol* **14**(11): 953-64.

Hoyt, M. A., Totis L. and Roberts B. T. (1991). "S. cerevisiae genes required for cell cycle arrest in response to loss of microtubule function." *Cell* **66**(3): 507-17.

Hsu, J. Y., Sun Z. W., Li X., Reuben M., Tatchell K., Bishop D. K., Grushcow J. M., Brame C. J., Caldwell J. A., Hunt D. F., Lin R., Smith M. M. and Allis C. D. (2000). "Mitotic phosphorylation of histone H3 is governed by Ipl1/aurora kinase and Glc7/PP1 phosphatase in budding yeast and nematodes." *Cell* **102**(3): 279-91.

Huang, L. E., Ho V., Arany Z., Krainc D., Galson D., Tendler D., Livingston D. M. and Bunn H. F. (1997). "Erythropoietin gene regulation depends on heme-dependent oxygen sensing and assembly of interacting transcription factors." *Kidney Int* **51**(2): 548-52.

Huang, X., Le Q. T. and Giaccia A. J. (2010). "MiR-210--micromanager of the hypoxia pathway." *Trends Mol Med* **16**(5): 230-7.

Hwang, E., Ryu K. S., Paakkonen K., Guntert P., Cheong H. K., Lim D. S., Lee J. O., Jeon Y. H. and Cheong C. (2007). "Structural insight into dimeric interaction of the SARAH domains from Mst1 and RASSF family proteins in the apoptosis pathway." *Proc Natl Acad Sci U S A* **104**(22): 9236-41.

Ikeda, M., Hirabayashi S., Fujiwara N., Mori H., Kawata A., Iida J., Bao Y., Sato Y., Iida T., Sugimura H. and Hata Y. (2007). "Ras-association domain family protein 6 induces apoptosis via both caspase-dependent and caspase-independent pathways." *Exp Cell Res* **313**(7): 1484-95.

Inoue, S. and Salmon E. D. (1995). "Force generation by microtubule assembly/disassembly in mitosis and related movements." *Mol Biol Cell* **6**(12): 1619-40.

Ishiguro, K., Avruch J., Landry A., Qin S., Ando T., Goto H. and Xavier R. (2006). "Nore1B regulates TCR signaling via Ras and Carma1." *Cell Signal* **18**(10): 1647-54.

Jelluma, N., Brenkman A. B., van den Broek N. J., Cruijsen C. W., van Osch M. H., Lens S. M., Medema R. H. and Kops G. J. (2008). "Mps1 phosphorylates Borealin to control Aurora B activity and chromosome alignment." *Cell* **132**(2): 233-46.

Jeyaprakash, A. A., Klein U. R., Lindner D., Ebert J., Nigg E. A. and Conti E. (2007). "Structure of a Survivin-Borealin-INCENP core complex reveals how chromosomal passengers travel together." *Cell* **131**(2): 271-85.

Ji, L., Nishizaki M., Gao B., Burbee D., Kondo M., Kamibayashi C., Xu K., Yen N., Atkinson E. N., Fang B., Lerman M. I., Roth J. A. and Minna J. D. (2002). "Expression of several genes in the human chromosome 3p21.3 homozygous deletion region by an adenovirus vector results in tumor suppressor activities in vitro and in vivo." *Cancer Res* **62**(9): 2715-20.

Kaira, K., Sunaga N., Tomizawa Y., Yanagitani N., Ishizuka T., Saito R., Nakajima T. and Mori M. (2007). "Epigenetic inactivation of the RAS-effector gene RASSF2 in lung cancers." *Int J Oncol* **31**(1): 169-73.

Kaitna, S., Mendoza M., Jantsch-Plunger V. and Glotzer M. (2000). "Incenp and an aurora-like kinase form a complex essential for chromosome segregation and efficient completion of cytokinesis." *Curr Biol* **10**(19): 1172-81.

Kallio, M., Weinstein J., Daum J. R., Burke D. J. and Gorbsky G. J. (1998). "Mammalian p55CDC mediates association of the spindle checkpoint protein Mad2 with the cyclosome/anaphase-promoting complex, and is involved in regulating anaphase onset and late mitotic events." *J Cell Biol* **141**(6): 1393-406.

Kallio, M. J., Beardmore V. A., Weinstein J. and Gorbsky G. J. (2002a). "Rapid microtubule-independent dynamics of Cdc20 at kinetochores and centrosomes in mammalian cells." *J Cell Biol* **158**(5): 841-7.

Kallio, M. J., McCleland M. L., Stukenberg P. T. and Gorbsky G. J. (2002b). "Inhibition of aurora B kinase blocks chromosome segregation, overrides the spindle checkpoint, and perturbs microtubule dynamics in mitosis." *Curr Biol* **12**(11): 900-5.

Karpen, G. H. and Allshire R. C. (1997). "The case for epigenetic effects on centromere identity and function." *Trends Genet* **13**(12): 489-96.

Katagiri, K., Imamura M. and Kinashi T. (2006). "Spatiotemporal regulation of the kinase Mst1 by binding protein RAPL is critical for lymphocyte polarity and adhesion." *Nat Immunol* **7**(9): 919-28.

Katagiri, K., Maeda A., Shimonaka M. and Kinashi T. (2003). "RAPL, a Rap1-binding molecule that mediates Rap1-induced adhesion through spatial regulation of LFA-1." *Nat Immunol* **4**(8): 741-8.

Katagiri, K., Ohnishi N., Kabashima K., Iyoda T., Takeda N., Shinkai Y., Inaba K. and Kinashi T. (2004). "Crucial functions of the Rap1 effector molecule RAPL in lymphocyte and dendritic cell trafficking." *Nat Immunol* **5**(10): 1045-51.

Katayama, H., Zhou H., Li Q., Tatsuka M. and Sen S. (2001). "Interaction and feedback regulation between STK15/BTAK/Aurora-A kinase and protein phosphatase 1 through mitotic cell division cycle." *J Biol Chem* **276**(49): 46219-24.

Kawajiri, A., Yasui Y., Goto H., Tatsuka M., Takahashi M., Nagata K. and Inagaki M. (2003). "Functional significance of the specific sites phosphorylated in desmin at cleavage furrow: Aurora-B may phosphorylate and regulate type III intermediate filaments during cytokinesis coordinatedly with Rho-kinase." *Mol Biol Cell* **14**(4): 1489-500.

Kemp, C. A., Kopish K. R., Zipperlen P., Ahringer J. and O'Connell K. F. (2004). "Centrosome maturation and duplication in C. elegans require the coiled-coil protein SPD-2." *Dev Cell* **6**(4): 511-23.

Kenneth, N. S. and Rocha S. (2008). "Regulation of gene expression by hypoxia." *Biochem J* **414**(1): 19-29.

Khokhlatchev, A., Rabizadeh S., Xavier R., Nedwidek M., Chen T., Zhang X. F., Seed B. and Avruch J. (2002). "Identification of a novel Ras-regulated proapoptotic pathway." *Curr Biol* **12**(4): 253-65.

Kim, J. H., Kang J. S. and Chan C. S. (1999). "Sli15 associates with the ipl1 protein kinase to promote proper chromosome segregation in Saccharomyces cerevisiae." *J Cell Biol* **145**(7): 1381-94.

Kimmins, S., Crosio C., Kotaja N., Hirayama J., Monaco L., Hoog C., van Duin M., Gossen J. A. and Sassone-Corsi P. (2007). "Differential functions of the Aurora-B and Aurora-C kinases in mammalian spermatogenesis." *Mol Endocrinol* **21**(3): 726-39.

Kimura, M., Kotani S., Hattori T., Sumi N., Yoshioka T., Todokoro K. and Okano Y. (1997). "Cell cycle-dependent expression and spindle pole localization of a novel human protein kinase, Aik, related to Aurora of Drosophila and yeast Ipl1." *J Biol Chem* **272**(21): 13766-71.

Kinashi, T. and Katagiri K. (2005). "Regulation of immune cell adhesion and migration by regulator of adhesion and cell polarization enriched in lymphoid tissues." *Immunology* **116**(2): 164-71.

King, J. M., Hays T. S. and Nicklas R. B. (2000). "Dynein is a transient kinetochore component whose binding is regulated by microtubule attachment, not tension." *J Cell Biol* **151**(4): 739-48.

King, J. M. and Nicklas R. B. (2000). "Tension on chromosomes increases the number of kinetochore microtubules but only within limits." *J Cell Sci* **113 Pt 21**: 3815-23.

Kitagawa, D., Kajiho H., Negishi T., Ura S., Watanabe T., Wada T., Ichijo H., Katada T. and Nishina H. (2006). "Release of RASSF1C from the nucleus by Daxx degradation links DNA damage and SAPK/JNK activation." *EMBO J* **25**(14): 3286-97.

Klein, U. R., Nigg E. A. and Gruneberg U. (2006). "Centromere targeting of the chromosomal passenger complex requires a ternary subcomplex of Borealin, Survivin, and the N-terminal domain of INCENP." *Mol Biol Cell* **17**(6): 2547-58.

Kline-Smith, S. L. and Walczak C. E. (2004). "Mitotic spindle assembly and chromosome segregation: refocusing on microtubule dynamics." *Mol Cell* **15**(3): 317-27.

Knowlton, A. L., Lan W. and Stukenberg P. T. (2006). "Aurora B is enriched at merotelic attachment sites, where it regulates MCAK." *Curr Biol* **16**(17): 1705-10.

Korkola, J. E., Houldsworth J., Chadalavada R. S., Olshen A. B., Dobrzynski D., Reuter V. E., Bosl G. J. and Chaganti R. S. (2006). "Down-regulation of stem cell genes, including those in a 200-kb gene cluster at 12p13.31, is associated with in vivo differentiation of human male germ cell tumors." *Cancer Res* **66**(2): 820-7.

Kraft, C., Herzog F., Gieffers C., Mechtler K., Hagting A., Pines J. and Peters J. M. (2003). "Mitotic regulation of the human anaphase-promoting complex by phosphorylation." *EMBO J* **22**(24): 6598-609.

Krontiris, T. G., Devlin B., Karp D. D., Robert N. J. and Risch N. (1993). "An association between the risk of cancer and mutations in the HRAS1 minisatellite locus." *N Engl J Med* **329**(8): 517-23.

Krontiris, T. G., DiMartino N. A., Colb M. and Parkinson D. R. (1985). "Unique allelic restriction fragments of the human Ha-ras locus in leukocyte and tumour DNAs of cancer patients." *Nature* **313**(6001): 369-74.

Kufer, T. A., Sillje H. H., Korner R., Gruss O. J., Meraldi P. and Nigg E. A. (2002). "Human TPX2 is required for targeting Aurora-A kinase to the spindle." *J Cell Biol* **158**(4): 617-23.

Kumari, G., Singhal P. K., Suryaraja R. and Mahalingam S. (2010). "Functional interaction of the Ras effector RASSF5 with the tyrosine kinase Lck: critical role in nucleocytoplasmic transport and cell cycle regulation." *J Mol Biol* **397**(1): 89-109.

Kuzmin, I., Gillespie J. W., Protopopov A., Geil L., Dreijerink K., Yang Y., Vocke C. D., Duh F. M., Zabarovsky E., Minna J. D., Rhim J. S., Emmert-Buck M. R., Linehan W. M. and Lerman M. I. (2002). "The RASSF1A tumor suppressor gene is inactivated in prostate tumors and suppresses growth of prostate carcinoma cells." *Cancer Res* **62**(12): 3498-502.

Lampson, M. A., Renduchitala K., Khodjakov A. and Kapoor T. M. (2004). "Correcting improper chromosome-spindle attachments during cell division." *Nat Cell Biol* **6**(3): 232-7.

Lan, W., Zhang X., Kline-Smith S. L., Rosasco S. E., Barrett-Wilt G. A., Shabanowitz J., Hunt D. F., Walczak C. E. and Stukenberg P. T. (2004). "Aurora B phosphorylates centromeric MCAK and regulates its localization and microtubule depolymerization activity." *Curr Biol* **14**(4): 273-86.

Lane, H. A. and Nigg E. A. (1996). "Antibody microinjection reveals an essential role for human polo-like kinase 1 (Plk1) in the functional maturation of mitotic centrosomes." *J Cell Biol* **135**(6 Pt 2): 1701-13.

Langton, P. F., Colombani J., Chan E. H., Wepf A., Gstaiger M. and Tapon N. (2009). "The dASPP-dRASSF8 complex regulates cell-cell adhesion during Drosophila retinal morphogenesis." *Curr Biol* **19**(23): 1969-78.

Lazcoz, P., Munoz J., Nistal M., Pestana A., Encio I. and Castresana J. S. (2006). "Frequent promoter hypermethylation of RASSF1A and CASP8 in neuroblastoma." *BMC Cancer* **6**: 254.

Lee, M. G., Kim H. Y., Byun D. S., Lee S. J., Lee C. H., Kim J. I., Chang S. G. and Chi S. G. (2001). "Frequent epigenetic inactivation of

RASSF1A in human bladder carcinoma." *Cancer Res* **61**(18): 6688-92.

Lens, S. M., Wolthuis R. M., Klompmaker R., Kauw J., Agami R., Brummelkamp T., Kops G. and Medema R. H. (2003). "Survivin is required for a sustained spindle checkpoint arrest in response to lack of tension." *EMBO J* **22**(12): 2934-47.

Li, C., Issa R., Kumar P., Hampson I. N., Lopez-Novoa J. M., Bernabeu C. and Kumar S. (2003). "CD105 prevents apoptosis in hypoxic endothelial cells." *J Cell Sci* **116**(Pt 13): 2677-85.

Li, J., El-Naggar A. and Mao L. (2005). "Promoter methylation of p16INK4a, RASSF1A, and DAPK is frequent in salivary adenoid cystic carcinoma." *Cancer* **104**(4): 771-6.

Li, J., Wang F., Protopopov A., Malyukova A., Kashuba V., Minna J. D., Lerman M. I., Klein G. and Zabarovsky E. (2004a). "Inactivation of RASSF1C during in vivo tumor growth identifies it as a tumor suppressor gene." *Oncogene* **23**(35): 5941-9.

Li, R. and Murray A. W. (1991). "Feedback control of mitosis in budding yeast." *Cell* **66**(3): 519-31.

Li, X. and Nicklas R. B. (1995). "Mitotic forces control a cell-cycle checkpoint." *Nature* **373**(6515): 630-2.

Li, X., Sakashita G., Matsuzaki H., Sugimoto K., Kimura K., Hanaoka F., Taniguchi H., Furukawa K. and Urano T. (2004b). "Direct association with inner centromere protein (INCENP) activates the novel chromosomal passenger protein, Aurora-C." *J Biol Chem* **279**(45): 47201-11.

Liang, G. P., Su Y. Y., Chen J., Yang Z. C., Liu Y. S. and Luo X. D. (2009). "Analysis of the early adaptive response of endothelial cells to hypoxia via a long serial analysis of gene expression." *Biochem Biophys Res Commun* **384**(4): 415-9.

Lipp, J. J., Hirota T., Poser I. and Peters J. M. (2007). "Aurora B controls the association of condensin I but not condensin II with mitotic chromosomes." *J Cell Sci* **120**(Pt 7): 1245-55.

Liu, L., Amy V., Liu G. and McKeehan W. L. (2002a). "Novel complex integrating mitochondria and the microtubular cytoskeleton with

chromosome remodeling and tumor suppressor RASSF1 deduced by in silico homology analysis, interaction cloning in yeast, and colocalization in cultured cells." *In Vitro Cell Dev Biol Anim* **38**(10): 582-94.

Liu, L., Baier K., Dammann R. and Pfeifer G. P. (2007). "The tumor suppressor RASSF1A does not interact with Cdc20, an activator of the anaphase-promoting complex." *Cell Cycle* **6**(13): 1663-5.

Liu, L., Guo C., Dammann R., Tommasi S. and Pfeifer G. P. (2008). "RASSF1A interacts with and activates the mitotic kinase Aurora-A." *Oncogene* **27**(47): 6175-86.

Liu, L., Tommasi S., Lee D. H., Dammann R. and Pfeifer G. P. (2003). "Control of microtubule stability by the RASSF1A tumor suppressor." *Oncogene* **22**(50): 8125-36.

Liu, L., Vo A. and McKeehan W. L. (2005). "Specificity of the methylation-suppressed A isoform of candidate tumor suppressor RASSF1 for microtubule hyperstabilization is determined by cell death inducer C19ORF5." *Cancer Res* **65**(5): 1830-8.

Liu, L., Yoon J. H., Dammann R. and Pfeifer G. P. (2002b). "Frequent hypermethylation of the RASSF1A gene in prostate cancer." *Oncogene* **21**(44): 6835-40.

Lock, F. E., Underhill-Day N., Dunwell T., Matallanas D., Cooper W., Hesson L., Recino A., Ward A., Pavlova T., Zabarovsky E., Grant M. M., Maher E. R., Chalmers A. D., Kolch W. and Latif F. (2010). "The RASSF8 candidate tumor suppressor inhibits cell growth and regulates the Wnt and NF-kappaB signaling pathways." *Oncogene* **29**(30): 4307-16.

Logarinho, E., Bousbaa H., Dias J. M., Lopes C., Amorim I., Antunes-Martins A. and Sunkel C. E. (2004). "Different spindle checkpoint proteins monitor microtubule attachment and tension at kinetochores in Drosophila cells." *J Cell Sci* **117**(Pt 9): 1757-71.

Logsdon, C. D., Simeone D. M., Binkley C., Arumugam T., Greenson J. K., Giordano T. J., Misek D. E., Kuick R. and Hanash S. (2003). "Molecular profiling of pancreatic adenocarcinoma and chronic

pancreatitis identifies multiple genes differentially regulated in pancreatic cancer." *Cancer Res* **63**(10): 2649-57.

Losada, A., Hirano M. and Hirano T. (2002). "Cohesin release is required for sister chromatid resolution, but not for condensin-mediated compaction, at the onset of mitosis." *Genes Dev* **16**(23): 3004-16.

Lowe, A. W., Olsen M., Hao Y., Lee S. P., Taek Lee K., Chen X., van de Rijn M. and Brown P. O. (2007). "Gene expression patterns in pancreatic tumors, cells and tissues." *PLoS One* **2**(3): e323.

Luders, J. and Stearns T. (2007). "Microtubule-organizing centres: a re-evaluation." *Nat Rev Mol Cell Biol* **8**(2): 161-7.

Ma, Y., Cai S., Lu Q., Lu X., Jiang Q., Zhou J. and Zhang C. (2008). "Inhibition of protein deacetylation by trichostatin A impairs microtubule-kinetochore attachment." *Cell Mol Life Sci* **65**(19): 3100-9.

Macheiner, D., Heller G., Kappel S., Bichler C., Stattner S., Ziegler B., Kandioler D., Wrba F., Schulte-Hermann R., Zochbauer-Muller S. and Grasl-Kraupp B. (2006). "NORE1B, a candidate tumor suppressor, is epigenetically silenced in human hepatocellular carcinoma." *J Hepatol* **45**(1): 81-9.

Macurek, L., Lindqvist A., Lim D., Lampson M. A., Klompmaker R., Freire R., Clouin C., Taylor S. S., Yaffe M. B. and Medema R. H. (2008). "Polo-like kinase-1 is activated by aurora A to promote checkpoint recovery." *Nature* **455**(7209): 119-23.

Maiato, H., DeLuca J., Salmon E. D. and Earnshaw W. C. (2004). "The dynamic kinetochore-microtubule interface." *J Cell Sci* **117**(Pt 23): 5461-77.

Mao, Y., Abrieu A. and Cleveland D. W. (2003). "Activating and silencing the mitotic checkpoint through CENP-E-dependent activation/inactivation of BubR1." *Cell* **114**(1): 87-98.

Mao, Y., Desai A. and Cleveland D. W. (2005). "Microtubule capture by CENP-E silences BubR1-dependent mitotic checkpoint signaling." *J Cell Biol* **170**(6): 873-80.

Marumoto, T., Honda S., Hara T., Nitta M., Hirota T., Kohmura E. and Saya H. (2003). "Aurora-A kinase maintains the fidelity of early and late mitotic events in HeLa cells." *J Biol Chem* **278**(51): 51786-95.

Maruyama, R., Akino K., Toyota M., Suzuki H., Imai T., Ohe-Toyota M., Yamamoto E., Nojima M., Fujikane T., Sasaki Y., Yamashita T., Watanabe Y., Hiratsuka H., Hirata K., Itoh F., Imai K., Shinomura Y. and Tokino T. (2008). "Cytoplasmic RASSF2A is a proapoptotic mediator whose expression is epigenetically silenced in gastric cancer." *Carcinogenesis* **29**(7): 1312-8.

Matallanas, D., Romano D., Yee K., Meissl K., Kucerova L., Piazzolla D., Baccarini M., Vass J. K., Kolch W. and O'Neill E. (2007). "RASSF1A elicits apoptosis through an MST2 pathway directing proapoptotic transcription by the p73 tumor suppressor protein." *Mol Cell* **27**(6): 962-75.

McCleland, M. L., Gardner R. D., Kallio M. J., Daum J. R., Gorbsky G. J., Burke D. J. and Stukenberg P. T. (2003). "The highly conserved Ndc80 complex is required for kinetochore assembly, chromosome congression, and spindle checkpoint activity." *Genes Dev* **17**(1): 101-14.

McCleland, M. L., Kallio M. J., Barrett-Wilt G. A., Kestner C. A., Shabanowitz J., Hunt D. F., Gorbsky G. J. and Stukenberg P. T. (2004). "The vertebrate Ndc80 complex contains Spc24 and Spc25 homologs, which are required to establish and maintain kinetochore-microtubule attachment." *Curr Biol* **14**(2): 131-7.

McGuinness, B. E., Hirota T., Kudo N. R., Peters J. M. and Nasmyth K. (2005). "Shugoshin prevents dissociation of cohesin from centromeres during mitosis in vertebrate cells." *PLoS Biol* **3**(3): e86.

McInnes, C., Mazumdar A., Mezna M., Meades C., Midgley C., Scaerou F., Carpenter L., Mackenzie M., Taylor P., Walkinshaw M., Fischer P. M. and Glover D. (2006). "Inhibitors of Polo-like kinase reveal roles in spindle-pole maintenance." *Nat Chem Biol* **2**(11): 608-17.

McIntosh, J. R., Grishchuk E. L. and West R. R. (2002). "Chromosome-microtubule interactions during mitosis." *Annu Rev Cell Dev Biol* **18**: 193-219.

Merdes, A. and De Mey J. (1990). "The mechanism of kinetochore-spindle attachment and polewards movement analyzed in PtK2 cells at the prophase-prometaphase transition." *Eur J Cell Biol* **53**(2): 313-25.

Mhawech-Fauceglia, P., Wang D., Kesterson J., Clark K., Monhollen L., Odunsi K., Lele S. and Liu S. (2010). "Microarray analysis reveals distinct gene expression profiles among different tumor histology, stage and disease outcomes in endometrial adenocarcinoma." *PLoS One* **5**(11): e15415.

Michaelis, C., Ciosk R. and Nasmyth K. (1997). "Cohesins: chromosomal proteins that prevent premature separation of sister chromatids." *Cell* **91**(1): 35-45.

Miertzschke, M., Stanley P., Bunney T. D., Rodrigues-Lima F., Hogg N. and Katan M. (2007). "Characterization of interactions of adapter protein RAPL/Nore1B with RAP GTPases and their role in T cell migration." *J Biol Chem* **282**(42): 30629-42.

Minoshima, Y., Kawashima T., Hirose K., Tonozuka Y., Kawajiri A., Bao Y. C., Deng X., Tatsuka M., Narumiya S., May W. S., Jr., Nosaka T., Semba K., Inoue T., Satoh T., Inagaki M. and Kitamura T. (2003). "Phosphorylation by aurora B converts MgcRacGAP to a RhoGAP during cytokinesis." *Dev Cell* **4**(4): 549-60.

Mishima, M., Kaitna S. and Glotzer M. (2002). "Central spindle assembly and cytokinesis require a kinesin-like protein/RhoGAP complex with microtubule bundling activity." *Dev Cell* **2**(1): 41-54.

Morris, J. A., Kandpal G., Ma L. and Austin C. P. (2003). "DISC1 (Disrupted-In-Schizophrenia 1) is a centrosome-associated protein that interacts with MAP1A, MIPT3, ATF4/5 and NUDEL: regulation and loss of interaction with mutation." *Hum Mol Genet* **12**(13): 1591-608.

Morrow, C. J., Tighe A., Johnson V. L., Scott M. I., Ditchfield C. and Taylor S. S. (2005). "Bub1 and aurora B cooperate to maintain BubR1-mediated inhibition of APC/CCdc20." *J Cell Sci* **118**(Pt 16): 3639-52.

Moshnikova, A., Frye J., Shay J. W., Minna J. D. and Khokhlatchev A. V. (2006). "The growth and tumor suppressor NORE1A is a

cytoskeletal protein that suppresses growth by inhibition of the ERK pathway." *J Biol Chem* **281**(12): 8143-52.

Murata-Hori, M., Fumoto K., Fukuta Y., Iwasaki T., Kikuchi A., Tatsuka M. and Hosoya H. (2000). "Myosin II regulatory light chain as a novel substrate for AIM-1, an aurora/Ipl1p-related kinase from rat." *J Biochem* **128**(6): 903-7.

Murata-Hori, M., Tatsuka M. and Wang Y. L. (2002). "Probing the dynamics and functions of aurora B kinase in living cells during mitosis and cytokinesis." *Mol Biol Cell* **13**(4): 1099-108.

Musacchio, A. and Salmon E. D. (2007). "The spindle-assembly checkpoint in space and time." *Nat Rev Mol Cell Biol* **8**(5): 379-93.

Mutter, G. L., Baak J. P., Fitzgerald J. T., Gray R., Neuberg D., Kust G. A., Gentleman R., Gullans S. R., Wei L. J. and Wilcox M. (2001). "Global expression changes of constitutive and hormonally regulated genes during endometrial neoplastic transformation." *Gynecol Oncol* **83**(2): 177-85.

Nicklas, R. B. and Ward S. C. (1994). "Elements of error correction in mitosis: microtubule capture, release, and tension." *J Cell Biol* **126**(5): 1241-53.

Nicklas, R. B., Ward S. C. and Gorbsky G. J. (1995). "Kinetochore chemistry is sensitive to tension and may link mitotic forces to a cell cycle checkpoint." *J Cell Biol* **130**(4): 929-39.

Nigg, E. A. (2001). "Mitotic kinases as regulators of cell division and its checkpoints." *Nat Rev Mol Cell Biol* **2**(1): 21-32.

Nosho, K., Yamamoto H., Takahashi T., Mikami M., Taniguchi H., Miyamoto N., Adachi Y., Arimura Y., Itoh F., Imai K. and Shinomura Y. (2007). "Genetic and epigenetic profiling in early colorectal tumors and prediction of invasive potential in pT1 (early invasive) colorectal cancers." *Carcinogenesis* **28**(6): 1364-70.

Ortiz-Vega, S., Khokhlatchev A., Nedwidek M., Zhang X. F., Dammann R., Pfeifer G. P. and Avruch J. (2002). "The putative tumor suppressor RASSF1A homodimerizes and heterodimerizes with the Ras-GTP binding protein Nore1." *Oncogene* **21**(9): 1381-90.

Paoletti, A., Moudjou M., Paintrand M., Salisbury J. L. and Bornens M. (1996). "Most of centrin in animal cells is not centrosome-associated and centrosomal centrin is confined to the distal lumen of centrioles." *J Cell Sci* **109 ( Pt 13)**: 3089-102.

Park, H. W., Kang H. C., Kim I. J., Jang S. G., Kim K., Yoon H. J., Jeong S. Y. and Park J. G. (2007). "Correlation between hypermethylation of the RASSF2A promoter and K-ras/BRAF mutations in microsatellite-stable colorectal cancers." *Int J Cancer* **120**(1): 7-12.

Park, S. J., Lee D., Choi C. Y. and Ryu S. Y. (2008). "Induction of apoptosis by NORE1A in a manner dependent on its nuclear export." *Biochem Biophys Res Commun* **368**(1): 56-61.

Peters, U., Cherian J., Kim J. H., Kwok B. H. and Kapoor T. M. (2006). "Probing cell-division phenotype space and Polo-like kinase function using small molecules." *Nat Chem Biol* **2**(11): 618-26.

Pfeifer, G. P. and Dammann R. (2005). "Methylation of the tumor suppressor gene RASSF1A in human tumors." *Biochemistry (Mosc)* **70**(5): 576-83.

Pidoux, A. L. and Allshire R. C. (2005). "The role of heterochromatin in centromere function." *Philos Trans R Soc Lond B Biol Sci* **360**(1455): 569-79.

Pinsky, B. A., Kung C., Shokat K. M. and Biggins S. (2006). "The Ipl1-Aurora protein kinase activates the spindle checkpoint by creating unattached kinetochores." *Nat Cell Biol* **8**(1): 78-83.

Polesello, C., Huelsmann S., Brown N. H. and Tapon N. (2006). "The Drosophila RASSF homolog antagonizes the hippo pathway." *Curr Biol* **16**(24): 2459-65.

Ponting, C. P. and Benjamin D. R. (1996). "A novel family of Ras-binding domains." *Trends Biochem Sci* **21**(11): 422-5.

Praskova, M., Khoklatchev A., Ortiz-Vega S. and Avruch J. (2004). "Regulation of the MST1 kinase by autophosphorylation, by the growth inhibitory proteins, RASSF1 and NORE1, and by Ras." *Biochem J* **381**(Pt 2): 453-62.

Putkey, F. R., Cramer T., Morphew M. K., Silk A. D., Johnson R. S., McIntosh J. R. and Cleveland D. W. (2002). "Unstable kinetochore-

microtubule capture and chromosomal instability following deletion of CENP-E." *Dev Cell* **3**(3): 351-65.

Quintyne, N. J., Gill S. R., Eckley D. M., Crego C. L., Compton D. A. and Schroer T. A. (1999). "Dynactin is required for microtubule anchoring at centrosomes." *J Cell Biol* **147**(2): 321-34.

Rabizadeh, S., Xavier R. J., Ishiguro K., Bernabeortiz J., Lopez-Ilasaca M., Khokhlatchev A., Mollahan P., Pfeifer G. P., Avruch J. and Seed B. (2004). "The scaffold protein CNK1 interacts with the tumor suppressor RASSF1A and augments RASSF1A-induced cell death." *J Biol Chem* **279**(28): 29247-54.

Recino, A., Sherwood V., Flaxman A., Cooper W. N., Latif F., Ward A. and Chalmers A. D. (2010). "Human RASSF7 regulates the microtubule cytoskeleton and is required for spindle formation, Aurora B activation and chromosomal congression during mitosis." *Biochem J* **430**(2): 207-13.

Reddy, S. K., Rape M., Margansky W. A. and Kirschner M. W. (2007). "Ubiquitination by the anaphase-promoting complex drives spindle checkpoint inactivation." *Nature* **446**(7138): 921-5.

Reeves, M. E., Baldwin S. W., Baldwin M. L., Chen S. T., Moretz J. M., Aragon R. J., Li X., Strong D. D., Mohan S. and Amaar Y. G. (2010). "Ras-association domain family 1C protein promotes breast cancer cell migration and attenuates apoptosis." *BMC Cancer* **10**(1): 562.

Reeves, N. and Posakony J. W. (2005). "Genetic programs activated by proneural proteins in the developing Drosophila PNS." *Dev Cell* **8**(3): 413-25.

Regnier, V., Vagnarelli P., Fukagawa T., Zerjal T., Burns E., Trouche D., Earnshaw W. and Brown W. (2005). "CENP-A is required for accurate chromosome segregation and sustained kinetochore association of BubR1." *Mol Cell Biol* **25**(10): 3967-81.

Resnick, T. D., Satinover D. L., MacIsaac F., Stukenberg P. T., Earnshaw W. C., Orr-Weaver T. L. and Carmena M. (2006). "INCENP and Aurora B promote meiotic sister chromatid cohesion through

localization of the Shugoshin MEI-S332 in Drosophila." *Dev Cell* **11**(1): 57-68.

Ribeiro, P. S., Josue F., Wepf A., Wehr M. C., Rinner O., Kelly G., Tapon N. and Gstaiger M. (2010). "Combined functional genomic and proteomic approaches identify a PP2A complex as a negative regulator of Hippo signaling." *Mol Cell* **39**(4): 521-34.

Richter, A. M., Pfeifer G. P. and Dammann R. H. (2009). "The RASSF proteins in cancer; from epigenetic silencing to functional characterization." *Biochim Biophys Acta* **1796**(2): 114-28.

Rieder, C. L. and Alexander S. P. (1990). "Kinetochores are transported poleward along a single astral microtubule during chromosome attachment to the spindle in newt lung cells." *J Cell Biol* **110**(1): 81-95.

Rieder, C. L., Cole R. W., Khodjakov A. and Sluder G. (1995). "The checkpoint delaying anaphase in response to chromosome monoorientation is mediated by an inhibitory signal produced by unattached kinetochores." *J Cell Biol* **130**(4): 941-8.

Rieder, C. L. and Salmon E. D. (1998). "The vertebrate cell kinetochore and its roles during mitosis." *Trends Cell Biol* **8**(8): 310-8.

Rieder, C. L., Schultz A., Cole R. and Sluder G. (1994). "Anaphase onset in vertebrate somatic cells is controlled by a checkpoint that monitors sister kinetochore attachment to the spindle." *J Cell Biol* **127**(5): 1301-10.

Rodriguez-Viciana, P., Sabatier C. and McCormick F. (2004). "Signaling specificity by Ras family GTPases is determined by the full spectrum of effectors they regulate." *Mol Cell Biol* **24**(11): 4943-54.

Rong, R., Jiang L. Y., Sheikh M. S. and Huang Y. (2007). "Mitotic kinase Aurora-A phosphorylates RASSF1A and modulates RASSF1A-mediated microtubule interaction and M-phase cell cycle regulation." *Oncogene* **26**(55): 7700-8.

Rong, R., Jin W., Zhang J., Sheikh M. S. and Huang Y. (2004). "Tumor suppressor RASSF1A is a microtubule-binding protein that stabilizes microtubules and induces G2/M arrest." *Oncogene* **23**(50): 8216-30.

Rosasco-Nitcher, S. E., Lan W., Khorasanizadeh S. and Stukenberg P. T. (2008). "Centromeric Aurora-B activation requires TD-60, microtubules, and substrate priming phosphorylation." *Science* **319**(5862): 469-72.

Roscioli, E., Bolognesi A., Guarguaglini G. and Lavia P. (2010). "Ran control of mitosis in human cells: gradients and local signals." *Biochem Soc Trans* **38**(6): 1709-14.

Ruchaud, S., Carmena M. and Earnshaw W. C. (2007). "Chromosomal passengers: conducting cell division." *Nat Rev Mol Cell Biol* **8**(10): 798-812.

Saavedra, H. I., Knauf J. A., Shirokawa J. M., Wang J., Ouyang B., Elisei R., Stambrook P. J. and Fagin J. A. (2000). "The RAS oncogene induces genomic instability in thyroid PCCL3 cells via the MAPK pathway." *Oncogene* **19**(34): 3948-54.

Sampath, S. C., Ohi R., Leismann O., Salic A., Pozniakovski A. and Funabiki H. (2004). "The chromosomal passenger complex is required for chromatin-induced microtubule stabilization and spindle assembly." *Cell* **118**(2): 187-202.

Sasai, K., Katayama H., Stenoien D. L., Fujii S., Honda R., Kimura M., Okano Y., Tatsuka M., Suzuki F., Nigg E. A., Earnshaw W. C., Brinkley W. R. and Sen S. (2004). "Aurora-C kinase is a novel chromosomal passenger protein that can complement Aurora-B kinase function in mitotic cells." *Cell Motil Cytoskeleton* **59**(4): 249-63.

Saucedo, L. J. and Edgar B. A. (2007). "Filling out the Hippo pathway." *Nat Rev Mol Cell Biol* **8**(8): 613-21.

Schagdarsurengin, U., Richter A. M., Wohler C. and Dammann R. H. (2009). "Frequent epigenetic inactivation of RASSF10 in thyroid cancer." *Epigenetics* **4**(8): 571-6.

Scheel, H. and Hofmann K. (2003). "A novel interaction motif, SARAH, connects three classes of tumor suppressor." *Curr Biol* **13**(23): R899-900.

Seki, A., Coppinger J. A., Jang C. Y., Yates J. R. and Fang G. (2008). "Bora and the kinase Aurora a cooperatively activate the kinase Plk1 and control mitotic entry." *Science* **320**(5883): 1655-8.

Sekido, Y., Ahmadian M., Wistuba, II, Latif F., Bader S., Wei M. H., Duh F. M., Gazdar A. F., Lerman M. I. and Minna J. D. (1998). "Cloning of a breast cancer homozygous deletion junction narrows the region of search for a 3p21.3 tumor suppressor gene." *Oncogene* **16**(24): 3151-7.

Sessa, F., Mapelli M., Ciferri C., Tarricone C., Areces L. B., Schneider T. R., Stukenberg P. T. and Musacchio A. (2005). "Mechanism of Aurora B activation by INCENP and inhibition by hesperadin." *Mol Cell* **18**(3): 379-91.

Shah, J. V., Botvinick E., Bonday Z., Furnari F., Berns M. and Cleveland D. W. (2004). "Dynamics of centromere and kinetochore proteins; implications for checkpoint signaling and silencing." *Curr Biol* **14**(11): 942-52.

Sharp-Baker, H. and Chen R. H. (2001). "Spindle checkpoint protein Bub1 is required for kinetochore localization of Mad1, Mad2, Bub3, and CENP-E, independently of its kinase activity." *J Cell Biol* **153**(6): 1239-50.

Sharpe, J. C., Arnoult D. and Youle R. J. (2004). "Control of mitochondrial permeability by Bcl-2 family members." *Biochim Biophys Acta* **1644**(2-3): 107-13.

Sherwood, V., Manbodh R., Sheppard C. and Chalmers A. D. (2008). "RASSF7 is a member of a new family of RAS association domain-containing proteins and is required for completing mitosis." *Mol Biol Cell* **19**(4): 1772-82.

Sherwood, V., Recino A., Jeffries A., Ward A. and Chalmers A. D. (2010). "The N-terminal RASSF family: a new group of Ras-association-domain-containing proteins, with emerging links to cancer formation." *Biochem J* **425**(2): 303-11.

Shivakumar, L., Minna J., Sakamaki T., Pestell R. and White M. A. (2002). "The RASSF1A tumor suppressor blocks cell cycle progression and inhibits cyclin D1 accumulation." *Mol Cell Biol* **22**(12): 4309-18.

Shweiki, D., Itin A., Soffer D. and Keshet E. (1992). "Vascular endothelial growth factor induced by hypoxia may mediate hypoxia-initiated angiogenesis." *Nature* **359**(6398): 843-5.

Skoufias, D. A., Andreassen P. R., Lacroix F. B., Wilson L. and Margolis R. L. (2001). "Mammalian mad2 and bub1/bubR1 recognize distinct spindle-attachment and kinetochore-tension checkpoints." *Proc Natl Acad Sci U S A* **98**(8): 4492-7.

Soares, D. G., Escargueil A. E., Poindessous V., Sarasin A., de Gramont A., Bonatto D., Henriques J. A. and Larsen A. K. (2007). "Replication and homologous recombination repair regulate DNA double-strand break formation by the antitumor alkylator ecteinascidin 743." *Proc Natl Acad Sci U S A* **104**(32): 13062-7.

Song, M. S., Chang J. S., Song S. J., Yang T. H., Lee H. and Lim D. S. (2005). "The centrosomal protein RAS association domain family protein 1A (RASSF1A)-binding protein 1 regulates mitotic progression by recruiting RASSF1A to spindle poles." *J Biol Chem* **280**(5): 3920-7.

Song, M. S. and Lim D. S. (2004). "Control of APC-Cdc20 by the tumor suppressor RASSF1A." *Cell Cycle* **3**(5): 574-6.

Song, M. S., Song S. J., Ayad N. G., Chang J. S., Lee J. H., Hong H. K., Lee H., Choi N., Kim J., Kim H., Kim J. W., Choi E. J., Kirschner M. W. and Lim D. S. (2004). "The tumour suppressor RASSF1A regulates mitosis by inhibiting the APC-Cdc20 complex." *Nat Cell Biol* **6**(2): 129-37.

Stearns, T., Evans L. and Kirschner M. (1991). "Gamma-tubulin is a highly conserved component of the centrosome." *Cell* **65**(5): 825-36.

Stearns, T. and Kirschner M. (1994). "In vitro reconstitution of centrosome assembly and function: the central role of gamma-tubulin." *Cell* **76**(4): 623-37.

Strunnikov, A. V. (2003). "Condensin and biological role of chromosome condensation." *Prog Cell Cycle Res* **5**: 361-7.

Sudakin, V., Chan G. K. and Yen T. J. (2001). "Checkpoint inhibition of the APC/C in HeLa cells is mediated by a complex of BUBR1, BUB3, CDC20, and MAD2." *J Cell Biol* **154**(5): 925-36.

Sumara, I., Vorlaufer E., Stukenberg P. T., Kelm O., Redemann N., Nigg E. A. and Peters J. M. (2002). "The dissociation of cohesin from chromosomes in prophase is regulated by Polo-like kinase." *Mol Cell* **9**(3): 515-25.

Takahashi, S., Ebihara A., Kajiho H., Kontani K., Nishina H. and Katada T. (2011). "RASSF7 negatively regulates pro-apoptotic JNK signaling by inhibiting the activity of phosphorylated-MKK7." *Cell Death Differ* **18**(4): 645-55.

Tamimi, R. M., Hankinson S. E., Ding S., Gagalang V., Larson G. P., Spiegelman D., Colditz G. A., Krontiris T. G. and Hunter D. J. (2003). "The HRAS1 variable number of tandem repeats and risk of breast cancer." *Cancer Epidemiol Biomarkers Prev* **12**(12): 1528-30.

Tan, D. S., Lambros M. B., Rayter S., Natrajan R., Vatcheva R., Gao Q., Marchio C., Geyer F. C., Savage K., Parry S., Fenwick K., Tamber N., Mackay A., Dexter T., Jameson C., McCluggage W. G., Williams A., Graham A., Faratian D., El-Bahrawy M., Paige A. J., Gabra H., Gore M. E., Zvelebil M., Lord C. J., Kaye S. B., Ashworth A. and Reis-Filho J. S. (2009). "PPM1D is a potential therapeutic target in ovarian clear cell carcinomas." *Clin Cancer Res* **15**(7): 2269-80.

Tan, K. O., Tan K. M., Chan S. L., Yee K. S., Bevort M., Ang K. C. and Yu V. C. (2001). "MAP-1, a novel proapoptotic protein containing a BH3-like motif that associates with Bax through its Bcl-2 homology domains." *J Biol Chem* **276**(4): 2802-7.

Tanaka, T. U. (2008). "Bi-orienting chromosomes: acrobatics on the mitotic spindle." *Chromosoma* **117**(6): 521-33.

Tanaka, T. U., Rachidi N., Janke C., Pereira G., Galova M., Schiebel E., Stark M. J. and Nasmyth K. (2002). "Evidence that the Ipl1-Sli15 (Aurora kinase-INCENP) complex promotes chromosome bi-orientation by altering kinetochore-spindle pole connections." *Cell* **108**(3): 317-29.

Tang, Z., Shu H., Oncel D., Chen S. and Yu H. (2004). "Phosphorylation of Cdc20 by Bub1 provides a catalytic mechanism for APC/C inhibition by the spindle checkpoint." *Mol Cell* **16**(3): 387-97.

Terada, Y., Tatsuka M., Suzuki F., Yasuda Y., Fujita S. and Otsu M. (1998). "AIM-1: a mammalian midbody-associated protein required for cytokinesis." *EMBO J* **17**(3): 667-76.

Terada, Y., Uetake Y. and Kuriyama R. (2003). "Interaction of Aurora-A and centrosomin at the microtubule-nucleating site in Drosophila and mammalian cells." *J Cell Biol* **162**(5): 757-63.

Tommasi, S., Dammann R., Jin S. G., Zhang X. F., Avruch J. and Pfeifer G. P. (2002). "RASSF3 and NORE1: identification and cloning of two human homologues of the putative tumor suppressor gene RASSF1." *Oncogene* **21**(17): 2713-20.

Tommasi, S., Dammann R., Zhang Z., Wang Y., Liu L., Tsark W. M., Wilczynski S. P., Li J., You M. and Pfeifer G. P. (2005). "Tumor susceptibility of Rassf1a knockout mice." *Cancer Res* **65**(1): 92-8.

Tsai, M. Y., Wiese C., Cao K., Martin O., Donovan P., Ruderman J., Prigent C. and Zheng Y. (2003). "A Ran signalling pathway mediated by the mitotic kinase Aurora A in spindle assembly." *Nat Cell Biol* **5**(3): 242-8.

Tsang, H. T., Connell J. W., Brown S. E., Thompson A., Reid E. and Sanderson C. M. (2006). "A systematic analysis of human CHMP protein interactions: additional MIT domain-containing proteins bind to multiple components of the human ESCRT III complex." *Genomics* **88**(3): 333-46.

Ura, S., Nishina H., Gotoh Y. and Katada T. (2007). "Activation of the c-Jun N-terminal kinase pathway by MST1 is essential and sufficient for the induction of chromatin condensation during apoptosis." *Mol Cell Biol* **27**(15): 5514-22.

Vader, G., Kauw J. J., Medema R. H. and Lens S. M. (2006a). "Survivin mediates targeting of the chromosomal passenger complex to the centromere and midbody." *EMBO Rep* **7**(1): 85-92.

Vader, G., Medema R. H. and Lens S. M. (2006b). "The chromosomal passenger complex: guiding Aurora-B through mitosis." *J Cell Biol* **173**(6): 833-7.

Vaisberg, E. A., Koonce M. P. and McIntosh J. R. (1993). "Cytoplasmic dynein plays a role in mammalian mitotic spindle formation." *J Cell Biol* **123**(4): 849-58.

van der Weyden, L. and Adams D. J. (2007). "The Ras-association domain family (RASSF) members and their role in human tumourigenesis." *Biochim Biophys Acta* **1776**(1): 58-85.

van der Weyden, L., Arends M. J., Dovey O. M., Harrison H. L., Lefebvre G., Conte N., Gergely F. V., Bradley A. and Adams D. J. (2008). "Loss of Rassf1a cooperates with Apc(Min) to accelerate intestinal tumourigenesis." *Oncogene* **27**(32): 4503-8.

van der Weyden, L., Tachibana K. K., Gonzalez M. A., Adams D. J., Ng B. L., Petty R., Venkitaraman A. R., Arends M. J. and Bradley A. (2005). "The RASSF1A isoform of RASSF1 promotes microtubule stability and suppresses tumorigenesis." *Mol Cell Biol* **25**(18): 8356-67.

Vasioukhin, V., Bauer C., Degenstein L., Wise B. and Fuchs E. (2001). "Hyperproliferation and defects in epithelial polarity upon conditional ablation of alpha-catenin in skin." *Cell* **104**(4): 605-17.

Vavvas, D., Li X., Avruch J. and Zhang X. F. (1998). "Identification of Nore1 as a potential Ras effector." *J Biol Chem* **273**(10): 5439-42.

Verma, S. K., Ganesan T. S. and Parker P. J. (2008). "The tumour suppressor RASSF1A is a novel substrate of PKC." *FEBS Lett* **582**(15): 2270-6.

Vichalkovski, A., Gresko E., Cornils H., Hergovich A., Schmitz D. and Hemmings B. A. (2008). "NDR kinase is activated by RASSF1A/MST1 in response to Fas receptor stimulation and promotes apoptosis." *Curr Biol* **18**(23): 1889-95.

Vogel, C., Kienitz A., Hofmann I., Muller R. and Bastians H. (2004). "Crosstalk of the mitotic spindle assembly checkpoint with p53 to prevent polyploidy." *Oncogene* **23**(41): 6845-53.

Vos, M. D. and Clark G. J. (2006). "RASSF family proteins and Ras transformation." *Methods Enzymol* **407**: 311-22.

Vos, M. D., Dallol A., Eckfeld K., Allen N. P., Donninger H., Hesson L. B., Calvisi D., Latif F. and Clark G. J. (2006). "The RASSF1A tumor

suppressor activates Bax via MOAP-1." *J Biol Chem* **281**(8): 4557-63.

Vos, M. D., Ellis C. A., Bell A., Birrer M. J. and Clark G. J. (2000). "Ras uses the novel tumor suppressor RASSF1 as an effector to mediate apoptosis." *J Biol Chem* **275**(46): 35669-72.

Vos, M. D., Ellis C. A., Elam C., Ulku A. S., Taylor B. J. and Clark G. J. (2003a). "RASSF2 is a novel K-Ras-specific effector and potential tumor suppressor." *J Biol Chem* **278**(30): 28045-51.

Vos, M. D., Martinez A., Elam C., Dallol A., Taylor B. J., Latif F. and Clark G. J. (2004). "A role for the RASSF1A tumor suppressor in the regulation of tubulin polymerization and genomic stability." *Cancer Res* **64**(12): 4244-50.

Vos, M. D., Martinez A., Ellis C. A., Vallecorsa T. and Clark G. J. (2003b). "The pro-apoptotic Ras effector Nore1 may serve as a Ras-regulated tumor suppressor in the lung." *J Biol Chem* **278**(24): 21938-43.

Wada, T., Joza N., Cheng H. Y., Sasaki T., Kozieradzki I., Bachmaier K., Katada T., Schreiber M., Wagner E. F., Nishina H. and Penninger J. M. (2004). "MKK7 couples stress signalling to G2/M cell-cycle progression and cellular senescence." *Nat Cell Biol* **6**(3): 215-26.

Waizenegger, I. C., Hauf S., Meinke A. and Peters J. M. (2000). "Two distinct pathways remove mammalian cohesin from chromosome arms in prophase and from centromeres in anaphase." *Cell* **103**(3): 399-410.

Wei, Y., Mizzen C. A., Cook R. G., Gorovsky M. A. and Allis C. D. (1998). "Phosphorylation of histone H3 at serine 10 is correlated with chromosome condensation during mitosis and meiosis in Tetrahymena." *Proc Natl Acad Sci U S A* **95**(13): 7480-4.

Weiser, K. C., Liu B., Hansen G. M., Skapura D., Hentges K. E., Yarlagadda S., Morse Iii H. C. and Justice M. J. (2007). "Retroviral insertions in the VISION database identify molecular pathways in mouse lymphoid leukaemia and lymphoma." *Mamm Genome* **18**(10): 709-22.

Weitzel, J. N., Ding S., Larson G. P., Nelson R. A., Goodman A., Grendys E. C., Ball H. G. and Krontiris T. G. (2000). "The HRAS1 minisatellite locus and risk of ovarian cancer." *Cancer Res* **60**(2): 259-61.

Weitzel, J. N., Kasperczyk A., Mohan C. and Krontiris T. G. (1992). "The HRAS1 gene cluster: two upstream regions recognizing transcripts and a third encoding a gene with a leucine zipper domain." *Genomics* **14**(2): 309-19.

Welcsh, P. L., Lee M. K., Gonzalez-Hernandez R. M., Black D. J., Mahadevappa M., Swisher E. M., Warrington J. A. and King M. C. (2002). "BRCA1 transcriptionally regulates genes involved in breast tumorigenesis." *Proc Natl Acad Sci U S A* **99**(11): 7560-5.

Whang, Y. M., Kim Y. H., Kim J. S. and Yoo Y. D. (2005). "RASSF1A suppresses the c-Jun-NH2-kinase pathway and inhibits cell cycle progression." *Cancer Res* **65**(9): 3682-90.

Wheatley, S. P., Carvalho A., Vagnarelli P. and Earnshaw W. C. (2001). "INCENP is required for proper targeting of Survivin to the centromeres and the anaphase spindle during mitosis." *Curr Biol* **11**(11): 886-90.

Wong, I. H., Chan J., Wong J. and Tam P. K. (2004). "Ubiquitous aberrant RASSF1A promoter methylation in childhood neoplasia." *Clin Cancer Res* **10**(3): 994-1002.

Yamamoto, T., Taya S. and Kaibuchi K. (1999). "Ras-induced transformation and signaling pathway." *J Biochem* **126**(5): 799-803.

Yan, P. S., Shi H., Rahmatpanah F., Hsiau T. H., Hsiau A. H., Leu Y. W., Liu J. C. and Huang T. H. (2003). "Differential distribution of DNA methylation within the RASSF1A CpG island in breast cancer." *Cancer Res* **63**(19): 6178-86.

Yan, X., Cao L., Li Q., Wu Y., Zhang H., Saiyin H., Liu X., Zhang X., Shi Q. and Yu L. (2005). "Aurora C is directly associated with Survivin and required for cytokinesis." *Genes Cells* **10**(6): 617-26.

Yang, J. and Weinberg R. A. (2008). "Epithelial-mesenchymal transition: at the crossroads of development and tumor metastasis." *Dev Cell* **14**(6): 818-29.

Zeitlin, S. G., Shelby R. D. and Sullivan K. F. (2001). "CENP-A is phosphorylated by Aurora B kinase and plays an unexpected role in completion of cytokinesis." *J Cell Biol* **155**(7): 1147-57.

Zhang, Z., Sun D., Van do N., Tang A., Hu L. and Huang G. (2007). "Inactivation of RASSF2A by promoter methylation correlates with lymph node metastasis in nasopharyngeal carcinoma." *Int J Cancer* **120**(1): 32-8.

Zheng, Y., Wong M. L., Alberts B. and Mitchison T. (1995). "Nucleation of microtubule assembly by a gamma-tubulin-containing ring complex." *Nature* **378**(6557): 578-83.

Zinkowski, R. P., Meyne J. and Brinkley B. R. (1991). "The centromere-kinetochore complex: a repeat subunit model." *J Cell Biol* **113**(5): 1091-110.

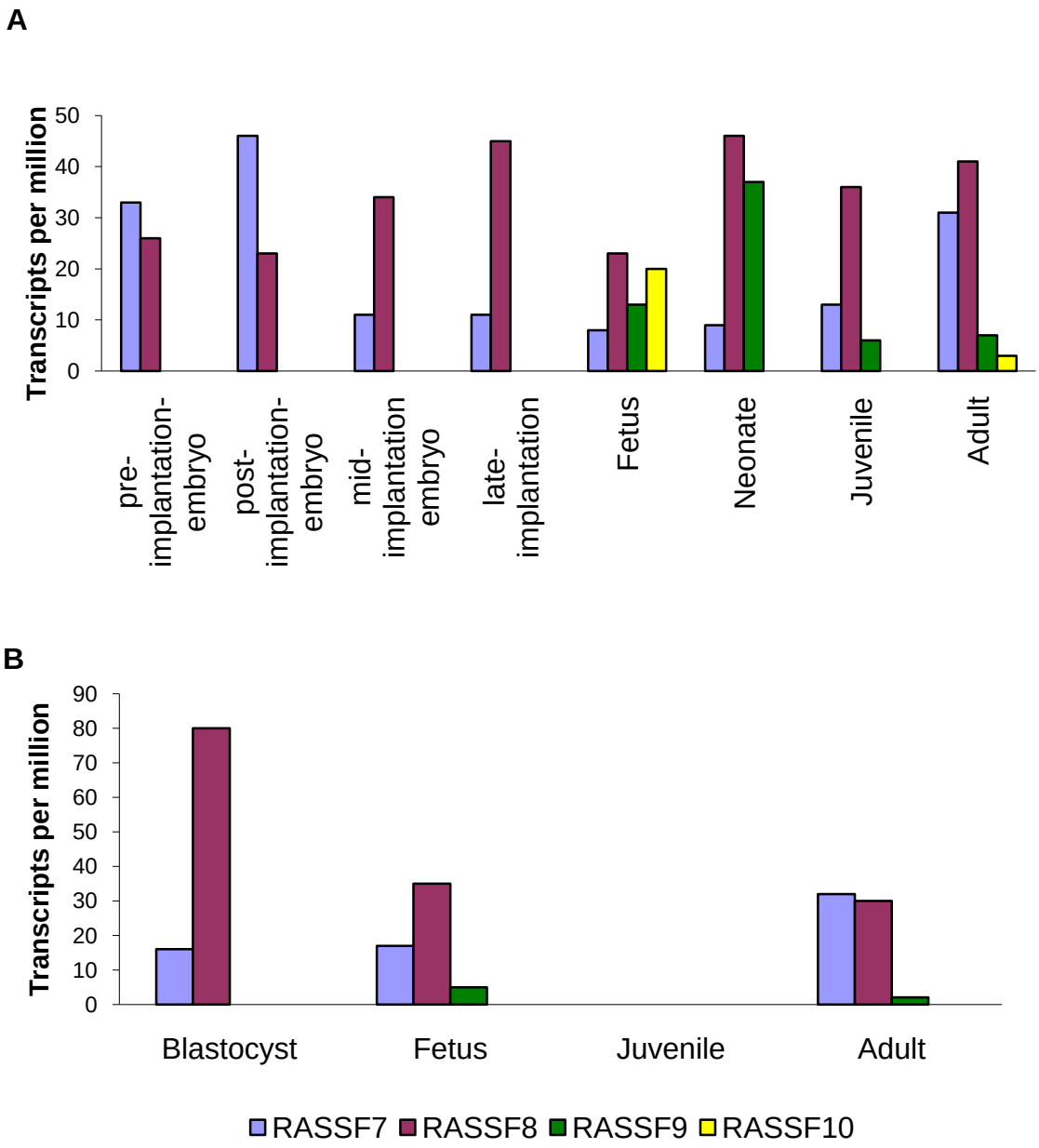


**Figure 3.1: RASSF7, RASSF8, RASSF9 and RASSF10 are predicted to be differentially expressed during mammalian development**. In *silico* temporal *N-Terminal RASSF* expression analysis in mouse (A) and in human (B) according to the NCBI database (http://www.ncbi.nlm.nih.gov/UniGene/ESTProfile). Only the stages with total expressed sequence tags (EST) counts exceeding 50,000 were considered.

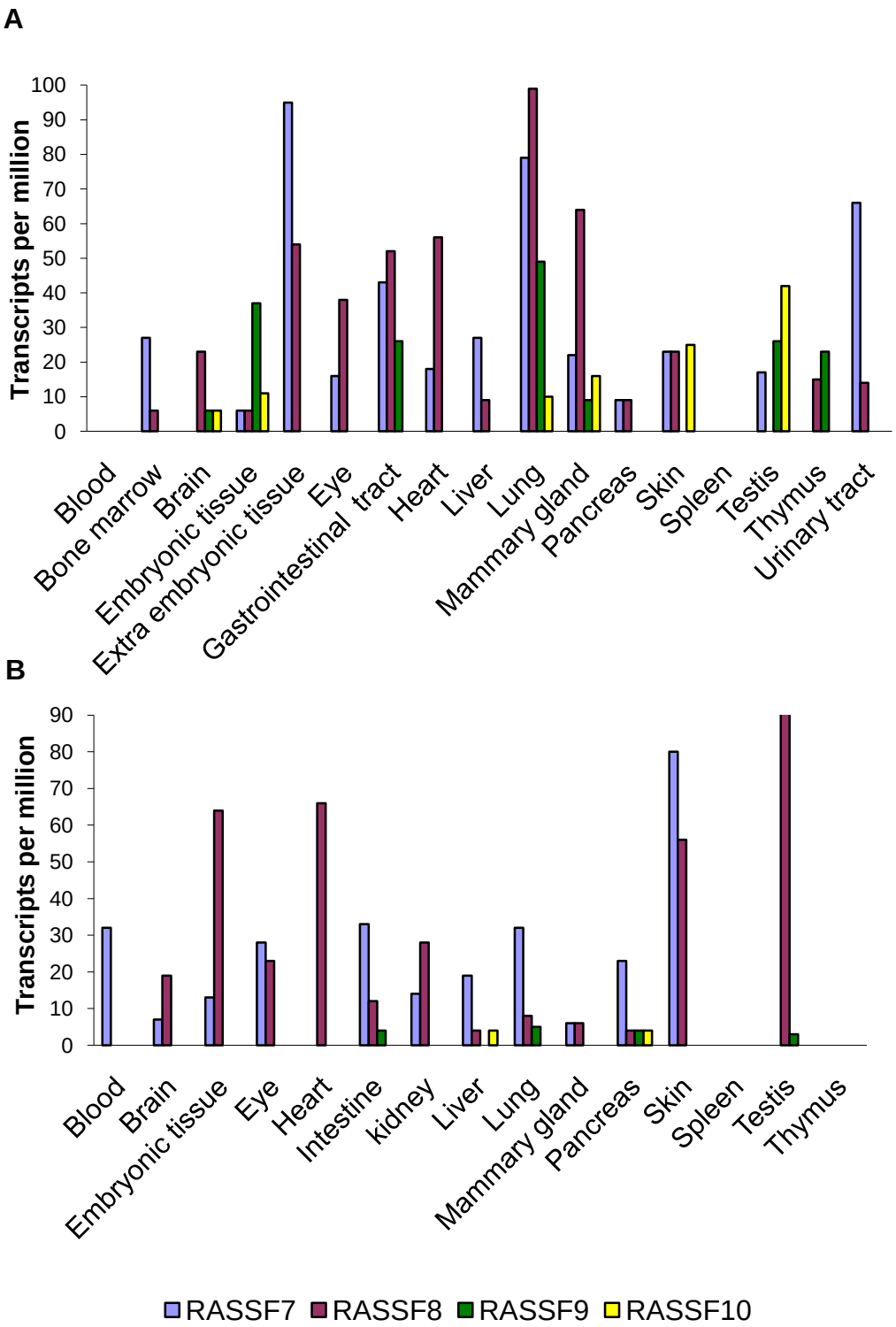


**Figure 3.2: RASSF7 and RASSF8 EST are more frequent than RASSF9 and RASS10 predicted transcripts in mammalian tissues**. In *silico* spatial *N-Terminal RASSF* expression analysis in mouse (A) and in human (B) according to the NCBI database (http://www.ncbi.nlm.nih.gov/UniGene/ESTProfile). Only the tissues with total EST counts exceeding 50,000 were considered.

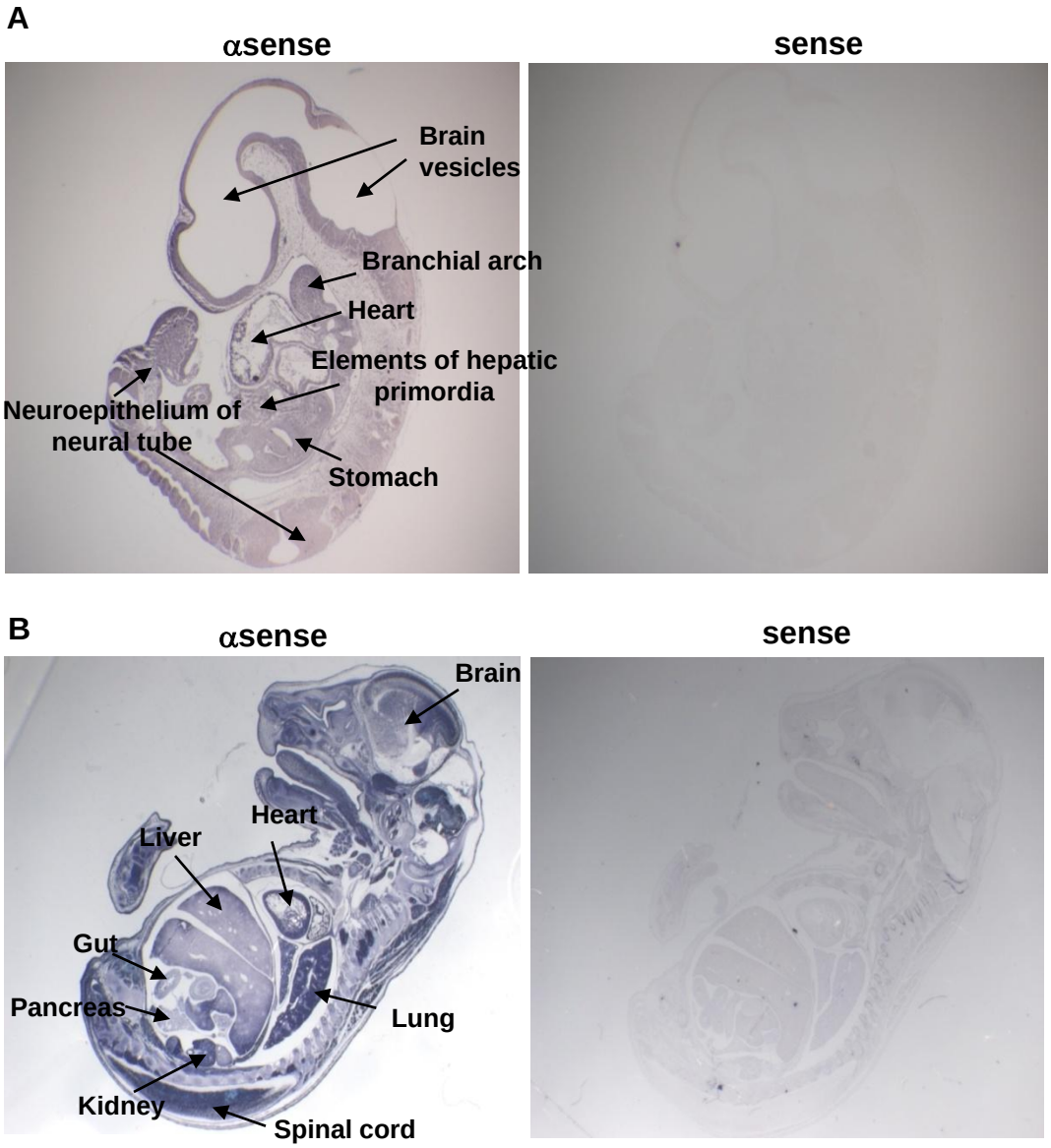


**Figure 3.3: *Rassf7* is ubiquitously expressed during mid and late mouse embryogenesis**. In *situ* hybridisation (ISH) on E10.5 (A, 22x) and E15.5 (B, 8x) mouse sagittal sections. Both *Rassf7* RNA probed (left panel) and negative control (right panel) are shown. The images are representative of at least three independent experiments.

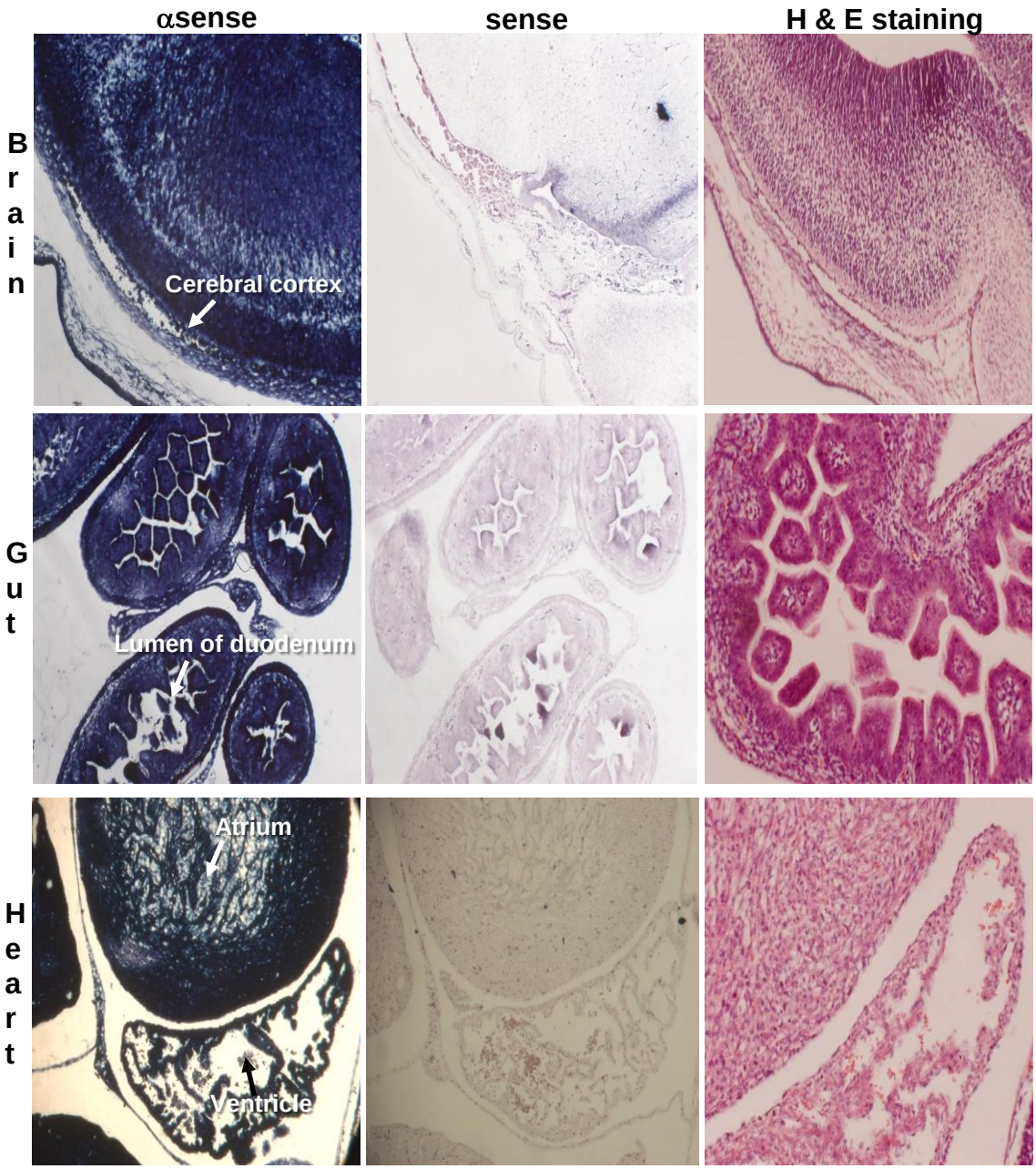


**Figure 3.4: *Rassf7* expression is high during late mouse embryogenesis**. High magnification images of the brain cortex, the gut and the heart of a E15.5 mouse embryo probed for *Rassf7* RNA (left panel) and negative control (central panel) (100x). Haematoxylin and Eosin (H & E) staining is shown as reference (200x). The images are representative of at least three independent experiments.

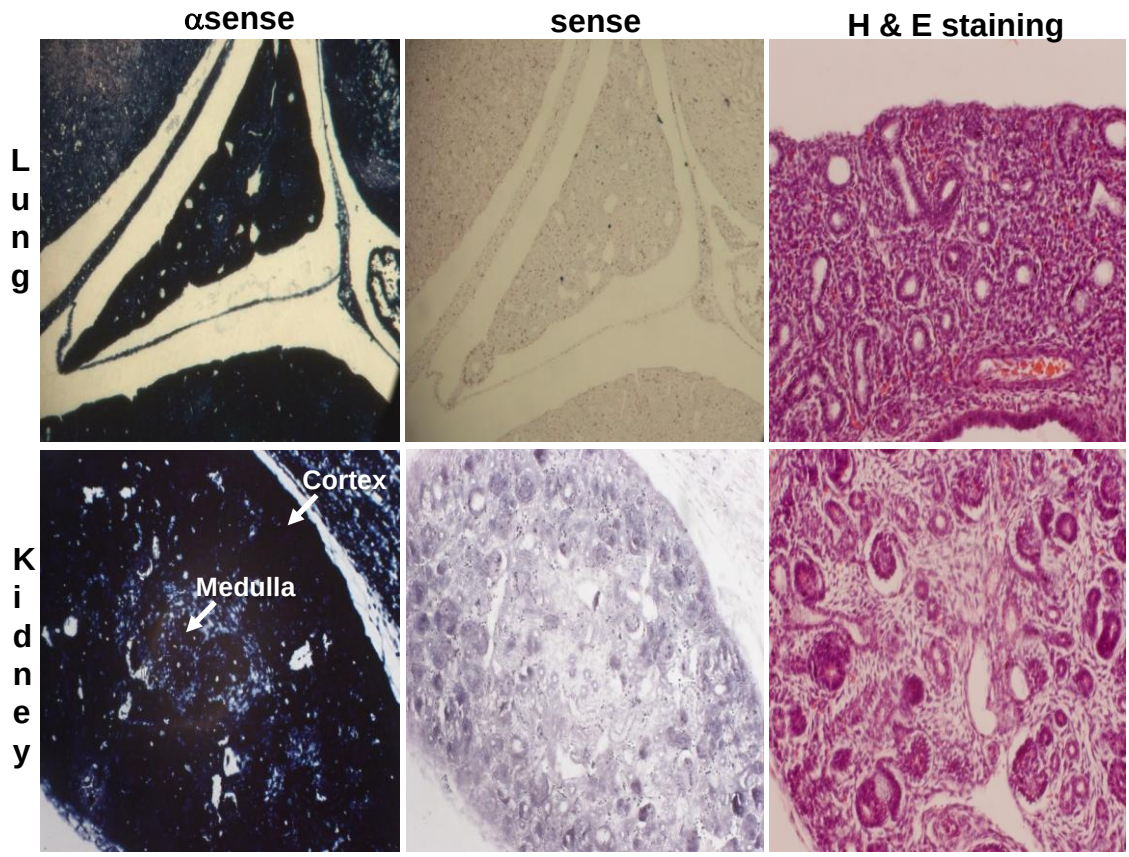


**Figure 3.5: *Rassf7* expression is high during late mouse embryogenesis**. High magnification images of the lung and the kidney of a E15.5 mouse embryo probed for *Rassf7* RNA (left panel) and negative control (central panel) (100x). H a E staining is shown as reference (200x). The images are representative of at least three independent experiments.

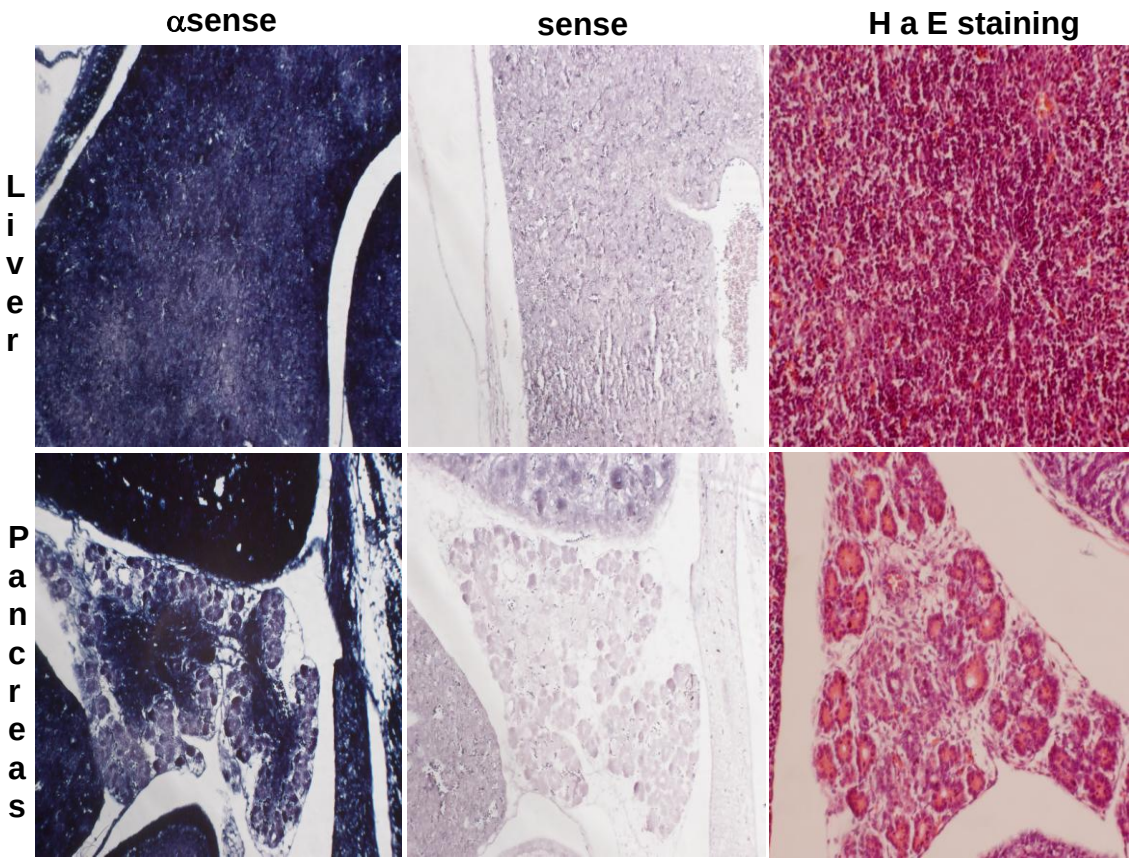


**Figure 3.6: *Rassf7* expression is high during late mouse embryogenesis**. High magnification images of the liver and the pancreas of a E15.5 mouse embryo probed for *Rassf7* RNA (left panel) and negative control (central panel) (100x). H a E staining is shown as reference (200x). The images are representative of at least three independent experiments.

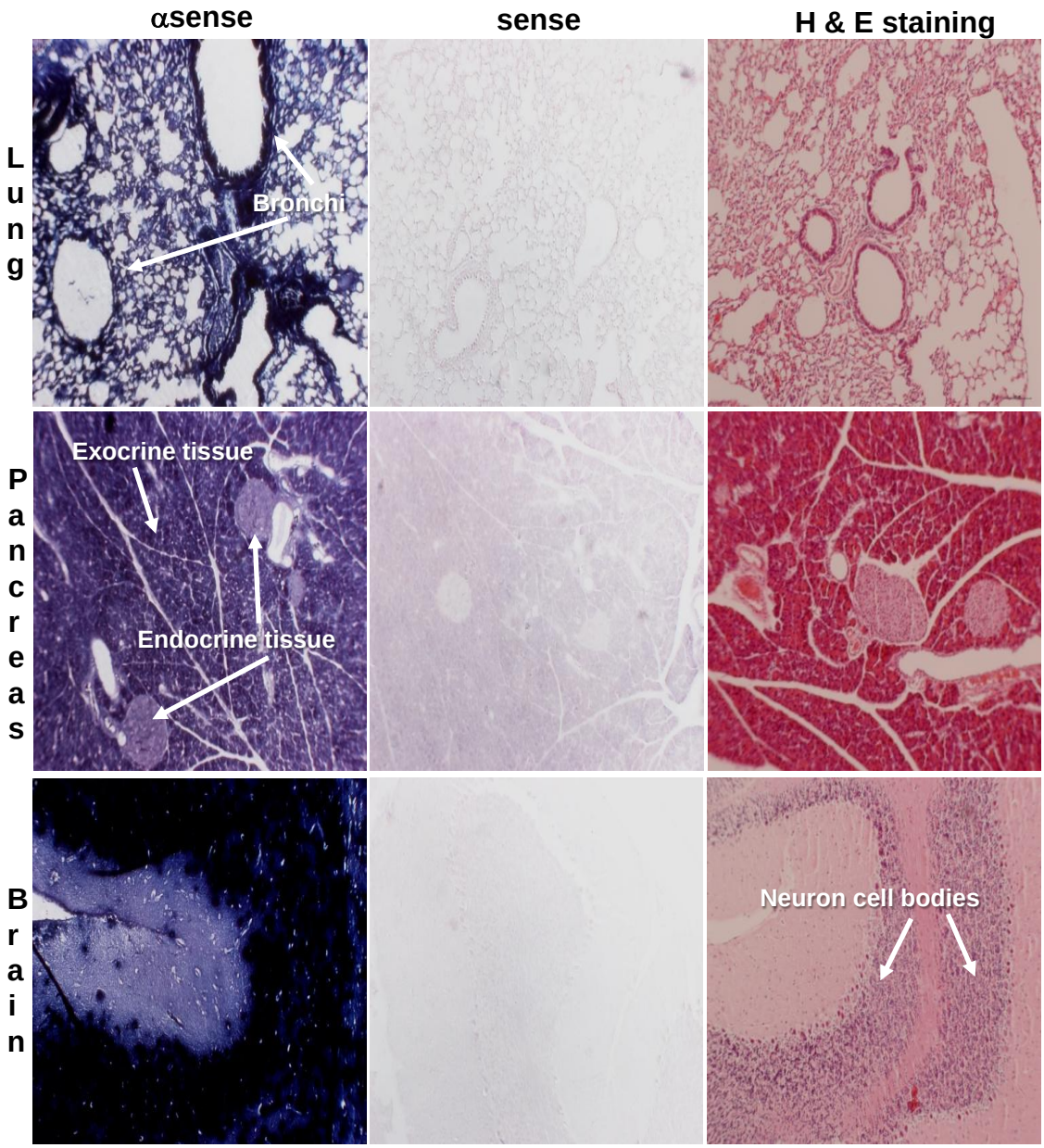


**Figure 3.7: *Rassf7* expression is high in adult mouse organs.** The strong signal detected in the adult mouse lung, pancreas and brain indicates high *Rassf7* expression levels. Both *Rassf7* RNA probed (left panel) and negative control (central panel) are shown (50x). H a E staining is shown as reference (100x). Relevant organ structures are pointed by arrows. The images are representative of at least three independent experiments.

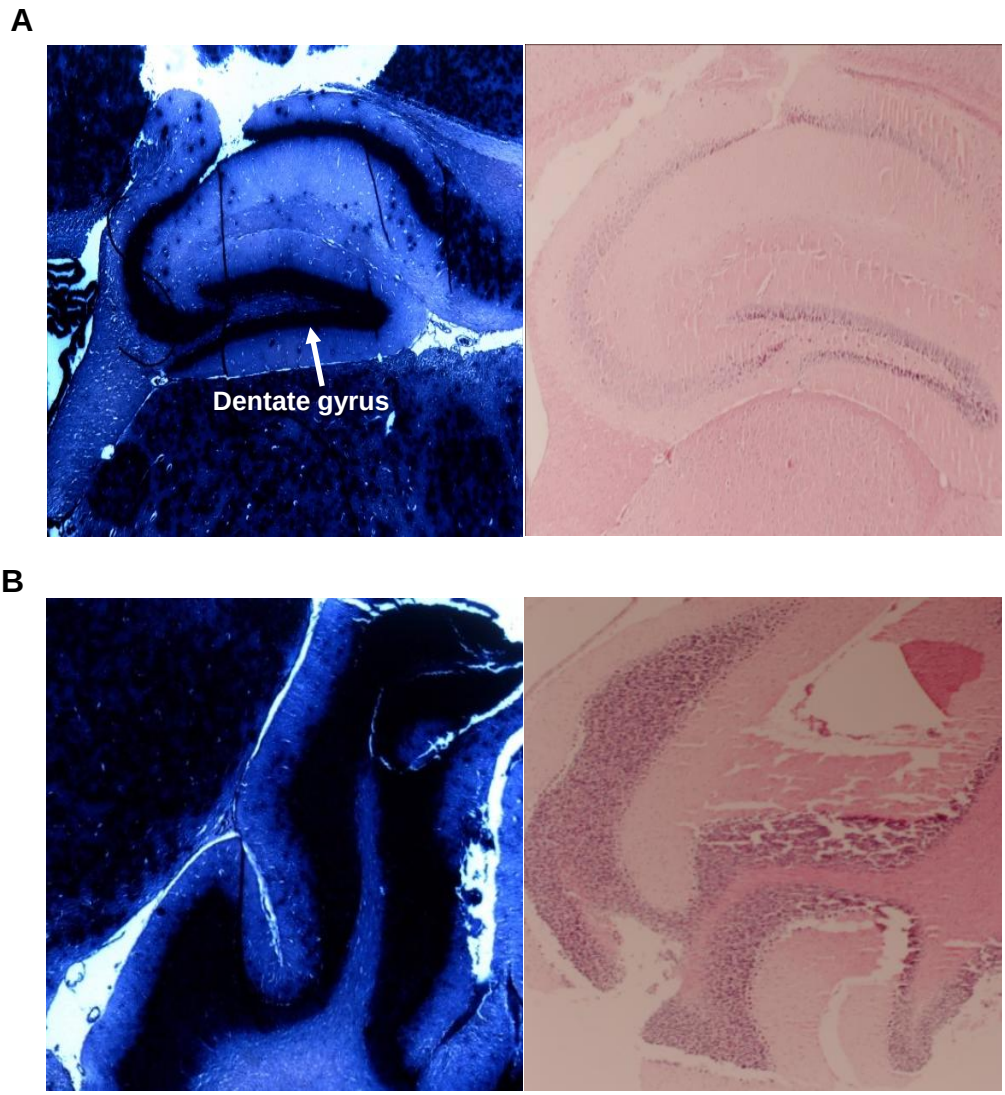


**Figure 3.8: High *Rassf7* expression in the adult mouse brain correlates with high cell density.** High magnification images of the dentate gyrus (pointed by arrow), a region of the hippocampus (A), and the cerebellum (B) probed for *Rassf7* RNA (left panel, 20x). The corresponding H and E staining is shown in the right panel (50x) for cell number reference.

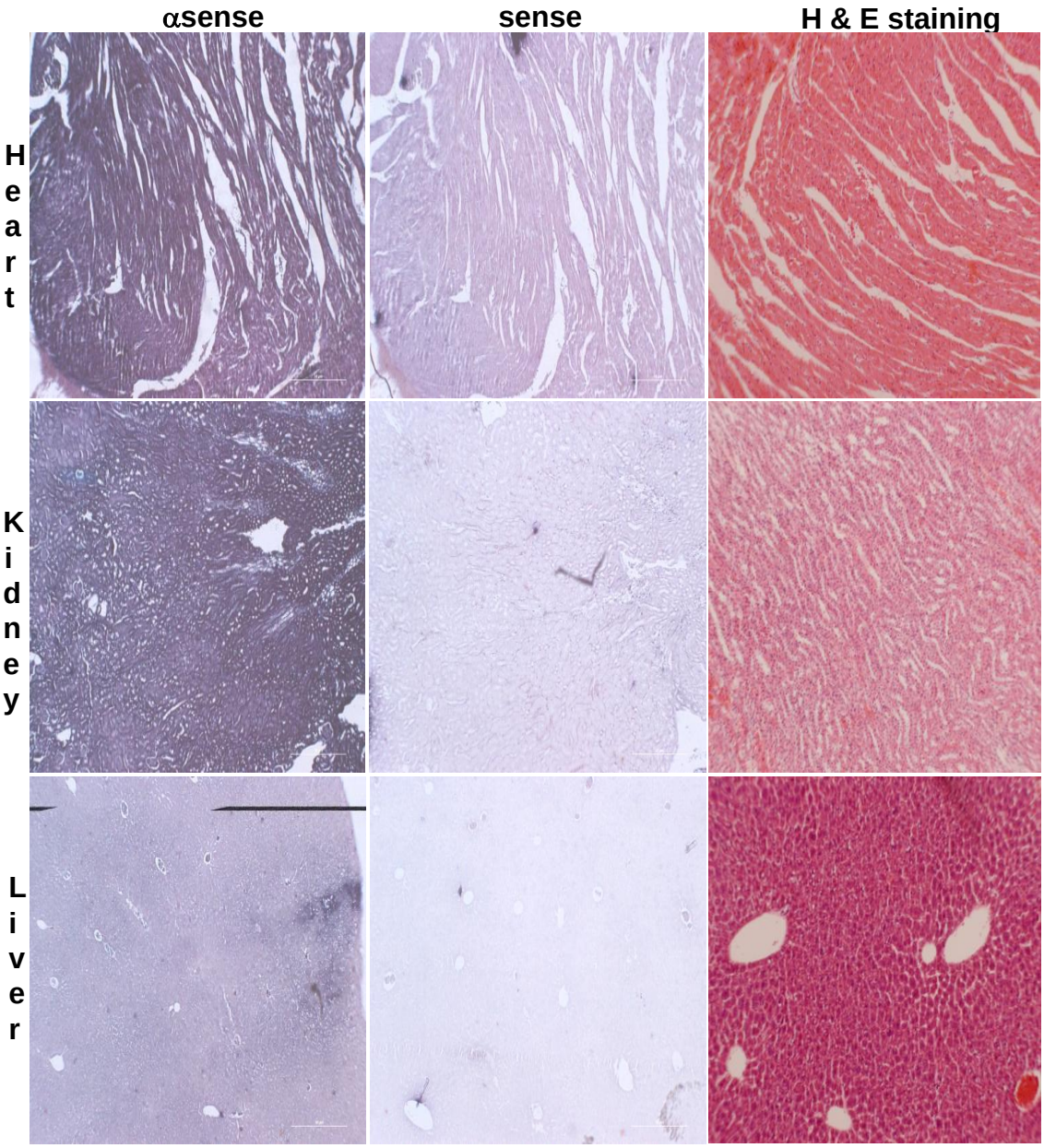


**Figure 3.9: RASSF7 is weakly expressed in the heart, the kidney and the liver during mouse adulthood.** The low intensity of the staining for the heart, the kidney and the liver indicates a low *Rassf7* expression. Both *Rassf7* RNA probed (left panel) and negative control (central panel) are shown (50x). H a E staining is shown as reference (100x). The images are representative of at least three independent experiments.

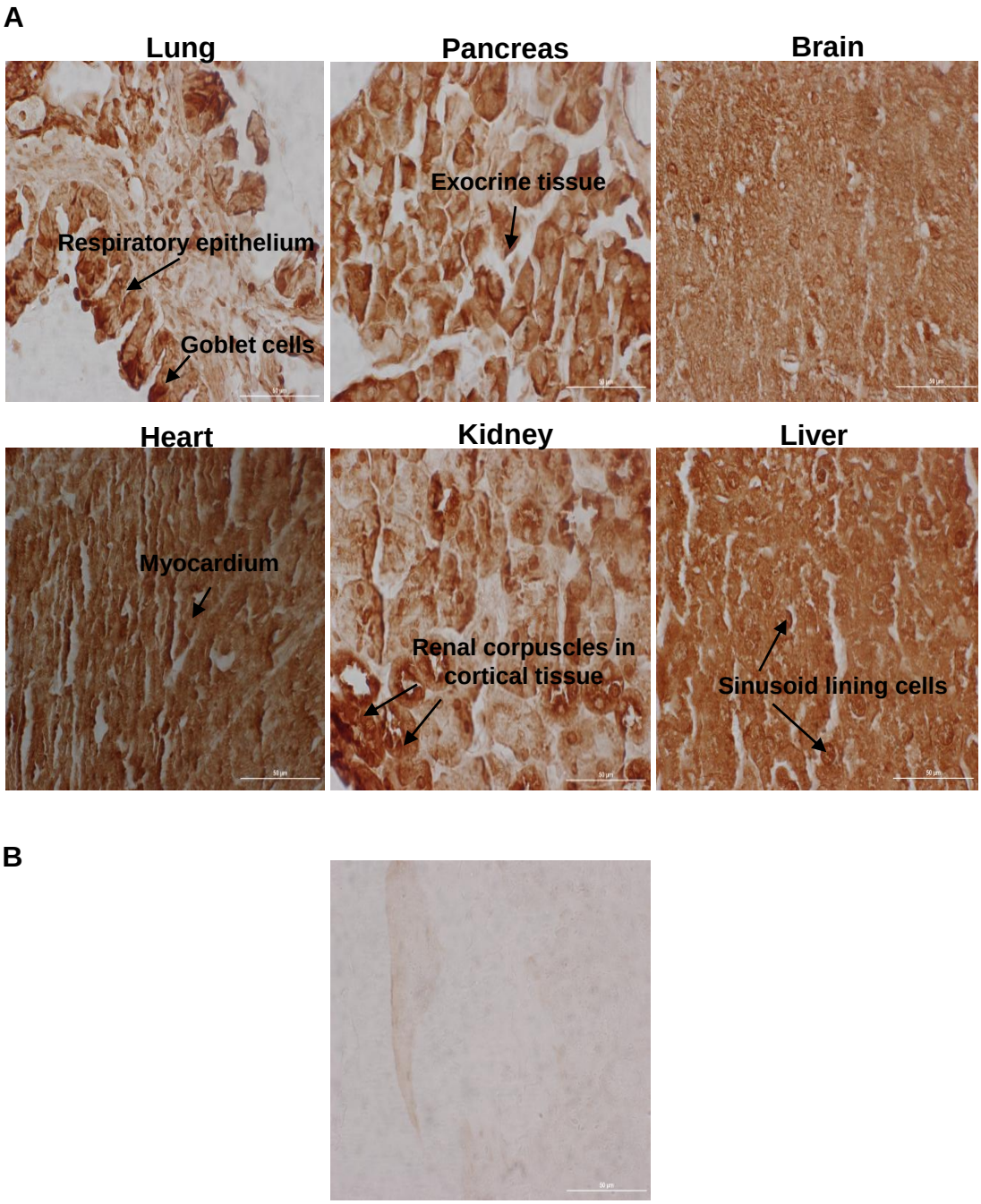


**Figure 3.10: Rassf7 protein is expressed in many organs from an adult mouse.** Immunohistochemistry (IHC) conducted on adult mouse organs (60x) using AVIVA rabbit anti RASSF7 antibody (A). The signal displayed by the corresponding negative controls, probed for rabbit serum, was too weak for imaging (as shown in B). Mouse tissue array kindly donated by Dr Jason Gill, University of Bradford).

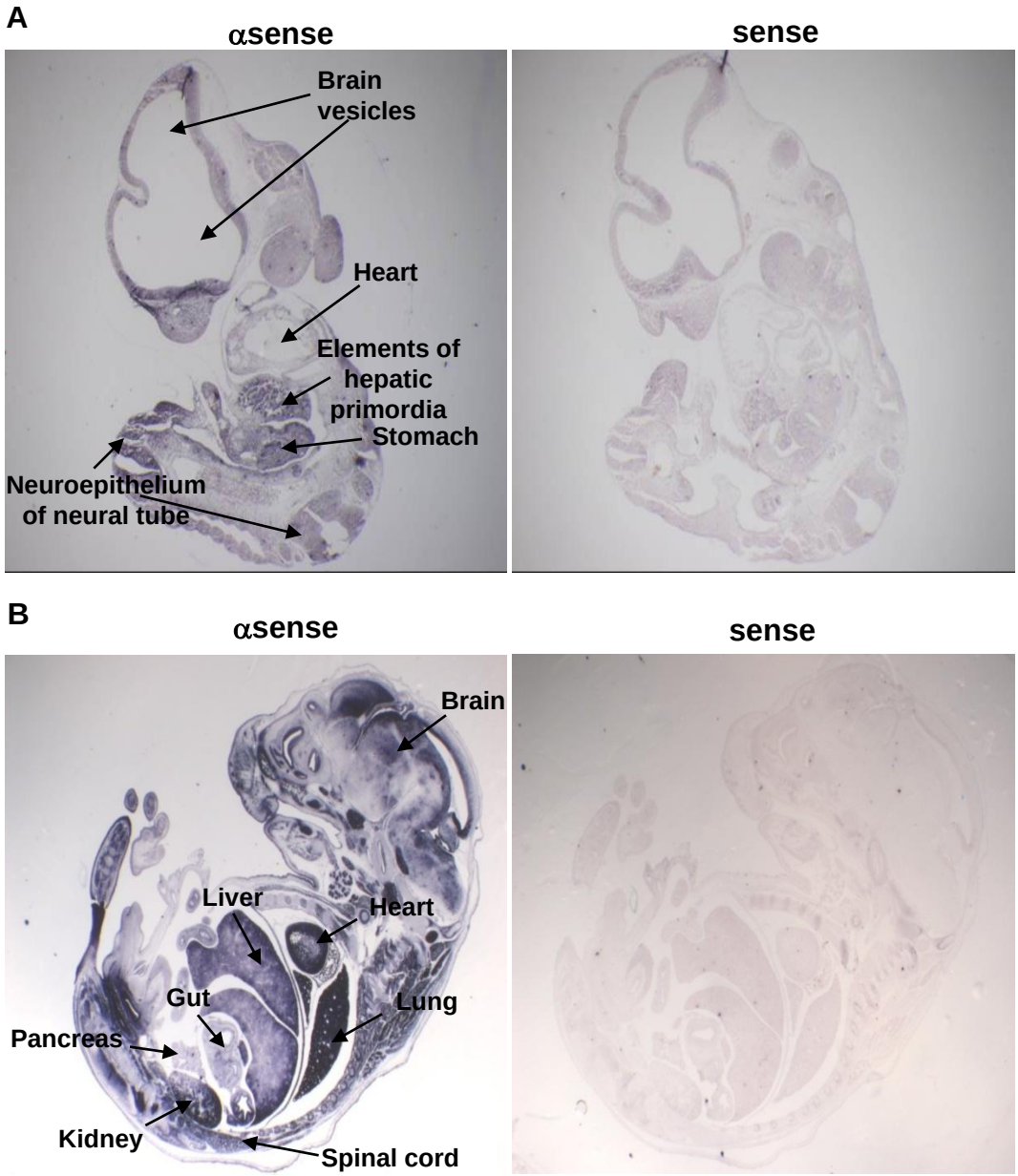


**Figure 3.11: Mouse *Rassf8* is expressed during mid and late mouse embryogenesis**. ISH on E10.5 (A, 22x) and E15.5 (B, 8x) mouse sagittal sections. Both *Rassf8* RNA probed (left panel) and negative control (right panel) are shown. The images are representative of at least three independent experiments.

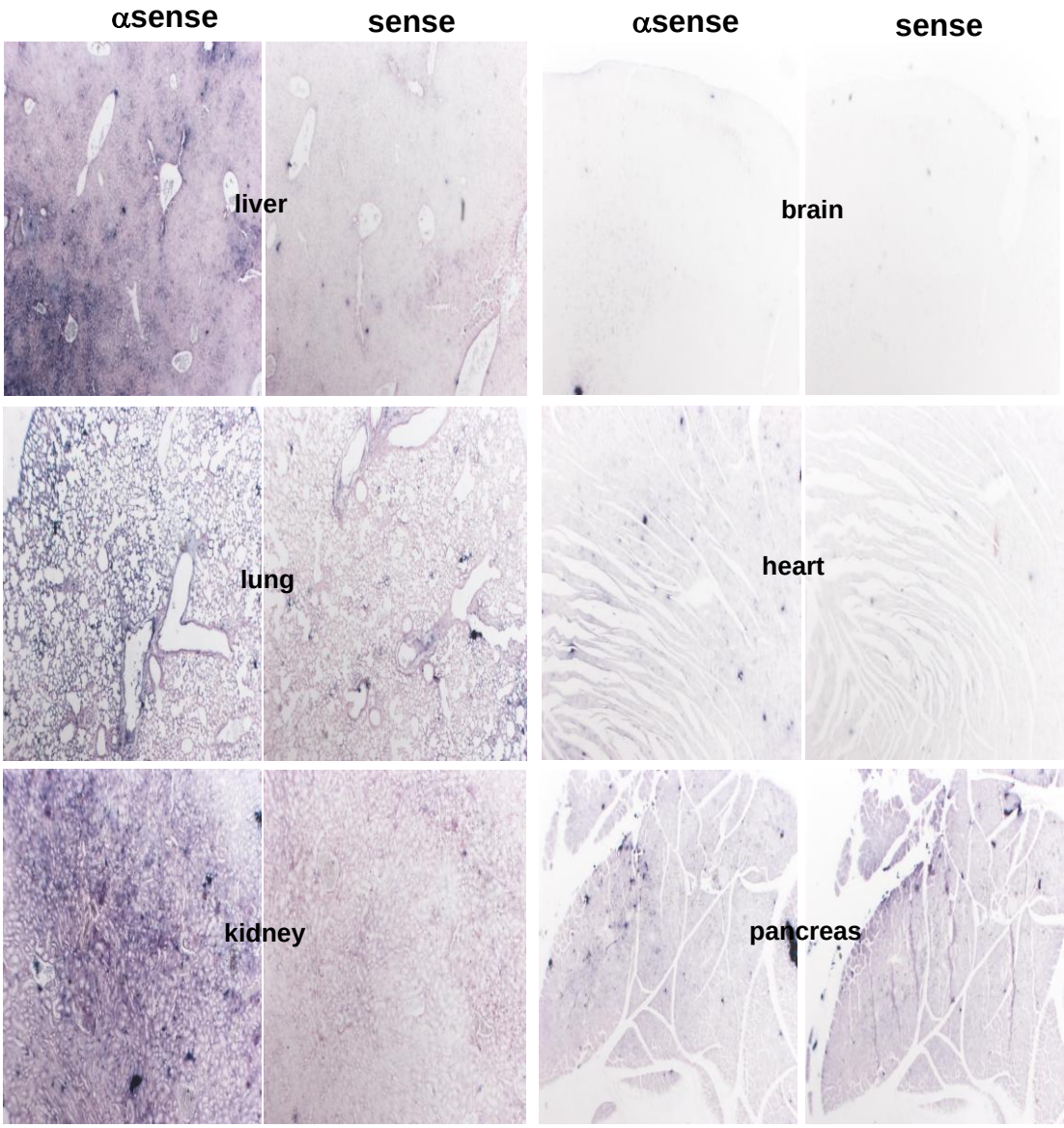


**Figure 3.12: *Rassf8* expression in the adult mouse organs**. Expression above the background is shown for the liver, the lung and the kidney (left) whereas the brain, the heart and the pancreas (right) do not show significant expression. Both *Rassf8* RNA probed (first and third panels) and negative control (second and fourth panels) are shown (50x). The images are representative of at least three independent experiments.

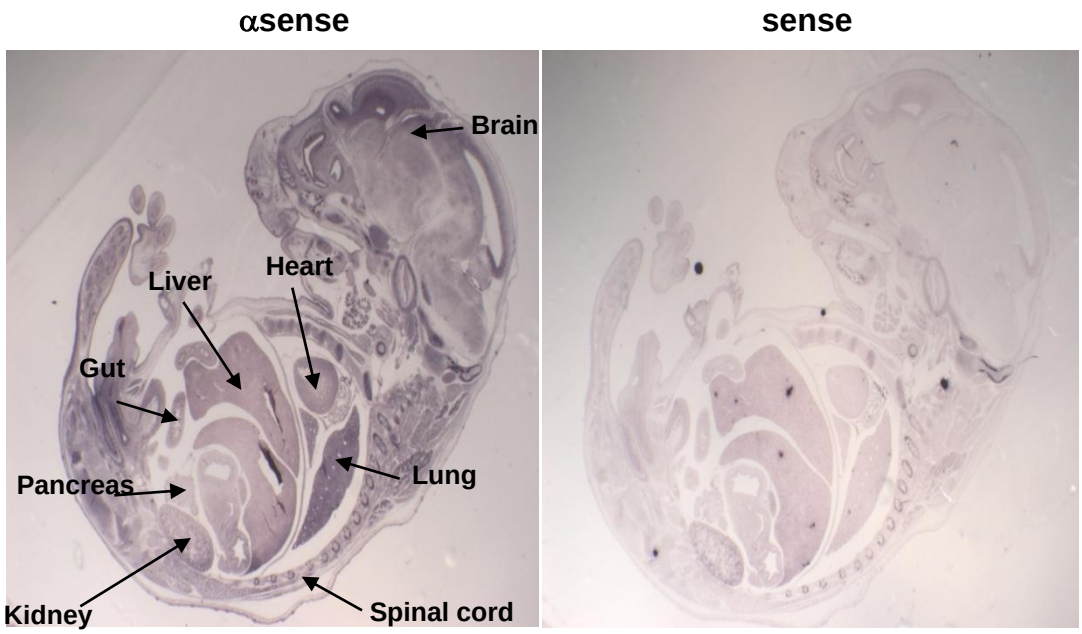


**Figure 3.13: *Rassf9* expression during late mouse embryogenesis.** ISH on E15.5 mouse sagittal sections. Both *Rassf9* RNA probed (left panel) and negative control (right panel) are shown (8x). The images are representative of two independent experiments.

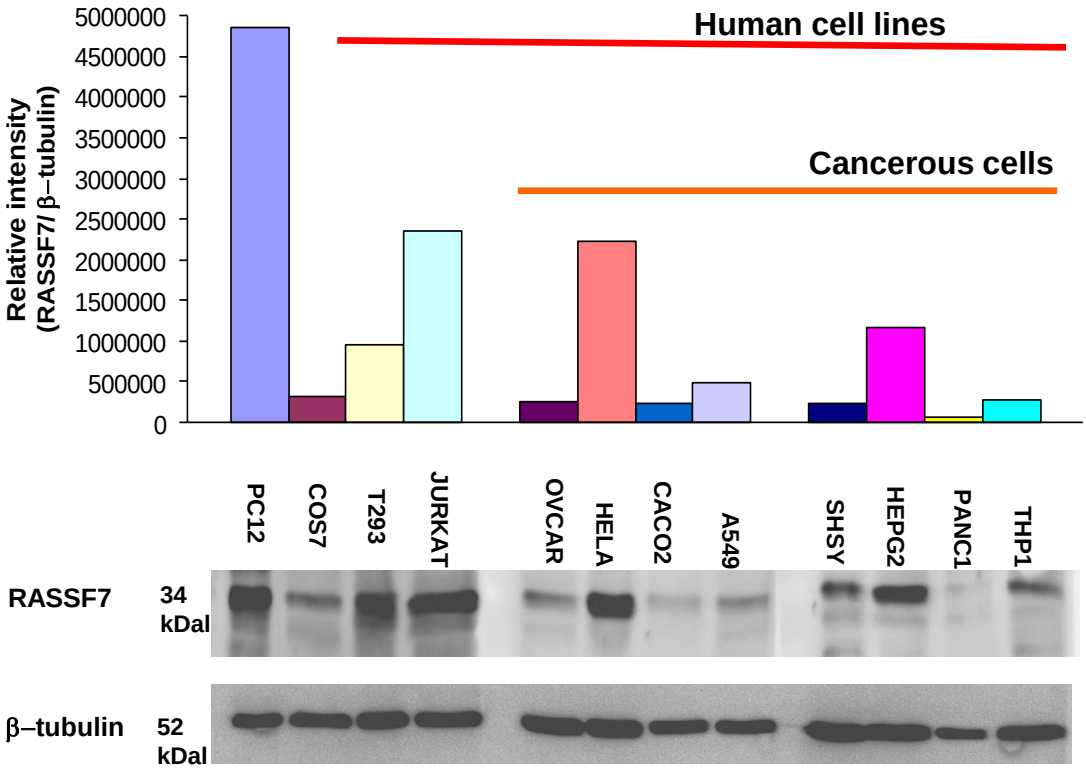


**Figure 3.14: Expression of RASSF7 protein in different mammalian cell lines.** Cell lysates were probed with AVIVA anti RASSF7 and the protein levels were normalised to β-tubulin. Data are representative of two independent experiments.

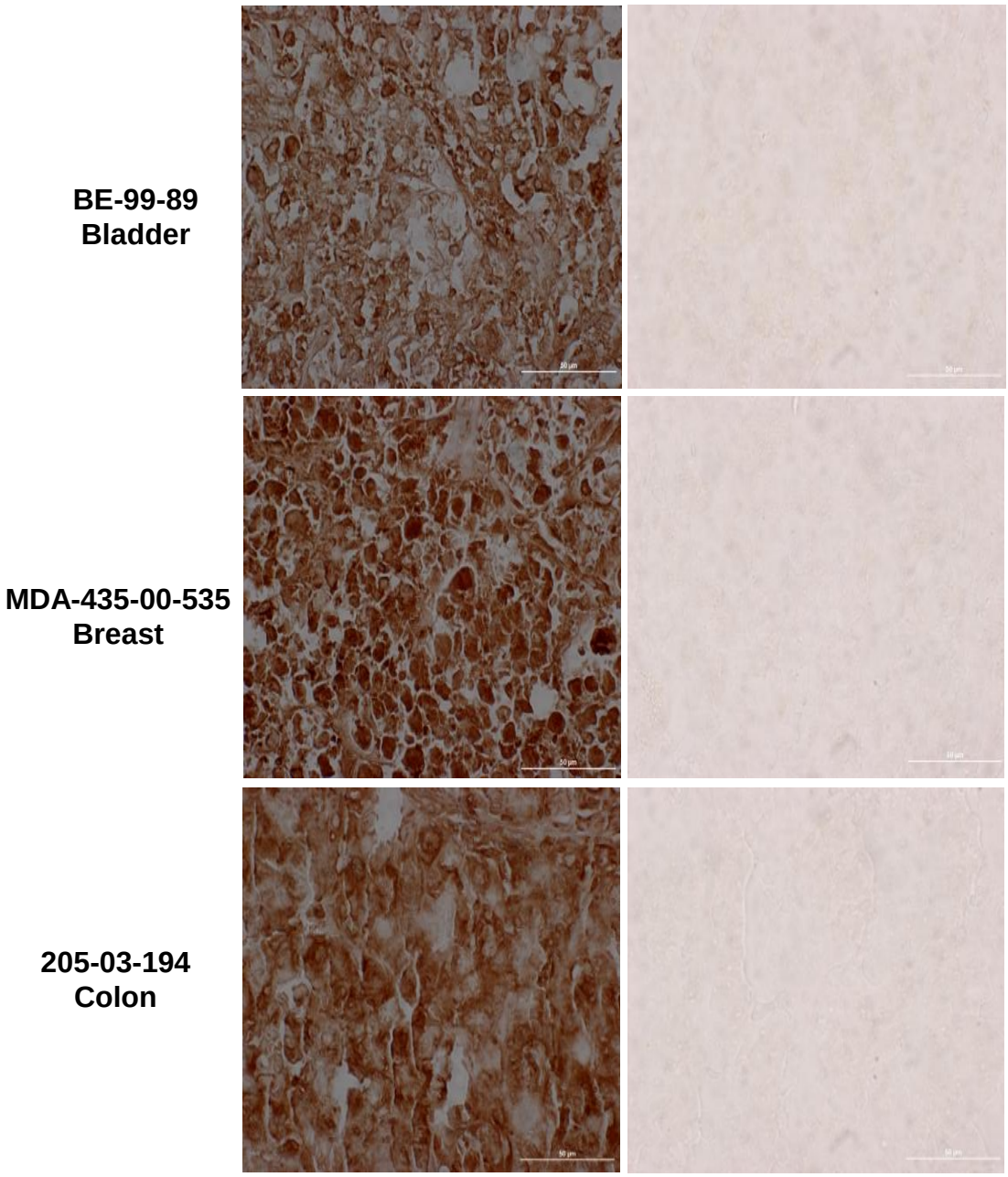


**Figure 3.15: RASSF7 protein is present in a range of human cancer cell types.** IHC conducted on human xenograft tumours grown in mice using AVIVA rabbit anti RASSF7 antibody (left panel) (60x). Negative controls, represented by samples probed for rabbit serum, (right panel) are shown. For each cell line name and organ of origin are indicated. Cancer tissue array kindly donated by Dr Jason Gill, University of Bradford.

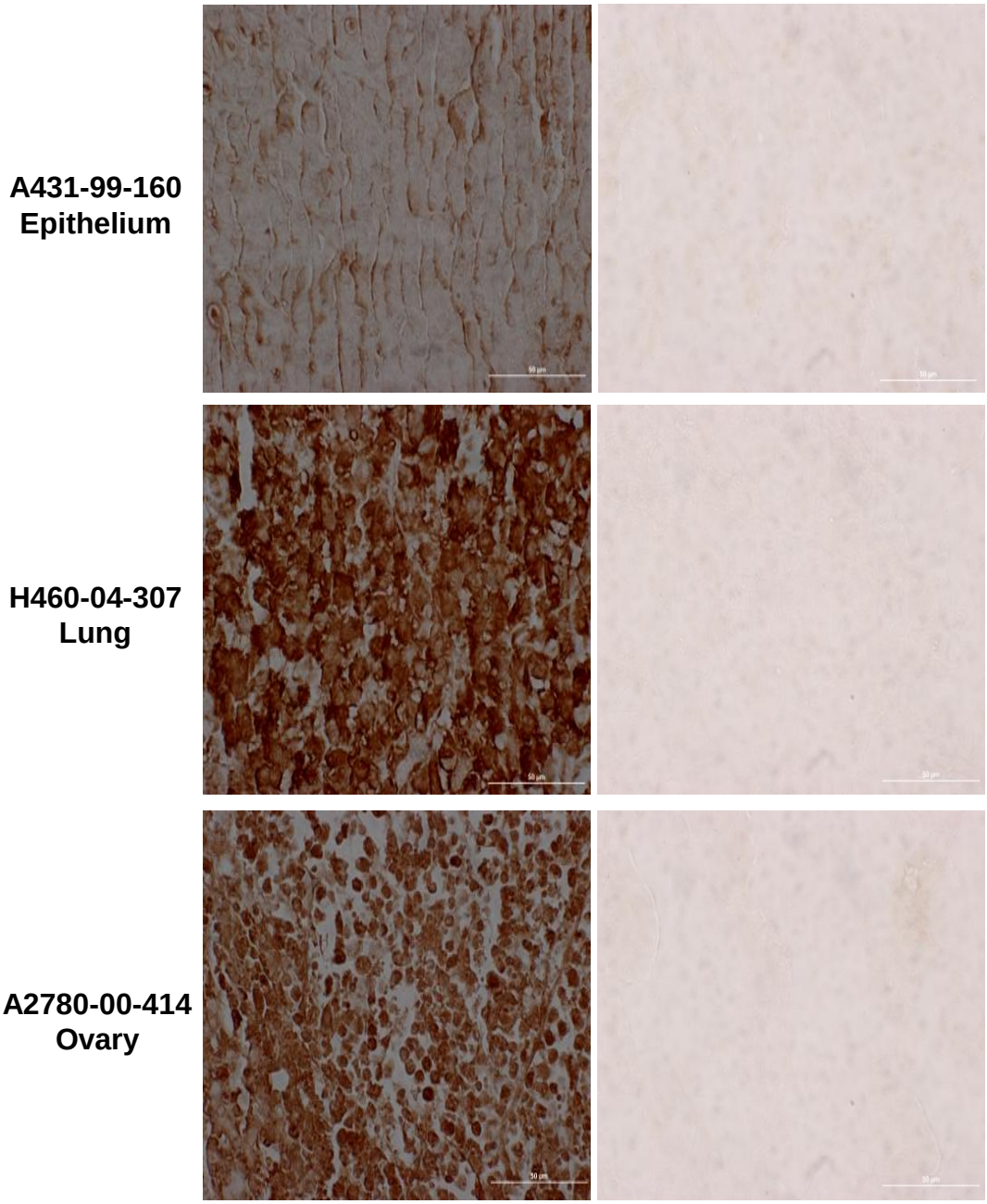


**Figure 3.16: RASSF7 protein is present in a range of human cancer cell types.** IHC conducted on human xenograft tumours grown in mice using AVIVA rabbit anti RASSF7 antibody (left panel) (60x). Negative controls, represented by samples probed for rabbit serum, (right panel) are shown. For each cell line name and organ of origin are indicated. Cancer tissue array kindly donated by Dr Jason Gill, University of Bradford.

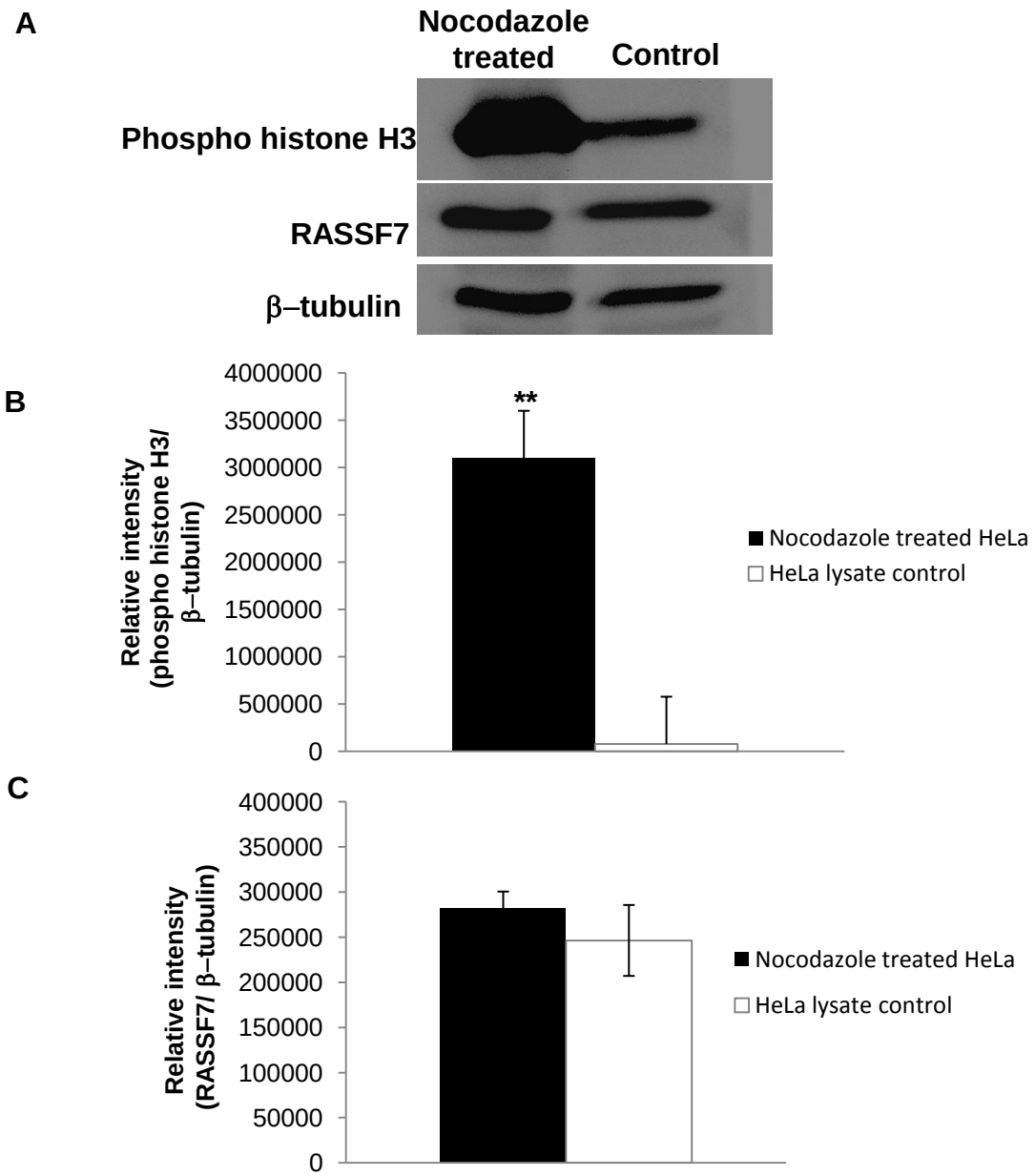


**Figure 3.17: RASSF7 levels of expression are not cell cycle dependent**. HeLa cell lysates were enriched with M phase cells through nocodazole treatment (75ng/ ml) for 18 hours followed by mitotic shake off. Lysates were then probed for either RASSF7 or phospho histone H3 (Ser10) considered as marker for dividing cells. β–tubulin was used as a loading control (A). Despite the dramatic difference for active H3 expression (B), RASSF7 expression levels are similar in nocodazole treated and untreated cells (C). **p<0.01. The average results shown derive from three independent experiments. Error bars, Standard Deviation (SD).

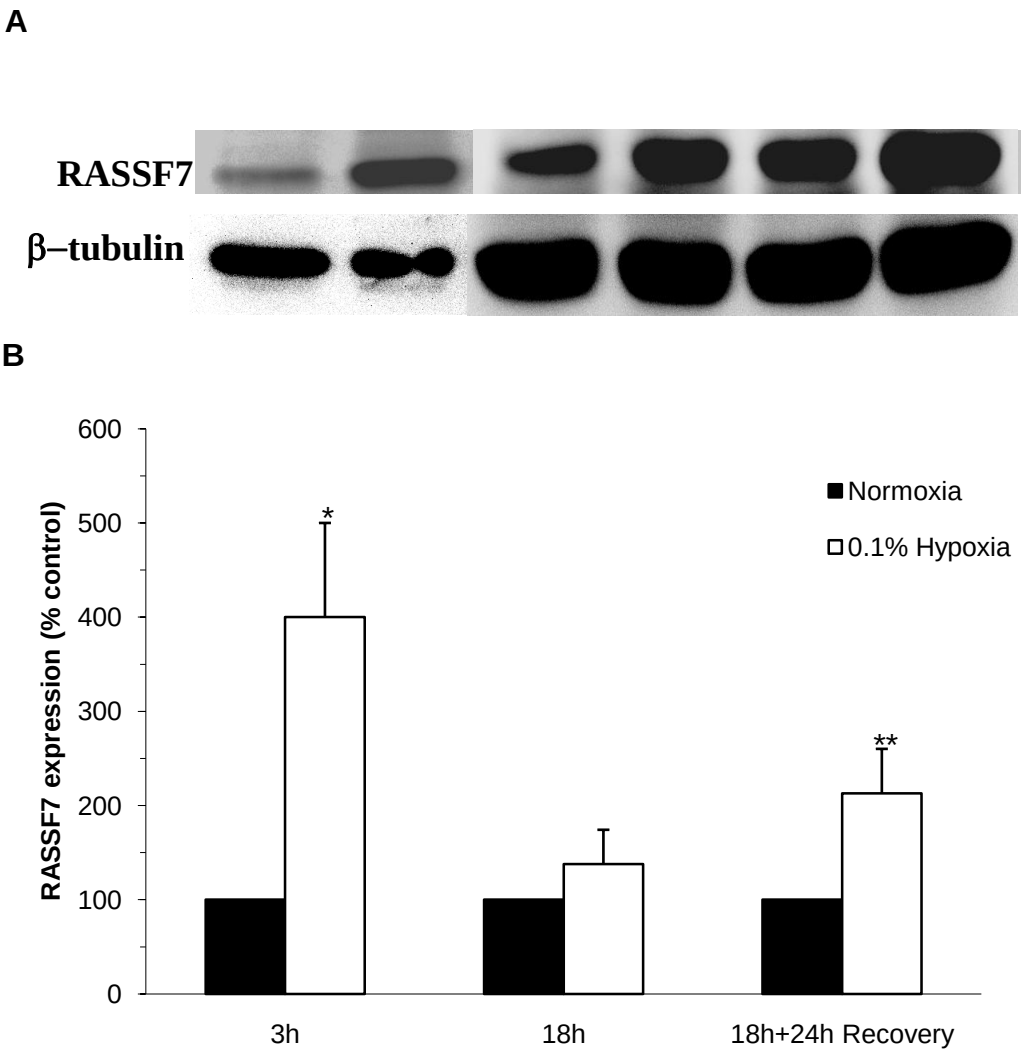


**Figure 3.18: RASSF7 protein is up-regulated under hypoxic conditions and its expression is maintained higher than the normoxic control during recovery.** Hela cells were subjected to hypoxic insult (0.1% Oxygen) for 3 hours, 18 hours, 18 hours + 24 hour recovery in normoxic conditions. Cell lysates from normoxic and hypoxic samples were probed for both RASSF7 and β–tubulin, used as a loading control (A). Both acute and prolonged hypoxic stress followed by recovery led to a significant RASSF7 over-expression compared to respective controls (B). *$p<0.05$, **$p<0.01$. The average results shown derive from three independent experiments. Error bars, SD.

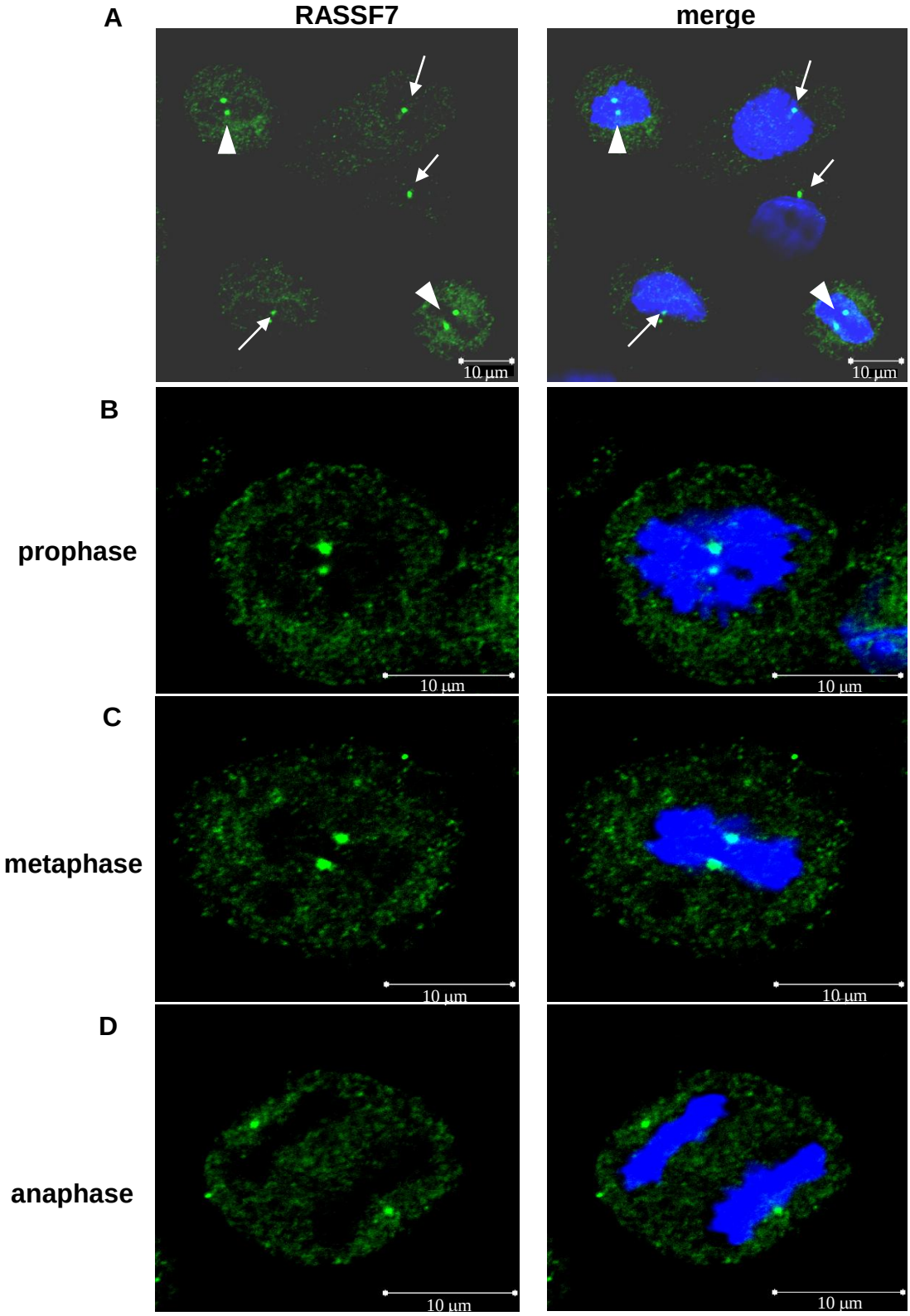


**Figure 4.2: Endogenous human RASSF7 localises to specific structures adjacent to the nucleus in a cell cycle independent fashion**. RASSF7 (green) labelling structures are detectable in both interphase (white arrows) and dividing (white arrowheads) HeLa cells (A). RASSF7 expression is maintained throughout M phase as shown in B, C and D. Blue: nuclear staining. The images are representative of three independent experiments.

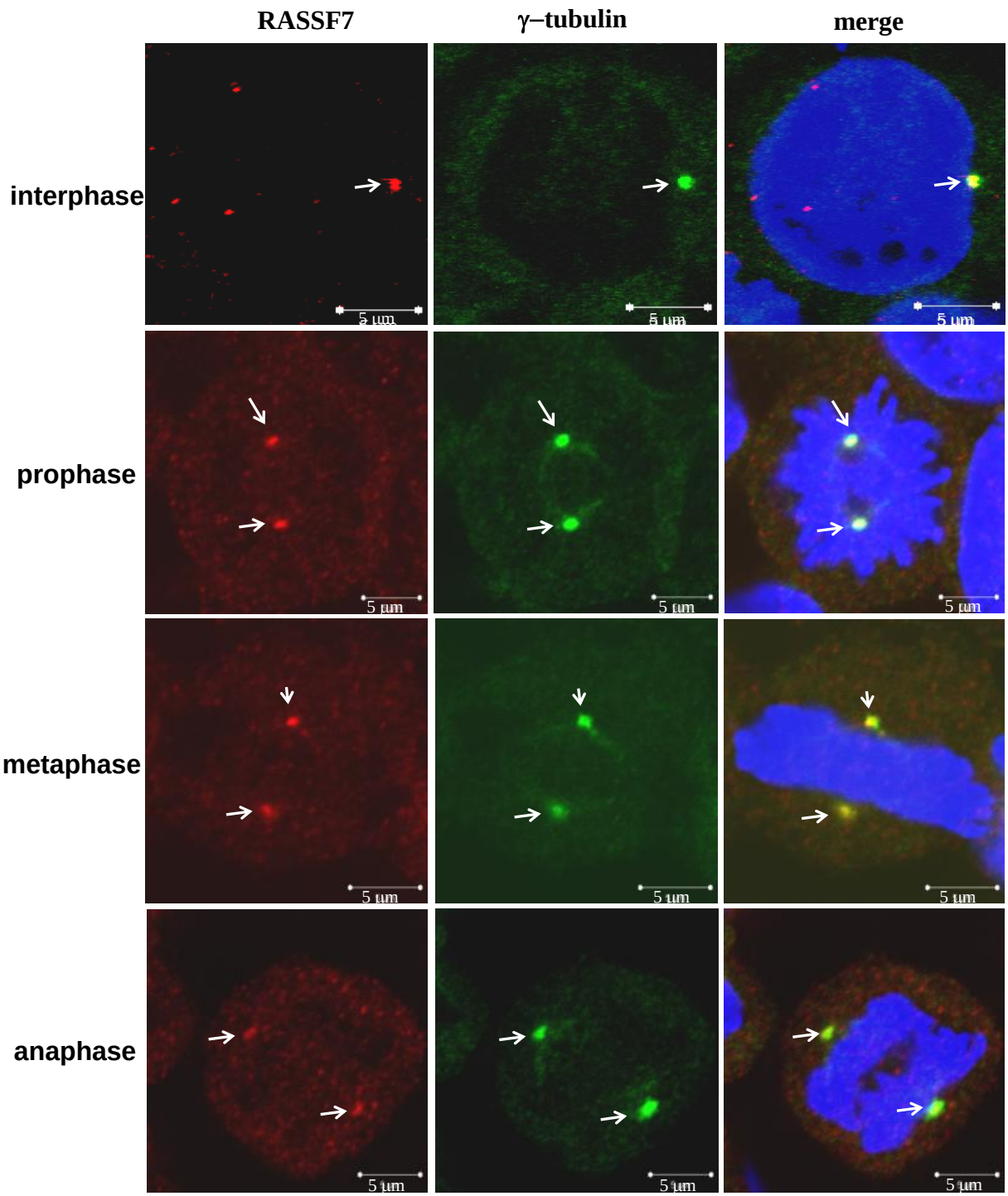


**Figure 4.3: Endogenous human RASSF7 localises to the centrosomes**. Co-localisation of RASSF7 (red) with the centrosomal marker γ-tubulin (green) (white arrows) in HeLa cells. Blue: nuclear staining. The images are representative of three independent experiments.

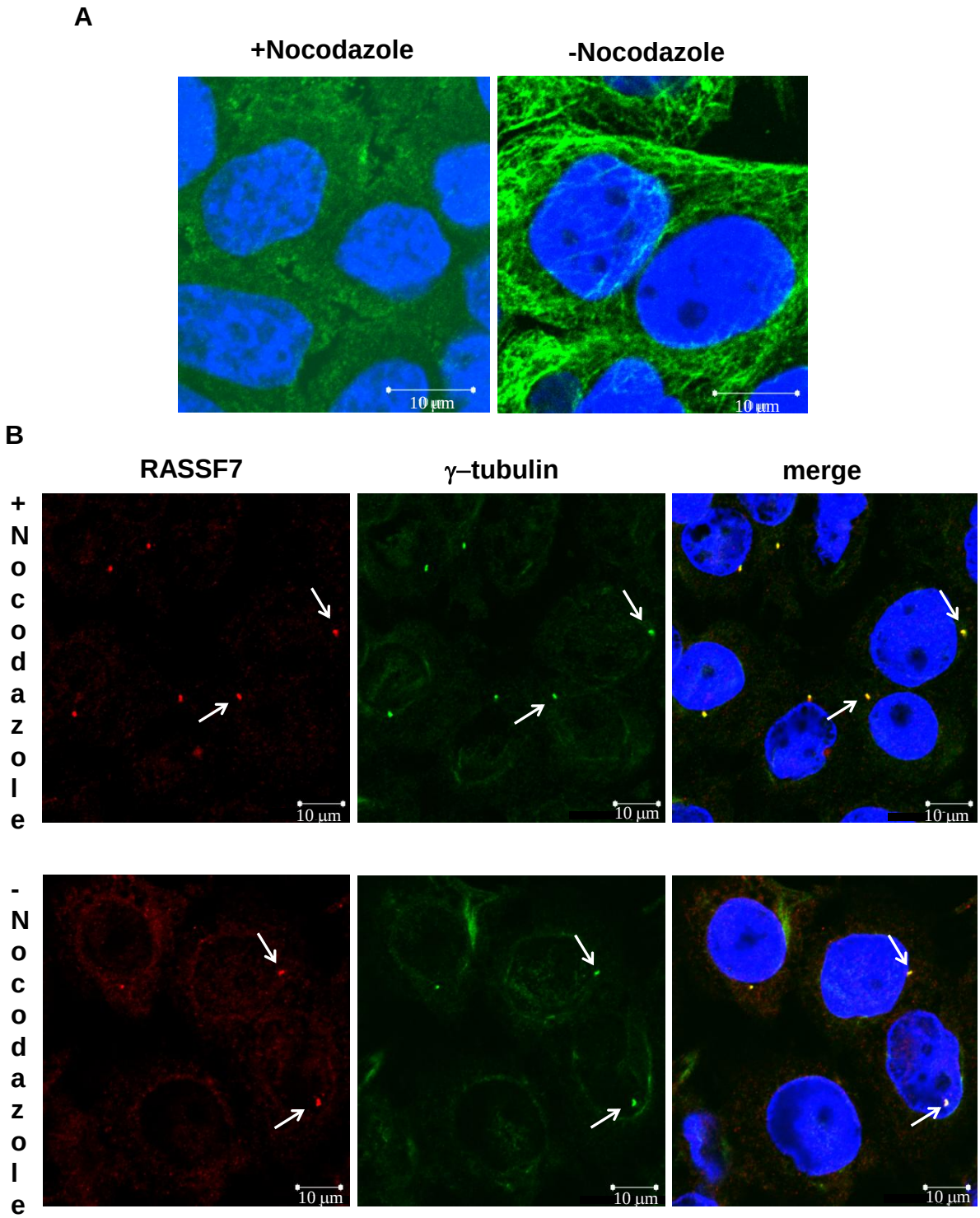


**Figure 4.4: Human RASSF7 localisation is maintained after microtubule disruption.** Microtubules were disrupted in HeLa cells when treated with 300ng/ml of nocodazole for one hour at 37°C. Microtubules were stained using α–tubulin (green) (A). Nocodazole treatment did not affect RASSF7 (red) localisation at the centrosomes (white arrows) which were stained for γ–tubulin (green) (B). Blue: nuclear staining. The images are representative of at least two independent experiments.

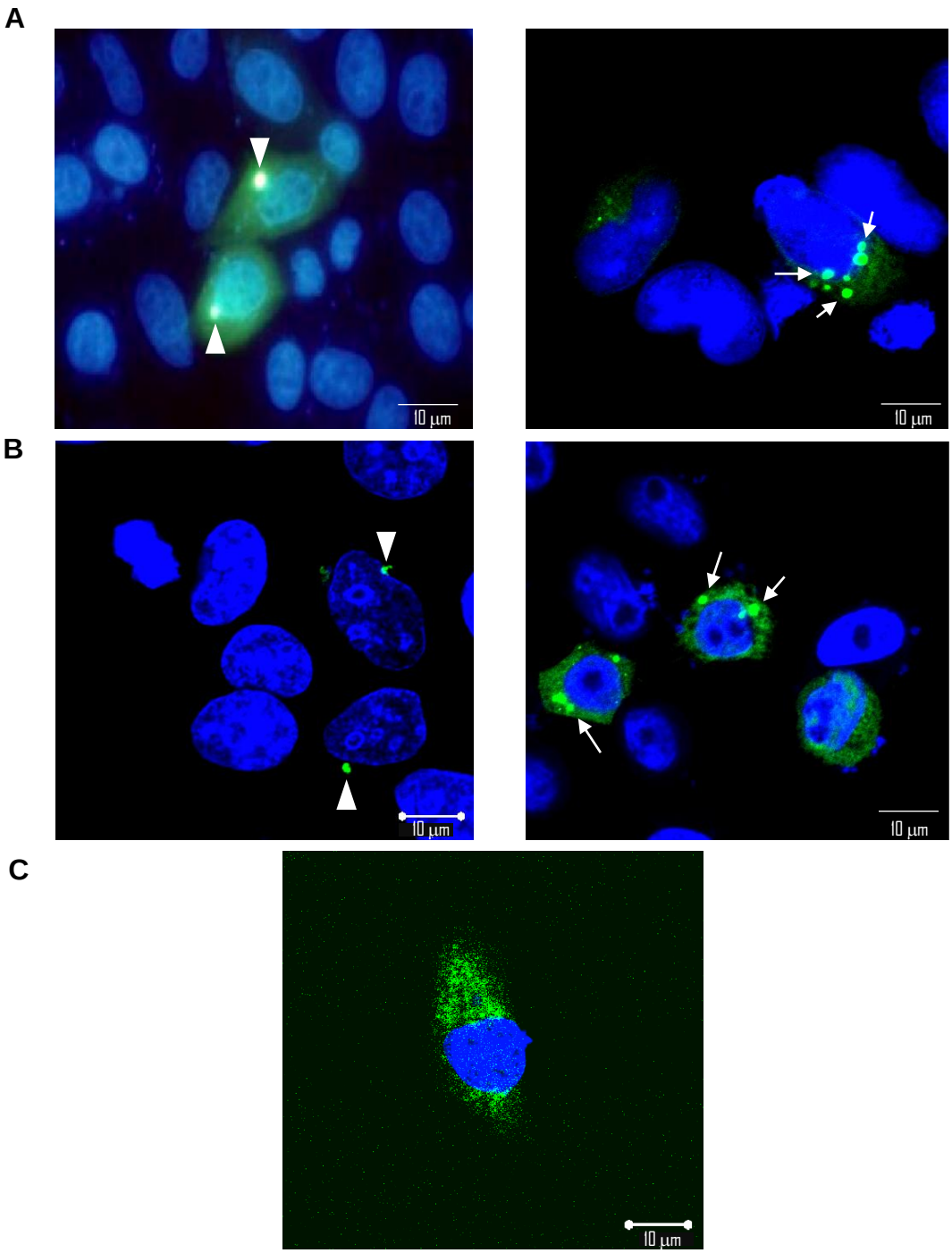


**Figure 4.5: Localisation of ectopic human RASSF7 does not depend on the way the fusion protein has been engineered.** The high over-expression of either N terminal GFP- (A) or C terminal V5- (B) tagged RASSF7 in HeLa cells causes the formation of cytoplasmic punctuate structures (white arrows) which vary in number and size within the cell. Transfected cells over-expressing RASSF7 at moderate levels present one inclusion (white arrowheads). GFP only transfected cell (C) is shown as control. Green: exogenous RASSF7. Blue: nuclear staining. The images are representative of three independent experiments.

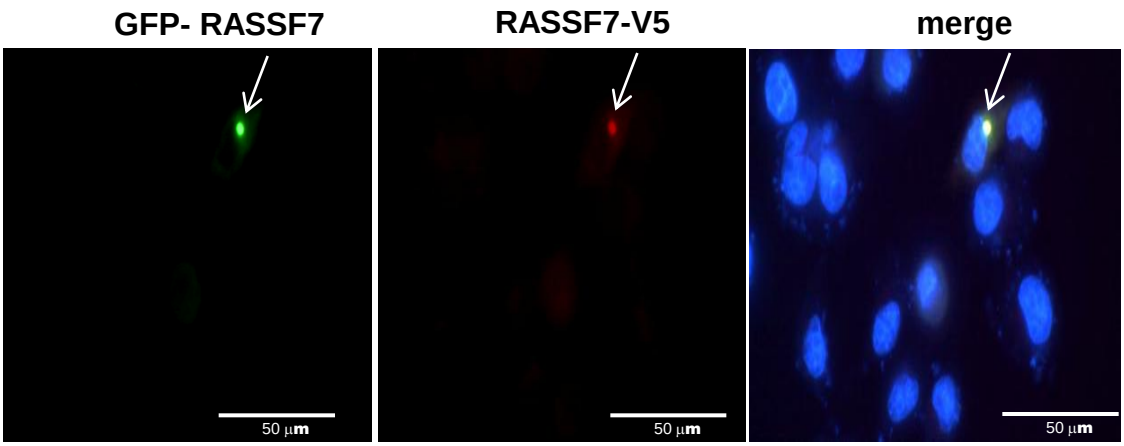


**Figure 4.6: Ectopic human RASSF7 localises to the same structures in HeLa cells despite the differently located tags**. GFP-RASSF7 (green) and RASSF7-V5 (red) exhibit the same localisation (white arrows) when co-transfected. Blue: nuclear staining. The images are representative of three independent experiments.

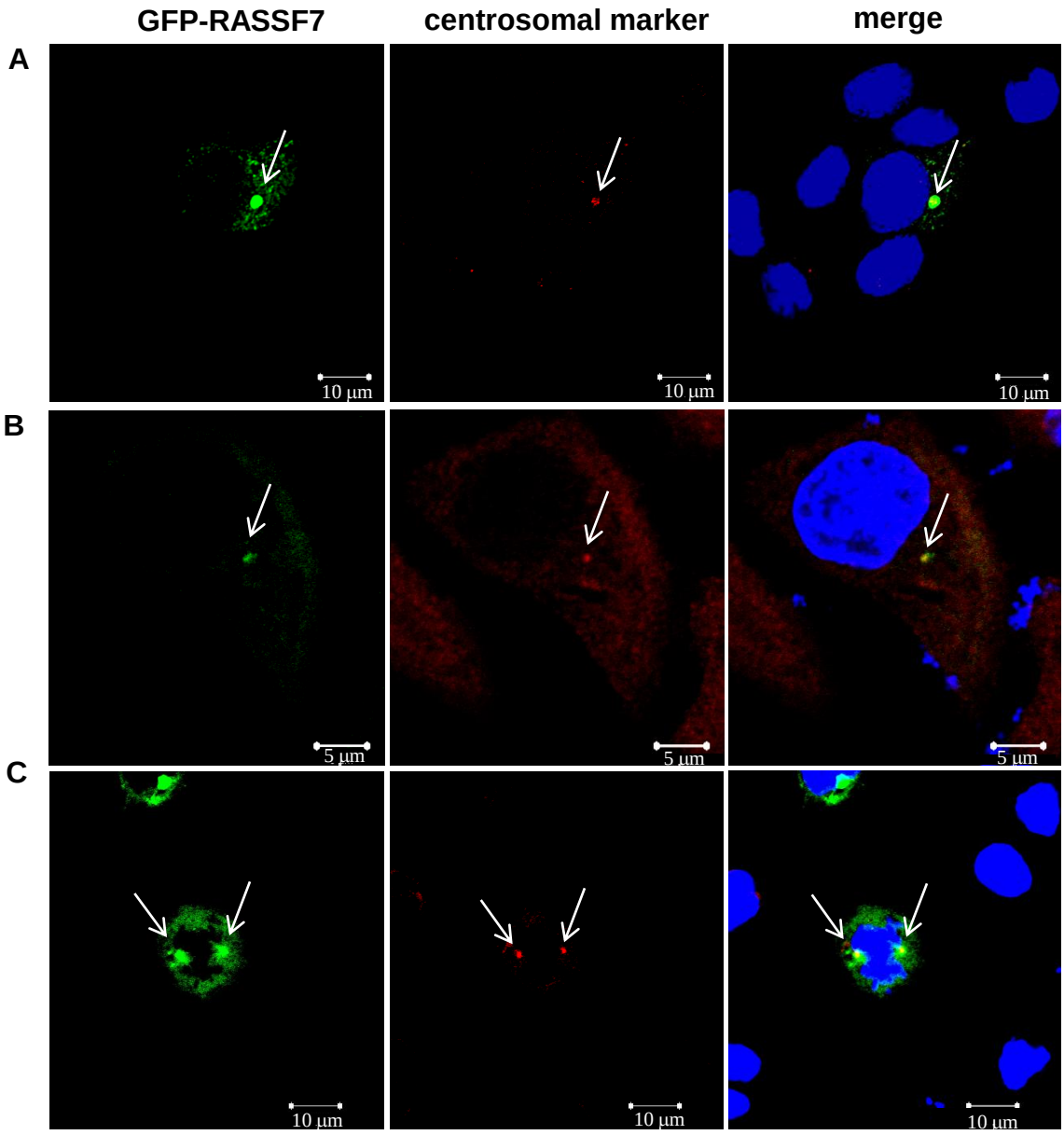


**Figure 4.7: Ectopic human RASSF7 is centrosomal in HeLa cells**. Co-localisation of GFP-RASSF7 (green) with centrosomal markers, pericentrin (red, A) and γ–tubulin (red, B, C) (white arrows) in both interphase (A, B) and diving cells (C). Blue: nuclear staining. The images relative to interphase cells are representative of at least three independent experiments. Only one transfected mitotic cell was found and imaged in all the specimens analysed.

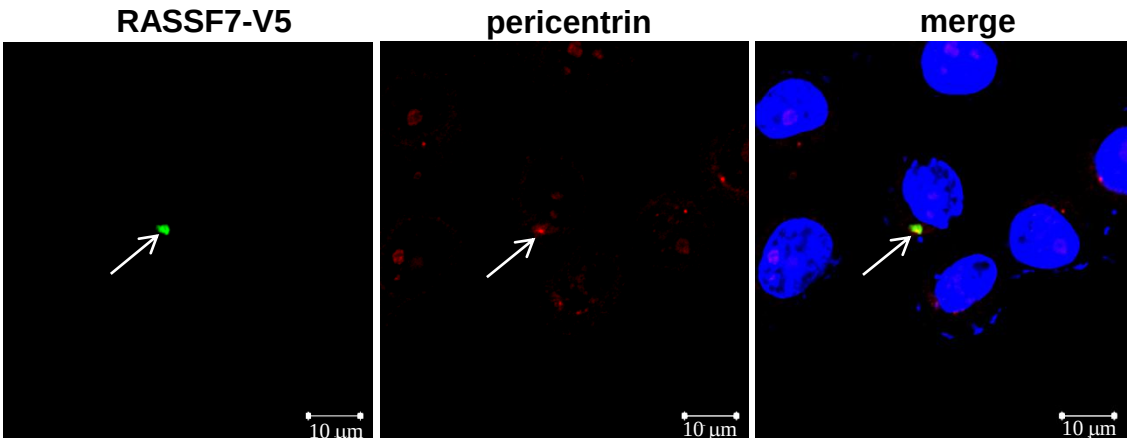


**Figure 4.8: Epitope tagged human RASSF7 localises to the centrosomes in HeLa cells.** Co-localisation of RASSF7-V5 (green) with the centrosomal marker pericentrin (red) (white arrows). Blue: nuclear staining. The images are representative of at least three independent experiments.

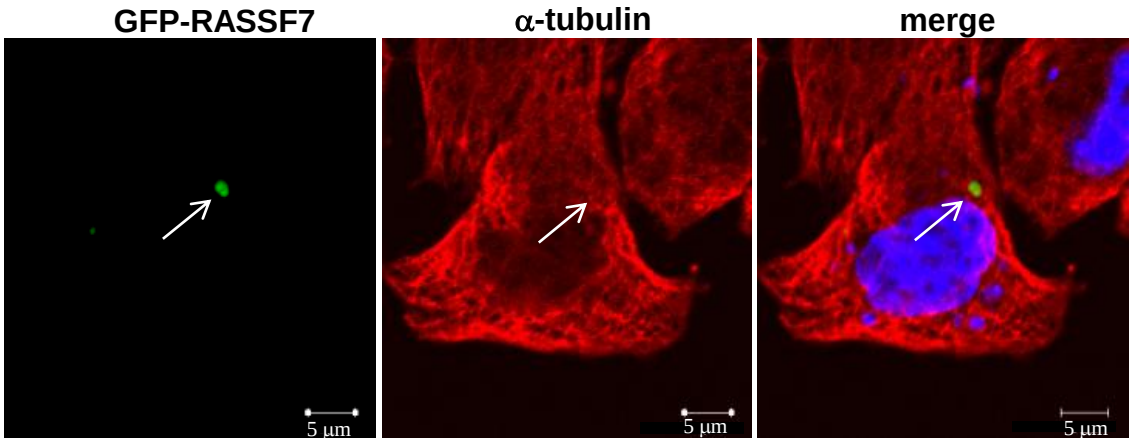


**Figure 4.9: Over-expressed human RASSF7 does not co-localise with microtubules.** The white arrow indicates the centrosome. Green: GFP-RASSF7, red: α-tubulin, blue: nuclear staining. The images are representative of at least three independent experiments.

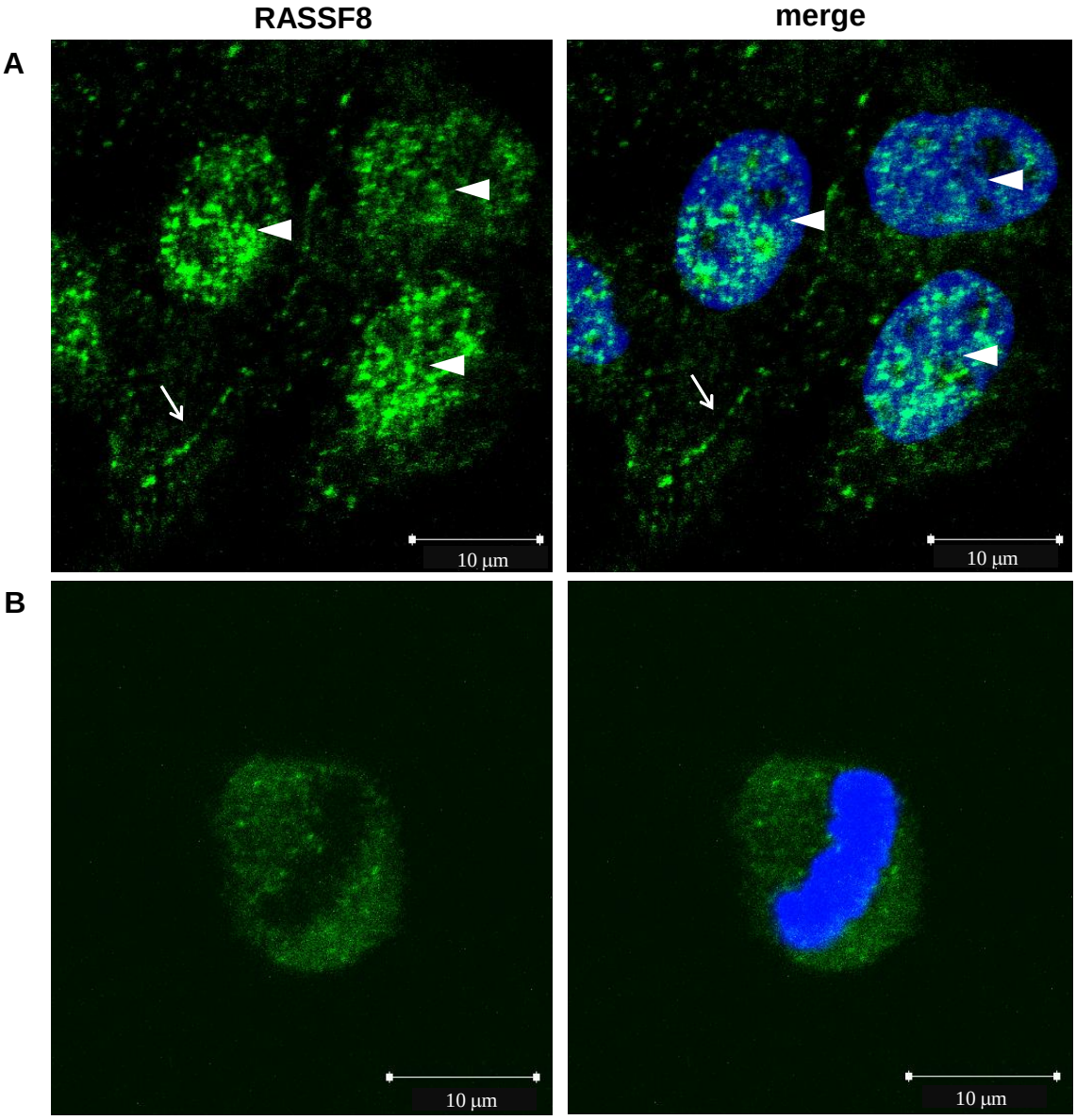


**Figure 4.10: Human RASSF8 localisation**. HeLa cells were stained for RASSF8 (green) and imaged in either interphase (A) or metaphase (B). In interphase, RASSF8 was observed within the nucleus (white arrowheads) and the cell membrane (white arrows). Blue: nuclear staining. The images are representative of at least two independent experiments.

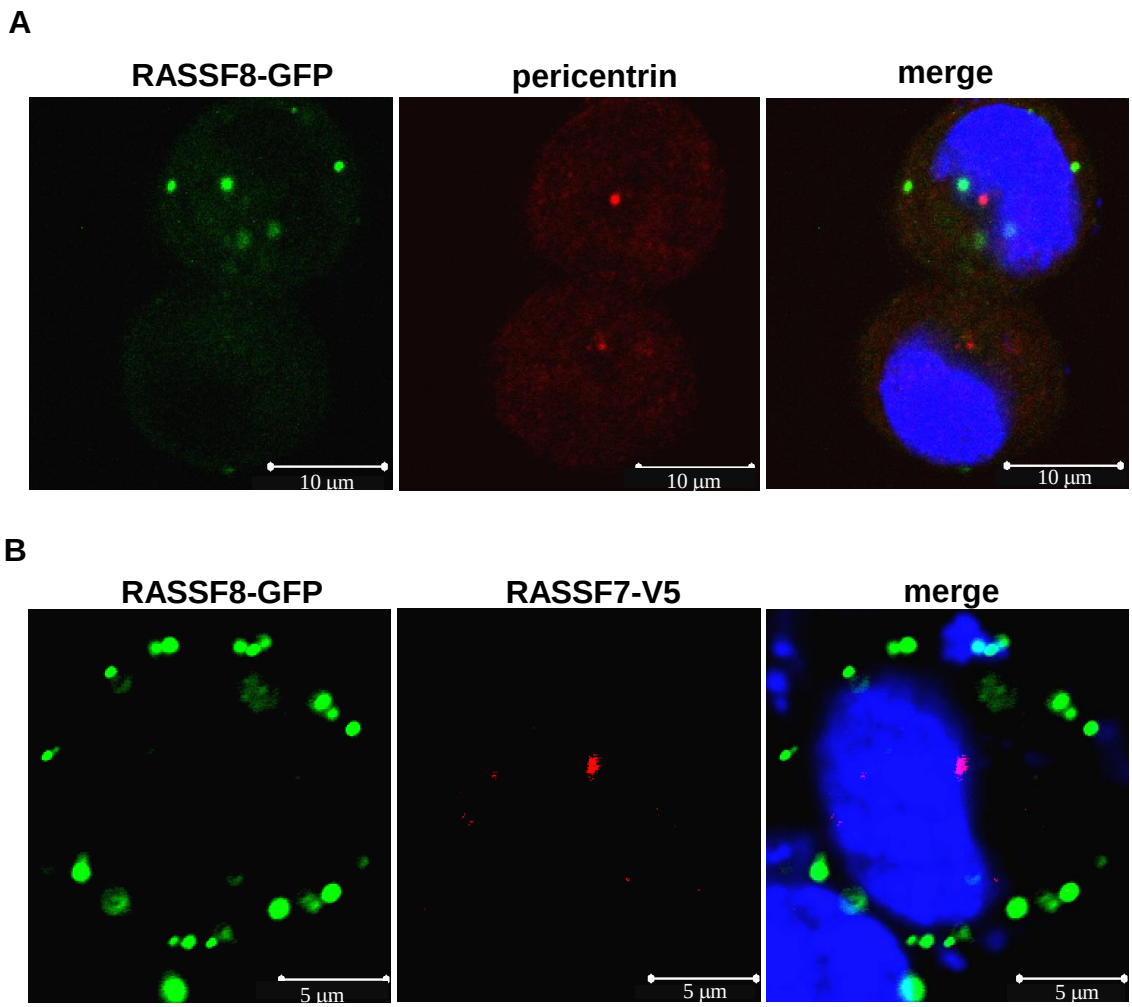


**Figure 4.11: Ectopic human RASSF8 localisation**. RASSF8-GFP (green) does not co-localise with either pericentrin (red, A) or RASSF7-V5 (red, B) in HeLa cells. Blue: nuclear staining. The images are representative of at least two independent experiments.

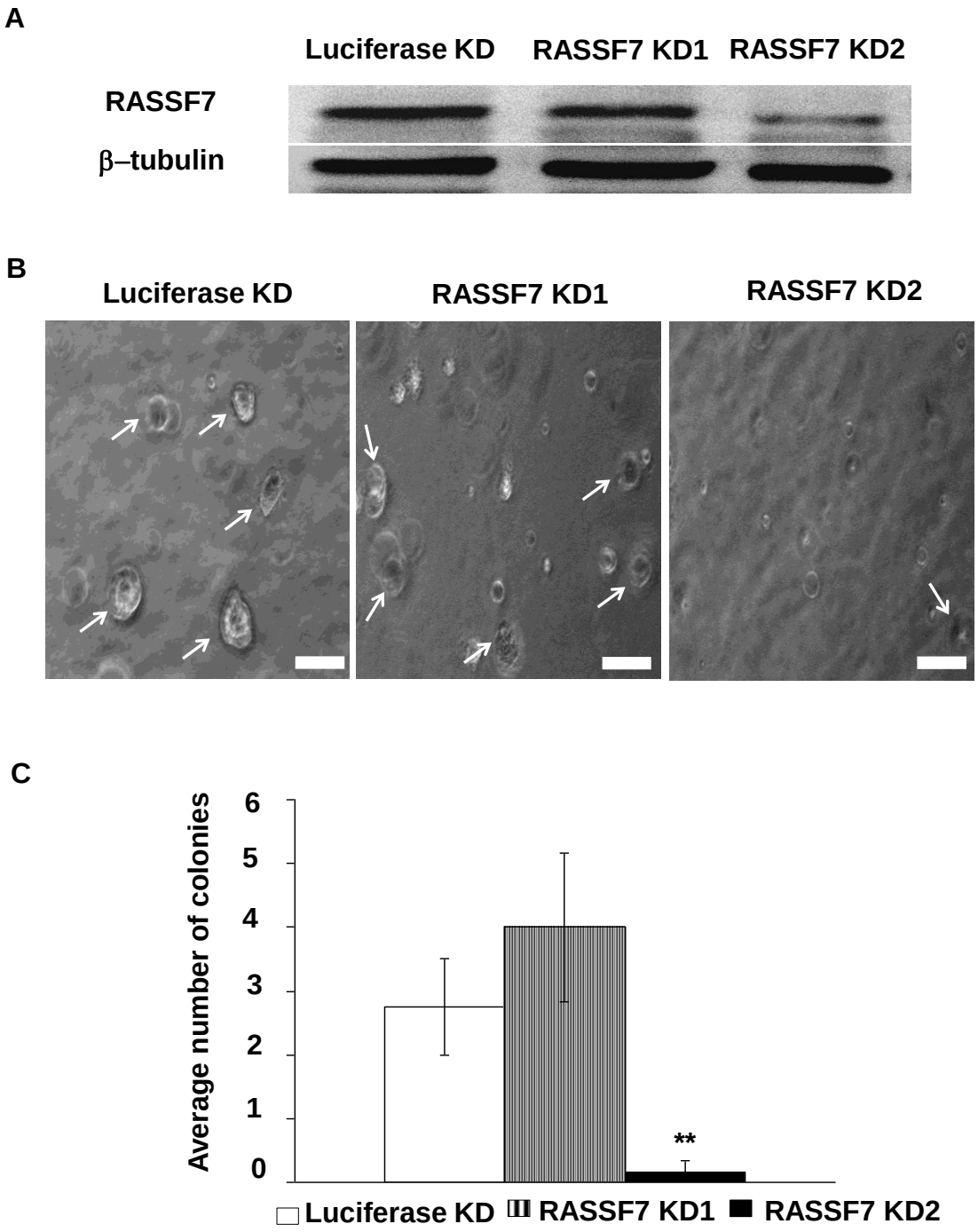


**Figure 5.2: RASSF7 knockdown prevents H1792 cells from forming anchorage independent growth colonies.** RASSF7 siRNA 2 specifically targeted RASSF7 as shown by the immunoblot (A). Two weeks after transfecting RASSF7 KD2 in H1792 cells, both the number and the size of the colonies (white arrows) were affected if compared to control (B) and the difference is statistically significant (C). **p<0.01 vs Luciferase KD and RASSF7 KD1. Error bars, SD. Scale bars, 100 μM. Results of three independent experiments.

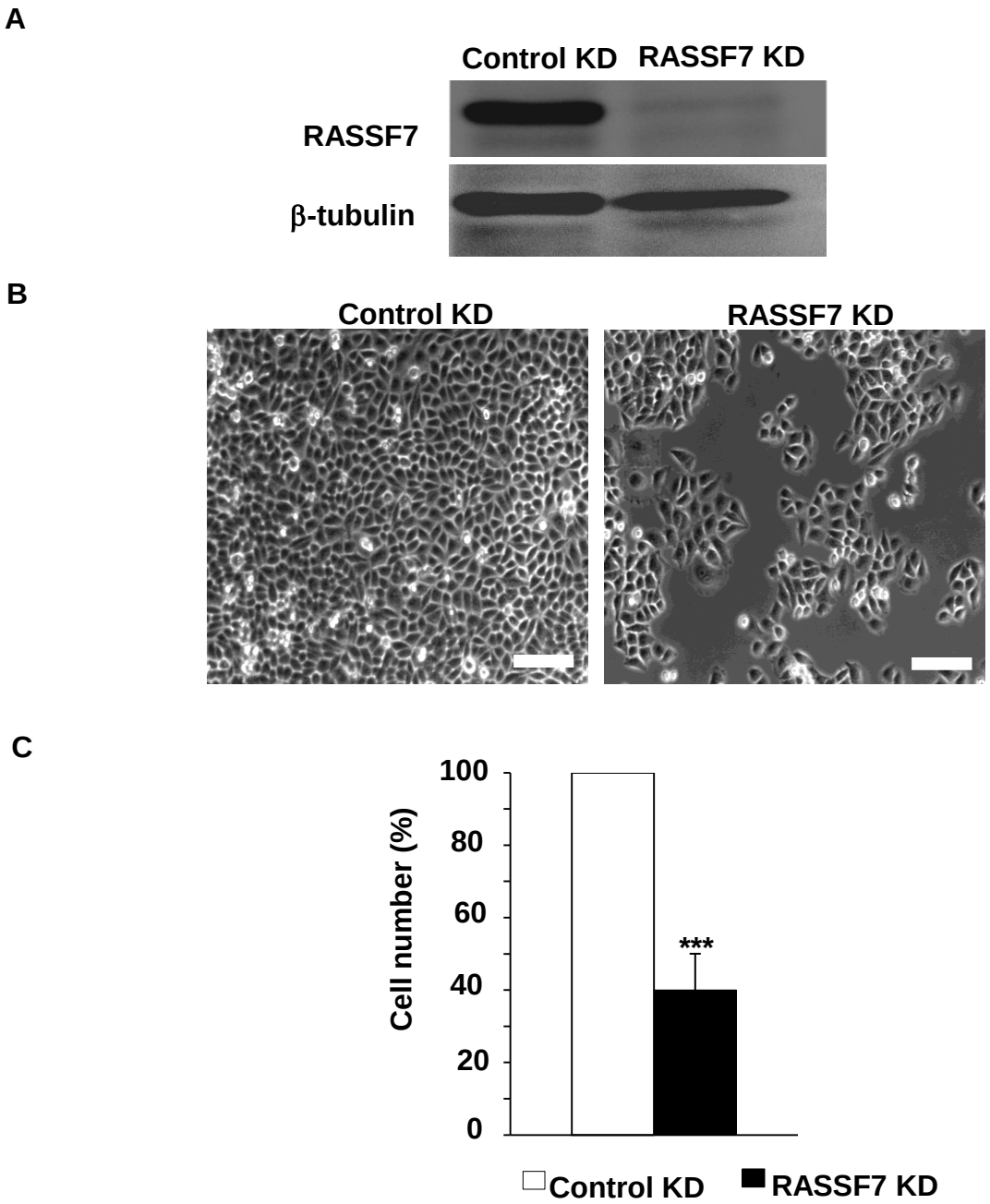


**Figure 5.4: RASSF7 shRNAi knockdown results in reduced numbers of HeLa cells.** Immunoblot of RASSF7 from control and RASSF7 knockdown (KD) cells. β–tubulin was used as a loading control (A). HeLa cells were seeded at the same density and transfected with constructs encoding resistance for G418 and shRNAi either targeting or non targeting RASSF7. After the end for selection for G418, cells were allowed to grow and subsequently counted (B). The difference in cell numbers between control and RASSF7 depleted HeLa was 2.6 $\pm$ 0.6 fold (***p<0.001). The average cell reduction was calculated from five independent experiments (C). Error bars, SD. Scale bars, 100 μM.

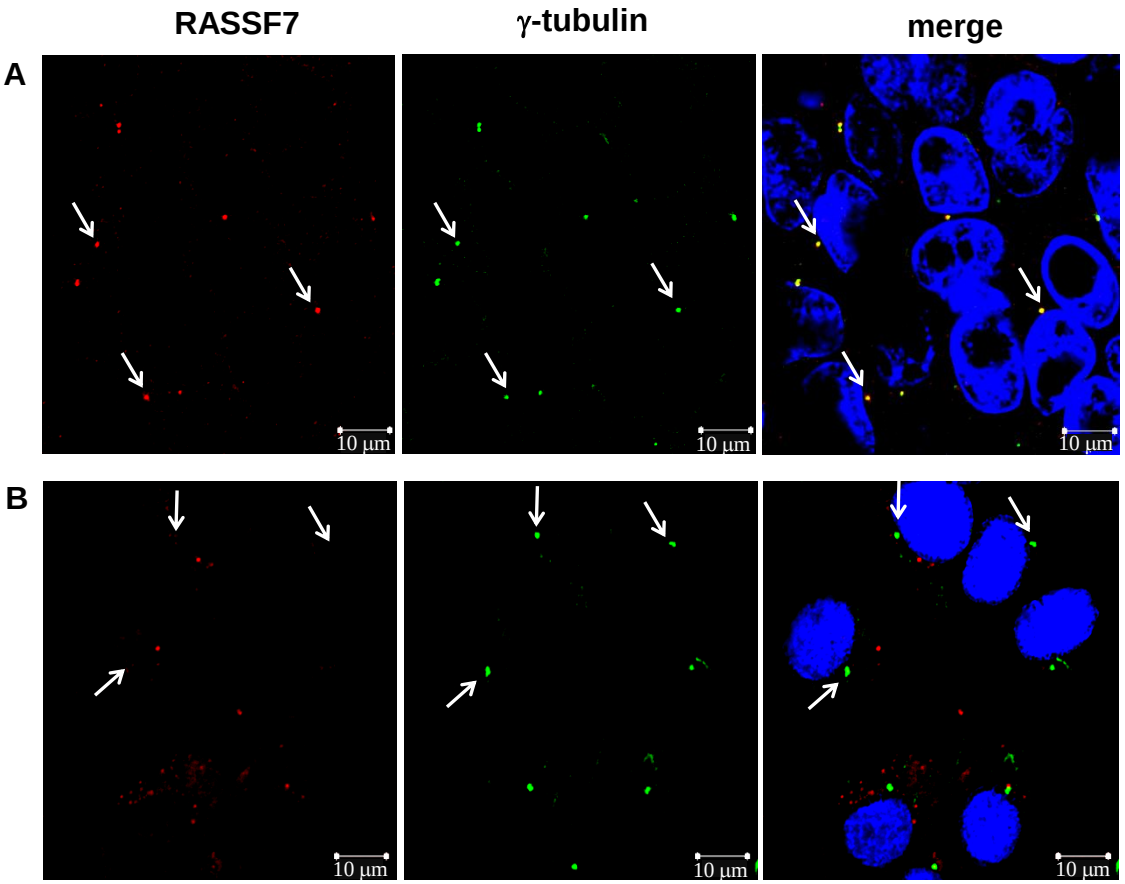


**Figure 5.5: RASSF7 centrosomal staining is lost in RASSF7 KD HeLa cells.** Control KD (A) and RASSF7 shRNAi containing (B) HeLa cells were fixed and co-stained for RASSF7 (red) and the centrosomal marker γ–tubulin (green) one day after the completion of G418 selection in transfected cells. In RASSF7 KD cells (B) there is some background staining but no detectable RASSF7 staining at the centrosomes (white arrows). Blue: nuclear staining. The images are representative of three independent experiments.

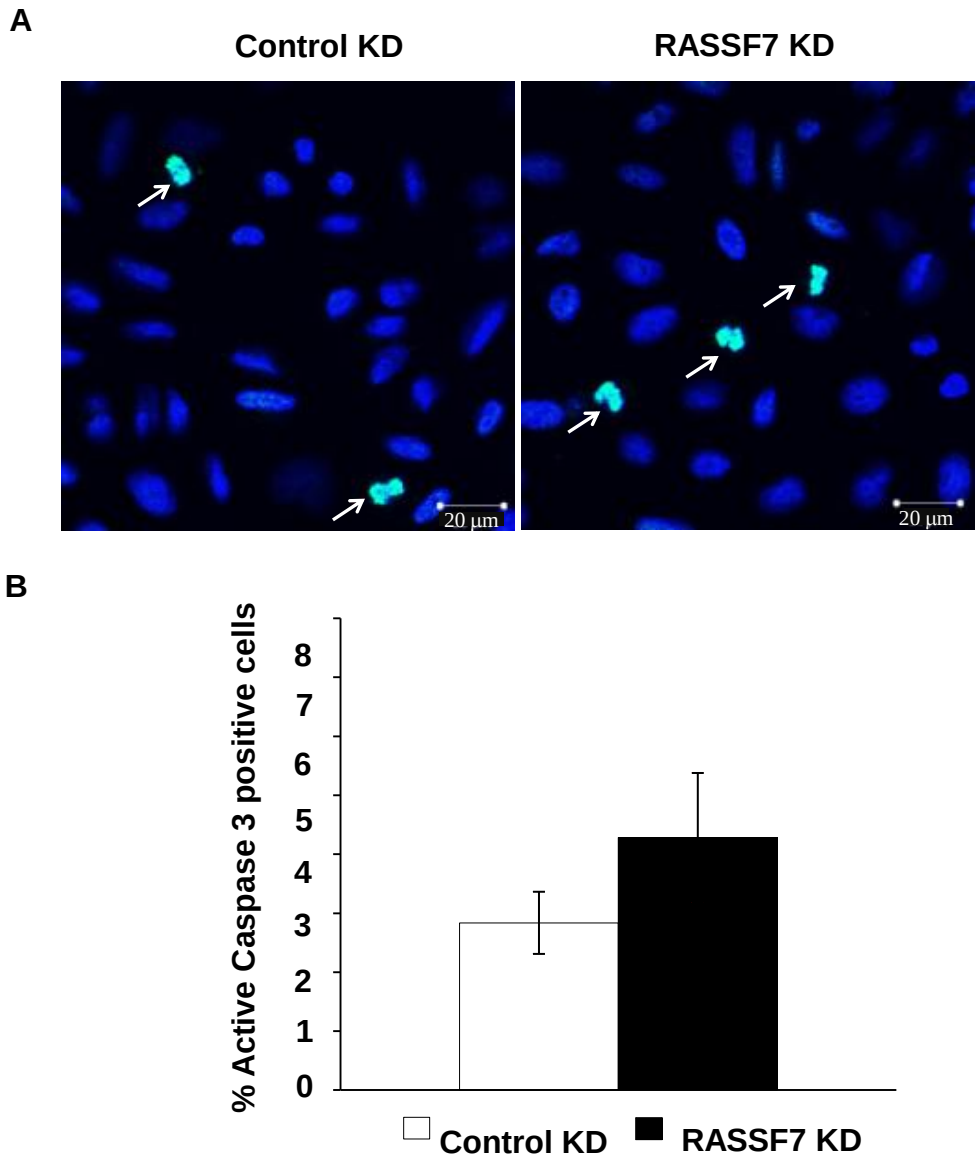


**Figure 5.6: RASSF7 KD did not cause a significant increase in apoptosis.** RASSF7 depletion in HeLa cells did not significantly increase the number of active caspase 3 positive cells (green, highlighted by arrows) compared with controls (A), as confirmed by statistical analysis (B). More than 500 cells were counted for each sample from three independent experiments. Blue: nuclear staining.

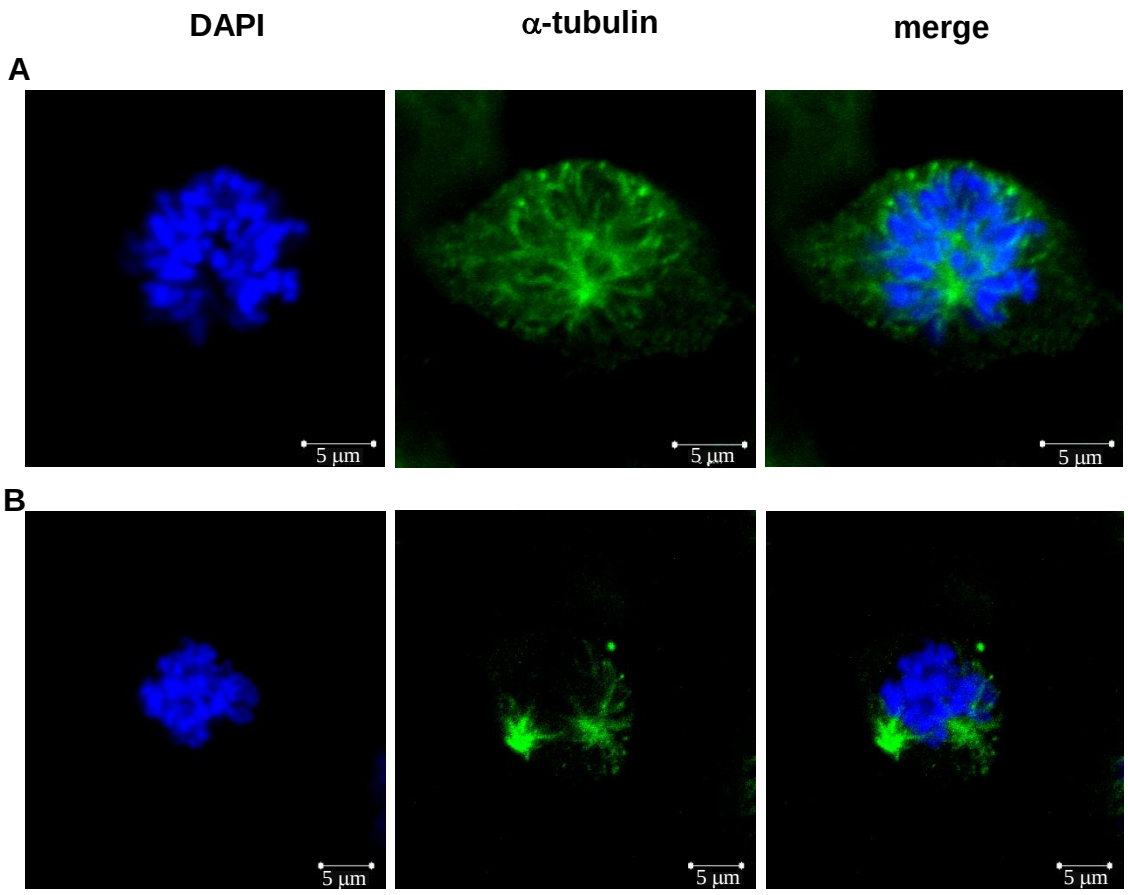


**Figure 5.7: Early events of mitosis are not compromised by RASSF7 depletion.** The onset of chromosome condensation occurs normally for both control KD (A) and RASSF7 KD (B) HeLa cells. Prophase cells were fixed and stained with the nuclear dye DAPI (blue) and the microtubule marker α–tubulin (green). Images are representative of at least three independent experiments.

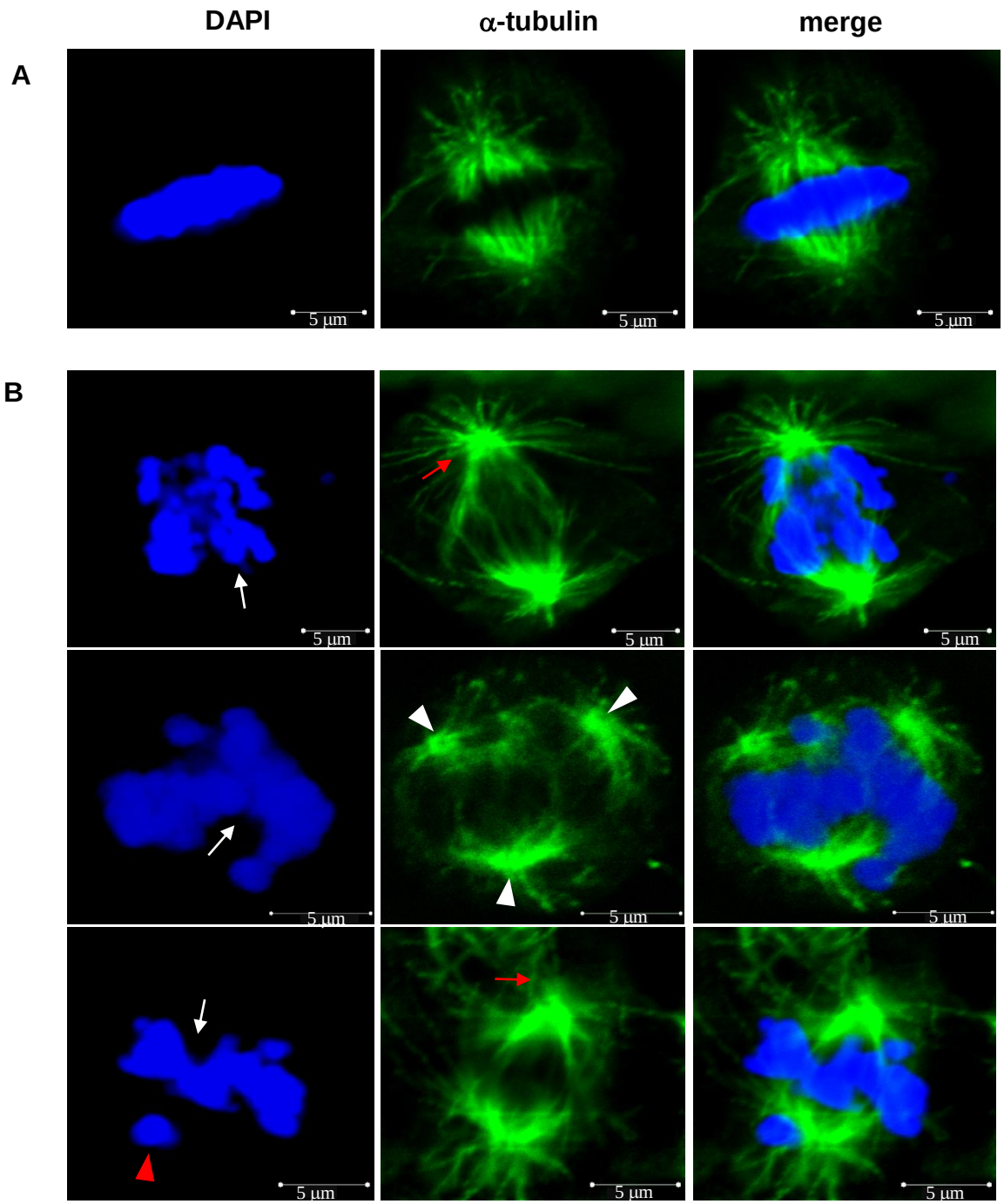


**Figure 5.8: RASSF7 KD by shRNA impairs mitosis in HeLa cells.** Metaphase RASSF7 KD cells (B) exhibit defects in spindle formation (red arrows highlight the more radial microtubules) and chromosomal congression (white arrows), with an increase in cells which had failed to align their DNA (left panel) and an increase in cells with lagging chromosomes (red arrowhead). There was also a small increase in tripolar spindles (white arrowheads). Control KD cell is shown in A). Cells were fixed and stained with the nuclear dye DAPI (blue) and the microtubule marker α–tubulin (green). Images are representative of at least three independent experiments.

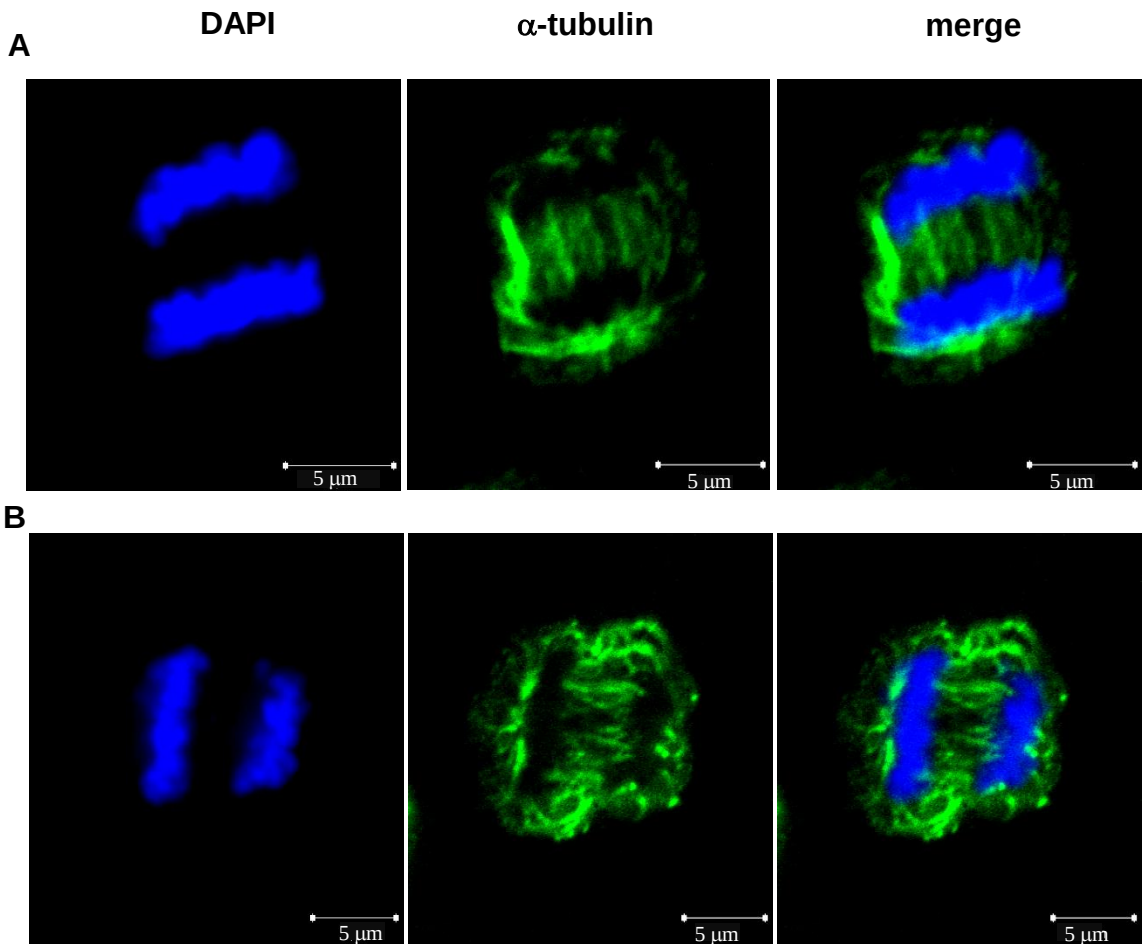


**Figure 5.9: Late events of mitosis are not compromised by RASSF7 depletion.** Anaphase occurs normally for both control KD (A) and RASSF7 KD (B) HeLa cells. Cells were fixed and stained with the nuclear dye DAPI (blue) and the microtubule marker α–tubulin (green). Images are representative of at least three independent experiments.

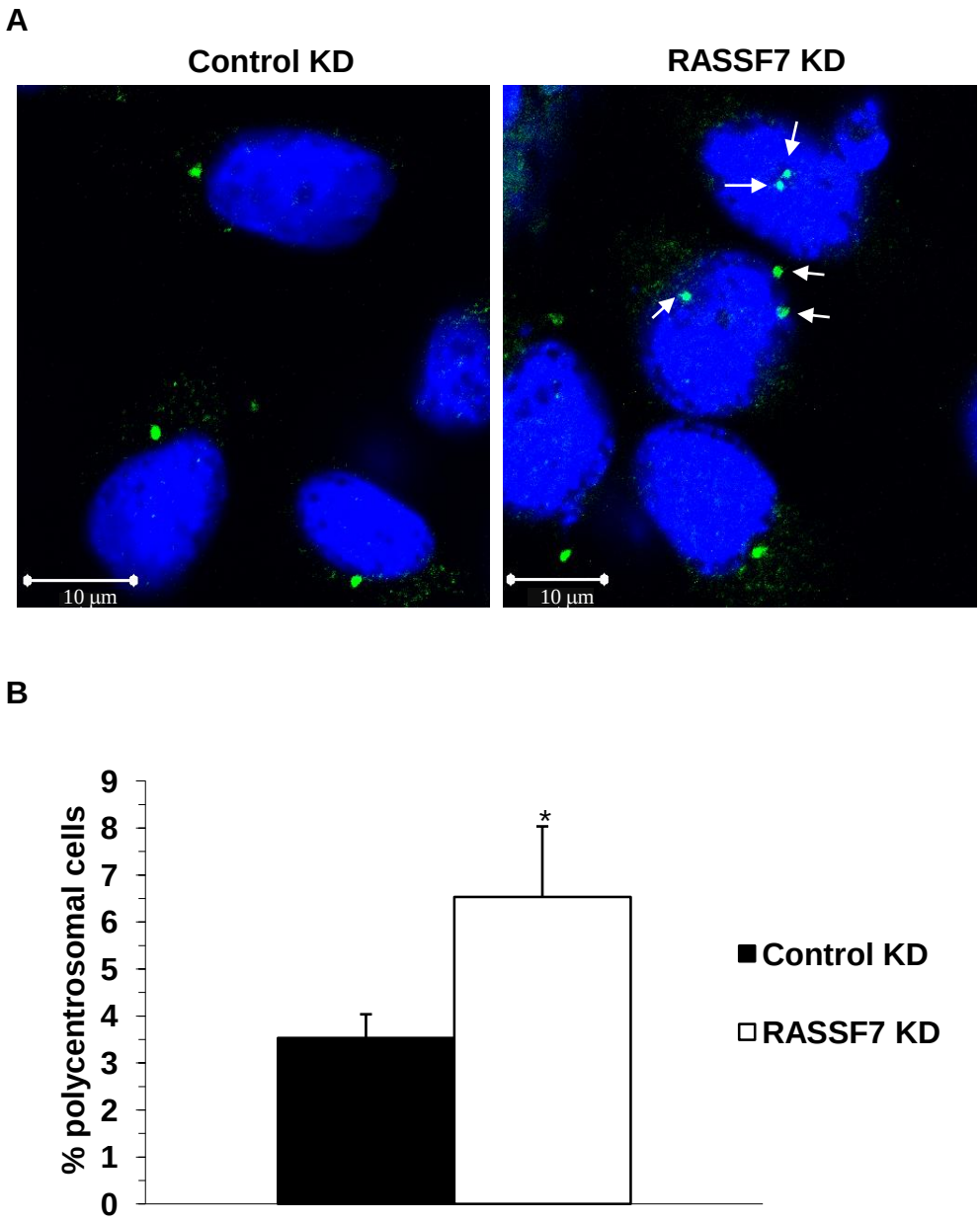


**Figure 5.10: RASSF7 KD leads to a higher rate of polycentrosomal interphase HeLa cells.** RASS7 KD cells often presented multiple centrosomes when in interphase, as indicated by arrows. Green: centrosomal marker pericentrin; Blue: nuclear staining (A). The rate of polycentrosomal non dividing cells was significantly higher for RASSF7 KD compared to controls as shown by the graph in B). *$p<0.05$, more than 500 cells were counted for each individual specimen from three independent experiments. Error bars, SD.

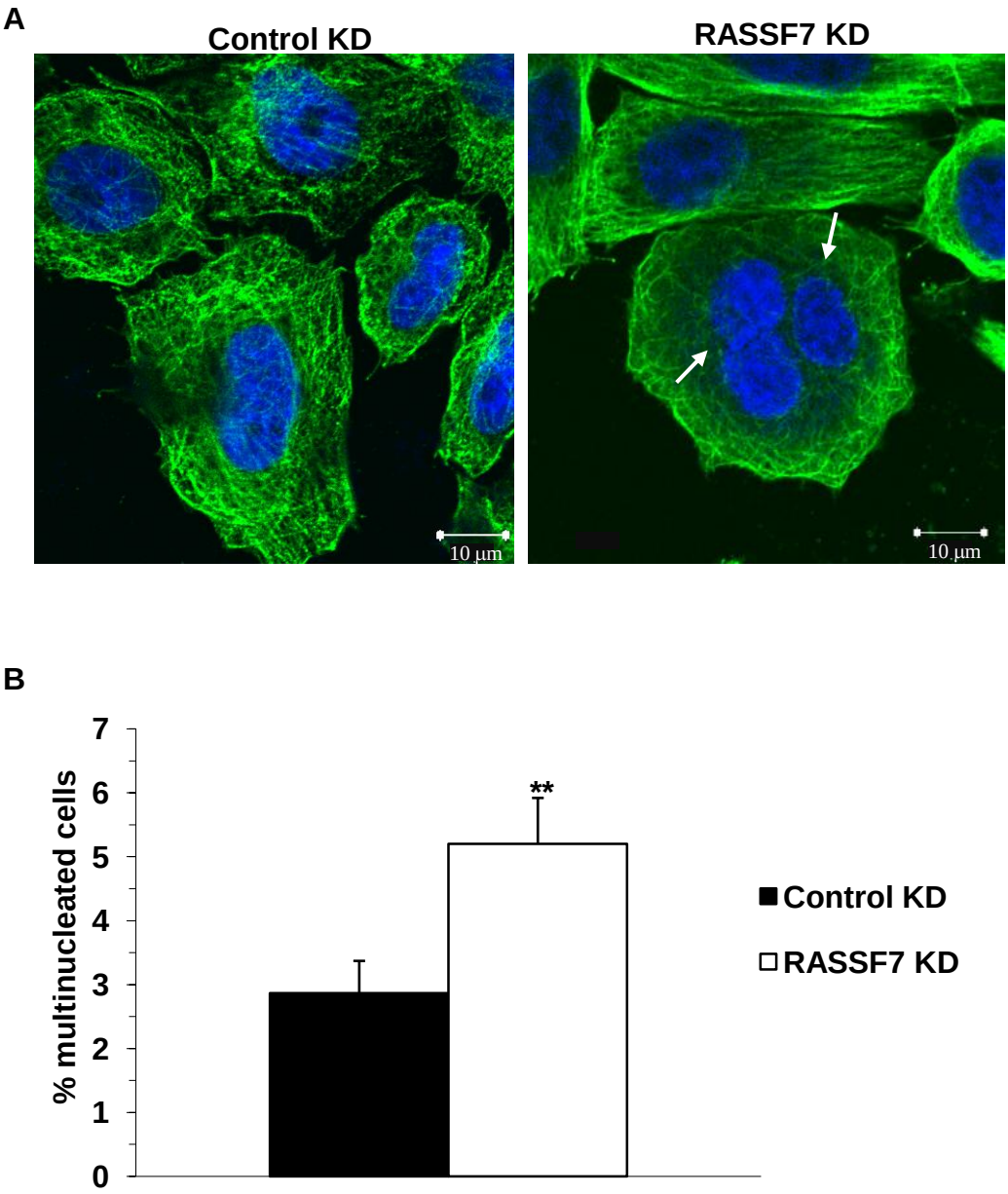


**Figure 5.11: RASSF7 depletion leads to polyploidy in interphase HeLa cells.** RASS7 disruption frequently resulted in the formation of multinucleated cells (as indicated by the arrows). Green: microtubule marker α–tubulin; Blue: nuclear staining (A). The graph shows the percentage of RASSF7 KD cells with abnormal DNA content compared to control (B). **p<0.01, more than 500 cells were counted for each individual specimen from three independent experiments. Error bars, SD.

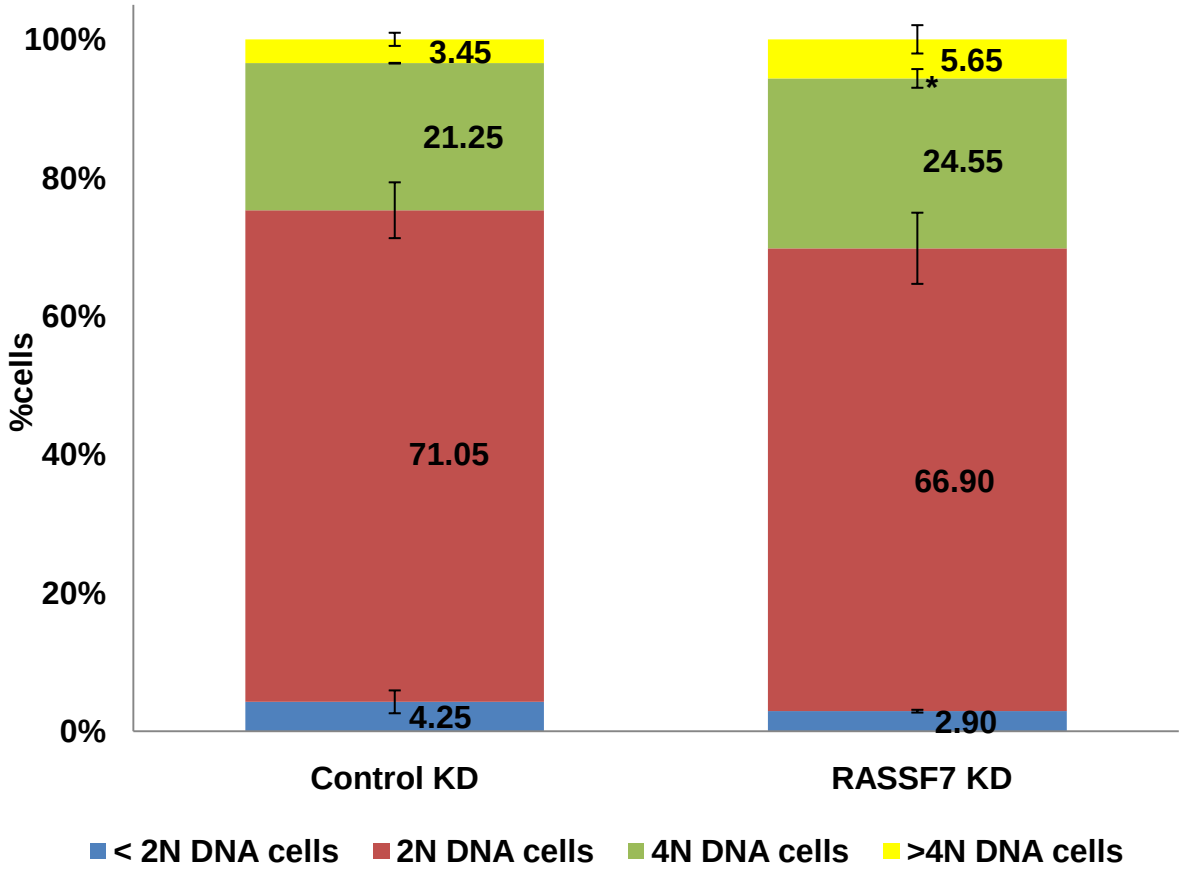


**Figure 5.12: RASSF7 KD caused a slight but statistically significant increase of tetraploid cells.** Cytofluorimetric estimation of control and RASSF7 KD HeLa cell cycle stages. Sub G1, G1, G2/M and polyploid cells were sorted according to DNA content (<2N, 2N, 4N and >4N respectively), gated accordingly and then counted. The graph shows the average result of three independent experiments. *p<0.05. One million events were considered each time. Error bars, SD.

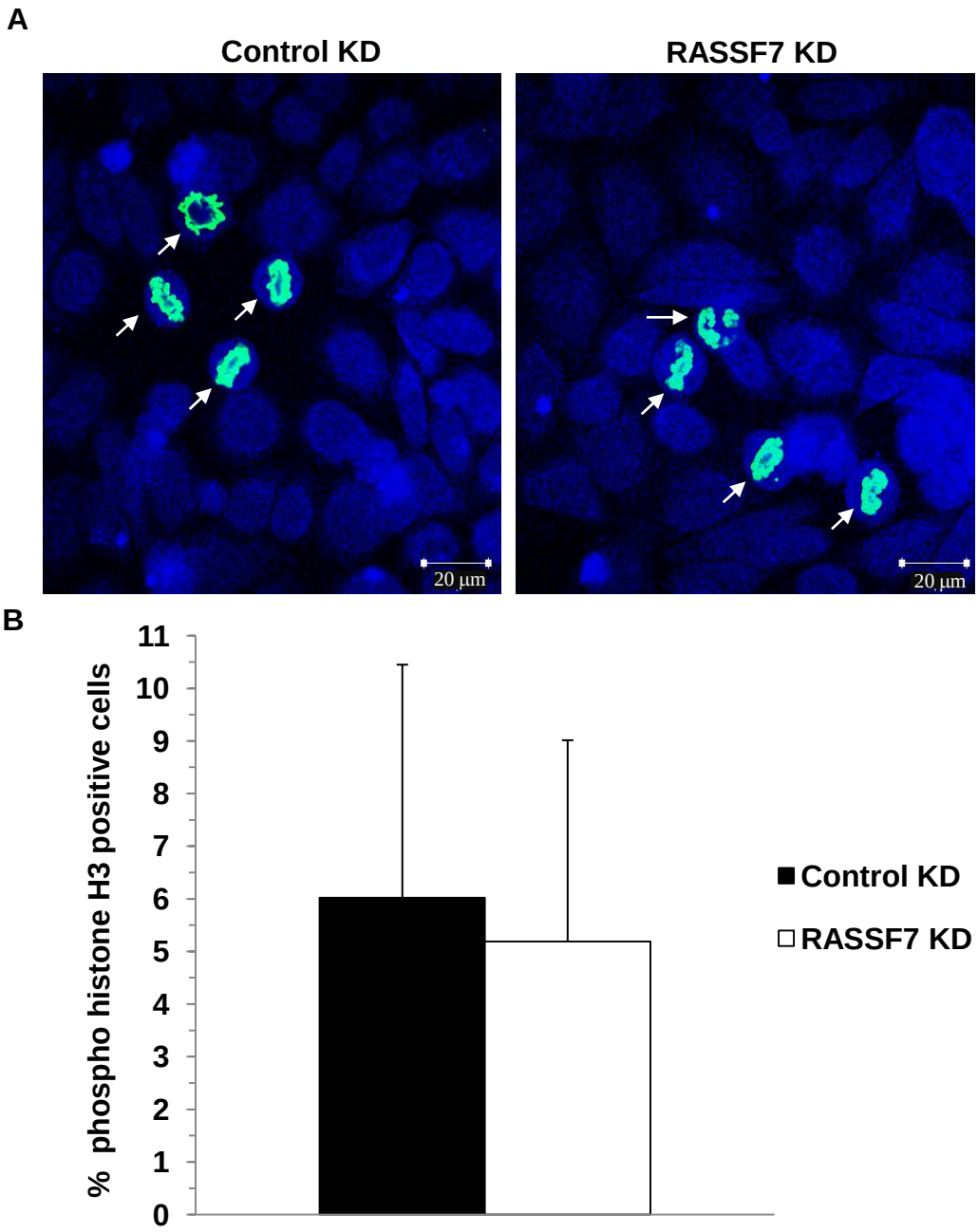


**Figure 5.13: RASSF7 KD did not cause a significant increase in mitotic cells.** RASSF7 depletion in HeLa cells did not significantly increase the number of phospho histone H3 (Ser10) positive cells (green, highlighted by arrows) compared with controls (A), as confirmed by statistical analysis (B). More than 500 cells were counted for each sample from three independent experiments. Blue: nuclear staining.

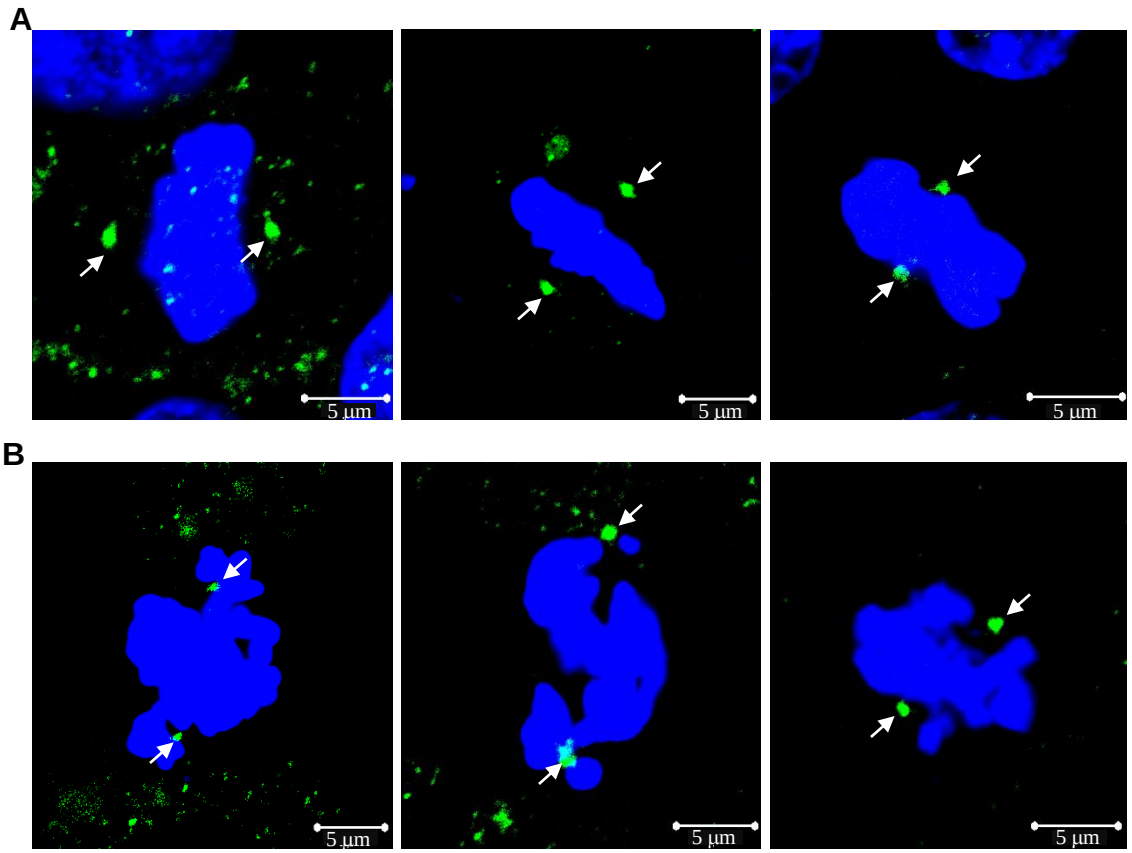


**Figure 5.14: Active Polo Like Kinese 1 (PLK1) localises to the centrosomes in RASSF7 KD cells.** Control (A) and RASSF7 KD (B) cells were stained for phospho PLK1 (Thr210) (green, white arrows) and DAPI (blue). The images are representative of at least two independent experiments.

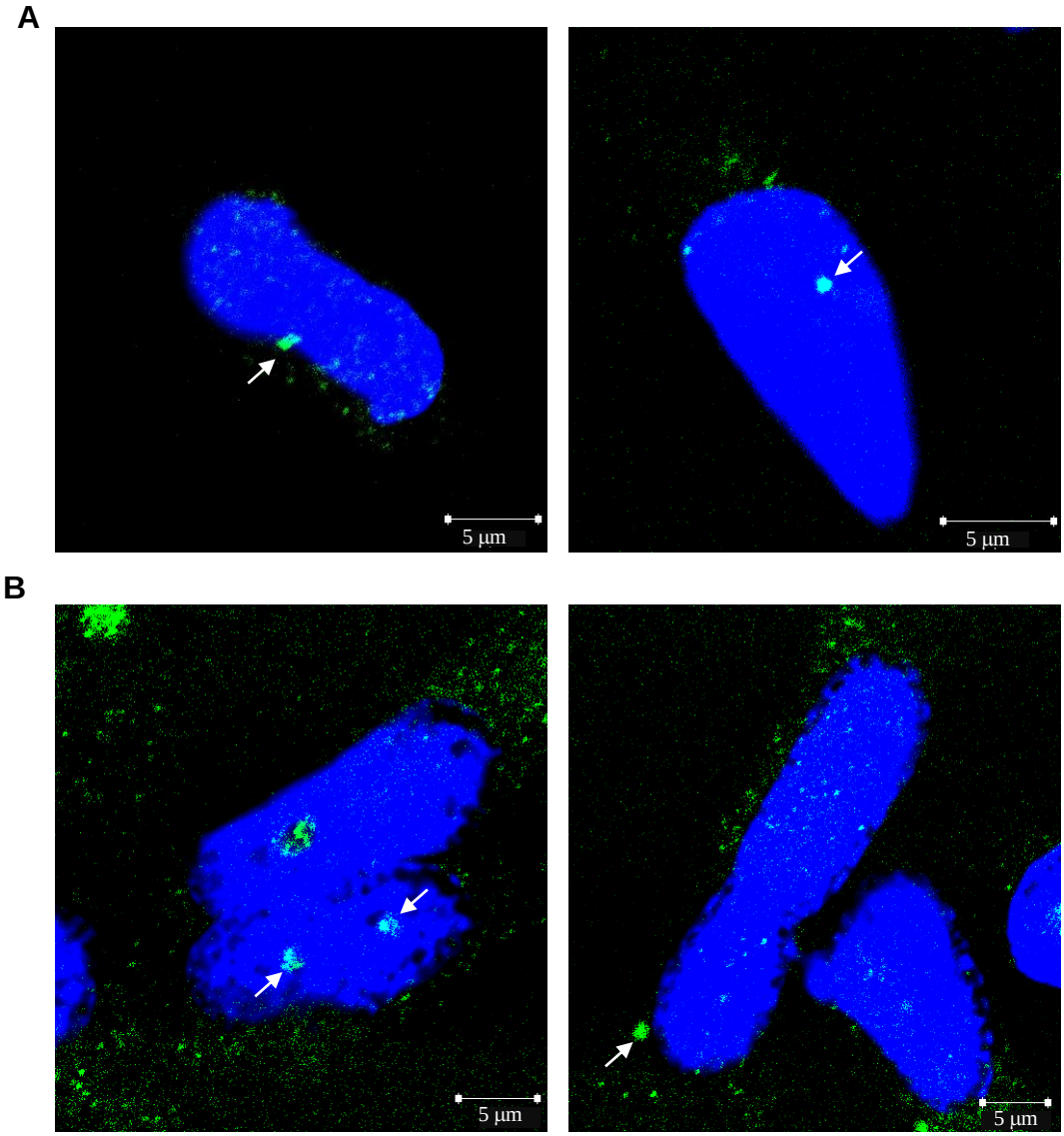


**Figure 5.15: RASSF1A continues being localised in RASSF7 KD cells.** RASSF7 KD HeLa cells exhibit normal centrosomal localisation of RASSF1A (green, white arrows) (B) as in control cells (A). Blue: nuclear staining.

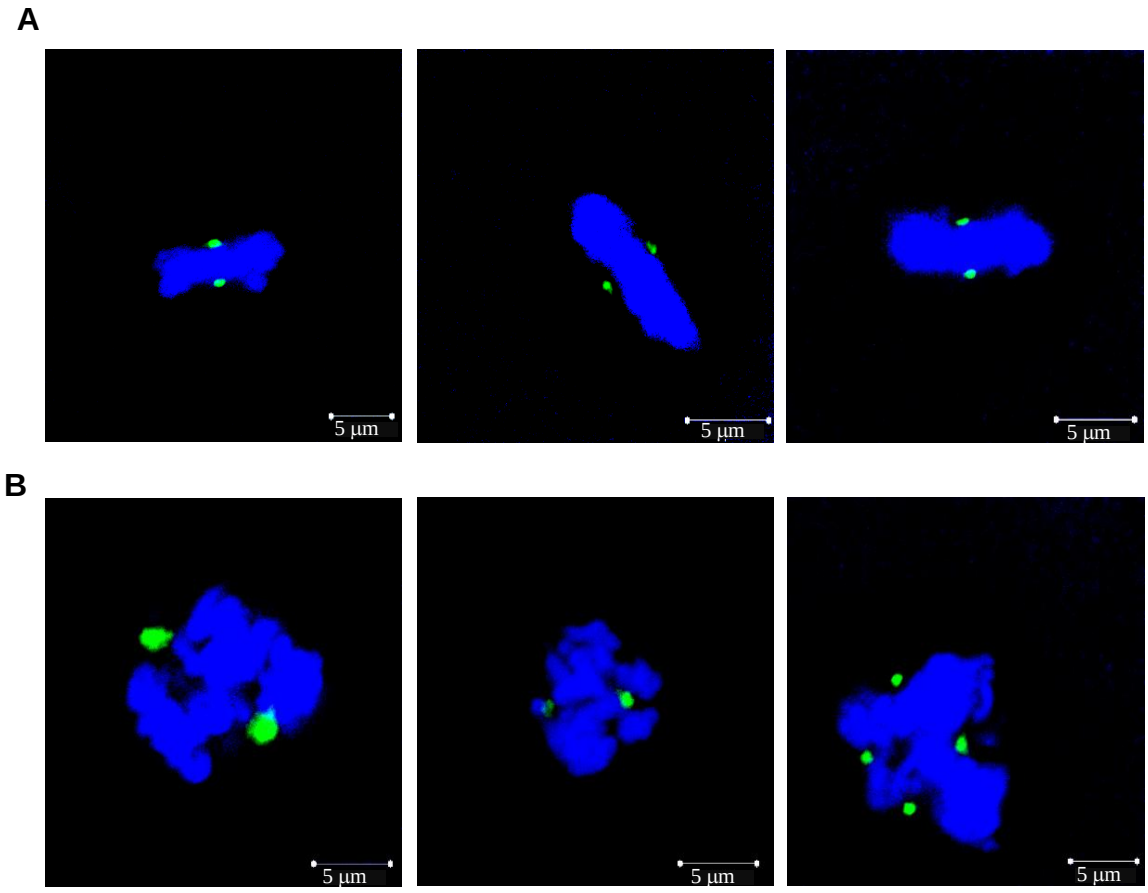


**Figure 5.16: Aurora A localises to the centrosomes in RASSF7 KD cells.** Control (A) and RASSF7 depleted (B) HeLa cells were stained for Aurora A (green) and DAPI (blue). Images are representative of at least three independent experiments**.**

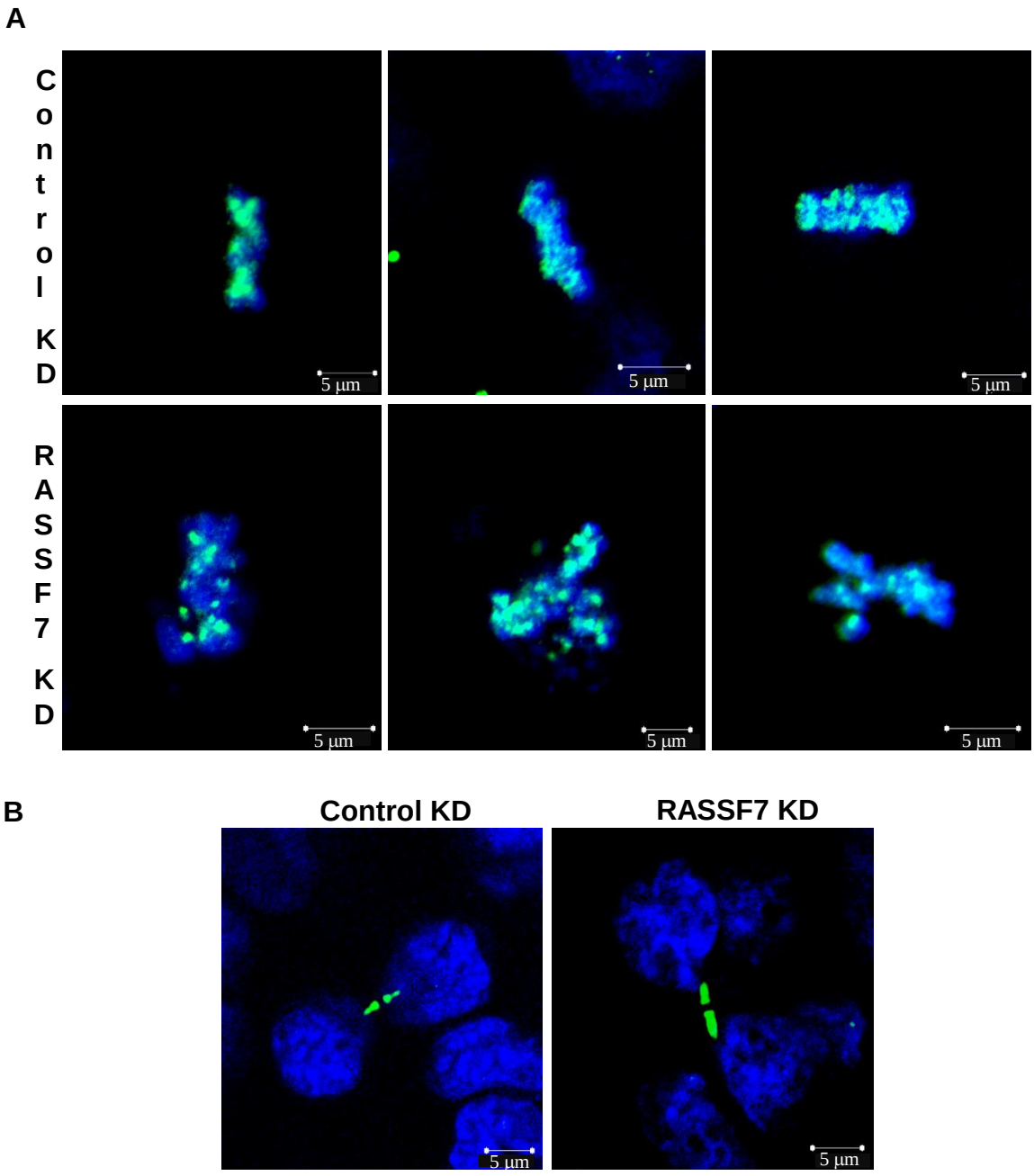


**Figure 5.17: Aurora B localisation is maintained throughout mitosis in RASSF7 KD HeLa cells.** RASSF7 KD cells show Aurora B (green) localisation at the kinetochore as controls during metaphase (A) and exhibit Aurora B at the mid body during cytokinesis (B). Blue: nuclear staining. Images are representative of at least three independent experiments.

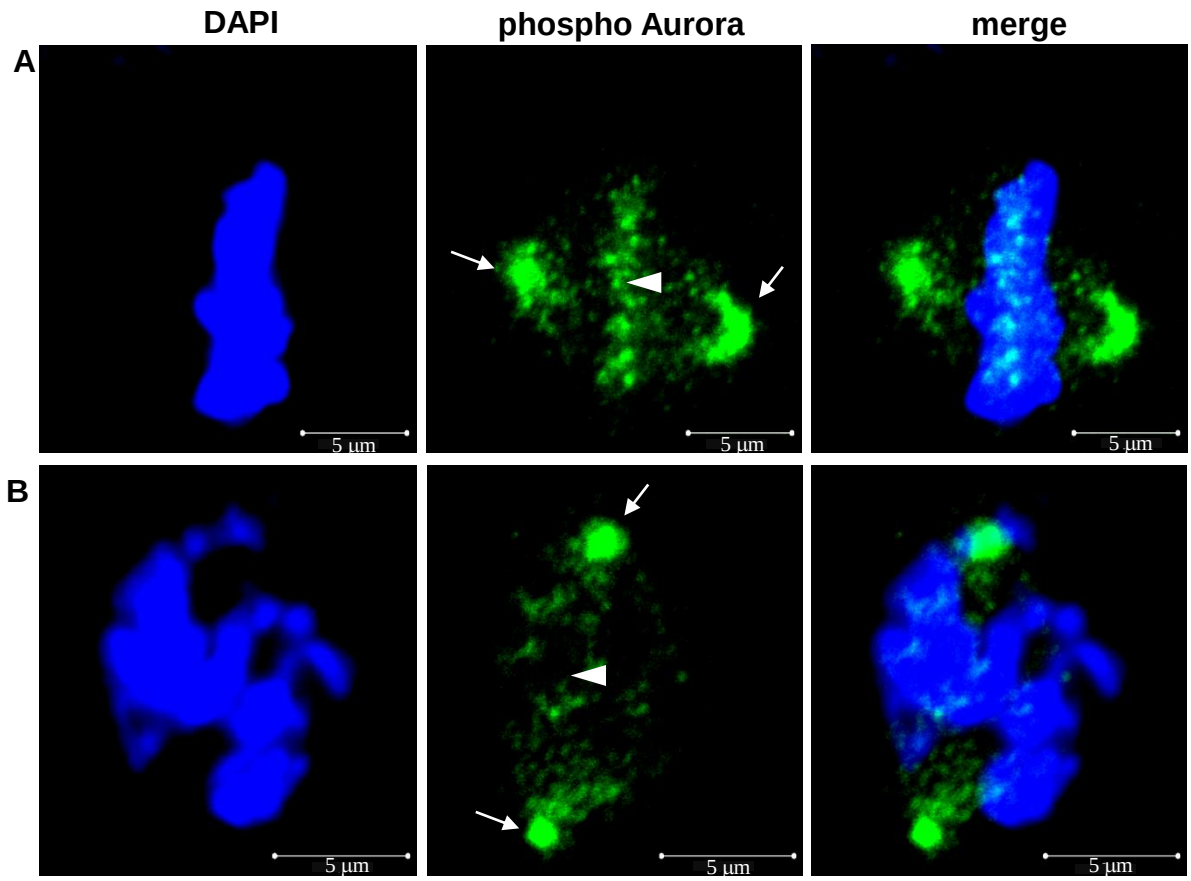


**Figure 5.18: There is reduced Aurora kinase activation at the kinetochore of RASSF7 KD cells.** Cells were stained with an antibody recognising the phosphorylated forms of Aurora A (Thr288), Aurora B (Thr232), Aurora C (Thr198). In a normal control cell (A) phospho Aurora (green) was detectable at both the centrosomes (white arrows) and at the kinetochore (white arrowhead). RASSF7 depleted HeLa cells (B) were positive for phospho Aurora at the centrosomes (white arrows) whereas reduced specific phospho Aurora staining was detectable at the kinetochore (white arrowhead). Blue: nuclear staining. Images are representative of at least three independent experiments.

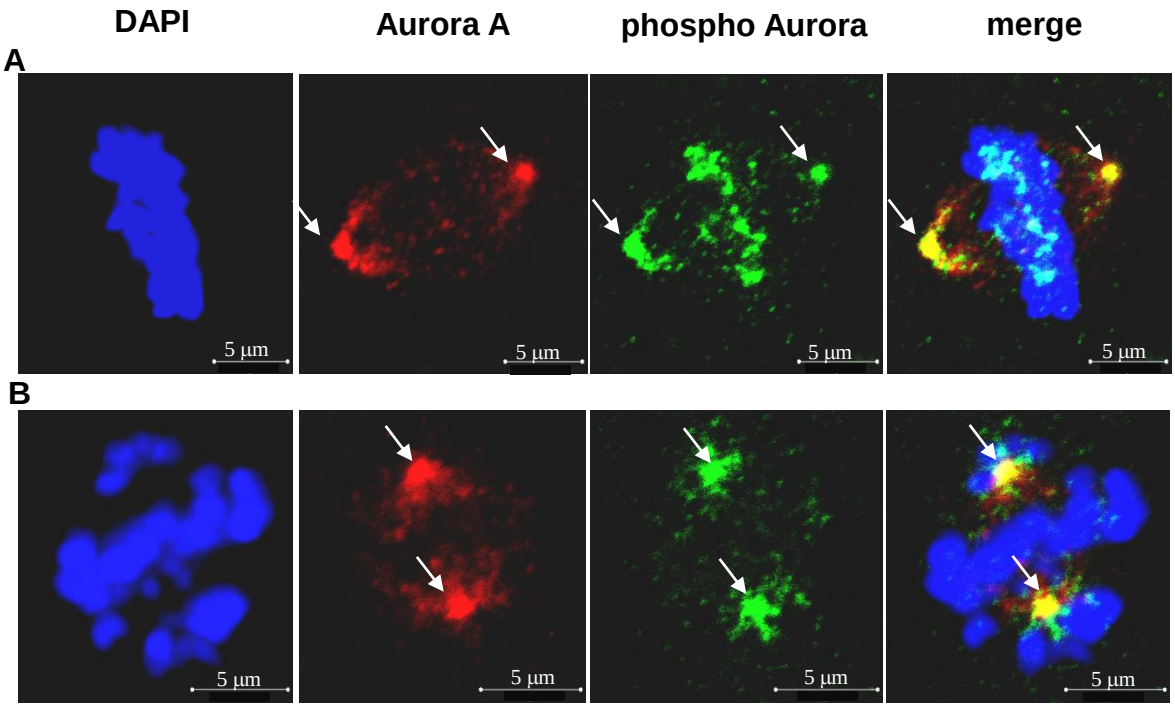


**Figure 5.19: Aurora A is expressed and active at the centrosomes of RASSF7 KD cells.** Co-localisation of Aurora A (red) and phospho Aurora (green). The two signals coincide at the centrosomes (white arrows) for both control (A) and RASSF7 KD (B) HeLa cells. Blue: nuclear staining. The images are representative of at least three indipendent experiments.

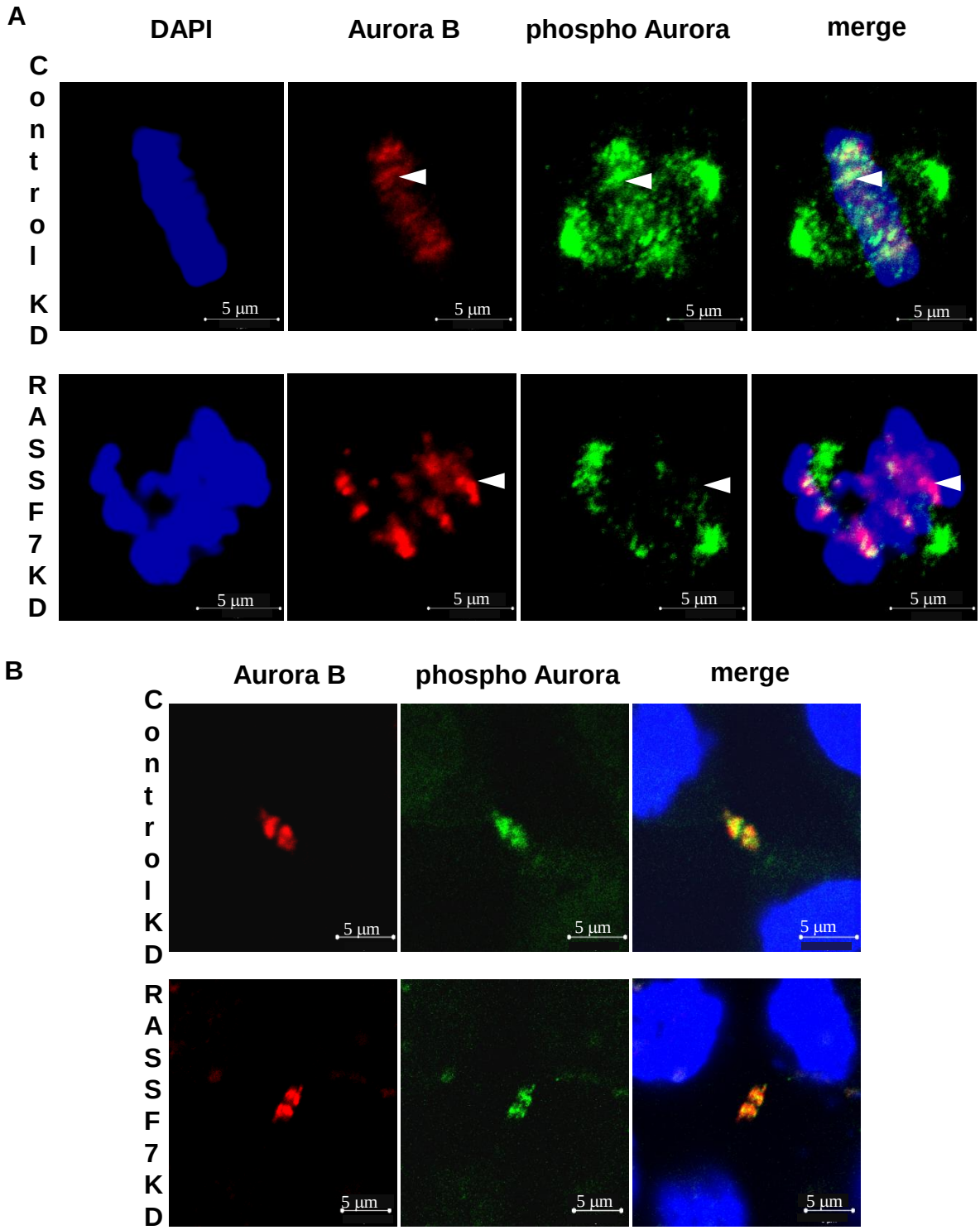


**Figure 5.20: RASSF7 KD compromises Aurora B activity during metaphase but not cytokinesis.** Aurora B co-localises with Phospho-Aurora at the kinetochore (white arrowheads) only in control metaphase cells (A). At the end of M phase Aurora B activity at the mid body of RASSF7 KD HeLa cells is almost comparable to controls (B). Blue: nuclear staining. Images are representative of at least three independent experiments.

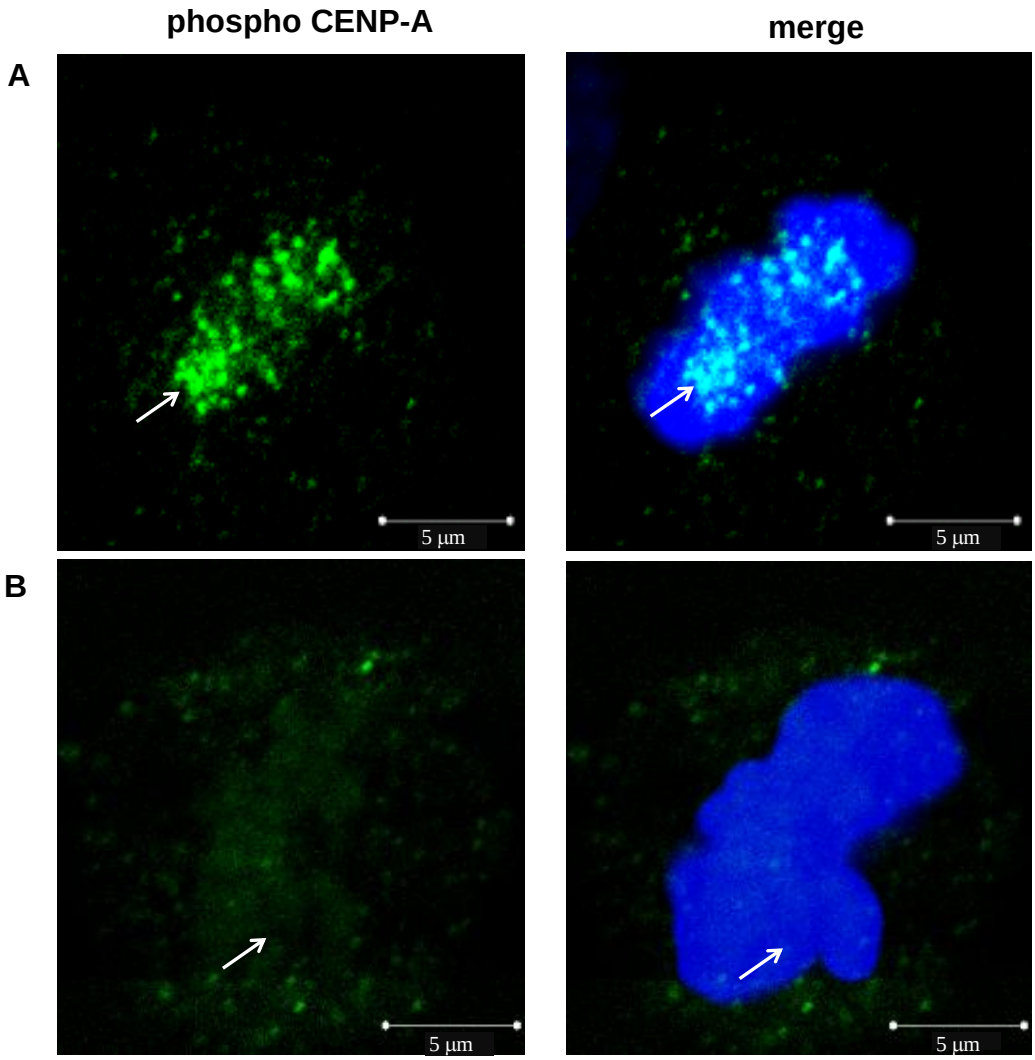


**Figure 5.21: RASSF7 KD causes the reduced phosphorylation of CENP-A, a prometaphase target of Aurora B.** Control (A) and RASSF7 KD (B) HeLa cells were stained for phospho CENP-A (Ser7) and DAPI (blue). Phospho CENP-A localises to the kinetochore (white arrows) only in control cells. Images are representative of at least three independent experiments**.**

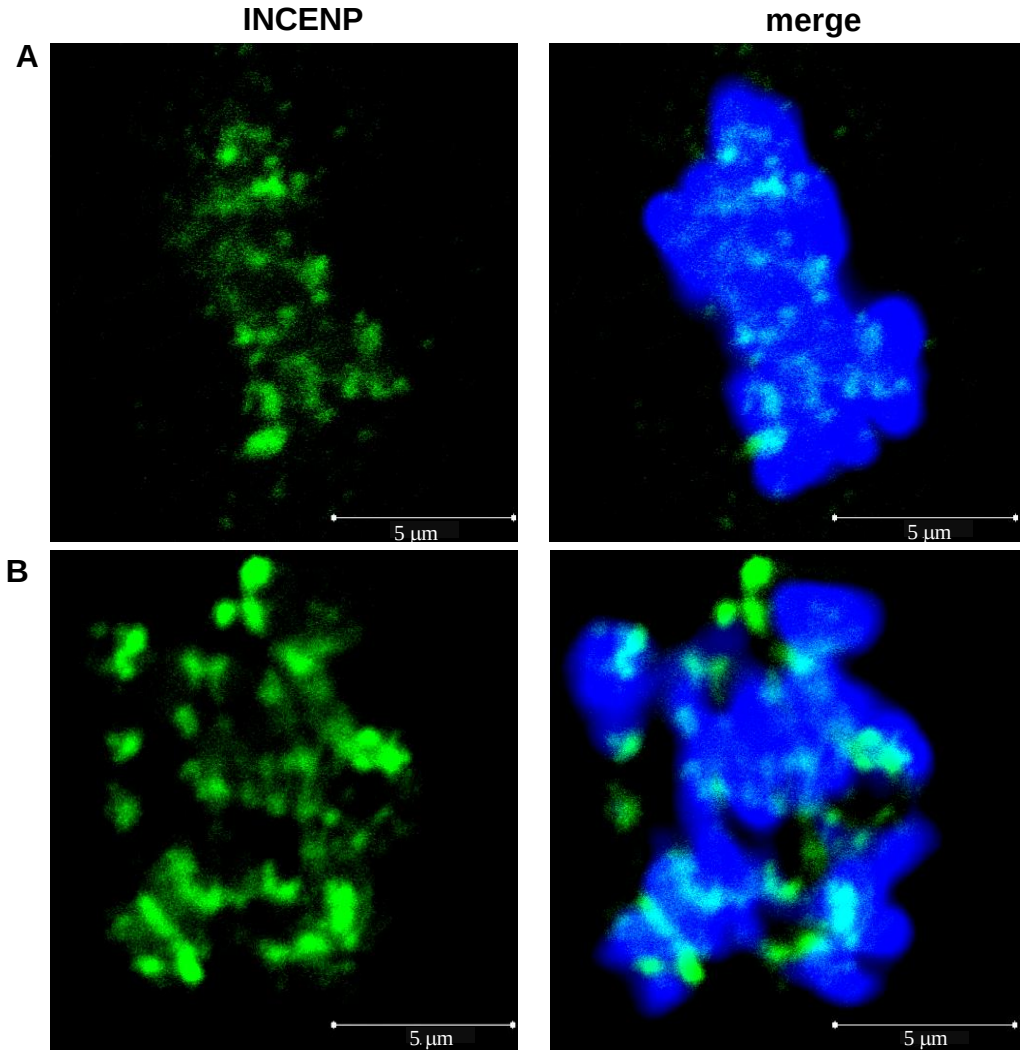


**Figure 5.22: INCENP, which is required for Aurora B activation, is correctly recruited to the kinetochore in RASSF7 KD cells.** Control (A) and RASSF7 KD (B) HeLa cells were stained for INCENP and DAPI (blue). Images are representative of at least three independent experiments.

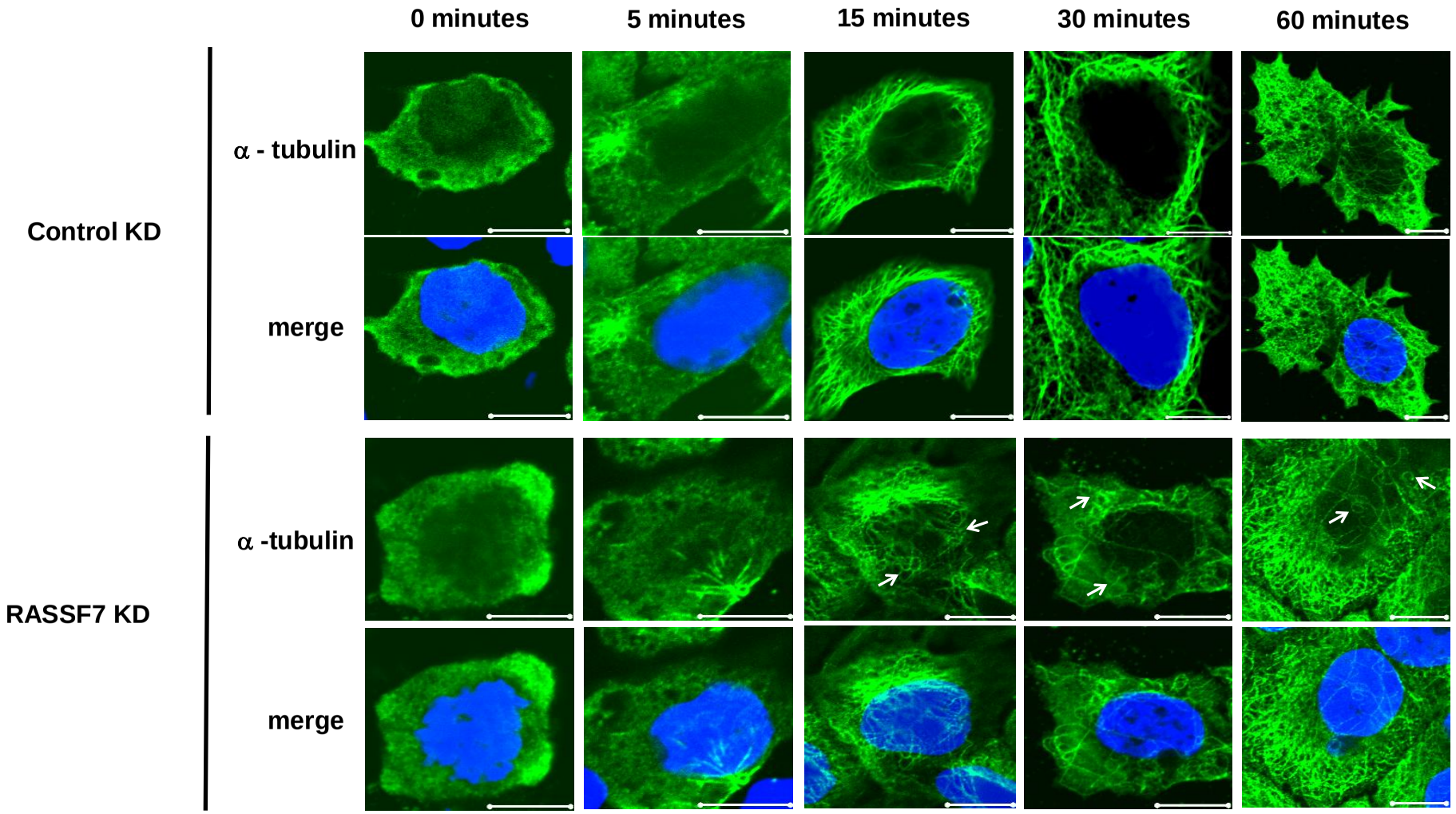


**Figure 5.23: Down-regulation of RASSF7 protein expression in HeLa cells causes delays and abnormalities in microtubule initial polymerisation.** RASSF7 KD and control cells were nocodazole treated (300ng/ml) for 1 hour at 37°C for disrupting the microtubules. Cells were subsequently incubated in nocodazole free medium and microtubule re-growth was monitored at different time points. Despite microtubule nucleation occurring fine in RASSF7 KD cells (5'), microtubule fibres (labelled by α–tubulin, green) took longer to form and are more irregular compared to controls (white arrows). Blue: nuclear staining. .Scale bars, 10 μm. Images are representative of two independent experiments.